# IODP HOLE 1256D: PETROLOGICAL AND TEXTURAL VARIATIONS DOWN-CORE

by

Khalhela E. Zoeller

Submitted in partial fulfilment of the requirements for the
degree of Combined Honours Bachelor of Science in Earth Sciences and
Oceanography

at

Dalhousie University
Halifax, Nova Scotia
April, 2011

# Distribution License

DalSpace requires agreement to this non-exclusive distribution license before your item can appear on DalSpace.

NON-EXCLUSIVE DISTRIBUTION LICENSE

You (the author(s) or copyright owner) grant to Dalhousie University the non-exclusive right to reproduce and distribute your submission worldwide in any medium.

You agree that Dalhousie University may, without changing the content, reformat the submission for the purpose of preservation.

You also agree that Dalhousie University may keep more than one copy of this submission for purposes of security, back-up and preservation.

You agree that the submission is your original work, and that you have the right to grant the rights contained in this license. You also agree that your submission does not, to the best of your knowledge, infringe upon anyone's copyright.

If the submission contains material for which you do not hold copyright, you agree that you have obtained the unrestricted permission of the copyright owner to grant Dalhousie University the rights required by this license, and that such third-party owned material is clearly identified and acknowledged within the text or content of the submission.

If the submission is based upon work that has been sponsored or supported by an agency or organization other than Dalhousie University, you assert that you have fulfilled any right of review or other obligations required by such contract or agreement.

Dalhousie University will clearly identify your name(s) as the author(s) or owner(s) of the submission, and will not make any alteration to the content of the files that you have submitted.

If you have questions regarding this license please contact the repository manager at dalspace@dal.ca.

Grant the distribution license by signing and dating below.

Name of signatory

Date

## TABLE OF CONTENTS

## ACKNOWLEDGMENTS

I would like to thank my supervisors Rebecca Jamieson and Matthew Salisbury for all of their support and encouragement while supervising this thesis. Without their patience and guidance this would not have been possible. I would also like to thank Lisa Gilbert for the many emails of helpful tips, and for providing the thin sections necessary to complete this thesis. Your comments and insight greatly improved this paper. Thank you to Patrick Ryall for his guidance in writing an honours thesis for the first time, and the many hours he spent reading paper after paper. Thank you to Dan MacDonald who patiently stood by while I learned to use the Electron Microprobe. I would also like to thank all the staff in the Earths Science office that successfully made sure my numerous rough drafts were received by the right people, and that I got the many comments back. Lastly I would like to thank all of my friends and family who stood by, pushed when I needed to be pushed, and were there for support whenever it was needed. I truly could not have done it without all of you.

## ABSTRACT

An intact core from IODP (Integrated Ocean Drilling Program) Site 1256, located in the eastern equatorial pacific (Cocos Plate), was collected on three different legs (legs 206, 309, and 312). This is the fourth deepest hole that IODP has drilled since 1968, and is the first hole to reach the uppermost portion of *in situ* gabbroic oceanic layer 3. The purpose of this study is to examine down-hole petrological and textural trends, including variations in hydrothermal alteration products.

Fifty-three thin sections were cut at specific depths down-core and point counts of primary and secondary minerals were done on all samples. Some systematic trends can be inferred from the modal analyses concerning the dominant minerals and alteration products. Trends include a change from possible smectites to chlorite at 1050 mbsf, concentrations of quartz at varying depths, and changes in opaque oxides at 1230 mbsf. Electron microprobe analysis was done on six representative thin sections to identify some unknown minerals, including amphiboles, opaque oxides, and possible clay minerals, suggested by previous work that showed clays to be present in the upper part of the core. Results show the presence of minimal sulphides, orthopyroxene and olivine, an abundance of clays, and amphiboles were determined to be hornblende and actinolite.

Point-counts and electron microprobe analyses from a core collected from the Kane Fracture Zone on the Mid-Atlantic Ridge were used to supplement data obtained from the Site 1256 core, in particular observing variations in texture and alteration minerals. Results from both cores will assist in understanding spatial variations in igneous and hydrothermal processes at mid-ocean ridges.

## LIST OF FIGURES

## LIST OF TABLES

# CHAPTER 1: INTRODUCTION

## 1.1 Site Location and Purpose of Study

Fast spreading mid-ocean ridges, including the East Pacific Rise (15 cm/yr (Sinton et al., 1991)), produce some of the thinnest oceanic crust in the world. Attempts to drill through a continuous section of oceanic crust have therefore focused on sites formed at these ridges. IODP Site 1256 is an ideal location to attempt to reach oceanic layer 3 by drilling, because it is located on the flank of the East Pacific Rise in the eastern equatorial Pacific (6º 44.2'N and 91º 56.1’W) in the Guatemala Basin on the Cocos Plate (figure 1.1). This site is located in approximately 3600m of water in ~15 Ma fast-spreading crust. Site 1256 is still a target for active IODP drilling projects, with a current depth of approximately 1500 meters below seafloor (mbsf). Since Hole 1256D is the first IODP hole drilled continuously through basalts and sheeted dikes into gabbro, data collected from this core will help determine the nature of Layer 3 and its boundaries with Layer 2, and any depth-controlled mineralogical or textural trends of oceanic crust at a fast-spreading ridge.

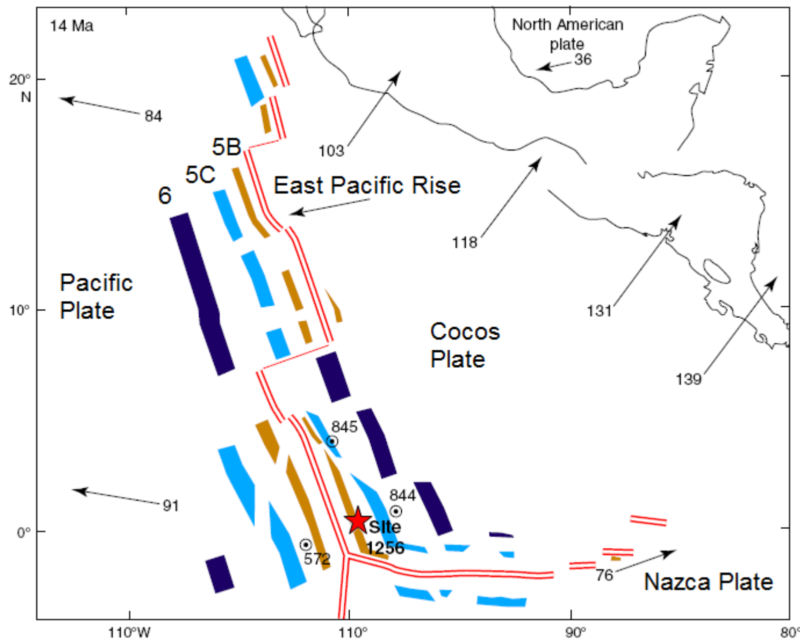


Figure 1.1: Reconstruction of Site 1256 and the Cocos Plate at approximately 14Ma, 1Ma after the formation of crust at Site 1256. Arrows show approximate direction of plate movement and average velocities in mm/yr. Coloured bars represent magnetic anomalies along the East Pacific Rise. (Teagle et al., 2006)

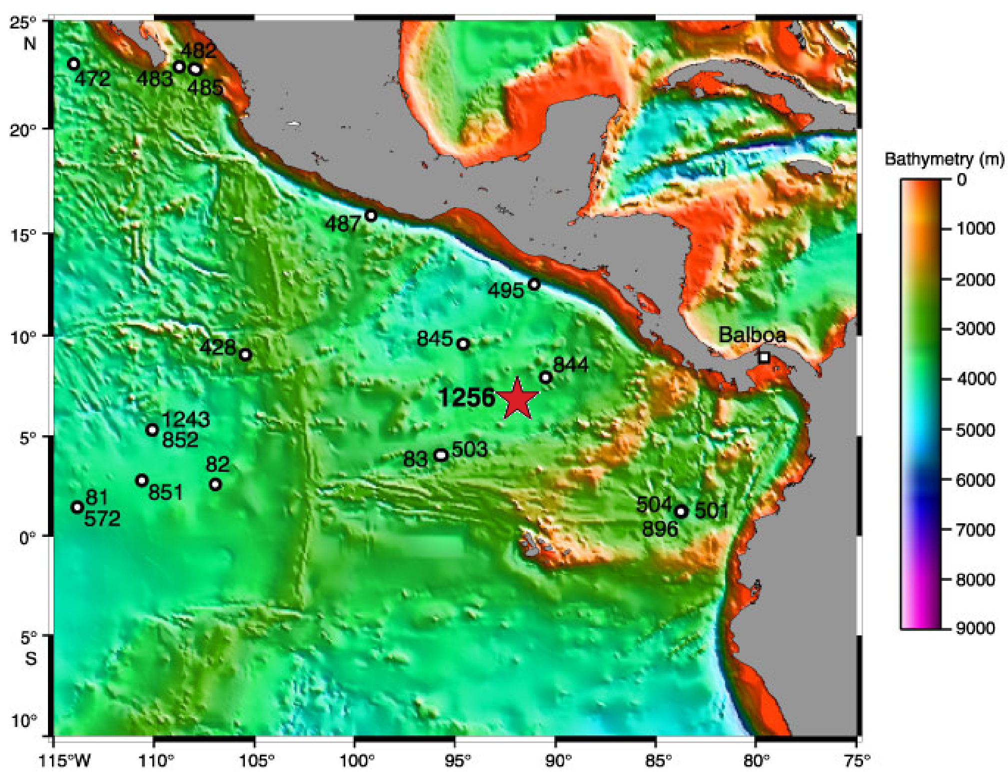


Figure 1.2: Location of IODP Site 1256 (represented by red star) and the general bathymetry of the surrounding area. Small circles show locations of other drill holes, along with IODP site numbers. (Teagle e al., 2006).

The purpose of this study is to provide the first quantitative petrologic modal analysis of primary and secondary minerals as a function of the depth in Hole 1256D. Although extensive petrologic analysis of the core has been performed previously (see below), the shipboard modal analyses were only qualitative and often failed to tally to 100%. There were also noticeable differences between observations recorded by different shipboard parties. Fifty-three thin sections were prepared from Hole 1256D for point count analysis and to describe the texture and mineralogy from top to bottom of the core. Six representative thin sections were analyzed using the 8200X JEOL Superprobe at the Dalhousie Regional Electron Microprobe Laboratory to aid in the identification of some unknown minerals within the samples. In addition, similar observations were made on a core collected from the Kane Fracture Zone along the Mid-Atlantic Ridge in order to compare oceanic crust from a slow-spreading ridge with the fast-spreading crust at Site 1256. The observations from the two cores are compared to reveal similarities or differences between the two areas, specifically whether or not the same alteration minerals are present in both.

**1.2 Overview of Hole 1256D**

Oceanic crust is classically divided into three layers: Layer 1 is composed of sediments, while Layer 2 is composed of basaltic lavas and sheeted dikes, and Layer 3 is thought to be composed of gabbros. In Hole 1256D (Teagle et al., 2006) Layer 2 consists of pillow basalts, massive lava flows, and sheet flows of basaltic composition down to approximately 1050 mbsf, underlain by a sheeted dike complex, which consists of sub-vertical intrusions to a depth of about 1400 mbsf. The mineralogy of the sheeted dikes changes with depth, especially in terms of alteration products, however textural changes are obvious as well. Layer 3 comprises gabbros; at Hole 1256D these are reached at 1407 mbsf. The sediments of Layer 1 where not examined for this project. Detailed descriptions of rocks from Layers 2 and 3 at Hole 1256D are presented in Chapter 2. All have experienced hydrothermal alteration, however no faults or other evidence for tectonic activity has been found in the drill core.

### 1.3 Significance of Hole 1256D

More then 60% of the earth is covered by oceanic crust formed at mid-ocean ridges. Hole 1256D, which was drilled on three separate legs (ODP leg 206 and IODP legs 309 and 312), is the first hole to drill a continuous section through Layer 2 oceanic extrusive rocks (pillow basalts, sheet flows, and massive flows), and sheeted dikes, and into Layer 3 intrusive rocks (gabbros). Figure 1.3 shows a comparison of previous DSDP, ODP, and IODP legs and expeditions that have collected significant sections of oceanic crust. Previous samples of Layer 3 gabbros have been collected from tectonically exhumed oceanic Layer 3 and along walls of transform faults.

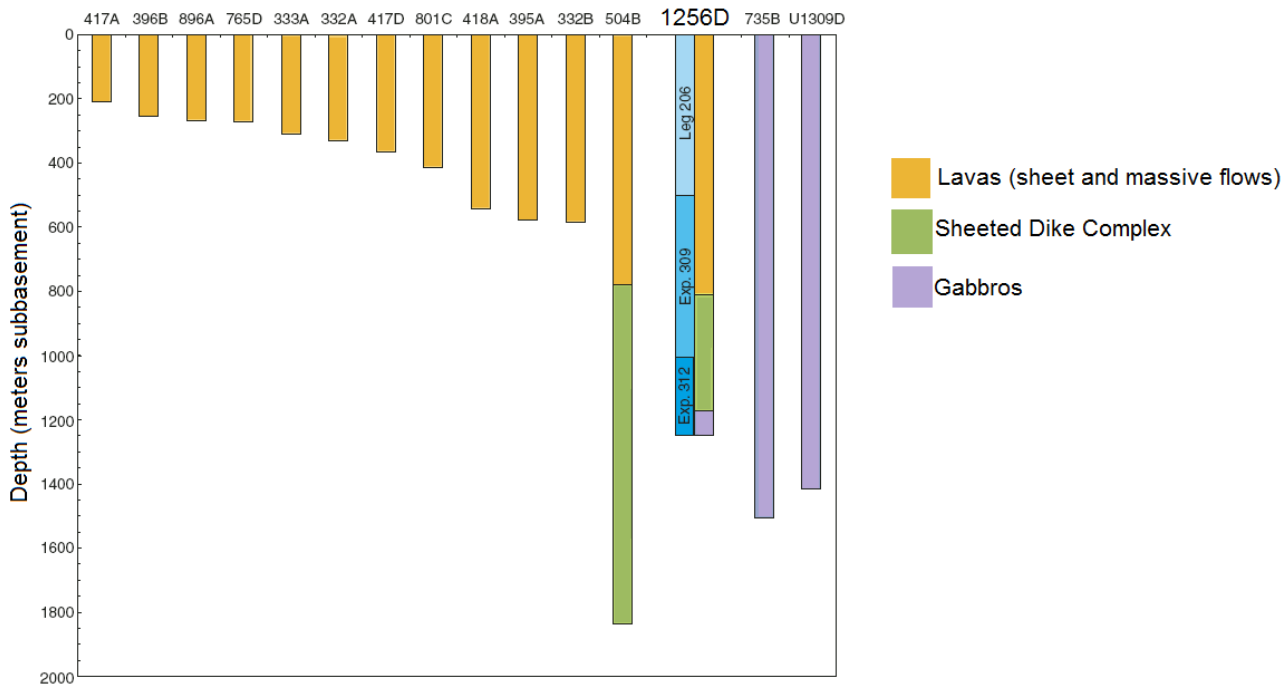


Figure 1.3: Comparison of basement holes drilled by DSDP, ODP, and IODP in the past. Hole 1256D is the only hole to have collected a continuous section through lavas, sheeted dikes, and gabbros. (Teagle et al., 2006)

In addition to advancing our understanding of the petrology and alteration of the crust, detailed point counts and petrographic analysis can eventually be used to calculate seismic and magnetic properties of the section for comparison with refraction and magnetic anomaly data and down-hole logs. Finally, with this detailed overview of crust formed at a fast-spreading ridge, comparisons of mineralogy, seismic properties, and magnetic data from other sites can be made to gain a better understanding of the crustal structure formed at mid-ocean ridges.

### 1.4 Geological Setting and Drilling Parameters

The general bathymetry at Site 1256 is relatively flat with no major fracture zones or seamounts observed in the area. The sediment overburden is approximately 250 m, and the total crustal thickness is 5-5.5 km based on seismic data collected from various expeditions. The crust at Site 1256 is thought to have formed at approximately 15 Ma and accreted at a superfast spreading rate of 20-22 cm/yr (Wilson et al., 2003). This site was chosen due to the inverse relationship between spreading rate and the depth to axial low-velocity zones, thought to be partially molten gabbros (Wilson et al., 2003; figure 1.4). Based on a spreading rate of 20cm/yr to 22cm/yr and seismic data collected previously, it was thought the depth to the gabbros would be less than at many other locations. Furthermore, since Site 1256 is tectonically stable it was thought that a continuous section of ocean crust could be obtained. Site 1256 comprises four different holes that were all originally drilled during the first expedition, Leg 206. After three pilot holes were drilled, Hole 1256D was selected for an attempt to drill 1.5-2 km into oceanic crust.

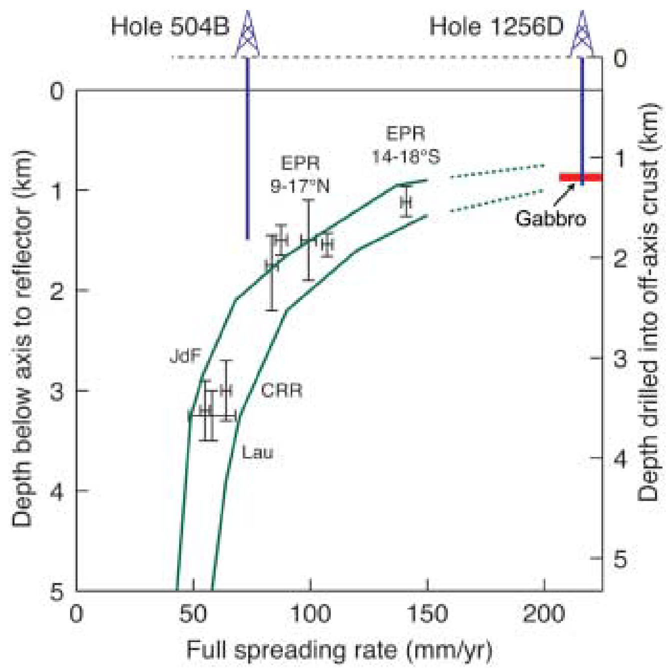


Figure 1.4: Depth to axial melt-lens reflector plotted against spreading rate. Penetration to date in Holes 504B and 1256D is shown by solid vertical lines, with the depth at which gabbros were intersected is indicated with a red horizontal line. (Wilson, 2006)

Three legs, 206, 309, and 312, have deepened Hole 1256D. The exploratory leg 206 drilled approximately 750 mbsf into the crust, remaining in the lavas. Leg 309 deepened the hole to 1255 mbsf, which penetrated into the sheeted dike complex. The most recent of the expeditions, leg 312, deepened the hole to approximately 1507mbsf (Teagle et al., 2006; figure 1.5).

Seismic data have shown Layer 3, at Site 1256, to begin somewhere between 1270-1570 mbsf, and the gabbro was reached at 1407 mbsf. Although this suggests that the Layer 3 was reached, it is possible that the drill only penetrated into the transition zone between the sheeted dike complex and the gabbros. Therefore, in spring 2011, a fourth leg will return to Hole 1256D to deepen the hole further and determine if the third layer has in fact been reached. For now, Hole 1256D is the fourth deepest hole into oceanic crust, and the second deepest hole drilled into a continuous section of normal oceanic crust (Teagle et al., 2006).

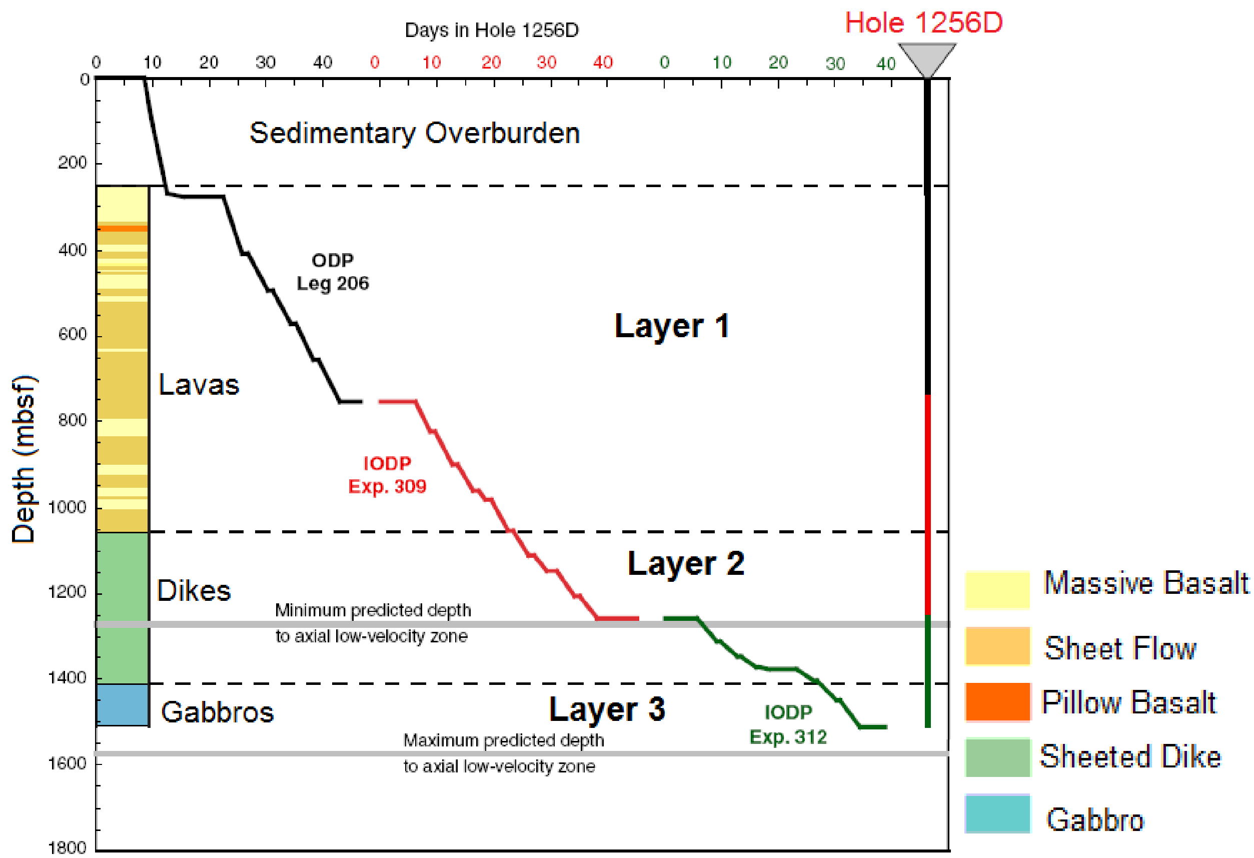


Figure 1.5: Drilling progress of Hole 1256D during ODP leg 206, and IODP expeditions 309 and 312, showing generalized lithostratigraphy. (Modified from Wilson, 2003)

**1.5 Previous Work**

Expedition reports for Legs 206, 309, and 312 have been published in the ODP/IODP Proceedings (Teagle et al., 2006). These review all aspects of the expeditions and scientific results to date. The four main objectives of the expeditions are as follows: (Teagle et al., 2006)

> 1. Test the prediction, from the correlation of spreading rate with decreasing depth to the axial low-velocity zones (e.g., Purdy et al., 1992), that gabbros representing the crystallized melt lens will be encountered at 1000–1300 msb (1250-1550 mbsf) at Site 1256.
>
> 2. Determine the lithology and structure of the upper oceanic crust from a superfast spreading rate end-member.
>
> 3. Correlate and calibrate seismic and magnetic imaging of the crustal structure with basic geological observations.
>
> 4. Investigate the interactions between magmatic and alteration processes, including the relationships between extrusive volcanic rocks, sheeted dikes, and underlying gabbroic rocks.

While these objectives have been met, the most comprehensive results to date are petrographic.

Each subdivision of the recovered section is described in general terms by Teagle et al. (2006). Figure 1.6 shows the generalized basement stratigraphy including the percentage of phenocrysts vs. depth. The subdivisions of the upper oceanic crust in Hole 1256D include sheet and massive flows, a basalt/dike transition zone, the underlying sheeted dikes, and the uppermost plutonic section. The sheet and massive flows are described as predominantly aphyric (<1% phenocrysts),with grain size ranging from glassy along chilled margins to cryptocrystalline or microcrystalline (Teagle, 2006). The groundmass of the sheet flows generally consists of plagioclase and clinopyroxene microlites, with interstitial titanomagnetite and altered glass. Where phenocrysts are present they include plagioclase, clinopyroxene, and olivine (in order of decreasing abundance). The transition zone consists of volcanic breccias interbedded with sheet flows. In the upper section, fine- to medium-grained basalt is in contact with cryptocrystalline basalt (Teagle et al., 2006). This subdivision typically includes flow structures, and with increasing down-hole distance from the upper section, the igneous textures are better preserved and more homogenous. The sheeted dike complex was subdivided into at least 15 lithological units based mostly on changes in texture or grain size. All basalts in the sheeted dike complex have been hydrothermally altered, changing down-core from subgreenshist/greenshist minerals to amphibole-bearing assemblages (Teagle et al., 2006). The deepest plutonic section consists of gabbros. Two different gabbroic intrusions were recognized, which produced contact metamorphism in the surrounding sheeted dikes. The gabbros are medium-grained and mineralogically homogenous.

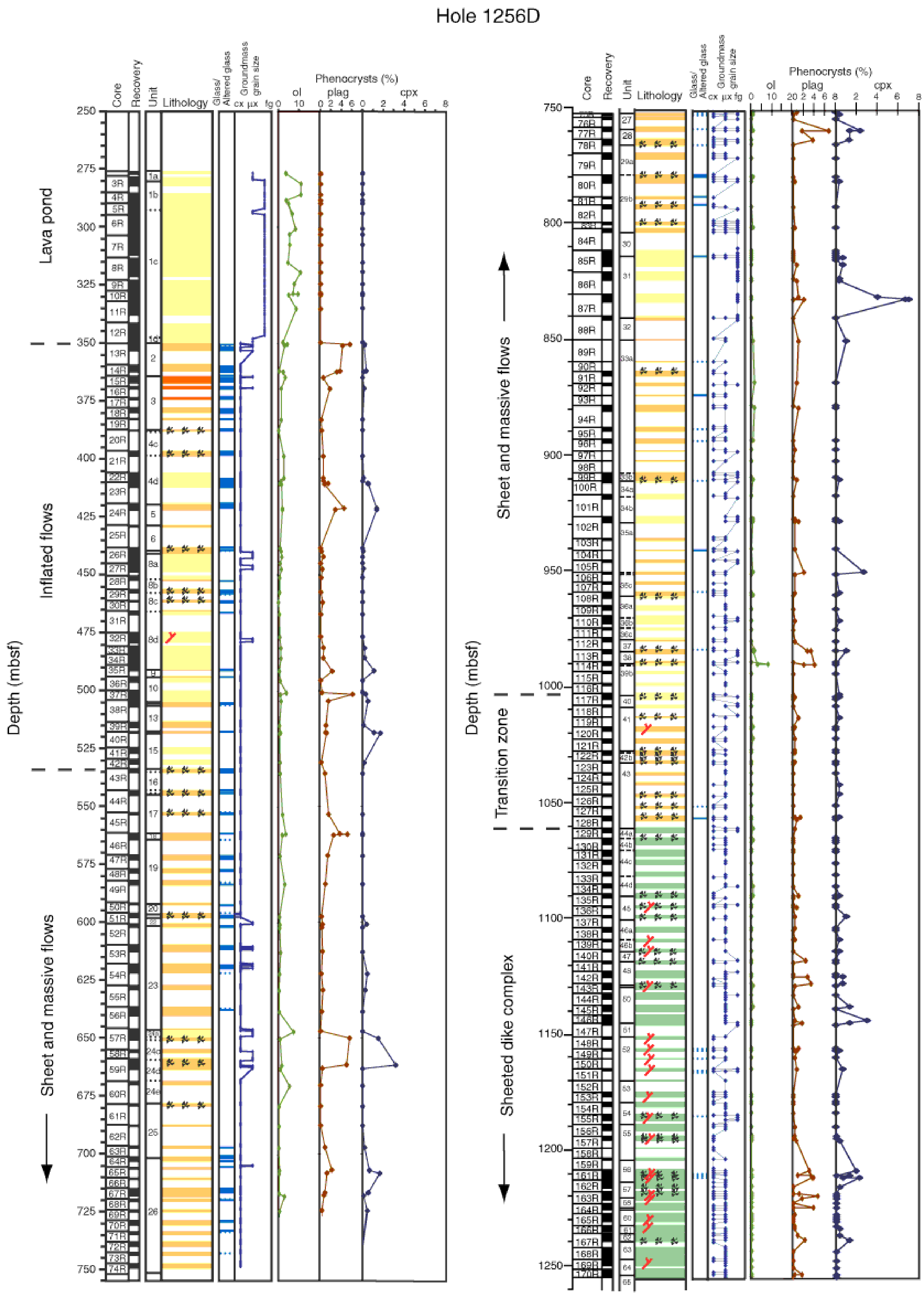

Hole 1256D
Core
Recovery
Unit
Lithology
Glass/ Altered glass
Groundmass grain size
cx µx fg
Phenocrysts (%)
ol
plag
cpx
Depth (mbsf)
Lava pond
Inflated flows
Sheet and massive flows
Transition zone
Sheeted dike complex

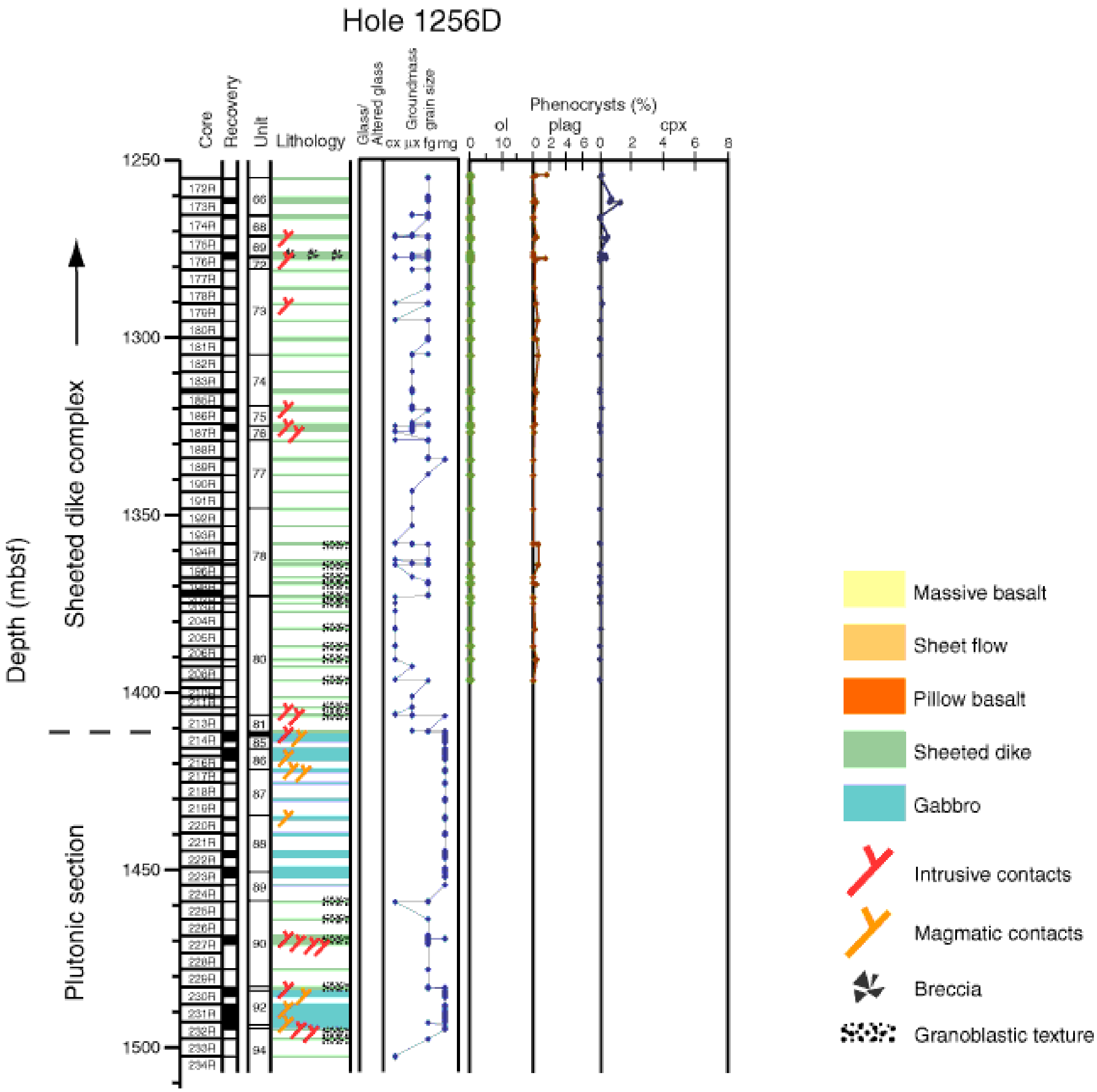


Figure 1.6: Basement stratigraphy in Hole 1256D showing (from left) depth scale, core numbers, recovered intervals, unit and subunit boundaries, igneous lithology, locations of glass and altered glass (solid/stippled line), groundmass grain size, and phenocryst percentage based on thin section descriptions. cx = cryptocrystalline, µx =microcrystalline, fg = fine grained, ol = olivine, plag = plagioclase, cpx = clinopyroxene (Teagle et al., 2006)

### 1.6 Approach and Organization

The approach taken in this study was to document the mineralogical and textural variations down-core at IODP Hole 1256D and then explain why these variations are occurring. The following paper has been organized into the following chapters to document the findings as concisely as possible:

Chapter 2: IODP Hole 1256D Down-core Petrography- This chapter focuses on the mineralogical and textural observations of fifty-three thin sections collected from Hole 1256D. Detailed descriptions of primary and secondary minerals found down-core will be given, along with electron microprobe data collected for six representative thin sections.

Chapter 3: Kane Fracture Zone Core Summary- This chapter will focus on ten thin sections from five cores collected along the Kane Fracture Zone. Detailed descriptions of primary and secondary minerals in the core will be given, along with the electron microprobe data collected from three representative thin sections. Furthermore a brief mineralogical and textural comparison of Hole 1256D and the Kane Fracture Zone core will be available.

Chapter 4: Discussion- This chapter will discuss possible explanations for trends observed down-core at IODP Hole 1256D. The primary focus will be on temperature changes down-core, and why this change is occurring. Observed trends and previous work will try to answer this question.

Chapter 5: Conclusions- This chapter will summarize the major findings of this paper and possible future work.

# CHAPTER 2: IODP HOLE 1256D DOWN-CORE PETROGRAPHY

## 2.1 Analytical Methods

The techniques used for this thesis included point counting a total of 61 thin sections, along with petrographic and textural observations of each thin section. A systematic process was needed to keep the necessary data organized. Each thin section had a total of 500 points counted with a small stage step interval, corresponding to grain size. Along with point counting, mineralogical, textural, and other important features were noted. Each thin section was described in detail and notes were made of any unusual features in the thin sections.

In some cases, however, optical analysis was not enough to confidently identify important minerals. Therefore representative thin sections were chosen for electron microprobe analysis. From Hole 1256D, six thin sections were selected and for the Kane Fracture Zone three thin sections were used. Due to the poor quality of the thin sections collected from Hole 1256D (they were uncovered but not polished) electron microprobe data were of variable quality. Representative thin sections from Hole 1256D and the Kane Fracture zone were therefore compared to determine the presence of some minerals. Fifty-three thin sections from IODP site 1256 were studied and point-counted to get an accurate analysis of the down-core mineralogical variation (Table 2.1). Thin sections were provided by Lisa Gilbert[1] and were cut at predetermined depths. The study included an overview of each section, briefly describing texture, general grain size, minerals present, and any other important characteristics. The point-counts were done on the basis of 500 points per section with a stage interval of 1; this gave the best overall count for each section, based on grain size and the circular shape of the sections. The point counts

[1] The Maritime Studies Program of Williams College and Mystic Seaport, Connecticut

included major minerals as well as vesicles, glass, and any unknown mineral, or fine-grained groundmass.

Electron microprobe work was done on six representative thin sections, selected to reflect variations in textures and mineralogy throughout the core. Back-scattered electron (BSE) imaging was done of selected areas in each of the six sections to show and record the location of the selected points. Energy dispersive (EDS) X-ray maps of the areas were collected to show details of chemical compositions. Specific minerals and areas of groundmass were analyzed to determine compositions of major minerals and to identify unknowns. Point counts can be found in table 2.1, general descriptions of each thin section can be found in Appendix A, and the data from the EMP analysis can be found in Appendix B.

The term “groundmass” was used to describe the areas of the thin sections that were too fine-grained to allow optical mineral idenification, which made point counting the individual minerals impossible. EMP data helped to determine the general composition of the groundmass in the analysed thin sections. “Porphyritic” was used to describe a thin section dominated by groundmass with some phenocrysts. The term “poikiolitic” related to a section that had many large grains (e.g., plagioclase) that contained fine-grained inclusions (e.g., clinopyroxene).

| Thin Section | mbsf | Rock Type | plg | cpx | opx | qtz | chl | hbl | act | epi | oli | ves | glass | ulvospinel | fe-oxides* | smectites | groundmass** | total |
|---|---|---|---|---|---|---|---|---|---|---|---|---|---|---|---|---|---|---|
| 48 | 253 | Basalt, sheet flow | 36.80% | 31.80% | | | | | | | | | | 13.00% | | 1.60% | 16.80% | 100.00% |
| 49 | 258 | Basalt, sheet flow | 32.80% | 5.20% | | | | | | | | | | 11.00% | | 0.60% | 50.40% | 100.00% |
| 50 | 267 | Basalt, sheet flow | 15.00% | 1.20% | 1.80% | | | | | | | | | 14.40% | | 2.00% | 65.60% | 100.00% |
| 36 | 277 | basalt, massive | 47.20% | 15.00% | | 1.40% | | | | | | | | 8.00% | | 4.80% | 23.60% | 100.00% |
| 37 | 279 | basalt, massive | 46.40% | 12.00% | 1.00% | 2.00% | | | | | | | | 7.80% | | 9.60% | 21.20% | 100.00% |
| 35 | 285 | basalt, massive | 41.20% | 22.20% | 0.40% | 6.40% | | | | | | | | 11.00% | | 12.60% | 6.20% | 100.00% |
| 38 | 290 | basalt, massive | 42.80% | 28.20% | 0.80% | 2.20% | 0.20% | | 0.40% | | | 1.20% | | 7.40% | | 2.00% | 14.80% | 100.00% |
| 39 | 295 | basalt, massive | 45.80% | 26.20% | | 4.60% | | | | | | 1.00% | | 6.20% | | 0.80% | 15.40% | 100.00% |
| 40 | 304 | basalt, massive | 49.40% | 31.60% | | 1.60% | 0.40% | | | | | 0.40% | | 4.00% | | 0.80% | 11.80% | 100.00% |
| 41 | 314 | basalt, massive | 51.60% | 27.20% | | 1.80% | 1.00% | | | | | 0.80% | | 5.80% | | 0.80% | 11.00% | 100.00% |
| 42 | 323 | basalt, massive | 46.00% | 26.80% | | 1.80% | 0.60% | | | | | 1.80% | | 6.80% | | 1.40% | 14.80% | 100.00% |
| 43 | 327 | basalt, massive | 50.00% | 30.60% | | 2.80% | | | | | | 2.00% | | 3.80% | | 1.20% | 9.60% | 100.00% |
| 44 | 332 | basalt, massive | 51.20% | 30.40% | | 2.80% | | | | | | 1.00% | | 5.40% | | 3.60% | 5.60% | 100.00% |
| 45 | 342 | basalt, massive | 44.80% | 30.00% | | 4.40% | | | | | | 1.00% | | 5.60% | | 4.60% | 9.60% | 100.00% |
| 46 | 350 | basalt, massive | 40.40% | 7.80% | | | | | | | | 1.40% | 0.20% | 8.60% | | 18.60% | 23.00% | 100.00% |
| 47 | 361 | basalt, massive | 38.20% | 22.20% | | | | | | | | | 0.60% | 11.00% | | 8.20% | 19.80% | 100.00% |
| 27 | 475 | basalt, massive | 42.40% | 40.80% | | | | | | | | | 0.20% | 8.80% | | 2.80% | 5.00% | 100.00% |
| 28 | 482 | basalt, massive | 38.80% | 38.40% | | | | | | | | | 0.20% | 9.40% | | 5.80% | 7.40% | 100.00% |
| 29 | 514 | Basalt, sheet flow | 43.80% | 44.60% | | | | | | | | | | 7.00% | | 4.60% | | 100.00% |
| 30 | 578 | Basalt, sheet flow | 13.00% | 10.80% | | | | | | | | | 0.20% | 7.20% | | 12.40% | 56.40% | 100.00% |
| 31 | 619 | Basalt, sheet flow | 39.40% | 35.60% | | | | | | | | | | 8.80% | | 4.00% | 12.20% | 100.00% |
| 32 | 660 | Basalt, sheet flow | 38.80% | 42.60% | | | | | | | | | | 6.60% | | 4.20% | 7.80% | 100.00% |
| 33 | 715 | Basalt, sheet flow | 45.80% | 22.40% | | | | | | | | | | 7.40% | | 22.00% | 2.40% | 100.00% |
| 34 | 716 | Basalt, sheet flow | 38.40% | 26.60% | | | | | | | | | | 10.40% | | 8.80% | 15.80% | 100.00% |
| 1 | 772 | Basalt, sheet flow | 35.80% | 28.40% | | | | | | | | 0.40% | | 9.40% | | 4.80% | 21.20% | 100.00% |
| 2 | 818 | basalt, massive | 44.00% | 37.20% | | | | | | | | | 1.20% | 4.40% | | 13.20% | | 100.00% |
| 3 | 823 | basalt, massive | 39.00% | 39.20% | | | | | | | | | | 6.80% | | 15.00% | | 100.00% |
| 4 | 842 | basalt, massive | 33.80% | 35.40% | | 0.20% | | | | | | | | 10.00% | | 6.60% | 14.00% | 100.00% |
| 5 | 908 | basalt, massive | 40.40% | 44.20% | 0.20% | | | | | | | | | 5.80% | | 9.40% | | 100.00% |
| 6 | 927 | basalt, massive | 35.80% | 38.60% | | | | | | | | | | 8.00% | | 17.60% | | 100.00% |
| 7 | 946 | basalt, massive | 67.40% | 10.00% | | | | | | | | | | 7.00% | | 5.60% | 10.00% | 100.00% |
| 8 | 972 | basalt, massive | 36.40% | 42.40% | | | | | | | | | | 7.60% | | 13.60% | | 100.00% |
| 9 | 995 | basalt, massive | 34.00% | 47.40% | | | | | | | | | | 4.80% | | 13.80% | | 100.00% |
| 10 | 1008 | Basalt, dikes | 42.80% | 34.80% | | 4.20% | | | | | | 1.00% | | 5.60% | | 11.60% | | 100.00% |
| 11 | 1068 | Basalt, dikes | 39.80% | 32.40% | | 7.20% | 14.00% | | | | | | | 6.60% | | | | 100.00% |
| 12 | 1087 | Basalt, dikes | 32.60% | 37.80% | | 8.40% | 11.40% | | | | | | | 5.00% | | | 4.80% | 100.00% |
| 13 | 1106 | Basalt, dikes | 39.20% | 44.40% | | 4.00% | 7.60% | | | | | | | 4.80% | | | | 100.00% |
| 14 | 1125 | Basalt, dikes | 34.00% | 34.40% | | 6.40% | 21.40% | | | | | | | 3.80% | | | | 100.00% |
| 15 | 1181 | Basalt, dikes | 35.60% | 41.80% | | 8.00% | 7.20% | | | | | | | 7.40% | | | | 100.00% |
| 16 | 1204 | Basalt, dikes | 38.80% | 31.60% | 0.60% | 2.40% | 8.20% | | | | | | | 6.20% | | | 12.20% | 100.00% |
| 17 | 1221 | Basalt, dikes | 31.20% | 48.00% | | 4.20% | 3.40% | | | | | | | 7.40% | | | 5.80% | 100.00% |
| 18 | 1235 | Basalt, dikes | 31.40% | 46.20% | | 6.00% | 4.40% | | | | | | | | 11.20% | | 0.80% | 100.00% |
| 19 | 1255 | Basalt, dikes | 29.20% | 46.00% | | 1.00% | 15.40% | | | | | | | | 8.40% | | | 100.00% |
| 22 | 1278 | Basalt, dikes | 33.60% | 42.80% | | 4.40% | 2.80% | | | | | | | | 16.40% | | | 100.00% |
| 20 | 1325 | Basalt, dikes | 30.40% | 32.00% | | 9.00% | 19.80% | | | | | | | | 8.80% | | | 100.00% |
| 23 | 1373 | Basalt, dikes | 46.00% | 21.20% | 7.20% | 3.00% | 3.60% | 6.80% | 0.20% | | | | | | 12.00% | | | 100.00% |
| (48) | 1374.9 | Basalt, dikes | 34.80% | 41.60% | | | | 0.60% | 19.80% | | | | | | 3.20% | | | 100.00% |
| (49) | 1382.2 | Basalt, dikes | 26.60% | 34.80% | | | | 2.00% | 20.40% | | | | | | 16.20% | | | 100.00% |
| (51) | 1387.1 | Basalt, dikes | 35.20% | 31.00% | | 1.40% | | 1.80% | 12.80% | | | | | | 17.80% | | | 100.00% |
| 24 | 1413 | Gabbro | 44.80% | 29.20% | | 1.20% | 3.80% | 10.60% | 2.40% | | | | | | 8.00% | | | 100.00% |
| 25 | 1448 | Gabbro | 45.80% | 10.00% | | | 1.00% | 39.20% | 0.40% | 0.40% | 1.40% | | | | 1.80% | | | 100.00% |
| 21 | 1470 | Basalt, dikes | 52.40% | 19.60% | | | 4.40% | 13.80% | 6.80% | | | | | | 3.00% | | | 100.00% |
| 26 | 1488 | Gabbro | 51.40% | 30.20% | | | 2.80% | 10.20% | 1.80% | | | | | | 3.60% | | | 100.00% |

Table 2.1: IODP Hole 1256D modal percentage of mineral content down-core for fifty-three thin sections. Percentages out of 500 point counts per slide. *Fe-oxides include ilmenite and titanomagnetite. **Groundmass is thought to be a composed of fine grain plagioclase an clinopyroxene. mbsf= meters below seafloor, plg=plagioclase, cpx=clinopyroxene, opx=orthopyroxene, qtz=quartz, chl=chlorite, hbl=hornblende, act=actinolite, epi=epidote, oli=olivine, ves=vesicles.

## 2.2 Thin Section Summary- IODP Hole 1256D

### 2.2.1 Petrography of IODP Hole 1256D

Plagioclase is present in all of the thin sections, with a modal percentage ranging from 15% to 70%, but averaging around 40% (figure 2.1). Clinopyroxene is also present in all of the sections, with a modal percentage ranging from 2% to 50%, averaging closer to 30% (figure 2.2). Plagioclase typically appears fresh and unaltered, however myrmekitic intergrowths of plagioclase and quartz are common. Orthopyroxene is present in some samples, with a maximum modal percentage of 7%.

The modal percentage of quartz varies down-core from <1% to 9% (figure 2.3), but is common only in two depth ranges: 280-345 mbsf and 1000-1415 mbsf. Where the amount of quartz is high it forms pockets of quartz grains that could be a result of alteration. At depths below1375mbsf quartz is restricted to veins. Whether quartz is primary or secondary is unknown. Textures of the quartz (forming in pockets and restriction to veins) could be a sign of secondary formation, but further analysis of the quartz must be completed to confirm whether quartz is primary or secondary.

Amphiboles, including hornblende and actinolite, are present in the lowermost basalts and in gabbros between 1370-1500mbsf (figure 2.4). Low to intermediate grade metamorphism is occurring in the lower basalts due to heating by underlying intrusive rocks. In many places secondary actinolite replaces clinopyroxene, forming both as a "rim" around the clinopyroxene and replacing the mineral as a whole. Both hornblende and actinolite are locally present in the same area, complicating their identification (actinolite vs. actinolitic-hornblende). EMP analysis shows that no actinolitic-hornblende is present, and thus actinolite was deemed to be the dominant amphibole present.

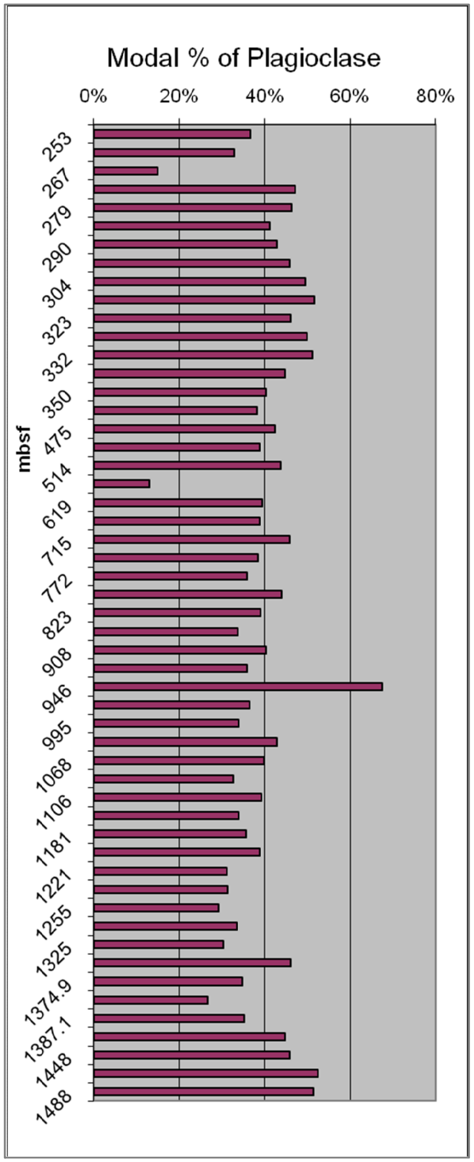


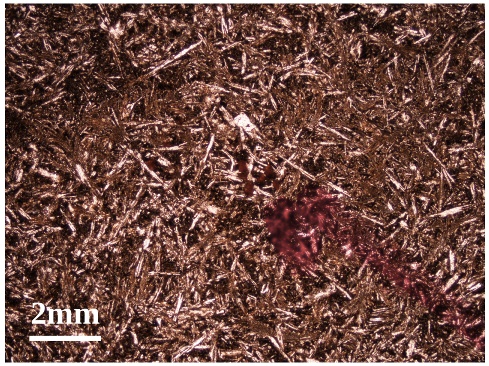


GIL 49: 258 mbsf., basalt sheet flow. Fine- grain euhedral plagioclase laths are predominant.

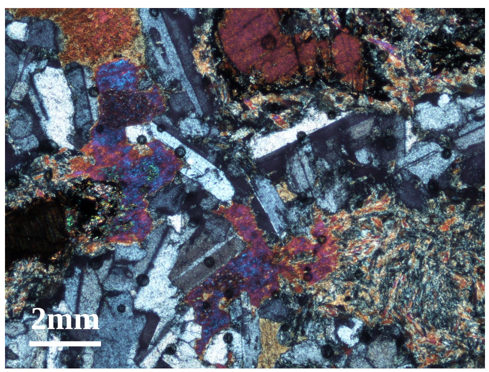


GIL 25: 1448 mbsf., Gabbro. Coarse-grain subhedral to euhedral plagioclase crystals present. (cross polarized)

Figure 2.1: down-hole variations in modal percentage of plagioclase determined from point counts. Horizontal axis in %; vertical axis in meters below sea floor (mbsf). Details in table 2.1.

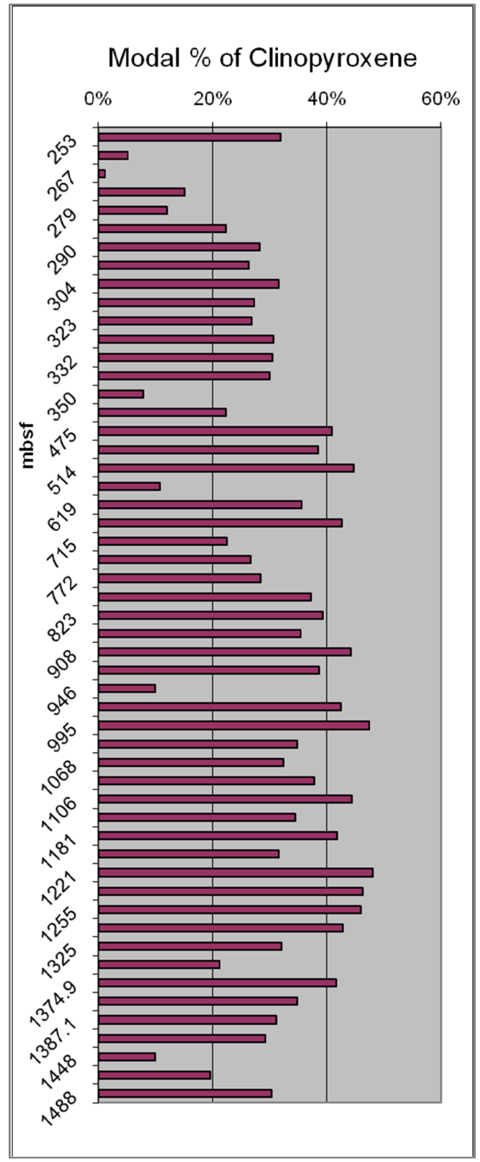


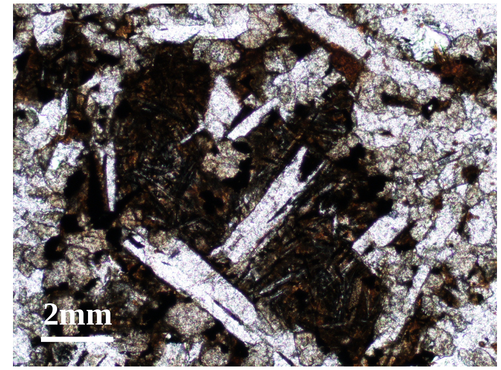


GIL 48: 253 mbsf., basalt sheet flow. Fine- grain anhedral clinopyroxene often as inclusions in plagioclase.

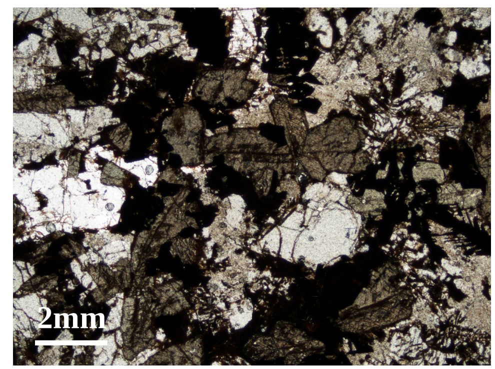


GIL 35: 285 mbsf., basalt, massive. Coarse-grain subhedral clinopyroxene (dirty looking minerals).

Figure 2.2: down-hole variations in modal percentage of clinopyroxene determined from point counts. Horizontal axis in %; vertical axis in meters below sea floor (mbsf). Details in table 2.1.

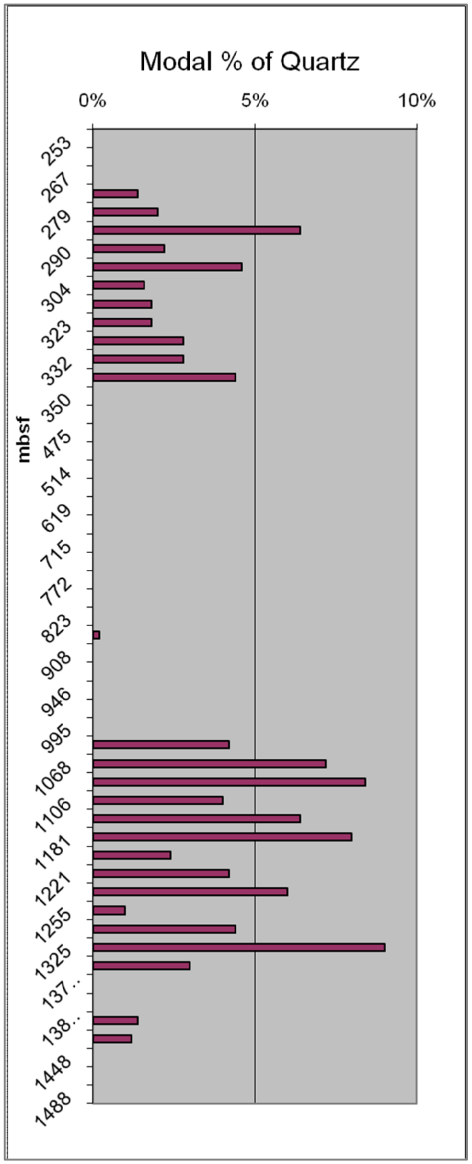


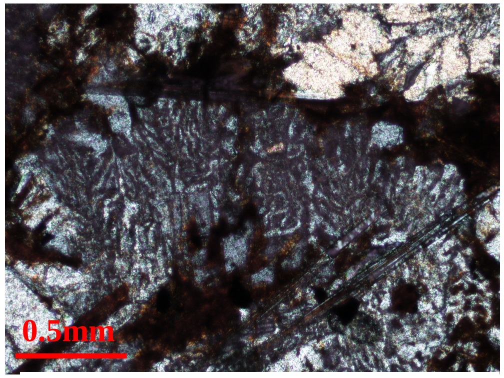


GIL 35: 285 mbsf., basalt, massive. Myrmekitic texture found in a few areas in the thin section.

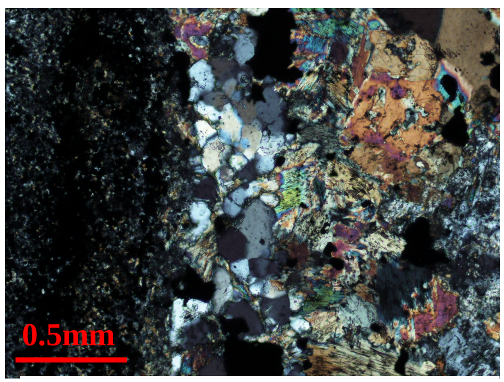


(51): 1387 mbsf., sheeted dike. Quartz is only found in veins present in the thin section and forms in fine- grain clumps.

Figure 2.3: down-hole variations in modal percentage of quartz determined from point counts. Horizontal axis in %; vertical axis in meters below sea floor (mbsf). Details in table 2.1.

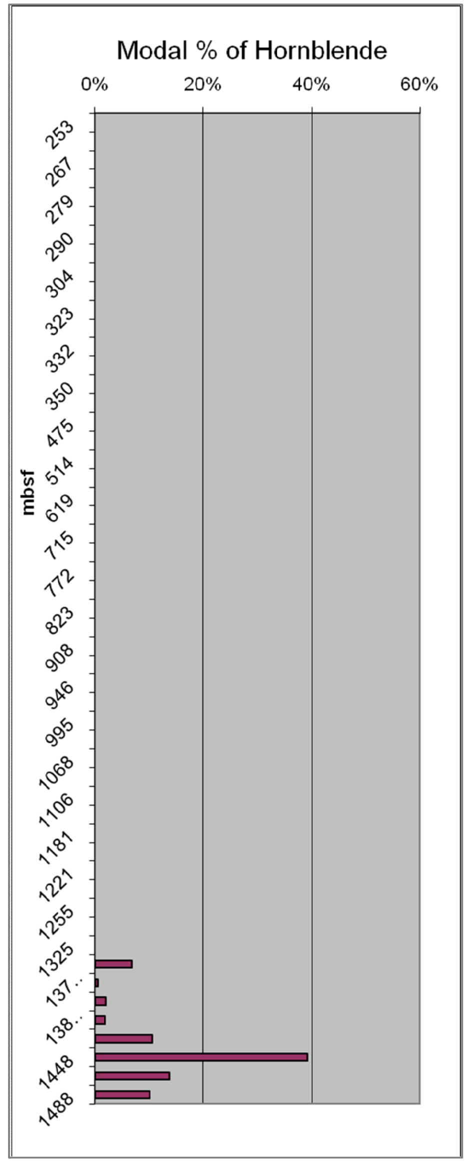


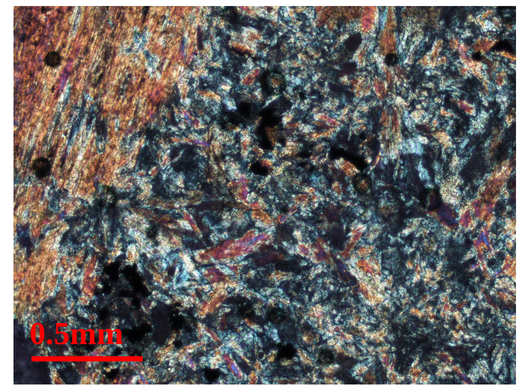


GIL 25: 1448 mbsf., gabbros. Intergrowths of hornblende and actinolite, primary hornblende in upper left corner.

Figure 2.4: down-hole variations in modal percentage of hornblende determined from point counts. Horizontal axis in %; vertical axis in meters below sea floor (mbsf). Details in table 2.1

Figure 2.5: down-hole variations in modal percentage of actinolite determined from point counts. Horizontal axis in %; vertical axis in meters below sea floor (mbsf). Details in table 2.1.

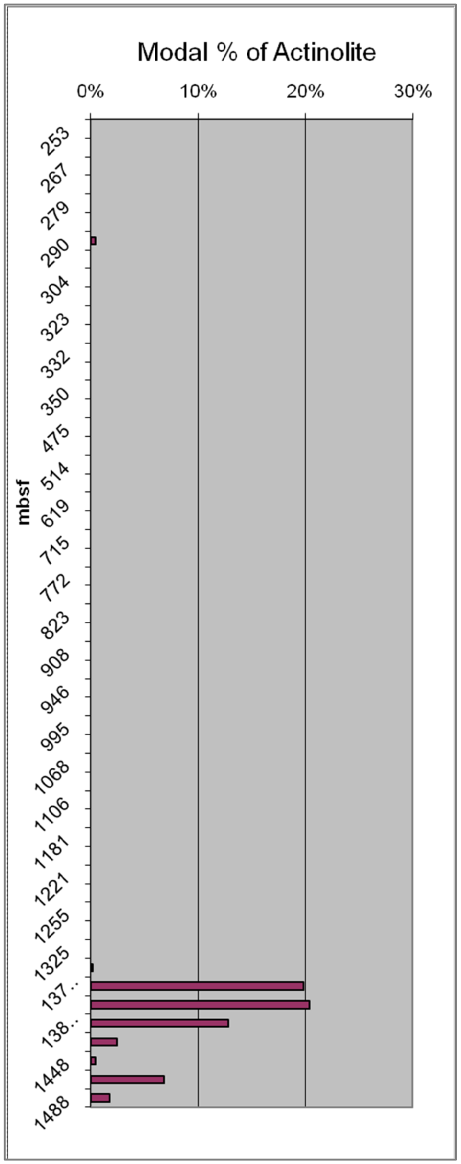


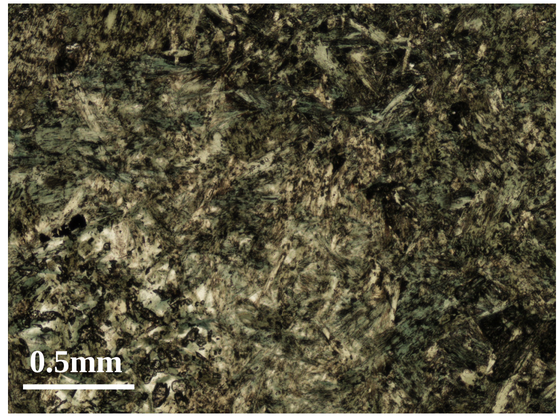


(48): 1375 mbsf., sheeted dike. Fine-grain intergowths of actinolite, chlorite, and possible hornblende. Actinolite creates the fibrous texture.

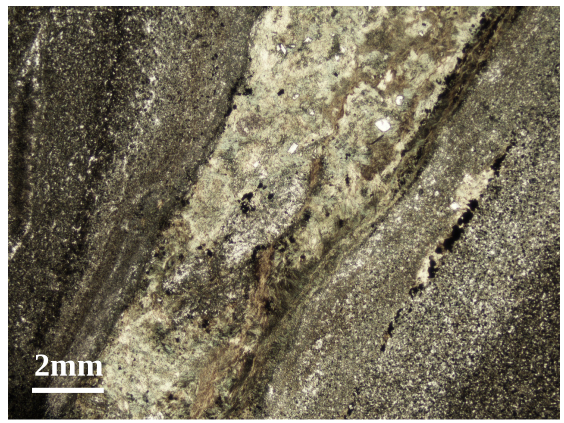


(49): 1382 mbsf., sheeted dike. Very fine-grain assemblage of actinolite and hornblende. Actinolite is concentrated in the veins

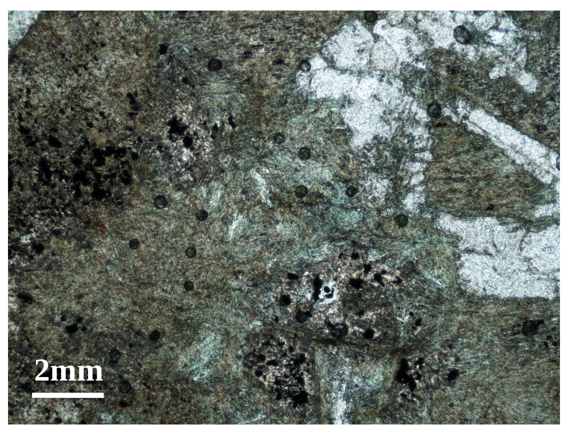


GIL 25: 1448 mbsf., gabbro. Fine-grain mass intergrowths of actinolite, hornblende, and minimal chlorite.

At about 1230mbsf the opaques change from ulvospinel to Fe-oxides (including both titano-magnetite and ilmenite) (figure 2.6 and 2.7). The individual percentages of titano-magnetite and ilmenite are not known as they could not be optically distinguished for point-counting, therefore they were counted together. The Fe-oxides typically appear to be secondary minerals and can also occur as inclusions in plagioclase and clinopyroxene. EMP studies showed that some sulphides are present, but sulphides were not included in the point-counts as they could not be distinguished from other opaque minerals. The (possible) sulphide was present in a sample that also contains abundant chlorite.

Alteration minerals consist primarily of fine-grained smectite (clay), chlorite, and actinolite. These minerals are difficult to identify using optical methods and XRD analysis was not possible due to the nature of the samples. EMP data was used for identification by looking for minerals with totals around 86% (due to water content), low Al values, and approximately equal Fe and Mg values. Smectites are present until ~1010 mbsf, where chlorite becomes the dominant alteration mineral (figure 2.8). Smectites replace glass and olivine. The former presence of olivine was determined by the characteristic fractures and shape of the original olivine, and vesicle infilling was evident by its circular form. Smectite is probably mainly present in the groundmass where it forms a dark matrix surrounding sparse plagioclase and clinopyroxene. Chlorite, which was more easily identified, is present from 1010 mbsf to the bottom of the core. Chlorite first appears at 290-323 mbsf with a modal percentage <1%, where it correlates with a decrease in smectites (figure 2.9). Therefore the two alteration minerals coexist in trace amounts. The significance of these secondary minerals is discussed in Chapter 4.

Actinolite is present as an alteration mineral in the gabbros where it replaces clinopyroxene.

Groundmass varies between 5% and 65%, and is not consistently present down-core. Where the percentage of groundmass increases, the percentages of plagioclase and clinopyroxene decrease (figure 2.10). This probably indicates the percentage of original glass. The EMP data showed that the groundmass is a very fine-grained equivalent of the rest of the rock, and contains abundant plagioclase, clinopyroxene and smectite in some areas. Since the groundmass is very fine-grained, the percentage of each mineral in the groundmass could not be determined optically. However future analysis of the EDS images may reveal approximate percentages of the plagioclase and clinopyroxene.

In addition to the aforementioned minerals, epidote and olivine are present, in trace amounts, in one section at 1448mbsf. Epidote is a secondary mineral replacing an unknown mineral, and olivine is a primary mineral.

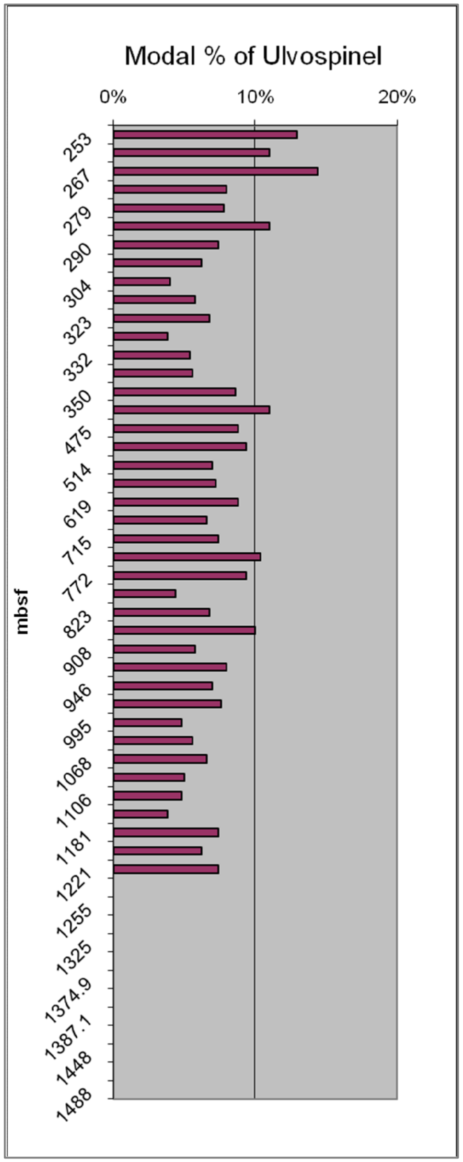


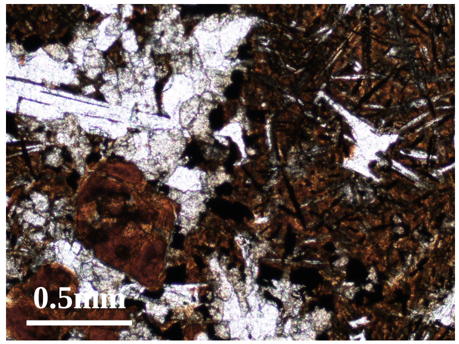


GIL 49: 258 mbsf., basalt, sheet flow. Fine-grain ulvospinel. Laths of ulvospinekl are located in the groundmass, and blocky opaques are formed near plagioclase and clinopyroxene.

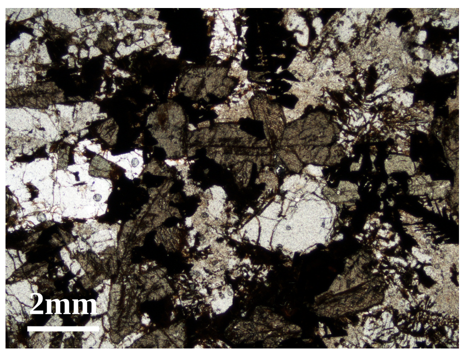


GIL 35: 285 mbsf., basalt, massive. Coarse-grain ulvospinel found throughout the thin section.

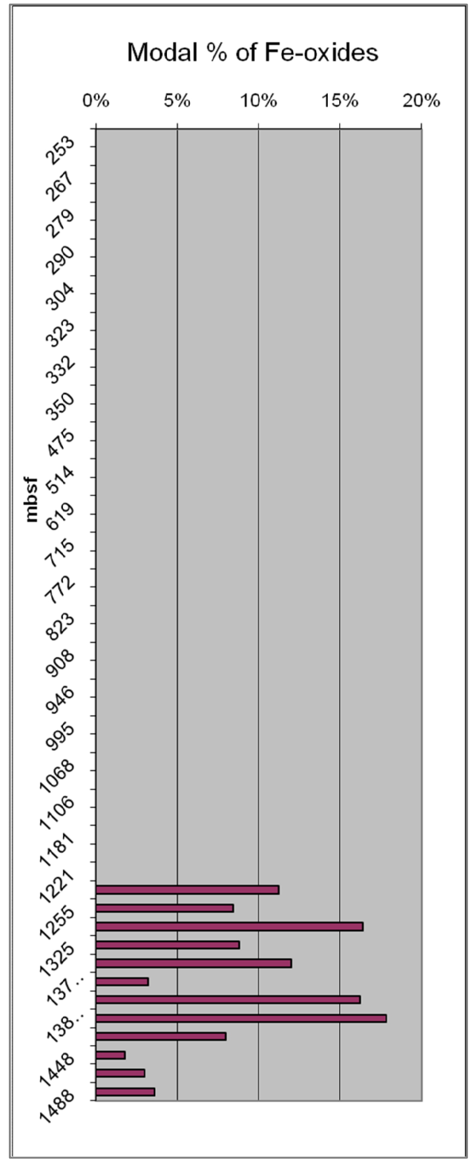


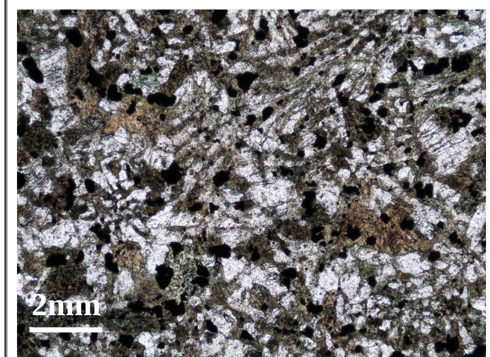


GIL 23: 1373 mbsf., sheeted dike. Fine-grain blocky opaque minerals. Predominantley titano-magetite.

Figure 2.6: down-hole variations in modal percentage of ulvospinel determined from point counts. Horizontal axis in %; vertical axis in meters below sea floor (mbsf). Details in table 2.1.

Figure 2.7: down-hole variations in modal percentage of Fe-oxides determined from point counts. Horizontal axis in %; vertical axis in meters below sea floor (mbsf). Details in table 2.1

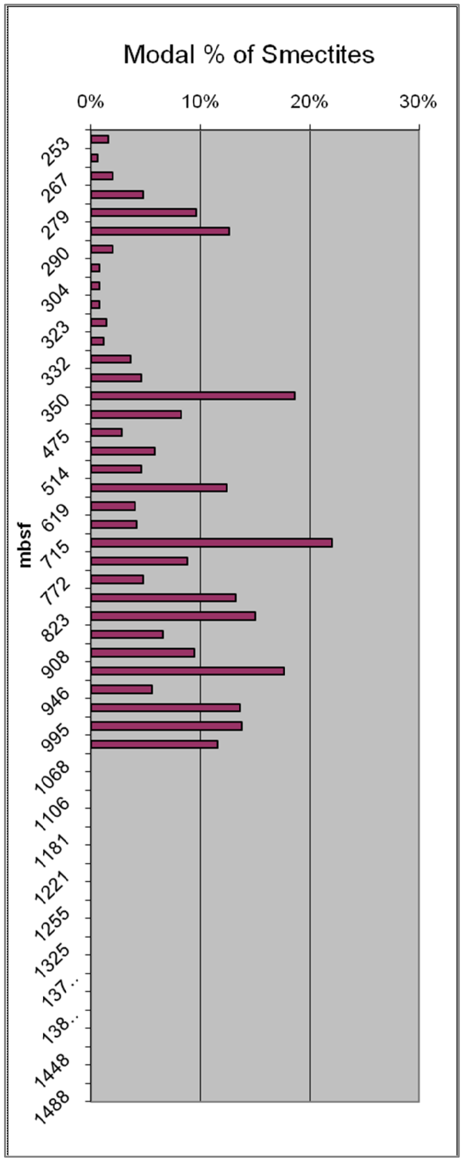


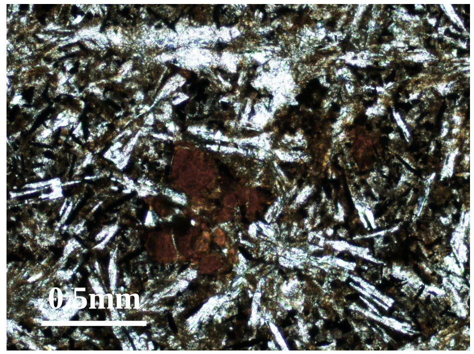


GIL 49: 258 mbsf., basalt, sheet flow. Smectite (center) replacing what appears to have been olivine.

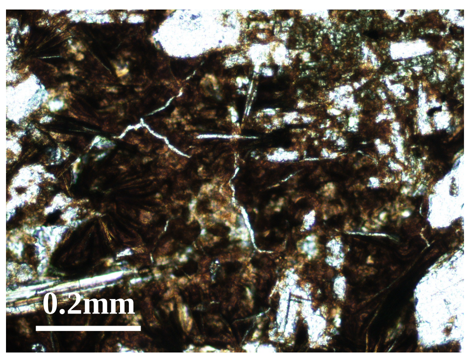


GIL 35: 285 mbsf., basalt, massive. Smectitre (dark brown) radiating throung the groundmass, inclusions of possible plagioclase and clinopyroxene are present.

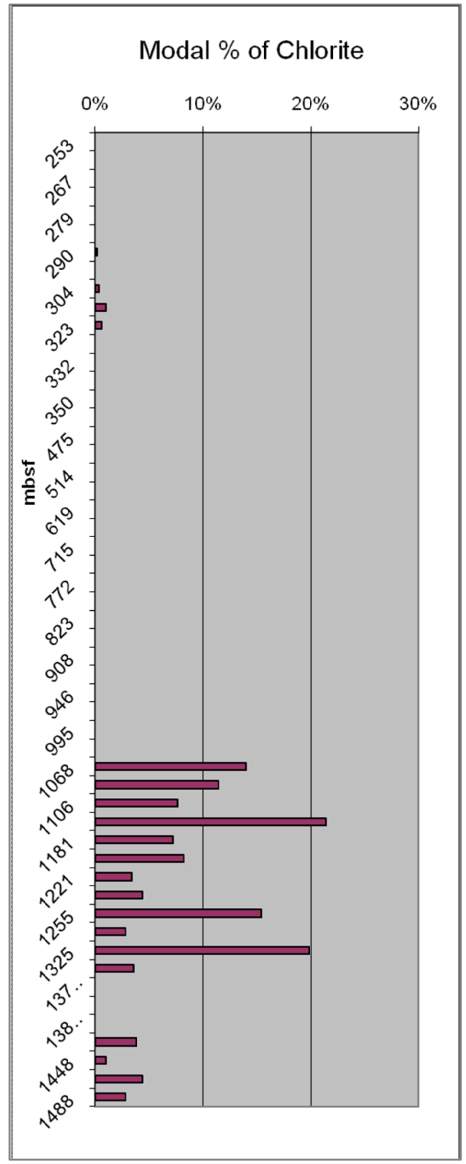


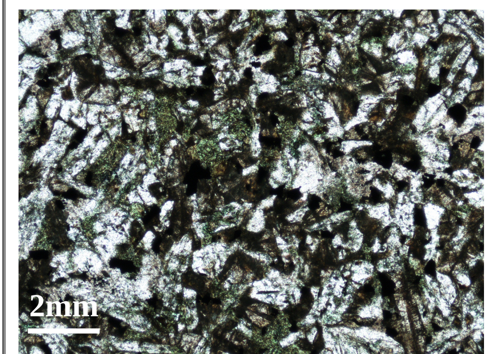


GIL 16: 1204 mbsf., sheeted dikes. Chlorite (green) replacing clinopyroxene in this thin section.

Figure 2.8: down-hole variations in modal percentage of smectite determined from point counts. Horizontal axis in %; vertical axis in meters below sea floor (mbsf). Details in table 2.1.

Figure 2.9: down-hole variations in modal percentage of chlorite determined from point counts. Horizontal axis in %; vertical axis in meters below sea floor (mbsf). Details in table 2.1.

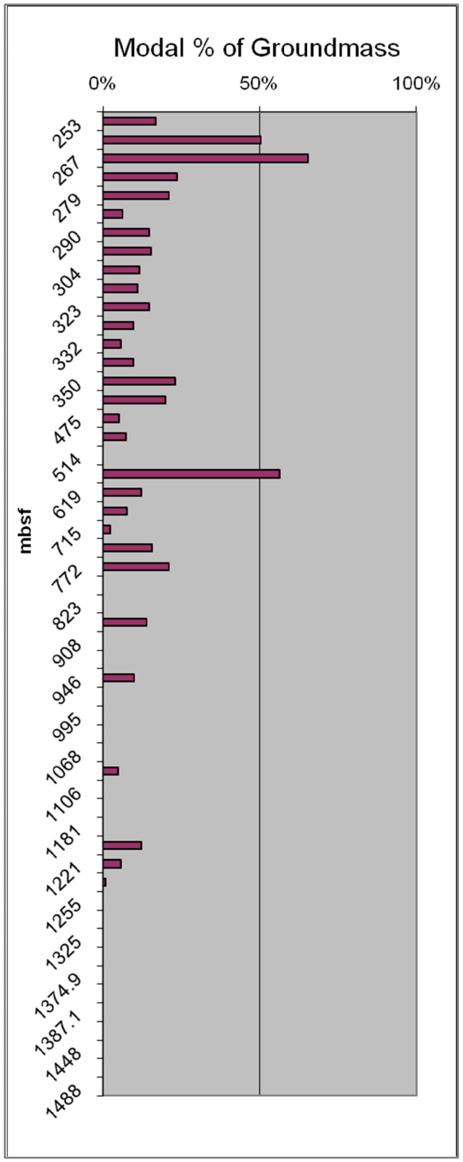


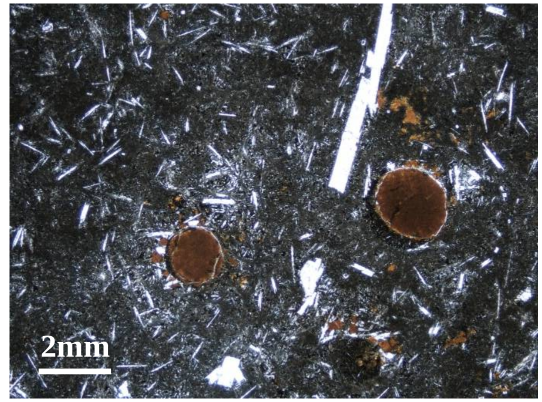


GIL 50: 267 mbsf., basalt, sheet flow. Groundmass makes up the majority of this thin section, making mineral identification difficult.

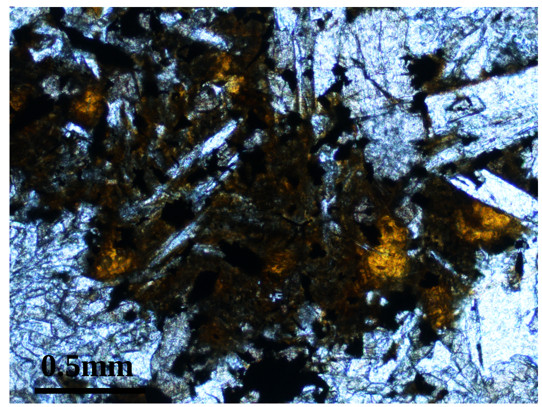


GIL 4: 842 mbsf., basalt, sheet flow. Dark brown groundmass that has inclusions of noticeable opaque minerals, and smectite. Smectite is most likely present in the groundmass.

Figure 2.10: down-hole variations in modal percentage of groundmass determined from point counts. Horizontal axis in %; vertical axis in meters below sea floor (mbsf). Details in table 2.1.

### 2.2.2 Textural Variations of IODP Hole 1256D

The basalt sheet flows at IODP Hole 1256D are fine-grained intergrowths of plagioclase, clinopyroxene and groundmass (appendix A). The grain size if often bimodal; where inter-grown skeletal plagioclase and clinopyroxene are fine-grained (<0.1mm) the phenocrysts of plagioclase are large (up to 3mm).This groundmass is dark brown and contains smectite, opaque minerals and what looks like plagioclase. Plagioclase is euhedral and fresh, while clinopyroxene is often anhedral and dusty in appearance. The ulvospinel varies in shape from thin fibers to blocky grains <0.5mm across. Amygdules with smectite vary from circular masses up to 2-3mm across, to small irregular shaped masses <0.5mm across.

The massive basalts are very consistent down-core. Plagioclase is euhedral, and the rock is relatively equigranular. Clinopyroxene is “dirty” looking, but the skeletal intergrowths are no longer present; clinopyroxene can have a grain size up to ~2mm. Myrmekitic textures are present in the massive basalts, and locally plagioclase is no longer euhedral or fresh. Some thin sections contain smectite along grain boundaries, and in one thin section a possible vein of smectite is present (Apendix A, GIL44). In many of the thin sections, vesicles are present but are not filled with smectite as in the basalt sheet flows. The opaque minerals appear to be secondary minerals as they form shapes not typically found in basalts (figure 2.11).

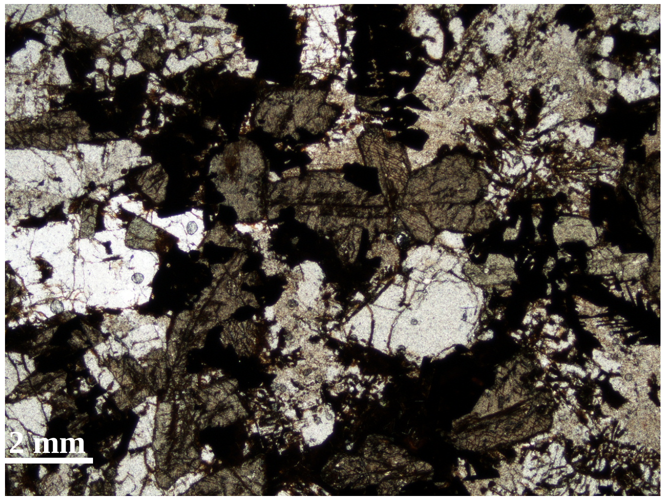


Figure 2.11: Irregular opaque minerals in massive basalts at IODP Hole 1256D. Thin section GIL35.

There are no consistent down-core textural trends in the sheeted dikes. In the upper sheeted dikes, grain size varies widely from <0.1mm to up to 4-5mm. Skeletal intergrowths of plagioclase and clinopyroxene are abundant, however the size of these intergrowths is often larger than in the basalt sheet flows. A change occurs close to the gabbro boundary where the sheeted dikes acquire a granoblastic texture which can signify contact metamorphism (figure 2.12). This texture is only present in a few thin sections. Where veins are present in the sample, masses of inter-grown alteration minerals (actinolite, chlorite, hornblende) form fibrous textures that often take up a large portion of the rock (Appendix A; Sections (48),(49), (51)). In some cases the only mineral that remains relatively unaltered is plagioclase. Opaques are blocky but consistently around 0.5-1mm in size.

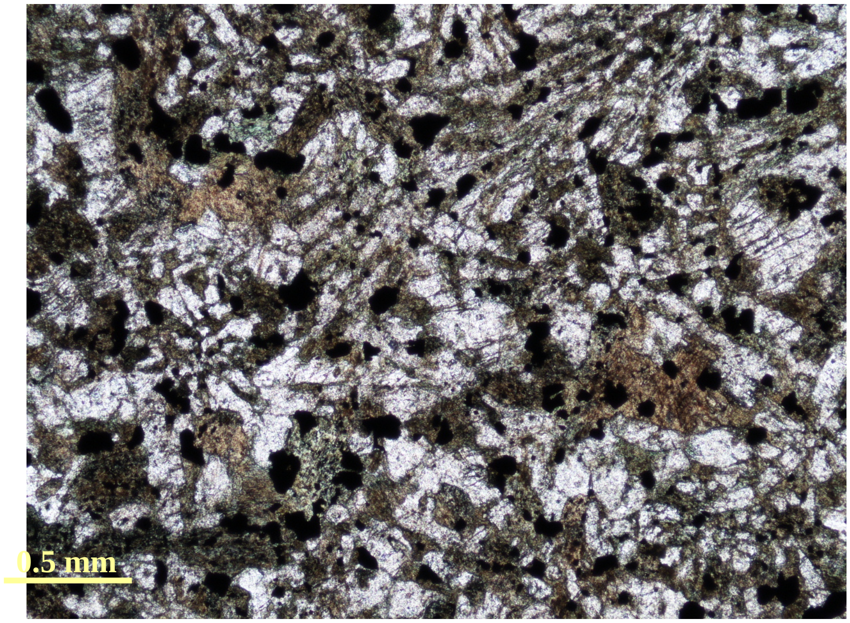


Figure 2.12: Granoblastic texture observed in the lower section of the sheeted dikes (1373 mbsf). Plane polarized light, thin section GIL23.

Gabbros at Hole 1256D are coarse-grained rocks, up to 5mm. Replacement of minerals in the gabbro creates masses of intergrown fine-grained fibrous minerals. The gabbros are consistent in their texture and grain size. Plagioclase is one of the only minerals that remains relatively fresh, minimal clinopyroxene is unaltered. Clinopyroxene appears “dirty”, and oxide stains are present in some areas.

## 2.3 Electron Microprobe Analysis

Electron microprobe analysis was conducted on six representative samples. The thin sections provided for this study were uncovered but not polished to the necessary standard for high quality analysis. The thin sections were too fragile to polish fully, therefore analyses were in some cases only semi-quantitative. All of the useable data collected from the EMP analysis can be found in Appendix B, along with pictures showing the analysed points. The electron microprobe was used to help identify some of the unknown minerals present in the thin sections, and provided compositional data from major minerals such as plagioclase and clinopyroxene.

The alteration products and groundmass were of greatest interest due to the difficulty in optical identification. However, the EMP also identified changes in the opaque minerals, plagioclase, and clinopyroxene mineral composition.

The alteration mineral of particular interest is a brown clay mineral that typically replaces glass and olivine. This clay is commonly intergrown with plagioclase, clinopyroxene, and opaque minerals. Its appearance changes slightly down-core from a rich brown to a dirty-looking brown-yellow mineral. However, the EMP data shows there is no compositional differences in the upper 1010 meters, and that the mineral has a composition resembling smectite (($\frac{1}{2}$Ca, Na)$_{0.7}$(Mg,Fe,Al)$_6$[(Si, Al)$_8$)$_{20}$](OH)$_4$.nH$_2$O). Smectite is a $Fe^-$ and $Mg^-$ rich clay mineral with totals averaging ~86%, excluding $H_20$ (Appendix B). However owing to the nature of the sections this could not be positively confirmed from EMP analysis alone.

Chlorite ((Mg,$Fe^{2+}$,$Fe^{3+}$,Mn,Al)$_{12}$[(Si,Al)$_8$O$_{20}$](OH)$_{16}$) has been identified by EMP analysis. These grains are $Fe^-$ rich, with variable $Mg^-$ content (Appendix B). The total of chlorite varies due to the quality of the sections and the grain being analyzed. Chlorite is fine-grained and commonly intergrown with other minerals. Optical identification was of more assistance for chlorite. Actinolite is very fine-grained and fibrous. Its composition is consistent (Appendix B), but data was only acquired from one thin section (GIL25).

EMP analysis was successful in determining a change in opaque minerals, that was not optically detectable (Appendix B). Ulvospinel ($Fe_2TiO_4$) was found in the upper 1221 meters of the core and then is succeded by Fe-oxides. The general term of Fe-oxides was used to describe the Fe-Ti minerals with variable element concentrations below 1221mbsf. The ratio between FeO and $TiO_2$ changes, ranging from ilmenite to magnetite and titano-magnetite.

The plagioclase composition has two noticeable trends: 1) anorthite content changes from $An_{45-70}$ in the lavas, to An10-50 in the sheeted dikes, then to $An_{77}$ in the gabbros, 2) anorthite content varies between plagioclase in the groundmass and the phenocrysts of plagioclase (from $An_{40}$ to $An_{70}$ respectively). Clinopyroxene is primarily augite/ferro-augite, although the presence of diopside or orthopyroxene cannot be ruled out.

# CHAPTER 3: KANE FRACTURE ZONE CORE SUMMARY

## 3.1 Introduction to Kane Fracture Zone

The Kane Fracture Zone is a left-lateral transform fault that crosses the Mid-Atlantic Ridge at 24˚N. About 150 km of offset is defined by the displacement trends of earthquakes and the offset of the 4000m depth contour (Louden et al., 1982). The fracture zone is a narrow, steep-sided trough that is continuous between 45˚W and 62˚W. The depth of the trough varies between 4.3km to 6km, and is bounded by escarpments that are between 1km and 2.5km above the fracture zone floor, with slopes between 15˚ and 25˚ (Louden et al., 1982). Magnetic anomalies define the age offset across the fault to be approximately 9Ma (Louden et al., 1982).

Five cores were collected from the Kane Fracture Zone in 1985 on cruise Hudson 85-010 (table 3.1, figure 3.1). The cruise, conducted in support of the Ocean Drilling Program, was an exploratory mission to survey the site to select targets suitable for bare rock drilling for the future ODP Leg 106 and was also a sampling test for the Dalhousie/BIO rock drill (Mayer, 1985).

Table 3.1: Locations and descriptions of the five cores collected from Hudson 85-010 along the Kane Fracture Zone. (Modified from Ryall, 1985)

| Core | Latitude (N) | Longitude (W) | Water Depth (m) | Core Length (cm) | Rock type |
|---|---|---|---|---|---|
| 08 | 23˚30.7’ | 45˚03.1’ | 1850 | 14 | Basalt |
| 09 | 23˚30.0’ | 45˚03.0’ | 1950 | 12 | Basalt |
| 11 | 23˚30.53’ | 45˚01.81’ | 2720 | 120 | Gabbro |
| 12 | 23˚30.25’ | 45˚01.60’ | 3120 | 76 | Gabbro |
| 14 | 23˚30.48’ | 45˚01.50’ | 3170 | 12 | Gabbro |

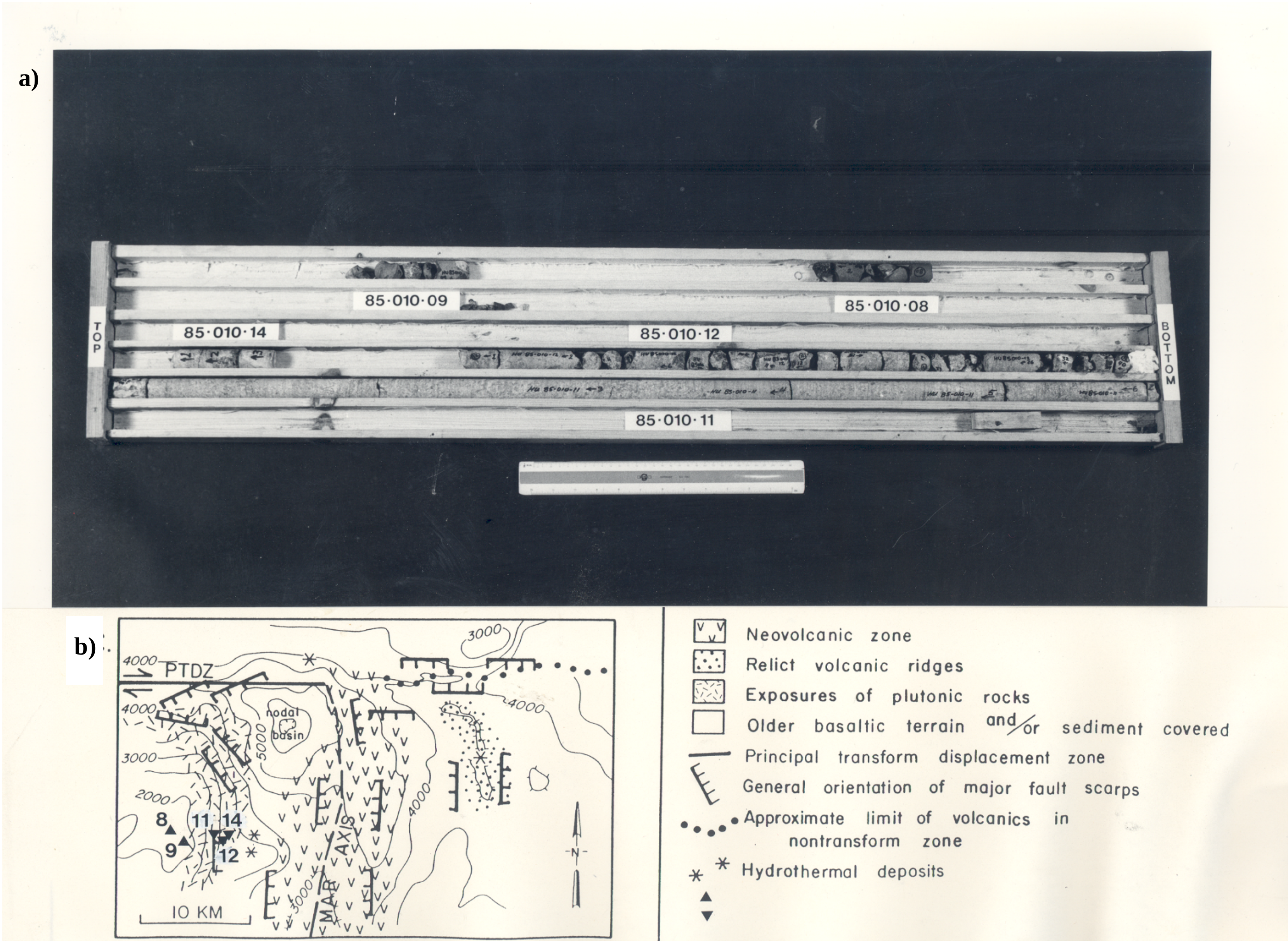


Figure 3.1: a) Photo of core collected in 1985, b) map of general lithologies and core sample locations along the Kane Fracture Zone (PTDZ (principal transform displacement zone) is equivalent to the Kane Fracture Zone), MAR= Mid-Atlantic Ridge. (Modififed from Ryall, 1985)

## 3.2 Lithology of Kane Fracture Zone core

Point counts (table 3.2) and EMP data were collected from thin sections cut from the Kane Fracture Zone core. Data was collected mainly to compare mineralogy and texture of the basalts and gabbros between the Kane Fracture Zone and Hole 1256D, focusing on alteration products formed in both. Appendix C presents descriptions and photos of all ten thin sections from the Kane Fracture Zone. Three thin sections of basalt and seven thin sections of gabbros were collected. Of the ten thin sections, three were analyzed using the EMP- one basalt and two gabbros. Because these thin sections were polished, EMP results were of better quality than those from Hole 1256D, improving confidence in mineral identification and composition (appendix D).

| Thin Section | mbsf | Rock Type | plg | cpx | opx | qtz | chl | hbl | act | epi | oli | ves | glass | total |
|---|---|---|---|---|---|---|---|---|---|---|---|---|---|---|
| 85-010-09-6 | | basalt | 53.60% | | | | | | | | 10.20% | 3.00% | 33.20% | 100.00% |
| 85-010-11-4 (top) | | gabbro | 34.20% | 37.20% | | 0.80% | 12.20% | 0.40% | 15.20% | | | | | 100.00% |
| 85-010-11-4 (bottom) | | gabbro | 43.80% | 36.80% | | 1.20% | 5.40% | 1.20% | 11.60% | | | | | 100.00% |
| 85-010-14-2 | | gabbro | 49.60% | 20.20% | | | 2.60% | 4.20% | 23.40% | | | | | 100.00% |
| 85-010-12-14 | | gabbro | 62.20% | 20.80% | | | 1.40% | 3.20% | 12.40% | | | | | 100.00% |
| 85-010-12-11 | | gabbro | 58.40% | 25.60% | | 4.80% | 0.40% | 5.60% | 5.20% | | | | | 100.00% |
| 85-010-11-2 | | gabbro | 37.40% | 38.80% | | 1.60% | 8.60% | | 13.60% | | | | | 100.00% |
| 85-010-12-7 | | gabbro | 47.20% | 48.40% | | | 2.20% | 1.20% | 1.00% | | | | | 100.00% |

Table 3.2: Modal percentage of minerals in the Kane Fracture Zone thin sections. plg=plagioclase, cpx=clinopyroxene, opx=orthopyroxene, qtz=quartz, chl=chlorite, hbl=hornblende, act=actinolite, epi=epidote, oli=olivine, ves=vesicles.

Unfortunately depth below sea floor cannot be correlated between the two cores because the Kane Fracture Zone core was tectonically exposed. Since this expedition was only an exploratory expedition, only the core length and location are known; information about the original depth below sea floor could not be collected. The Kane Fracture zone core was therefore divided into basalts and gabbros for purposes of comparison. Although primary mineralogy and textures in the gabbros and basalts vary between cores, the alteration minerals are similar and were useful to confirm identification of alteration minerals in IODP Hole 1256D (table 3.3).

| | Basalts | Gabbros |
|---|---|---|
| **IODP Hole 1256D (Appendix A)** | Typically has radiating intergrowths of plagioclase and clinopyroxene. Olivine has been altered to smectite. Plagioclase grain size can reach up to 1mm in length. Glass no longer is present. | Coarse-grained (up to 2mm). Plagioclase is subhedral and fresh looking. Clinopyroxene is altered to secondary actinolite, chlorite and hornblende. Intergrowths of actinolite and hornblende give a fibrous texture |
| **Kane Fracture Zone (Appendix C)** | Glassy, with few microphenocrysts of plagioclase and olivine. Clinopyroxene is not present. Microphenocrysts do not exceed 0.5mm in length. | Coarse-grained (up to 4mm). Plagioclase is subhedral to anhedral and relatively fresh. Clinopyroxene varies in degree of alteration, but is replaced by actinolite and chlorite (sometimes hornblende). Chlorite forms rims around the clinopyroxene and contains inclusions of actinolite. |

Table 3.3: Comparison of general mineralogy and textures found in the basalts and gabbros at IODP Hole 1256D and the Kane Fracture Zone.

### 3.2.1 Comparison of Kane Fracture Zone basalts and IODP Hole 1256D basalts

The basalts of the Kane Fracture Zone core are very different from those from Hole 1256D. The volcanic part of the Kane Fracture Zone core consists of pillow basalts with an aphyric texture. Of the three sections available, the tachylite glass in two cases is too fine-grained to point count, however one thin section was suitable for point counting (the groundmass in this case was not predominantly tachylite glass). EMP work on the Kane Fracture Zone showed that the matrix is composed largely of plagioclase, olivine, and glass. The presence of olivine in the Kane Fracture Zone core is interesting, especially since fresh olivine is minor in Hole 1256D basalts, where it has almost entirely been replaced (Chapter 4). EMP results did not detect smectites in the Kane Fracture Zone core. Hole1256D basalts consist primarily of plagioclase and clinopyroxene, with altered olivine and amygdules containing smectite. Hydrothermal alteration has not affected the basalts of the Kane Fracture Zone to the extent it has at Hole 1256D. The variation between the two cores reflects the lack of pillow basalts sampled at Hole 1256D (figures 3.2, 3.3, and 3.4.) Shipboard scientists from

Hudson 85-010 described clays (saponite, zeolite, and celadonite) in the vesicles and along some fracture boundaries (Mayer, 1985). This was not confirmed by EMP analysis, and XRD analysis was not completed due to time considerations and sample size limitations.

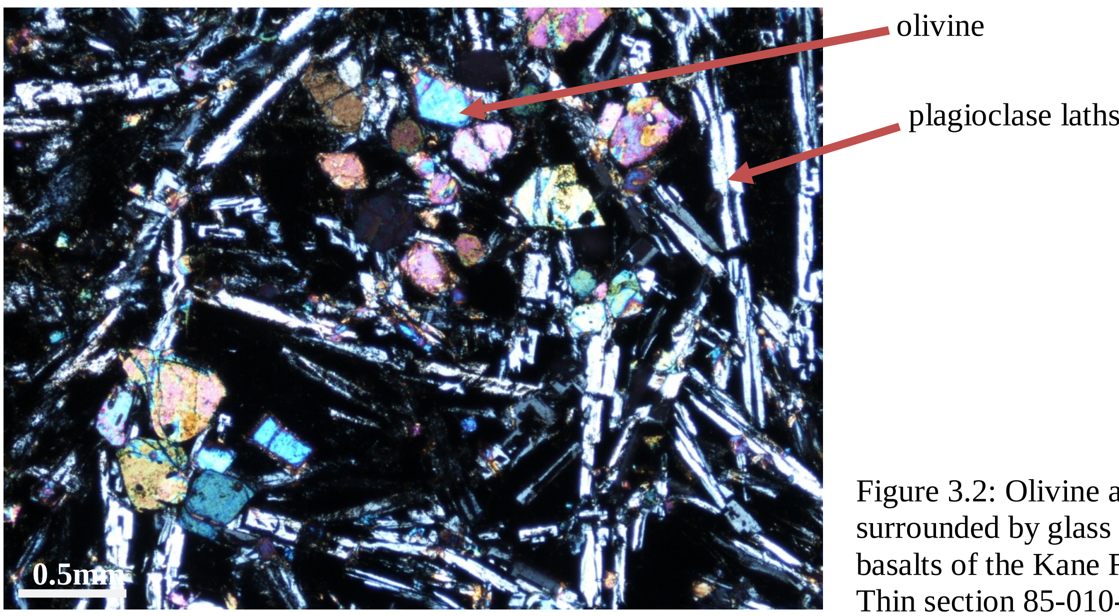


Figure 3.2: Olivine and plagioclase surrounded by glass in the pillow basalts of the Kane Fracture Zone. Thin section 85-010-9-6 (cross polarized light (XPL)).

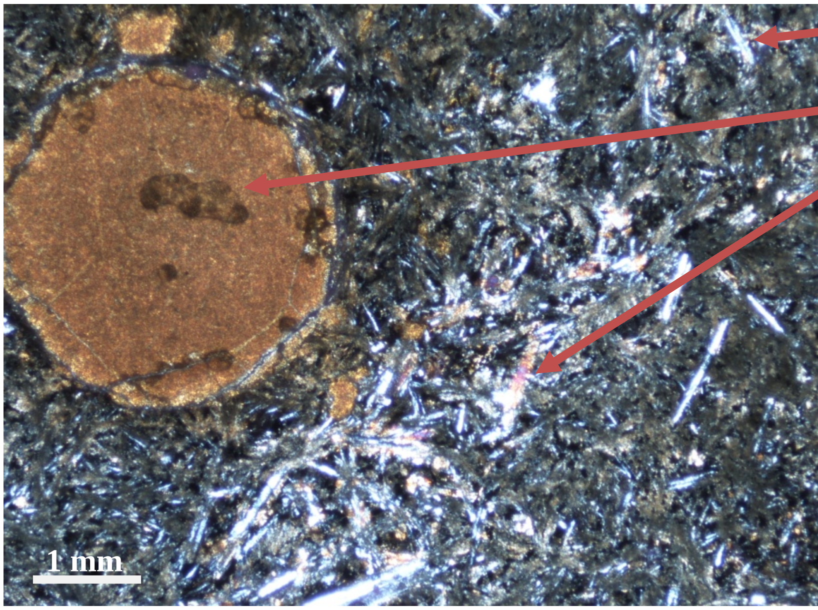


Figure 3.3: Groundmass consisting of plagioclase and clinopyroxene, with a vesicle filled by smectite, Hole 1256D basalts (oceanic layer 1). Glassy material is less dominant, with a dominant ultra-fine grained groundmass with a fibrous texture. Thin section GIL 50 (plane polarized light (PPL)).

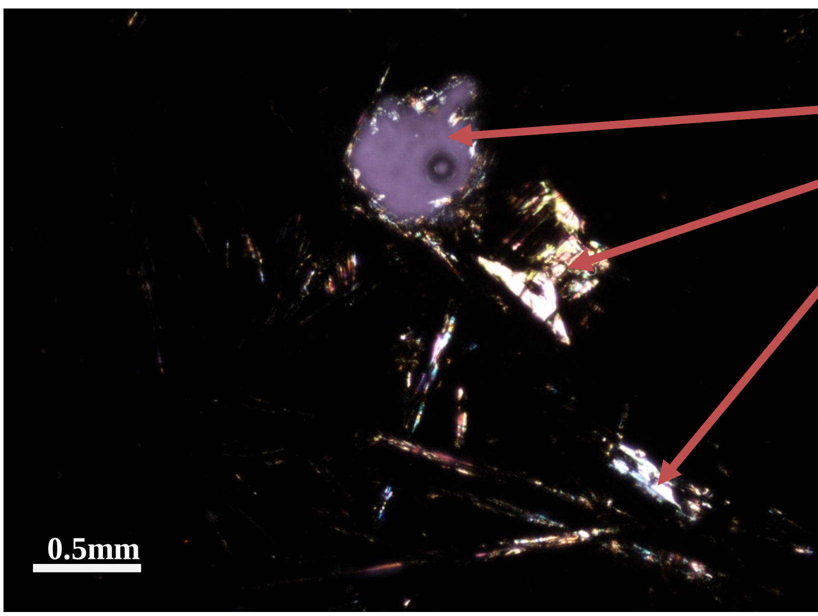


Figure 3.4: Swallow-tail olivine and plagioclase laths in glass. Pillow basalt from Kane Fracture Zone, thin section 85-010-8-2 (XPL).

### 3.2.2 Comparison of Kane Fracture Zone gabbros and IODP Hole 1256D gabbros

Gabbros in the Kane Fracture Zone and Hole 1256D cores are compositionally and texturally similar. Replacement of clinopyroxene by hornblende and actinolite is typical. Fibrous intergrowths of actinolite and chlorite are common in these rocks, however chlorite and actinolite are significantly more abundant in the Kane Fracture Zone cores than the Hole 1256D core. In Kane Fracture Zone core, fibrous intergrowths of chlorite and actinolite surround both clinopyroxene and plagioclase. The abundance of actinolite fibers varies from a few in chlorite to so many that the chlorite itself appears fibrous (fig 3.6 and 3.7). Pyroxene in Hole 1256D gabbros is mainly altered to hornblende, with minor actinolite and chlorite. Point counts of the Kane Fracture Zone samples show modal percentages of actinolite between 1% and 15.2% (avg: 10.34%), chlorite between 0.4 and 12.2% (avg: 4.69%), and hornblende between 0.4% and 5.6% (avg: 2.47%). Hole 1256D samples show modal percentages of actinolite between 0.4% and 6.8% (avg: 2.85%), chlorite between 1% and 4.4% (avg: 3.00%), and hornblende between 10.2% and 39.2% (avg: 18.45%). Temperature variations in hydrothermal fluids play the largest role in the formation of alteration products.

Plagioclase is relatively fresh in all of the gabbro samples from both cores, with minimal alteration. Anorthite content in the gabbros is between $An_{48}$-$An_{60.}$ All plagioclase crystals show typical polysynthetic twinning but vary markedly in grain size, from microns to millimeters. In some cases the boundaries of the plagioclase crystals appear to have been “eaten” by the alteration products of surrounding clinopyroxene. The texture of plagioclase is similar in the two cores.

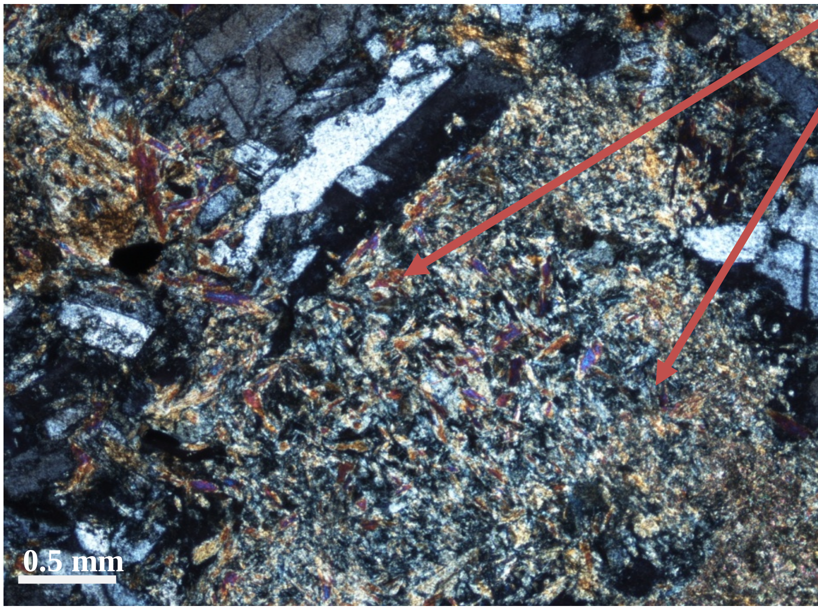


Figure 3.5: Replacement of clinopyroxene by actinolite and hornblende. Relatively fresh plagioclase surrounds intergrowths of actinolite and hornblende. IODP Hole 1256D, thin section GIL25 (XPL).

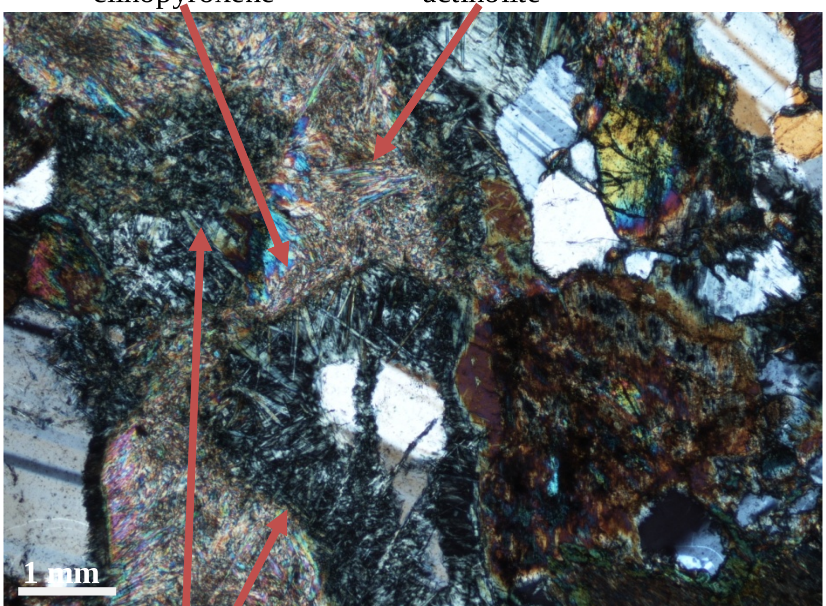


Figure: 3.6: Replacement of clinopyroxene by actinolite and chlorite. Actinolite alters the clinopyroxene core, with chlorite around the rim of altered clinopyroxene. Kane Fracture zone, thin section 85-010-11-2 (XPL).

Chlorite and actinolite intergrowth alteration rims. Present throughout the sample

plagioclase

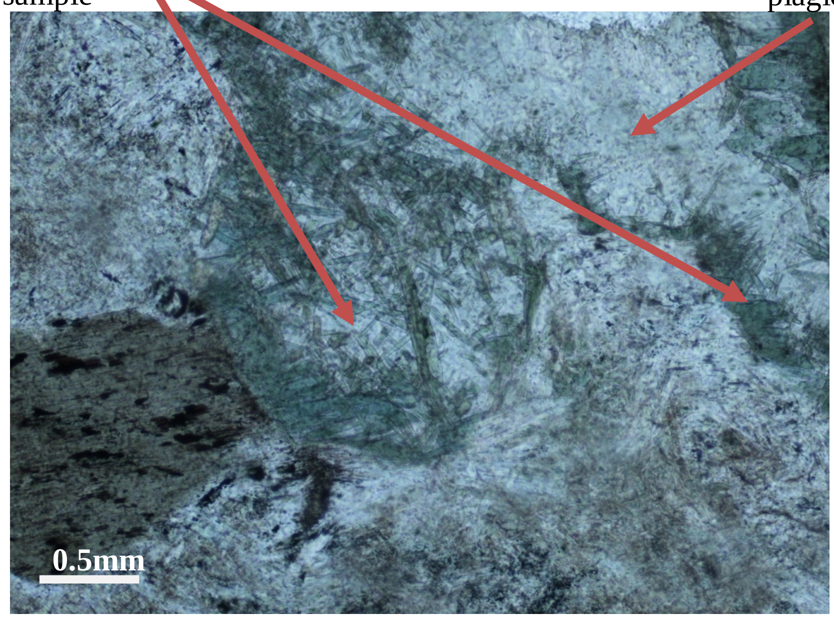


Figure 3.7: Fibrous intergrowth of chlorite with actinolite. Kane Fracture zone, thin section 85-010-11-2 (PPL).

# CHAPTER 4: DISCUSSION

## 4.1 Introduction

This chapter discusses the significance of the petrology and textures of IODP Hole 1256D, described in Chapter 2. The Kane Fracture Zone cores are discussed briefly for comparison. Hole 1256D was drilled in a tectonically stable area that formed at a fast-spreading ridge, while the Kane Fracture Zone cores come from a tectonically active area where a transform fault has offset the Mid-Atlantic Ridge. The similarities and differences in mineralogy and texture may therefore be related to the settings from which the samples were taken.

It is known that as mantle rises beneath a spreading center it decompresses, crosses the solidus, melts and then erupts or intrudes to form the oceanic crust we observe today (Sinton et al., 1992). The nature of primary mid-ocean ridge basalts is controversial. For example, the degree to which fractional crystallization and magma mixing processes contribute to magma chemistry is still subject to debate. Many marine geoscientists agree that a system of magma chambers occurs along mid-ocean ridges (Sinton et al., 1992), however the properties of these axial magma chambers (eg., dimensions and volumes) are debated. Seismic studies have shown that shallow magma chambers exist along the axes of mid-ocean ridges, and petrological evidence suggests fractionation of open system magma chambers, with both replenishment and magma mixing taking place (Macdonald et al., 1982). Magma chambers along a fast-spreading ridge such as the East Pacific Rise are thought to be narrow, sill-like bodies of melt that grade downward into a partially solidified crustal mush, which is surrounded by a transition zone to the still hot gabbros (Sinton et al., 1992; figure 4.1).

The magma chamber model illustrates the gradual crystallization of a primitive melt, which is dependent on the location of the solidus. The solidus can be found anywhere from the boundary of the mush zone to the axial low velocity zone (the gabbros) (Fig 4.1, Sinton et al., 1992). The axial low velocity zone is interpreted as a mostly solid hot material that contains ~5% melt. Based on seismic data from the East Pacific Rise, seismic velocities are low for long distances beneath the axial rift (Lamoureux et al., 1999). This axial magma chamber provides a reservoir from which melt can be injected to form dikes, or erupted to form lavas, but also provides a location where deeper crustal rocks (gabbros) can form by slow crystallization (Sinha et al., 1999). The contributions of fractional crystallization and magma mixing vary in each magma chamber and from ridge to ridge because they are spreading-rate dependent (Kelemen et al., 1999).

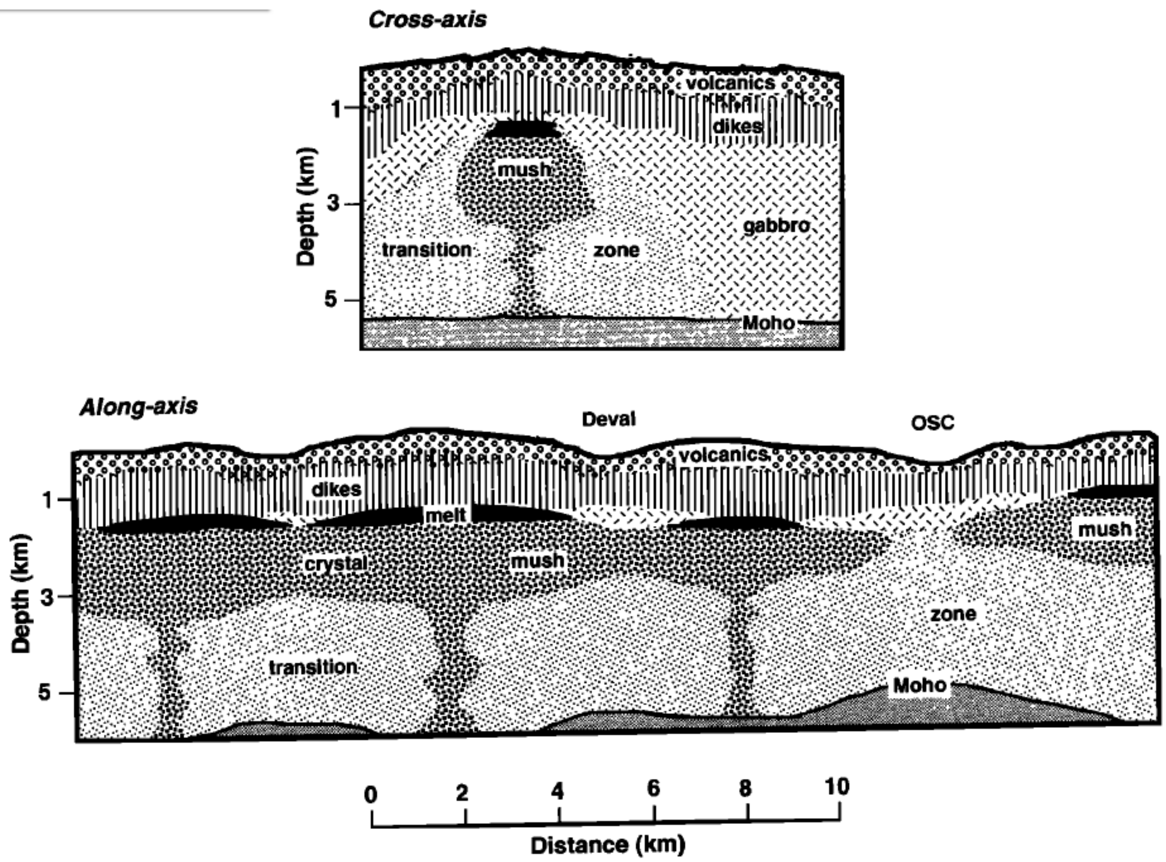


Figure 4.1: Interpretation of a magma chamber along a fast spreading ridge (cross-axis and along-axis). Note the narrow sill-like chamber (along-axis), comprising predominantly crystal mush surrounded by a transition zone to the hot gabbros (cross-axis). The axial chamber is not a continuous feature, and does not seem to be continuous along any mid-ocean ridge. However, slow-spreading ridges tend to have smaller, more localized chambers along the ridge (Sinton et al., 1992).

Alteration of oceanic crust is commonly caused by the interaction of hydrothermal fluids with rocks, causing chemical exchange between the fluid and the host rock and creation of secondary mineral assemblages (figure 4.2, Banerjee, 1996). At a fast-spreading ridge, hydrothermal circulation is typically focused at the top of the axial magma chamber (approximately the upper 1-2km below sea floor) where energy is derived from the latent heat of crystallization of magma and the heat released during cooling (Gillis, 2008). Hydrothermal fluids can circulate to great depths because fractures allow fluids to penetrate near the axial magma chamber where they can become super-heated (Manning, 2000). Fractures are thought to form due to the cooling of ocean crust. Since fast-spreading ridges rarely have a ductile zone, brittle failure is common, causing a downward-propagating cracking front that can travel as deep as the sheeted dike-gabbro transition zone (Manning et al., 2000). Furthermore, microfracturing that allows fluids to travel through the rocks is thought to first occur along grain boundaries on a micrometer-scale (Manning et al., 2000). The effect of off-axis hydrothermal circulation is important, as most of the heat loss (~70%) in the oceanic crust occurs in the ocean basins, driving off-axis fluid flux and geochemical exchange (Schramm, 2005). The pattern of circulation is created by down-flow and up-flow patterns caused by the creation of new crust at the axis providing a heat source to drive convective circulation (Alt et al., 1986). Convection and fracture/microfracture formation allow hydrothermal circulation to occur at great distances below and off-axis.

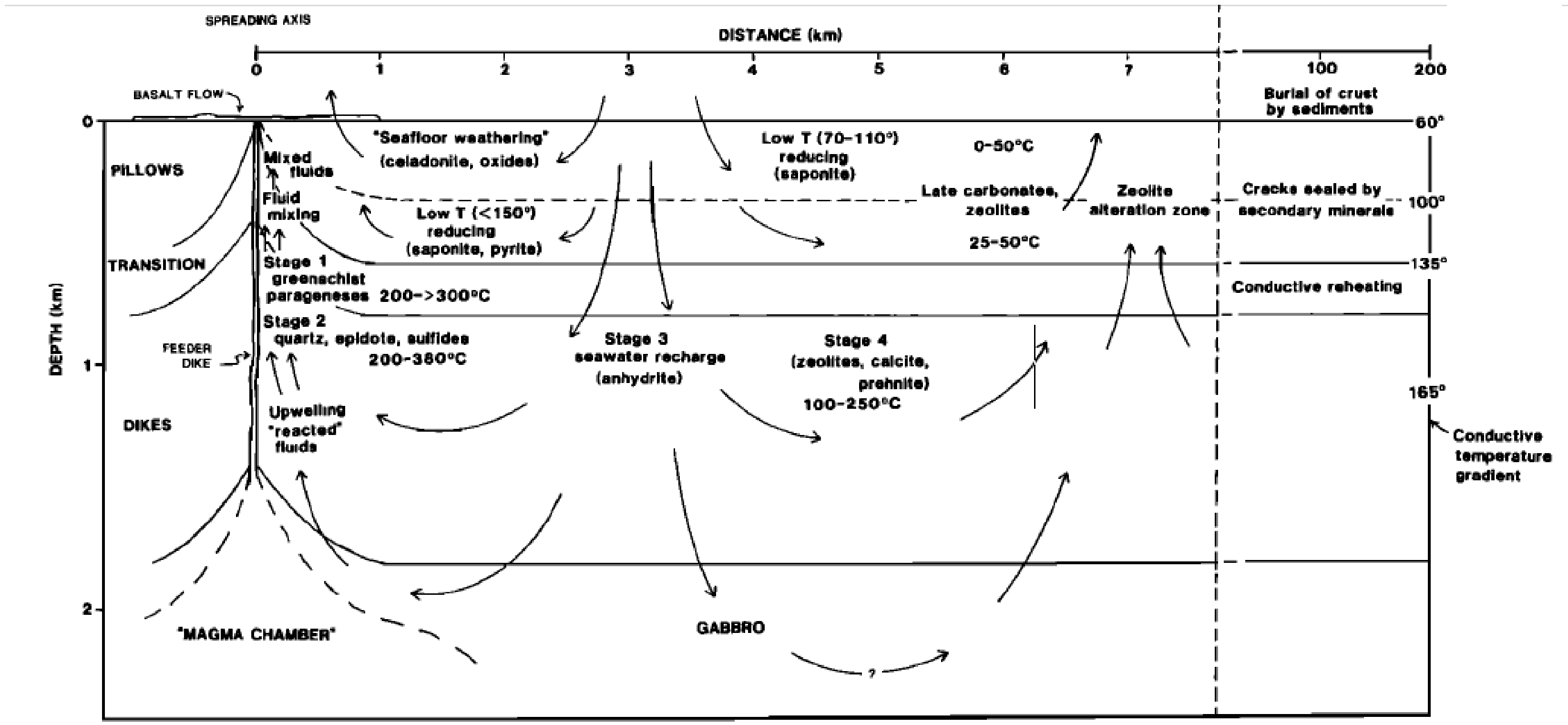


Figure 4.2: Schematic cross-section of oceanic crust that shows the distribution of convection cells and the alteration processes with distance from the spreading center. This is a summary of the evolution of the hydrothermal system at ODP Site 504 (figure 1.2). The hydrothermal convective cell is fixed in relation to the spreading center, therefore the alteration style will change as the crust moves through the varying convection cells. (Alt et al., 1986).

In oceanic crust, the intrusion of gabbros causes contact metamorphism of the sheeted dikes. A melt lens can form under the sheeted dikes and its effects may be observed in textural and petrological features of the sheeted dikes. The underlying melt lens can react with hydrothermal fluids that are able to reach this depth. Interaction of the hydrothermal fluids and the melt can lead to hydrous partial melting of the lower sheeted dikes (Manning et al., 2000; France et al., 2009). Vertical movement of the melt lens caused by inflation/deflation of the melt lens results in reheating and recrystallization (France et al., 2009), producing the granoblastic texture observed in the lower sheeted dikes at Hole 1256D.

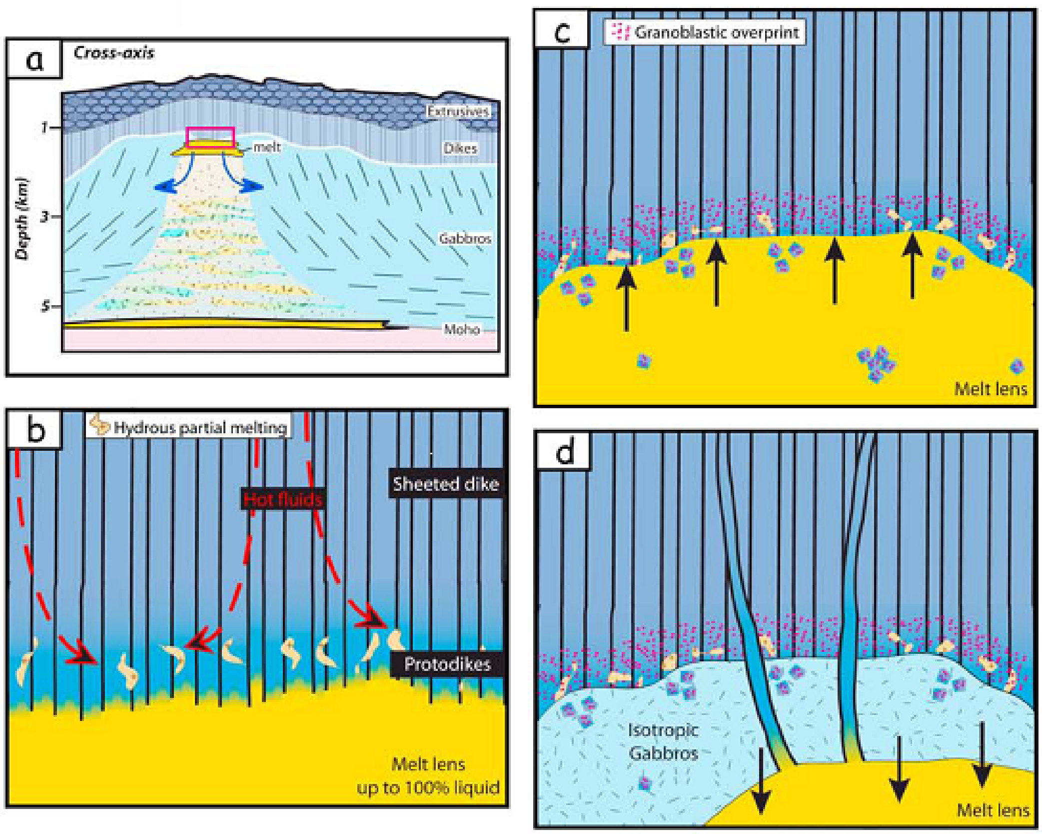


Figure 4.3. General schematic model for the dynamics of the melt lens underlying the sheeted dikes. A) a representative diagram of the cross-section of a fast-spreading ridge. Red box shows location of melt lens. B) Interaction of the hydrothermal fluids and the melt lens causing partial melting of the sheeted dikes. C) Upward movement of the melt lens resulting in reheating and recrystallization producing a granoblastic overprint. D) Downward motion of the melt lens and crystallization of isotropic gabbros, injection of new dikes is possible. (France et al., 2009)

**4.2 Alteration of oceanic lavas and sheeted dikes at IODP Hole 1256D**

Alteration of the oceanic crust is mainly caused by hydrothermal circulation. At the base of the sheeted dike complex, contact metamorphism by the underlying gabbros can affect the mineralogy of the lower sheeted dikes. Tectonic deformation did not affect the rocks of Hole 1256D, as no major faults or fractures occur in this area.

Fluid-rock interactions are the probable cause of alteration at Hole 1256D and the degree of alteration varies as defined by the modal percentage of alteration products. The main alteration mineral is smectite (figure 4.4). For the thin sections described in Chapter 2, alteration of basalt is apparent from the replacement of olivine or clinopyroxene or filling of vesicles. Alteration along fractures and veins was not observed as the thin sections did not contain any veins.  Smectite has a relatively narrow temperature range in which it is stable, between 28°C to 69°C (Alt et al., 2003).With a sediment overburden of 250 m, these lavas, sheeted dikes, and gabbros were increasingly buried as the site moved off-axis; this can restrict hydrothermal flow and produce a reducing environment (Hunter, 1998). However, due to the age of the crust at this location (~15 Ma) the heat flux would have declined over time affecting alteration at Hole 1256D (Schramm et al., 2005). Because this is an environment where hydrothermal circulation and elevated heat flux could occur off-axis for a long time and where sediment overburden creates a semi-reducing/reducing environment, smectite can form at great depth (Hunter, 1998; Schramm et al., 2005). Furthermore, higher ambient crustal temperatures increase the convection rate of fluids through the crust, leading to higher water-rock ratios and hence more intense alteration.

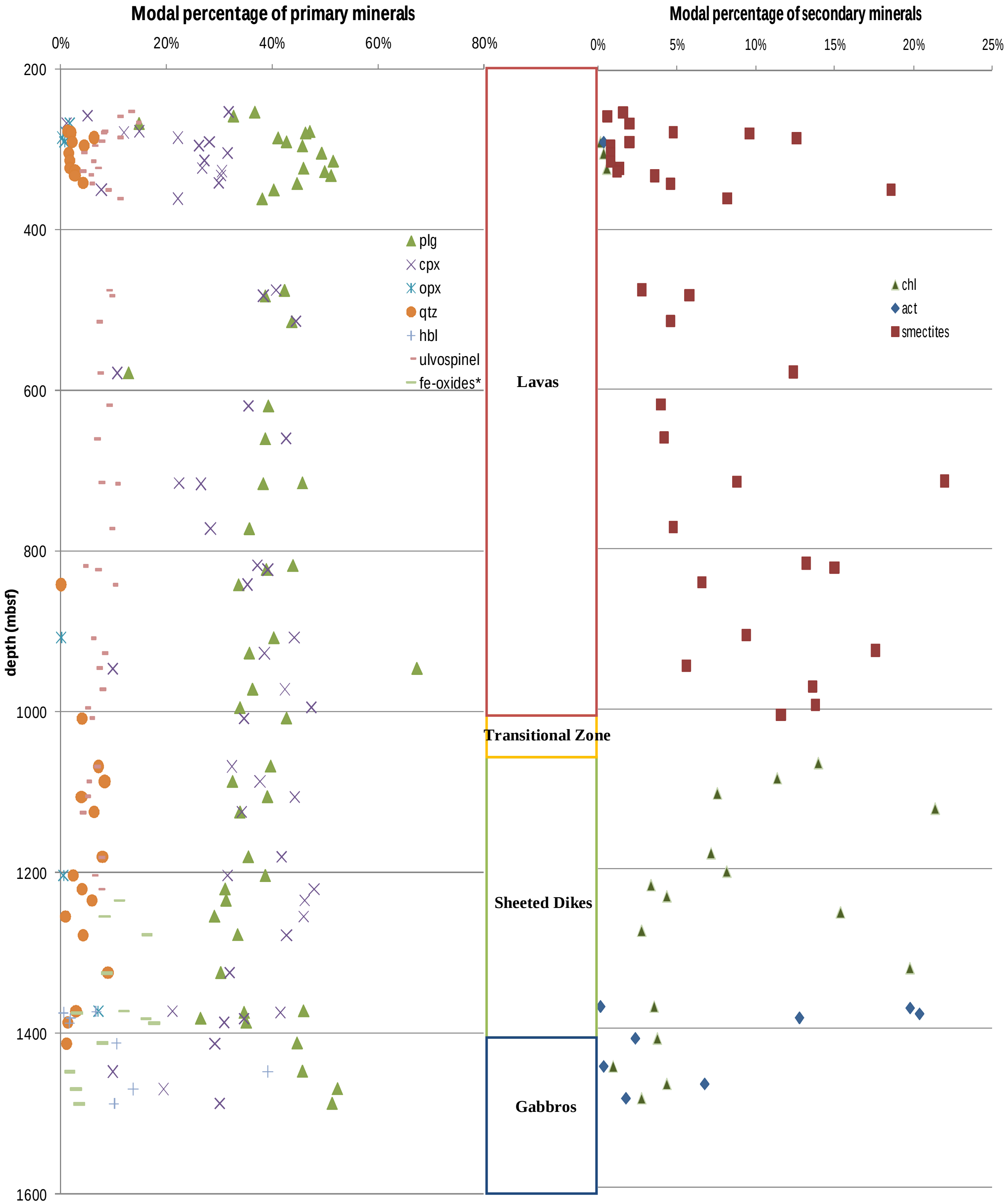


Figure 4.4: Modal percentage of primary and secondary minerals (both phenocrysts and groundmass minerals are included; olivine, glass, and epidote excluded) present down-hole in IODP Hole 1256D.

The presence of quartz (possibly secondary) at specific depths in the hole correlates with a variation in temperature. Quartz is stable at higher temperatures than smectite, 50°C to 110 °C (Alt, 2003). This temperature range was recorded from ODP Site 801 but temperatures between 200-400°C have been recorded (Rumyantsev, 2002)). Quartz is present between ~262 mbsf and ~336 mbsf, and then again below ~995 mbsf. The upper regions coincide with a lava pond that is a very thick, late stage flow that could have retained high temperatures for an extended period of time (Teagle et al., 2006). In the upper region where quartz is present, there is a decline in the smectite percentage, suggesting a possible temperature of approximately 70°C where quartz and smectite could coexist. In the lower section where quartz is stable an increase in temperature is evident from the presence of chlorite (figure 4.5). Temperatures become too high for quartz below ~1325 mbsf, where only a trace of quartz is present in a few samples, where it is restricted to veins that could have been formed by cooler hydrothermal fluids.

Plagioclase remains relatively fresh down-core, however noticeable changes in An content do occur. The anorthite content in the lavas ranges from $An_{45-70}$, in the sheeted dikes it can range from $An_{10-50}$, and in the gabbros it can range from $An_{60-80}$.
The persistence of calcic plagioclase is consistent with the phase relations illustrated in Fig. 4.5 (Winter, 2010), which show that at low pressures ($P < 2.5$ kbar) the assemblage An + Chl + Act is stable in the greenschist to amphibolite facies transition zone, with Ab + Ep + Hbl at higher pressures. The presence of some sodic plagioclase in the sheeted dikes may reflect incipient replacement of primary plagioclase by albite, perhaps in response to locally higher fluid pressures associated with reduced permeability.

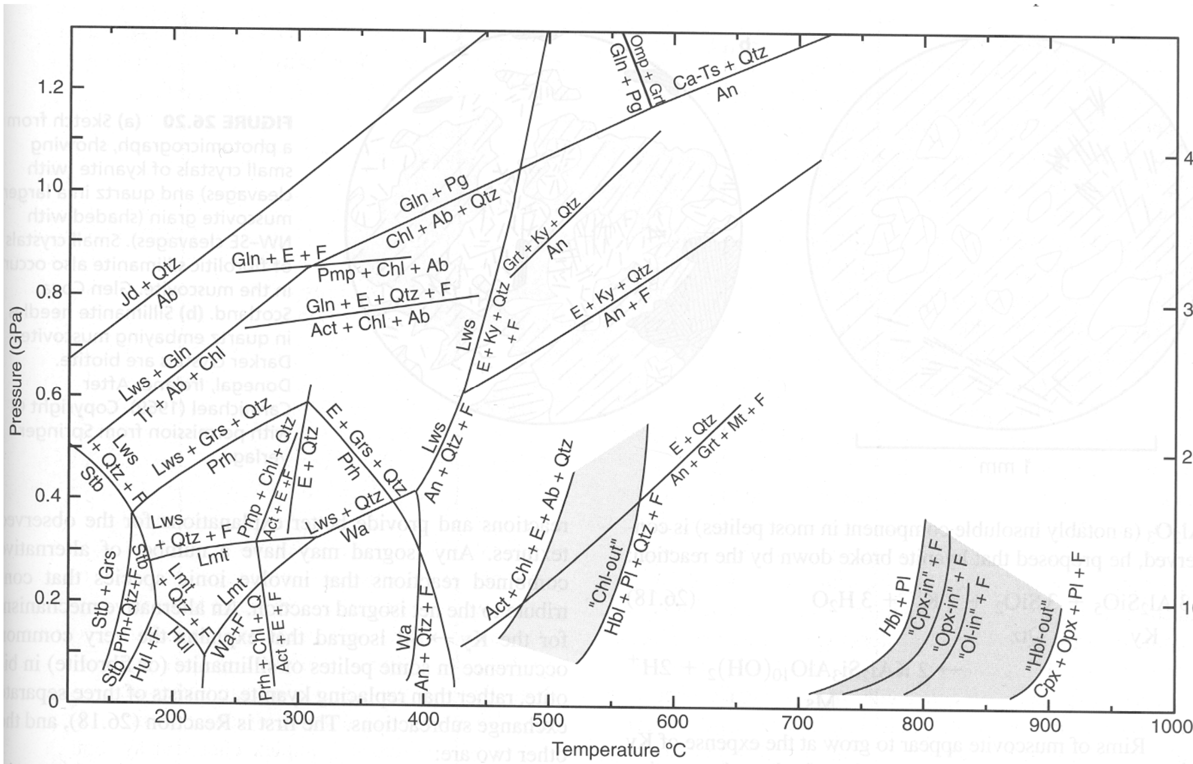

Figure 4.5: Petrogenetic grid for metabasites showing location of several reactions in the CaO-MgO-$Al_2O_3$-$SiO_2$-$H_2O$-($Na_2O$) system. (Winter, 2010)

The transition zone from lavas to sheeted dikes was, unfortunately, not well represented in the thin sections from IODP Hole 1256D. The transition zone, between 1004-1060 mbsf, is represented only by thin sections from 1008 mbsf and 1068 mbsf. Therefore a proper analysis could not be conducted for this region. Nonetheless a clear change in the predominant alteration minerals, from smectite to chlorite, occurs within this zone (figure 4.4).

The sheeted dike complex between 1060 and 1406 mbsf displays a significant change in alteration phases, with chlorite now the dominant alteration mineral. The appearance of chlorite marks the beginning of the greenschist facies (figure 4.6), with temperatures ≥250 °C (Umino et al., 2008). Veins of actinolite, hornblende, and chlorite are present in thin sections between 1375 and 1387 mbsf, indicating relatively high temperatures.

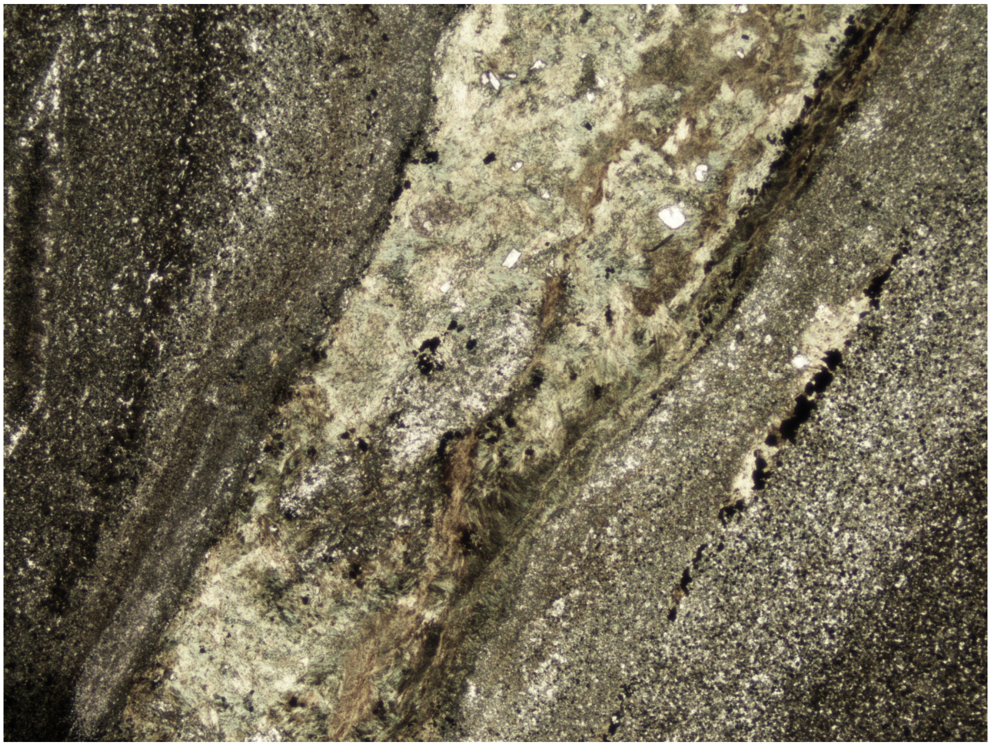

Figure 4.6: Vein of dominantly actinolite + hornblende, with some chlorite present along the margins. 1382 mbsf, Hole 1256D thin section (shown in plane polarize light, thin section (49)).

Textural changes have also occurred. The grain size of predominant primary minerals (clinopyroxene and plagioclase) has increased and chlorite occurs both as a replacement of these minerals and as an interstitial phase. A granoblastic texture at the base of the sheeted dike complex indicates metamorphic recrystallization, most likely caused by heat from the underlying gabbro (Koepke et al., 2008). The granoblastic texture is a sign of high temperature and is typical of contact metamorphism. Temperatures possibly have reached up to 1050°C right above the contact with gabbro (Koepke et al., 2008). This region experiences heat from both the intrusive body below plus heating of hydrothermal fluids by the same intrusive body. This can lead to partial melting and associated changes in the texture and composition of the rock, such as the granoblastic texture observed in the lower sheeted dikes at Hole 1256D (France et al., 2009, figure 4.3).

A change from ulvospinel ($Fe_2TiO_4$) to Fe-oxides (ilmenite and titanomagnetite) occurs at 1235 mbsf. This correlates with a sharp decrease in natural remnant magnetization (NRM) (figure 4.7). This also corresponds to an increase in ambient temperature and a gradual decrease in porosity and permeability as the dike/gabbro boundary at 1406 mbsf is approached. Koepke et al. (2008) discussed two possibilities for inferred highly oxidizing conditions that could be present in the transition from sheeted dikes to gabbros: (1) this condition could be inherited from the initial low-grade alteration of the dikes by oxidizing seawater-derived fluids, or (2) it could result from high water circulation during the process which formed the granoblastic texture seen at the base of the sheeted dikes. A shift from low water-rock ratios to high water-rock ratios could cause a shift toward highly oxidizing conditions. The change in opaque minerals suggests that oxidizing conditions occur lower in the crust, however how or when this oxidizing state formed is still unknown (Koepke et al., 2008).

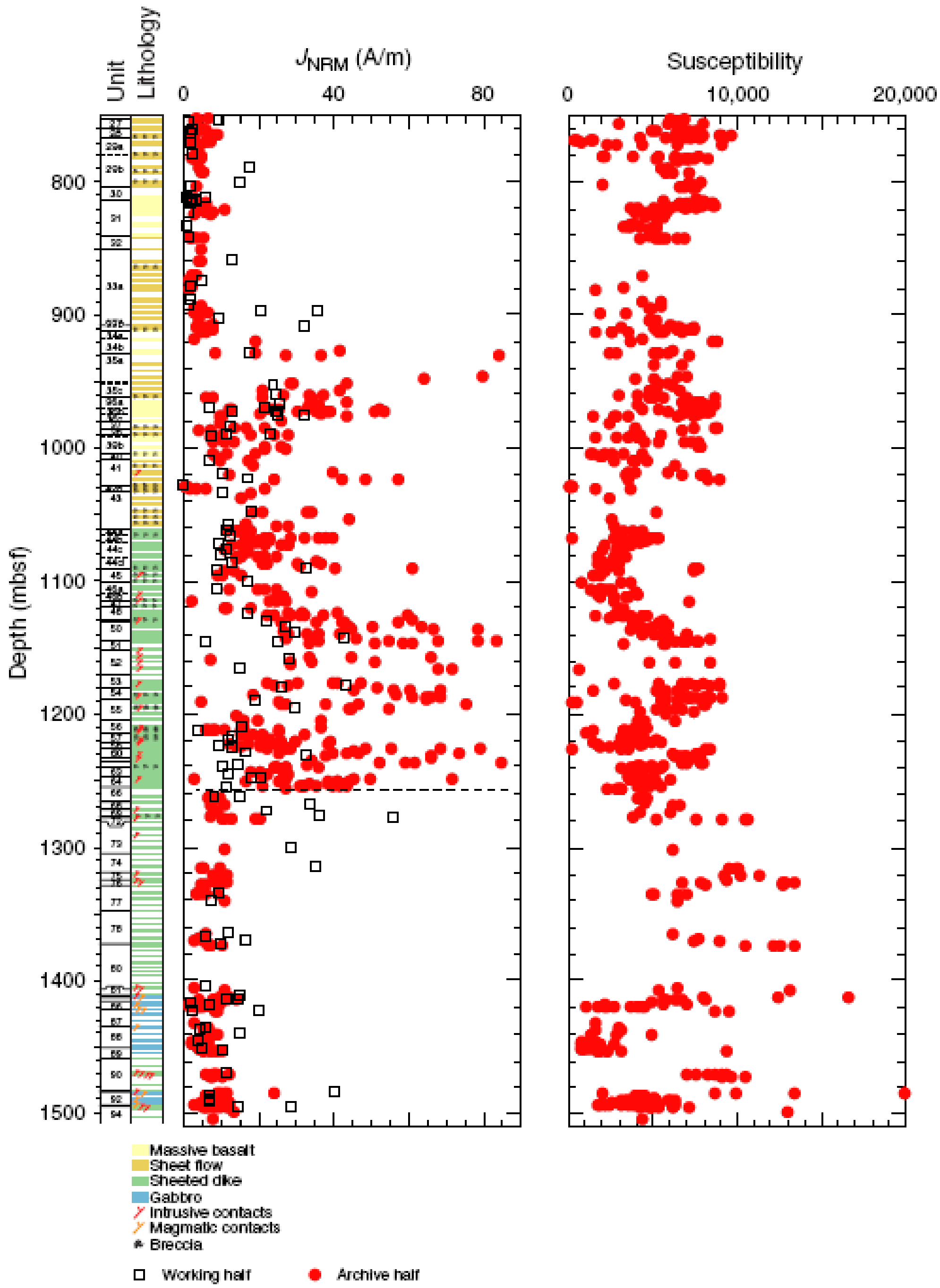


Figure 4.7: Down-core variations in natural remnant magnetization (NRM) intensity and magnetic susceptibility. A sharp decrease in NRM corresponds to the depth where ulvospinel is replaced by Fe-oxides. (Modified from Teagle et al., 2006)

**4.3 Alteration of gabbros at IODP Hole 1256D**

At Hole 1256D, gabbros are first found at 1406 mbsf and continue to the base of the hole (1507 mbsf), although the deepest thin section studied comes from 1488 mbsf. Within this zone there is at least one interval of sheeted dikes at 1470 mbsf, showing that the gabbros drilled so far are still in the transition zone between Layers 2 and 3.

Previous work comparing compositions of gabbros from fast and slow-spreading ridges suggests that those formed at a fast-spreading ridge have more fractionated compositions than those from a slow-spreading ridge (Sinton et al., 1992). Possible primary mantle melt compositions should have a Mg# of 70 to 78 and MgO of 9 to 14 wt% (figure 4.8) (Wilson, 2006). The average composition of gabbro is more primitive than the lavas and dikes, and less fractionated, but it is more evolved relative to primary magma in equilibrium with mantle olivine. Therefore the residue removed from the primary magma to form the observed gabbro and basalt compositions must be deeper than the uppermost gabbros in Hole 1256D (Wilson, 2006).

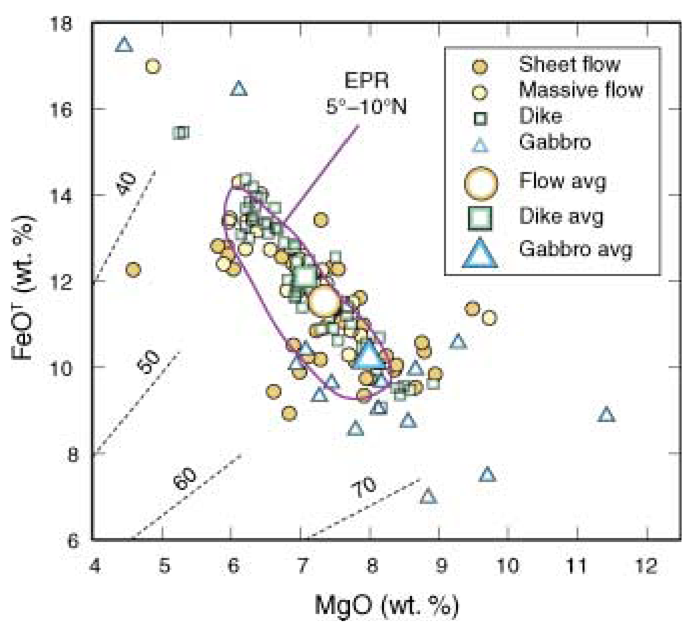


Figure 4.8: $FeO_T$ (total Fe expressed as FeO) versus MgO for the basalts, dikes and gabbros at Site 1256, compared with analyses from northern East Pacific Rise (outline). Dashed lines show constant Mg number. Wilson, 2006.

The gabbros at Hole 1256D are highly altered, with intricate intergrowths of clinopyroxene, hornblende and actinolite (figure 4.9). Grain size varies from fine- to coarse-grained, with alteration minerals often occurring as fine-grained intergrowths. Amphiboles are a major alteration product (figure 4.4). Distinguishing between magmatic amphibole and hydrothermally produced amphibole is difficult and could not be done with complete confidence in this study; although the possibility of determining the difference will be discussed.

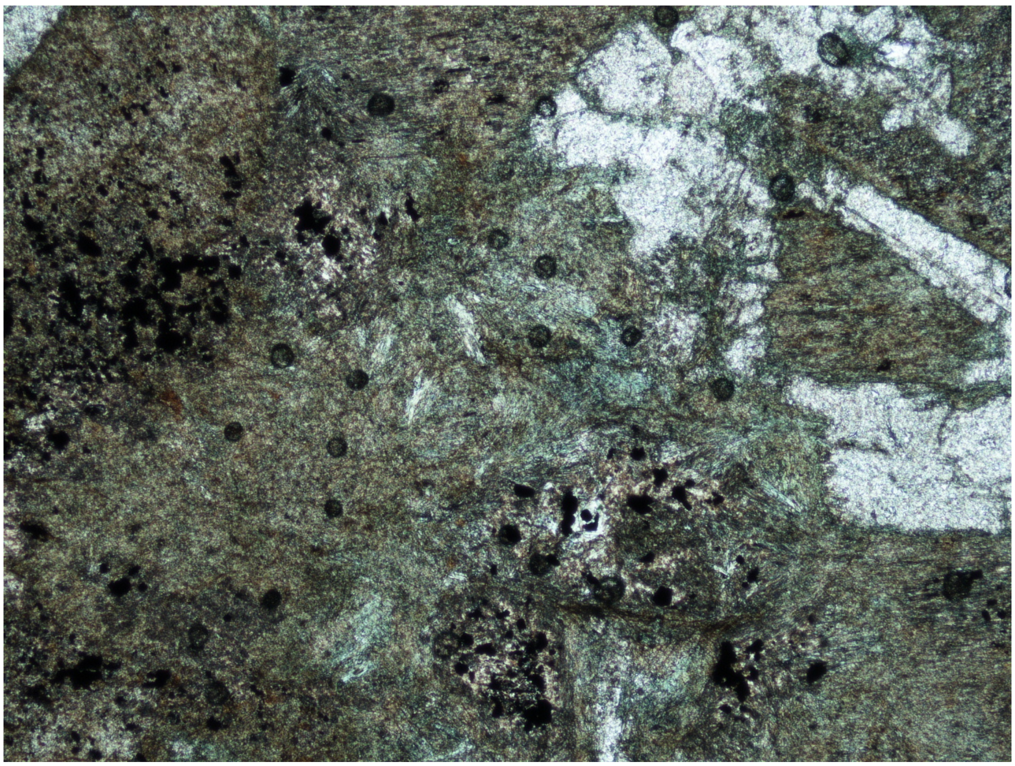

Figure 4.9: Fine grain intergrowths of actinolite, clinopyroxene and hornblende with minimal chlorite. Actinolite and hornblende are replacing the clinopyroxene. These masses of intergrown minerals are often difficult to differentiate. Hole 1256D thin section 25 (plane polarized light).

Although the lack of veins in the gabbros suggests that hydrothermal effects are limited, veins are present in the lower section of the sheeted dikes and hydrothermal alteration is known to occur there. Therefore a hydrothermal influence is likely within the upper section of gabbros. The idea that a significant volume of hydrothermal fluids could react with the intrusive body at near-solidus temperatures is still debated. Nonetheless, high temperature hydrothermal fluids (~750 °C) are known to penetrate into Layer 3 (Gillis, 2003).

A study conducted on oceanic gabbros from the MARK site/ODP Hole 923A (Mid-Atlantic Ridge south of the Kane Fracture Zone) tried to distinguish hydrothermal amphiboles from those produced from a hydrous silicate melt (magmatic amphibole) (Coogan et al., 2001). During the solidification of crystal mushes, interstitial melt migration can lead to the crystallization of secondary amphiboles without requiring externally derived hydrothermal fluid (Coogan et al., 2001). To distinguish magmatic amphibole from hydrothermal amphibole, Niobium (Nb) concentrations can be used. Since Nb is relatively immobile and the abundance of Nb in oceanic plagioclase, olivine, and pyroxene (the main silicate phases of oceanic crust) is known to be low, the interaction of hydrothermal fluids with a gabbroic assemblage would produce Nb-depleted fluids and thus form hydrothermal amphibole with low Nb abundances. In contrast, hydrous silicate melts, and the amphiboles that are formed from them, will be enriched in Nb. Using this method, hydrothermal and magmatic amphiboles can be differentiated (Coogan et al., 2001). Using Nb concentrations in the amphiboles may be a good strategy to determine how these amphiboles formed, but was not possible in the context of this study.

**4.4 Alteration of the Kane Fracture Zone core**

The Kane Fracture Zone is a tectonically active area that lies along the slow-spreading Mid-Atlantic Ridge. This setting is significantly different than that of IODP Hole 1256D which is in a stable region and formed at the fast-spreading East Pacific Rise. This difference could lead to texturally different rocks being formed and the degree to which they are altered could vary.

Kane Fracture Zone samples are from pillow basalts, which are quenched suddenly upon eruption (Winter, 2010), unlike the massive and sheet basalts examined at IODP Hole 1256D which have a slower cooling rate. Olivine and plagioclase are visible in some of the basalts both as microphenocrysts and part of the matrix, and their presence was confirmed based on EMP data. The absence of smectite indicates that the basalts have not been altered to any significant degree. Olivine remains fresh and unaltered, as does the plagioclase. It is surprising that the samples from the tectonically stable Site 1256 seem to be more altered than the Kane Fracture Zone samples.

The gabbros at the Kane Fracture Zone appear to have undergone alteration similar to those at IODP Hole 1256D, based on textures and mineralogy. Textures are similar in the two locations, including intergrowths of actinolite and hornblende, and actinolite and chlorite. Actinolite is the dominant alteration mineral (based on modal percentages) at the Kane Fracture Zone, unlike Hole 1256D where the dominant alteration mineral is hornblende. The abundance of actinolite could mean lower alteration temperatures in these gabbros (figure 4.5). Actinolite can form between ~300 °C - 500°C, and hornblende between ~500°C-700°C (Winter, 2010). A temperature close to (or just under) 500°C can be inferred based on the presence of both actinolite and hornblende, but the dominance of actinolite suggests the temperature will be in the lower part of this range for the Kane Fracture Zone samples.

# 5.0: CONCLUSIONS

## 5.1 Results from this study

Samples from IODP Hole 1256D were collected to observe petrographical and textural variations down-core. Fifty-three thin sections were examined, combining optical descriptions and electron microprobe analysis. Furthermore, ten thin sections from the Kane Fracture Zone cores were used to compare the mineralogy and textures of the two locations. The following results were obtained:

1. Primary plagioclase and clinopyroxene are abundant throughout Hole 1256D. Plagioclase is predominantly fresh, euhedral grains with An-Ab ratios varying depending on whether the plagioclase formed in the groundmass or as a phenocryst, with gabbroic plagioclase ranging up to An80. Clinopyroxene texture varies at Hole 1256D depending on the degree of alteration. In the basalt clinopyroxene is fine-grained and intergrown with plagioclase, whereas in the gabbros clinopyroxene is anhedral and with highly variable grain size. Olivine is present in the basalts from the Kane Fracture Zone, and there is little or no clinopyroxene. Plagioclase in the Kane Fracture Zone basalts forms euhedral microphenocrysts in the glassy matrix, and becomes coarse-grained and subhedral-anhedral in the gabbros.

2. At Hole 1256D the principal secondary minerals consist of smectite, chlorite, and actinolite (some secondary hornblende). The transition from smectite to chlorite occurs at ~1010 mbsf. Actinolite and secondary hornblende first occur at ~1373 mbsf, in the sheeted dike-gabbro transition zone. At the Kane Fracture Zone secondary minerals are not observed in the basalts; however the gabbros have secondary actinolite, hornblende, and chlorite. Actinolite is the dominant alteration mineral present in the gabbros.

3. The gabbros from IODP Hole 1256D and the Kane Fracture Zone are similar. Although minimal variations in modal percentages of secondary minerals occur, primary

minerals are comparable and both display intergrowths of secondary minerals, giving the rocks a microscopic fibrous texture. The major difference between the samples from the two locations occurs in the basalts. IODP Hole 1256D basalts are altered, with the dominant minerals being plagioclase, clinopyroxene and smectite. The Kane Fracture Zone basalts are fresh with primary minerals including plagioclase and olivine, and no secondary minerals.

4. A down-core increase in temperature and oxidation state is inferred at Hole 1256D, primarily based on secondary mineral assemblages (the smectite-chlorite transition and the change in opaque minerals). A granoblastic texture observed in the lower sheeted dikes is formed by contact metamorphism (caused by the intrusive gabbros) and hydrothermal alteration (transported through micro-cracks and fractures). Therefore hydrothermal alteration appears to affect the entire core, however with increasing depth temperature increases and the intrusion of the gabbros also has a strong effect on the lower section of the sheeted dikes.

5. The pillow basalts at the Kane Fracture Zone have not been altered (lack any secondary minerals), however the gabbros have. The abundance of actinolite in the Kane Fracture Zone gabbros suggests that the temperature of alteration was lower than that of Hole 1256D.

### 5.2: Recommendations for future work

Many variables have not yet been explored which could be the subject of future work. These include:

1) Niobium concentrations could be examined to determine the origin of the amphibole present in the gabbros.
2) Bulk rock geochemical data could be obtained to test alternative petrogenetic models.
3) More point counts on more thin sections throughout the core should be conducted and could reveal details of more changes and depths at which those changes occur.
4) A study of stable isotopes can help assess fluid-rock interactions down-core at Hole 1256D.
5) Obtaining polished thin sections from Hole 1256D would allow for more precise EMP analysis and would greatly aid in determining down-core trends of primary and secondary opaque minerals, and would give a more precise count of those opaque minerals. Also by using energy dispersive electron imaging from polished slides, modal percentages of groundmass minerals could be obtained.
6) Use of the modal percentage of each mineral in the rocks could be related to the seismic velocity of these rocks.
7) Collection of thin sections with presence of veins may be helpful to examine hydrothermal circulation and temperatures.

## REFERENCES


Alt, J.C., Honnorez, J., Laverne, C., Emmermann, R. 1986. Hydrothermal alteration of a 1 km section through the upper oceanic crust, Deep Sea Drilling Project Hole 504B, Mineralogy, Chemistry, and Evolution of Seawater-Basalt Interactions. Journal of Geophysical Research. **91**: 309-335.

Alt, J.C., Teagle, D.A.H. 2003. Hydrothermal alteration of upper oceanic crust formed at a fast-spreading ridge: mineral, chemical, and isotopic evidence from ODP Site 801. *Chemical Geology*. Elsevier Science Ltd. **201**: 191-211.

Banerjee, N.R. 1996. Geochemical effects of alteration in a section of lower ocean crust; ODP Hole 735B, Southwest Indian Ridge. M.Sc. thesis, Department of Earth Sciences, Dalhousie University, Halifax, NS.

Coogan, L.A., Wilson, R.N., Gillis, K.M., MacLeod, C.J. 2001. Near-solidus evolution of oceanic gabbros: Insights from amphibole geochemistry. *Geochimica et Cosmochimica Acta.* Elsevier Science Ltd. **65** (23): 4339-4357.

Duncan, R.A., Green, D. H. 1980. Role of multistage melting in the formation of oceanic crust. *Geology*. **8**: 22-26

France, L., Benoit, I., Koepke, J. 2009. Interactions between magma and hydrothermal system in Oman ophiolite and in IODP Hole 1256D: Fossilization of a dynamic melt lens at fast spreading ridges. *Geochemistry, Geophysics, Geosystems*. **10** (10): 16-30.

Gillis, K.M. 1995. Controls on hydrothermal alteration in a section of fast-spreading oceanic crust: *Earth and Planetary Science Letters*, **134:** 473-489.

Gillis, K.M. 2008. The roof of an axial magma chamber: A hornfelsic heat exchanger. *Geology*. The Geological Society of America. **36** (4): 299-302.

Gillis, K.M. 2003. Subseafloor Geology of hydrothermal root zones at oceanic spreading centers. *Energy and Mass Transfer in Marine Hydrothermal Systems*. Dahlem University Press, 53-66.

Hunter, A.G., ODP Leg 168 Shipboard Party. 1998. Petrological investigations of low temperature hydrothermal alteration of the upper crust, Juan de Fuca Ridge, ODP Leg 168. *Modern Ocean Floor Processes and the Geological Record.* The Geological Society. **148**: 99-126.

Keleman, P.B., Hirth, G., Shimizu, N., Spiegelman, M., Dick, H.J.B. 1999. A review of melt migration of processes in the adiabatically upwelling mantle beneath oceanic spreading ridges. *Mid-Ocean Ridges- Dynamic processes associated with creation of new ocean crust*. University of Cambridge. 67-102.

Koepke, J., Christie, D.M., Dziony, W., Holtz, F., Lattard D., Maclennan, J., Park, S., Scheibner, B., Yamasaki, T., Yamazaki, S. 2008. Petrography of the dike-gabbro transition at IODP Site 1256 (equatorial Pacific): The evolution of granoblastic dikes. *Geochemistry, Geophysics, Geosystems*. **9** (7): 17-29.

Louden, K.E., Forsyth, D.W. 1982. Crustal structure and isostatic compensation near the Kane Fracture Zone from topography and gravity measurements- I. Spectral analysis approach. *Geophys. J.R. Astr. Soc*. **68**: 725-750.

Lamoureux. 1999. Modelling the seismic properties of fast-spreading ridge crustal Low-Velocity Zones: insights from Oman gabbro textures. *Tectonophysics*. Elsevier Science Ltd. **312**: 283-301.

Mahoney, J.J., Fitton, J.G., Wallace, P.J., et al., 2001
Proceedings of the Ocean Drilling Program, Initial Reports, **192**: 25-32.

Macdonald, K.C. 1982. Mid-ocean ridges: fine scale tectonic, volcanic and hydrothermal processes within the plate boundary. Annual Review Earth Planet. *Science*. **10**: 155-191.

Manning, C.E., MacLeod, C.J., Weston, P.E. 2000. Lower-crustal cracking front at fast-spreading ridges: Evidence from the East Pacific Rise and the Oman ophiolite. *Geological Society of America Special Paper 349*. 261-272.

Mayer, L.A. 1985. Cruise Report: Hudson 85-010 ODP Site Surveys at the Kane Fracture zone. Dalhousie University, Department of Oceanography.

Robinson, D., Santana de Zamora,A. 1999. The smectite to chlorite transition in Chipilapa geothermal system, EL Salvador. American Mineralogist. **84**: 607-619.

Rumyanstev, V.N. 2002. Kinetics of Hydrothermal Crystallization of Quartz in $Na_2CO_3$ Solutions. *Crystallography Reports*. **47** (4): 691-694.

Ryall, P.J.C. 1985. Cruise Report: Hudson 85-010 rock drill operations. Dalhousie University, Department of Oceanography.

Schramm, B., Devey, C.W., Gillis, K.M., Lackschwitz, K. 2005. Quantitative assessment of chemical and mineralogical changes due to progressive low-temperature alteration of East Pacific Rise basalts between 0-9 Ma. *Chemical Geology*. Elsevier Science Ltd. **218**: 281-313.

Sinha, M.C., Navin, D.A., MacGregor, L.M., Constable, S., Peirce, C., White, A., Heinson, G., Inglis, M.A. 1999. Evidence for accumulated melt beneath the slow-spreading Mid-Atlantic Ridge. *Mid-Ocean Ridges- Dynamic processes associated with creation of new ocean crust*. University of Cambridge. 17-38.

Sinton, J.M., Detrick, R.S. 1992. Mid-ocean ridge magma chambers. *Journal of Geophysical Research*. **97:** 197-216.

Sinton, J.M., Smaglik, S.M., Mahoney, J.J., Macdonald, K.C. 1991. Magmatic Processes at Superfast Spreading Mid-Ocean Ridges: Glass Compositional Variations Along the East Pacific Rise 13 º -23 º S. *Journal of Geophysical Research*. **94:** 6133-6155. DOI:10.1029/90JB02454.

Teagle, D.A.H., Alt, J.C., Umino, S., Miyashita, S., Banerjee, N.R., Wilson, D.S., and the Expedition 309/312 Scientists. 2006. Proceedings of the Integrated Ocean Drilling Program, **309/312:** 1-6.

Umino, S., Crispini, L., et al. 2008. Origin of the sheeted dike complex at superfast spread East Pacific Rise revealed by deep ocean crust drilling at Ocean Drilling Program Hole 1256D. *Geochemistry, Geophysics, Geosystems*. **9** (6): 1-17.

Wilson, D.S., Teagle, D.A., Alt, J.C., et al. 2006. Drilling to Gabbro in Intact Ocean Crust. Science **312**: 1016. DOI:10.1126/science.1126090

Wilson, D.S., Teagle, D.A.H., Acton, G.D., et al., 2003. Proceedings of the Ocean Drilling Program, Initial Reports, **206:** 1-5, 11-13, 22-33. DOI:10.2973/odp.proc.ir.206.2003

Winter, J.D. 2010. Principles of Igneous and Metamorphic Petrology: Second Edition. Pearson Prentice Hall, New Jersey. 245-266, 520-575.

# APPENDIX A
# Petrographic Descriptions of IODP Hole 1256D Thin Sections

The following appendix includes descriptions of all 53 thin sections from IODP Hole 1256D. Descriptions contain thin section number, rock type, depth (meters below seafloor), grain size, textures, alteration/replacements, and any additional notes. The descriptions have been ordered in increasing depth. Included with descriptions are photomicrographs of each slide taken at the same optical zoom. All photos are in plane polarized light and are general images (they are not focused on features unique to that thin section).

| | |
|---|---|
| Thin Section<br>Rock Type<br>MBSF<br>ODP ID | GIL 48<br>Basalt, sheet flow<br>253<br>1713569 |
| Overall Grain Size | Fine to medium grain plagioclase (0.5-2mm), fine grain (~0.3mm) clinopyroxene, groundmass <0.1mm |
| Textures | Plagioclase grains with small clinopyroxene and opaque mineral inclusions. |
| Alteration/ Replacements | Clay replaces what may have been olivine based on the general habit and unique fracturing. |
| Notes | Although the opaque minerals are both blocky and fibrous, they are all ulvospinel, based on EMP analysis. |

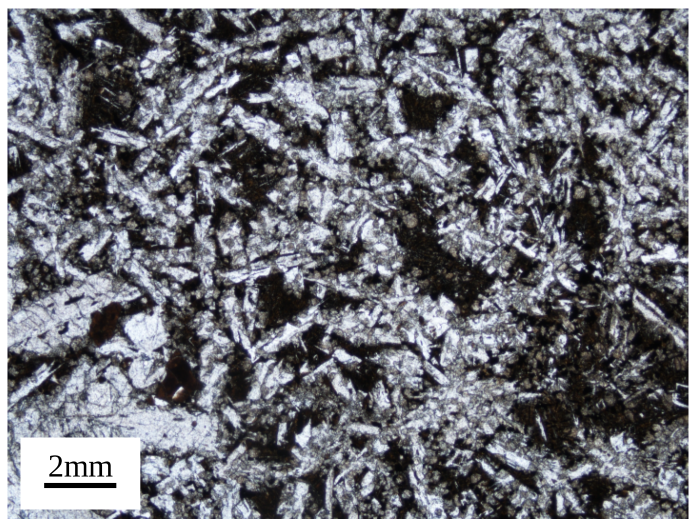

| | |
|---|---|
| Thin Section<br>Rock Type<br>MBSF<br>ODP ID | GIL 49<br>Basalt, sheet flow<br>258<br>1713570 |
| Overall Grain Size | Fine to medium grain (0.5-1mm), groundmass <0.1mm |
| Textures | Radiating intergrowths of plagioclase, clinopyroxene, and opaque minerals |
| Alteration/ Replacements | Clay replaces what may have been olivine based on the general habit and unique fracturing. |
| Notes | Although the opaque minerals are both blocky and fibrous, they are all ulvospinel, based on EMP analysis of similar sample. |

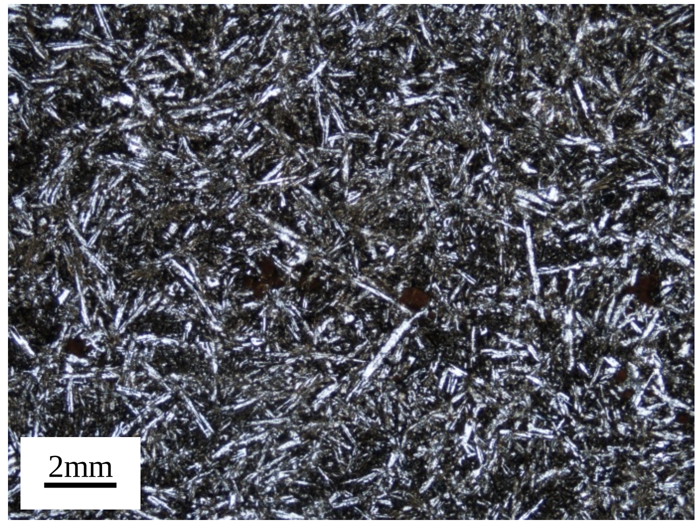


| | |
|---|---|
| Thin Section<br>Rock Type<br>MBSF<br>ODP ID | GIL 50<br>Basalt, sheet flow<br>267<br>1713571 |
| Overall Grain Size | Phenocrsyts (~3mm), groundmass <0.1mm |
| Textures | Porphyritic, with plagioclase phenocrysts (some clinopyroxene but not much) |
| Alteration/ Replacement s | Clay replaces what may have been olivine based on the general habit and unique fracturing and fills in vesicles present. |
| Notes | Although the opaque minerals are both blocky and fibrous, they are all ulvospinel, based on EMP analysis of similar sample. |

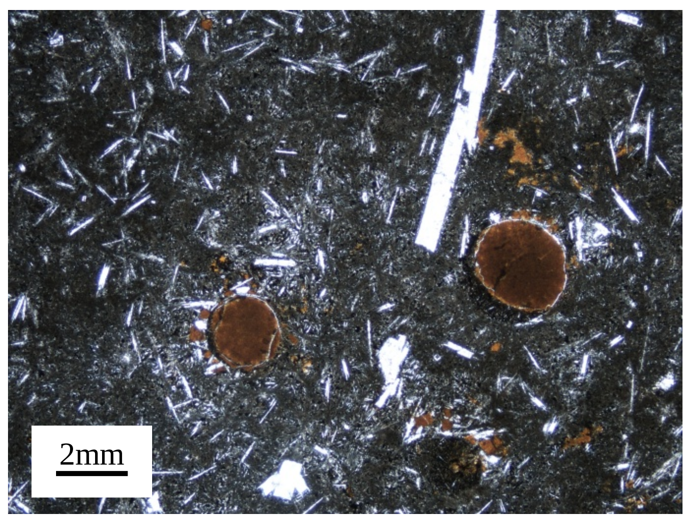

| | |
|---|---|
| Thin Section<br>Rock Type<br>MBSF<br>ODP ID | GIL 36<br>Basalt, massive<br>277<br>1713593 |
| Overall Grain Size | Medium to coarse grain (1-3mm), groundmass <0.1 |
| Textures | No relationship between minerals, and no textures are visible |
| Alteration/ Replacements | Clay replaces what may have been a pyroxene based on general habit, but that is not a definite. |
| Notes | Although quartz is present, it is minimal, and occurs randomly and has no affect on surrounding minerals. |

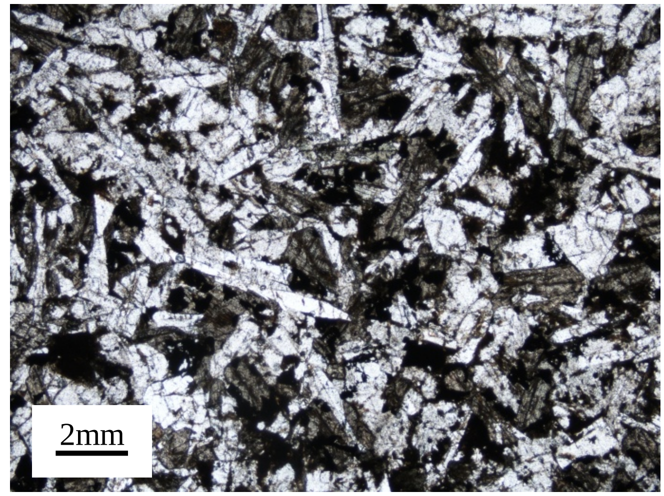


| | |
|---|---|
| Thin Section<br>Rock Type<br>MBSF<br>ODP ID | GIL 37<br>Basalt, massive<br>279<br>1713592 |
| Overall Grain Size | Fine to coarse grain (0.2-3mm), groundmass <0.1mm |
| Textures | No relationship between minerals, and no textures are visible |
| Alteration/ Replacements | Clay again replaces what may have been a pyroxene, based on the general habit, however this is not definite. |
| Notes | Quartz varies more in this sample (between 0.2mm-2mm in size); however it still does not have an affect on the surrounding minerals. The quartz can sometimes have inclusions of what may be plagioclase. |

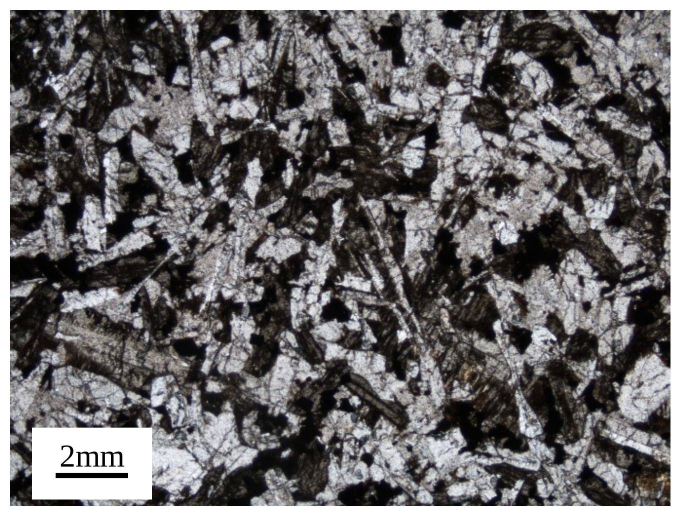

| | |
|---|---|
| Thin Section<br>Rock Type<br>MBSF<br>ODP ID | GIL 35<br>Basalt, massive<br>285<br>1713594 |
| Overall Grain Size | Fine grain (0.2-0.9mm), plagioclase can get to approx. 3mm, groundmass <0.1mm |
| Textures | Quartz and plagioclase show a myrmekitic texture, opaque minerals show unique habits (not simply blocky or fibrous); the minerals vary greatly throughout the sample. |
| Alteration/ Replacements | Clay replaces an unknown, sometimes located in the groundmass and thus may be altering many things. |
| Notes | |

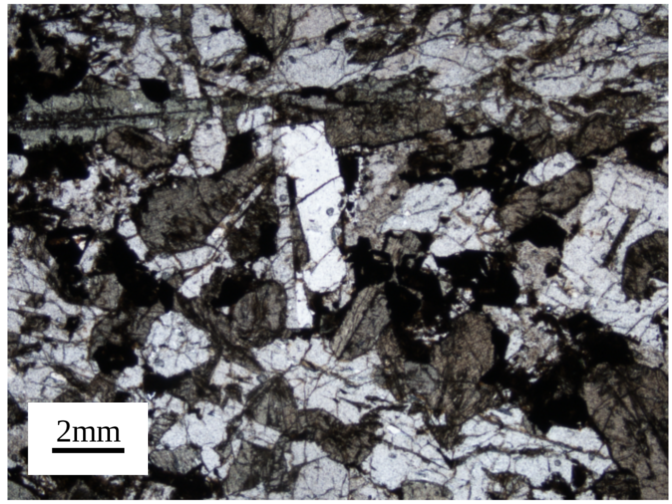


| | |
|---|---|
| Thin Section<br>Rock Type<br>MBSF<br>ODP ID | GIL 38<br>Basalt, massive<br>290<br>1713595 |
| Overall Grain Size | Fine to coarse grain (0.5-3mm), groundmass <0.1mm |
| Textures | A myrmekitic texture is present in the plagioclase, confirming the presence of quartz. |
| Alteration/ Replacements | Alteration of some sort occurs in this sample; in some cases a fibrous mineral is present with clinopyroxene, which is thought to be actinolite. Furthermore chlorite seems to make an appearance replacing clinopyroxene. Clay is also present, which may also be replacing clinopyroxene. |
| Notes | Groundmass is most often located between grain boundaries. Opaque minerals are forming unique shapes (Christmas tree-like), not the typical blocky habit. |

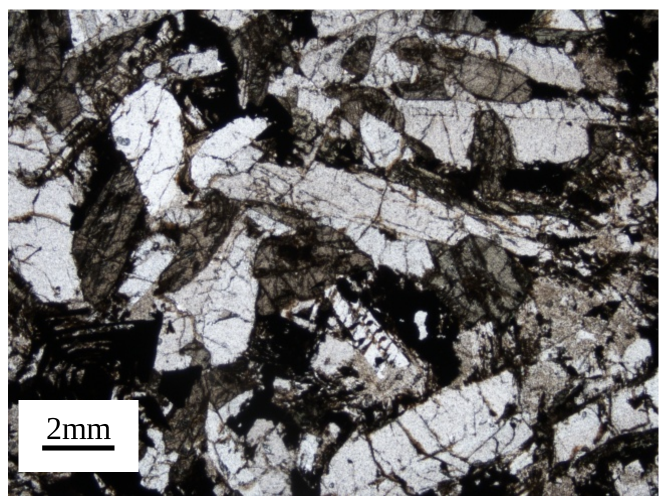

| | |
|---|---|
| Thin Section<br>Rock Type<br>MBSF<br>ODP ID | GIL 39<br>Basalt, massive<br>295<br>1713606 |
| Overall Grain Size | Fine to coarse grain (0.5-3mm), groundmass <0.1mm |
| Textures | A myrmekitic texture is present in the plagioclase, confirming the presence of quartz. |
| Alteration/ Replacements | Clay is replacing an unknown, and is often located within the fine grain groundmass, sometimes making it difficult to identify. |
| Notes | Unlike previously there is no sign of replacement products such as chlorite or actinolite. Reason unknown. |

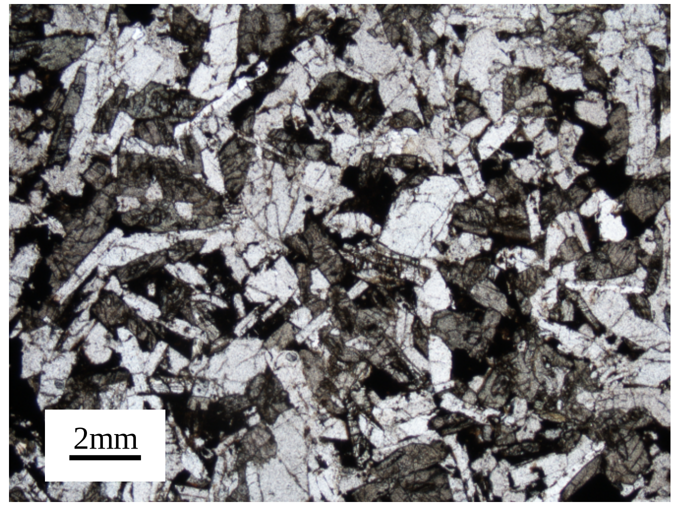


| | |
|---|---|
| Thin Section<br>Rock Type<br>MBSF<br>ODP ID | GIL 40<br>Basalt, massive<br>304<br>1713607 |
| Overall Grain Size | Fine to coarse grain (0.5-3mm), groundmass <0.1mm |
| Textures | A myrmekitic texture is present in some of the plagioclase, confirming the presence of quartz. |
| Alteration/ Replacements | Chlorite makes a tiny appearance, replacing an unknown mineral. Clay is also present, however much less then many previous samples. |
| Notes | |

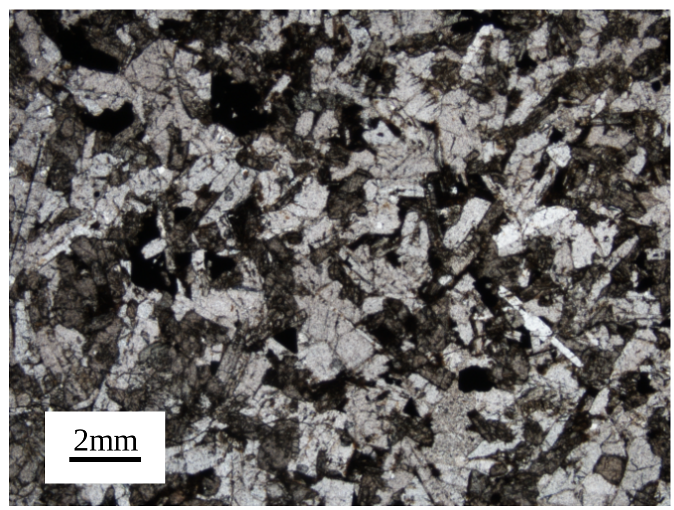

| | |
|---|---|
| Thin Section<br>Rock Type<br>MBSF<br>ODP ID | GIL 41<br>Basalt, massive<br>314<br>1713608 |
| Overall Grain Size | Medium grain (1-1.5mm), groundmass <0.1mm |
| Textures | The myrmekitic texture is abundant in this sample; very few grains of plagioclase have not interacted with quartz. |
| Alteration/ Replacements | Not much alteration, a little chlorite may be present, but what it is replacing is unknown. |
| Notes | Vesicles with no alteration are present in this sample, which is not common. |

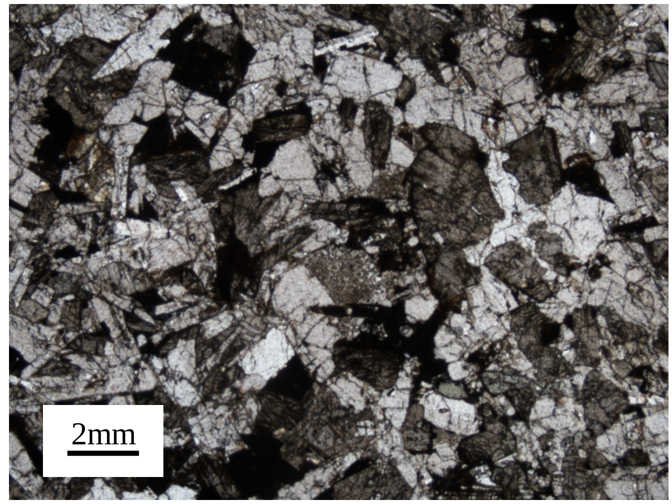


| | |
|---|---|
| Thin Section<br>Rock Type<br>MBSF<br>ODP ID | GIL 42<br>Basalt, massive<br>323<br>1713609 |
| Overall Grain Size | Medium grain (1-2mm), groundmass <0.1mm |
| Textures | Myrmekitic texture is present, however not affecting every plagioclase mineral. |
| Alteration/ Replacements | Not much alteration, a little chlorite may be present, but what it is replacing is unknown. |
| Notes | Again unaltered vesicles are present, often around 0.5mm |

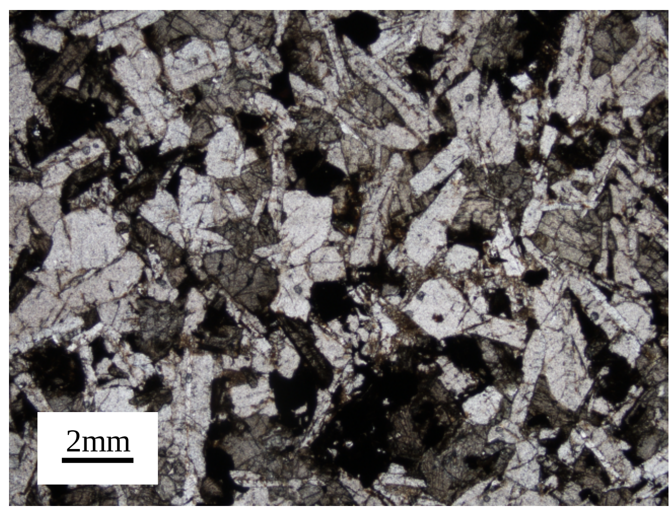

| | |
|---|---|
| Thin Section<br>Rock Type<br>MBSF<br>ODP ID | GIL 44<br>Basalt, massive<br>332<br>1713625 |
| Overall Grain Size | Fine grain (0.5-1mm) |
| Textures | A few plagioclase grains have a visible myrmekitic texture, confirming the presence of quartz in the sample. |
| Alteration/ Replacements | Clay is common along grain boundaries and fractures in this sample, and thus is replacing a number of minerals. |
| Notes | Chlorite is not present in this sample. Vesicles are present. |

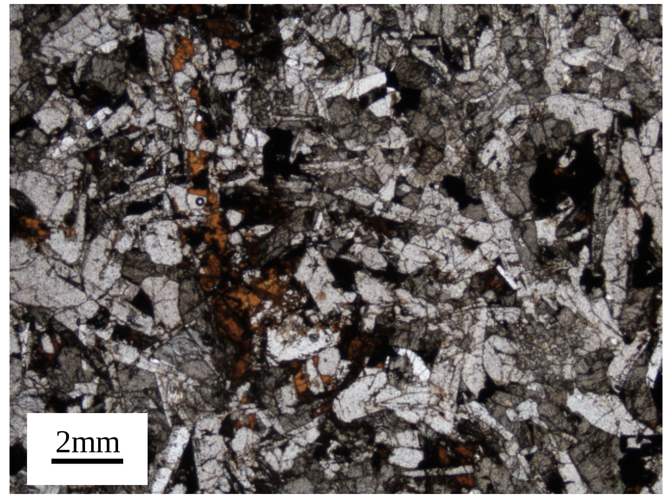


| | |
|---|---|
| Thin Section<br>Rock Type<br>MBSF<br>ODP ID | GIL 45<br>Basalt, massive<br>342<br>1713626 |
| Overall Grain Size | Fine to medium grain (0.5-1.5mm) |
| Textures | A few plagioclase grains have a visible myrmekitic texture, confirming the presence of quartz in the sample. |
| Alteration/ Replacements | Clay seems to be replacing glass, based on the presence of glass near the mineral, relatively abundant in this sample. |
| Notes | Vesicles are present. |

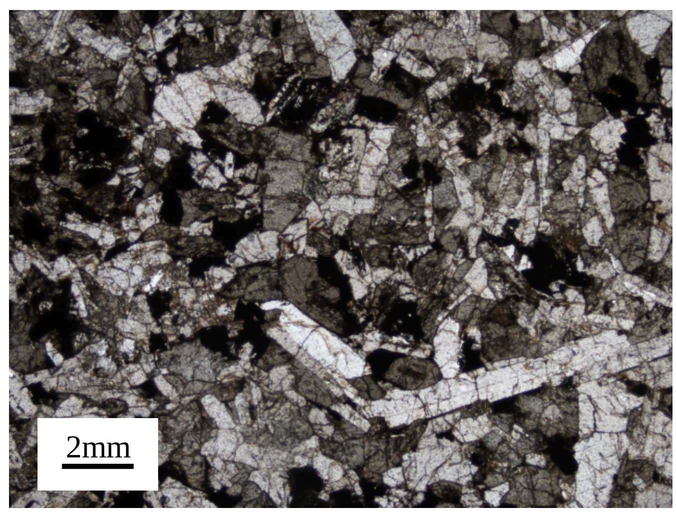

| | |
|---|---|
| Thin Section<br>Rock Type<br>MBSF<br>ODP ID | GIL 46<br>Basalt, massive<br>350<br>1713627 |
| Overall Grain Size | Fine grain (0.2-0.7mm), groundmass <0.1mm |
| Textures | Porphyritic, with phenocrysts of Clay. A sample with relatively no texture. |
| Alteration/ Replacements | Clay is somewhat common and seems to have replaced olivine, due to the habit and unique fracturing. |
| Notes | Although the opaque minerals are both blocky and fibrous, they are all ulvospinel, based on EMP analysis of similar sample. |

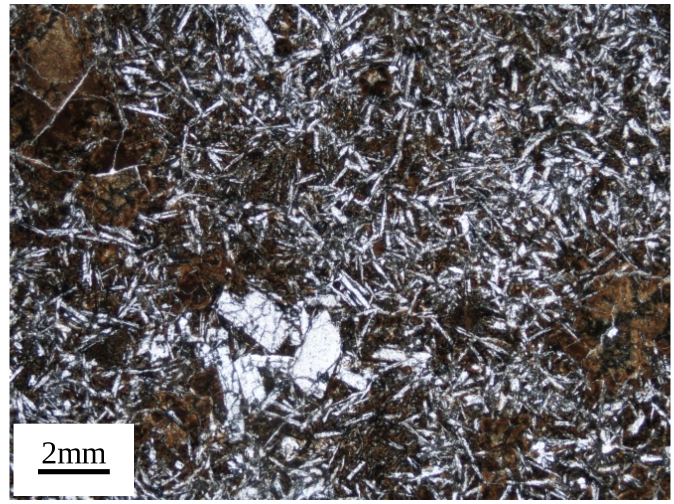


| | |
|---|---|
| Thin Section<br>Rock Type<br>MBSF<br>ODP ID | GIL 47<br>Basalt, massive<br>361<br>1713638 |
| Overall Grain Size | Fine grain (0.2-0.8mm), phenocrysts ~1mm, groundmass <0.1mm |
| Textures | Porphyritic, with phenocrysts of plagioclase, clinopyroxene, and Clay. |
| Alteration/ Replacements | Clay fills vesicles and replaces glass; glass is still present in the center of some vesicles. |
| Notes | Although the opaque minerals are both blocky and fibrous, they are all ulvospinel, based on EMP analysis of similar sample. |

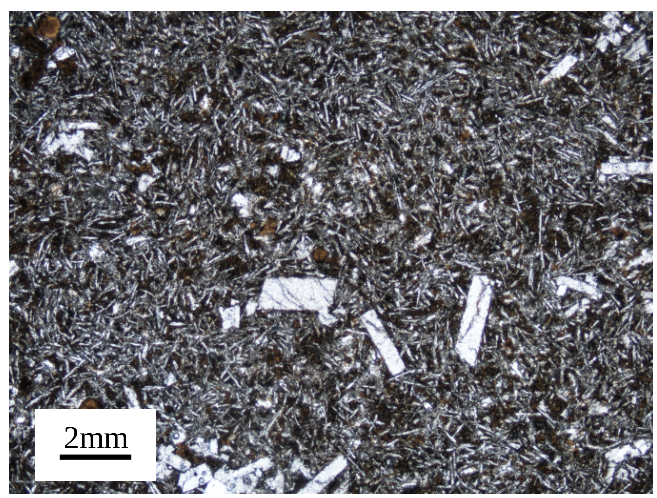

| | |
|---|---|
| Thin Section<br>Rock Type<br>MBSF<br>ODP ID | GIL 27<br>Basalt, massive<br>475<br>1713640 |
| Overall Grain Size | Fine grain (0.2-0.4mm), areas of groundmass <0.1mm |
| Textures | Minerals do not show any relationship and no distinctive texture in this sample. |
| Alteration/ Replacements | Clay replaces what appears to be glass, based on the shape being almost being perfectly circular. |
| Notes | |

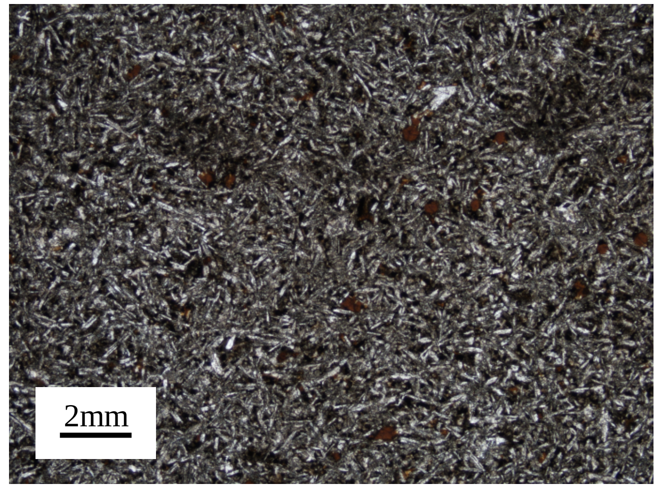


| | |
|---|---|
| Thin Section<br>Rock Type<br>MBSF<br>ODP ID | GIL 28<br>Basalt, massive<br>482<br>1713641 |
| Overall Grain Size | Fine grain (on avg. 0.3mm), groundmass <0.1mm |
| Textures | Minerals do not show any relationship and no distinctive texture in this sample. |
| Alteration/ Replacements | Clay is replacing what could have been glass, based on the almost circular shape. |
| Notes | The very fine grain groundmass often surrounds the clay vesicles. |

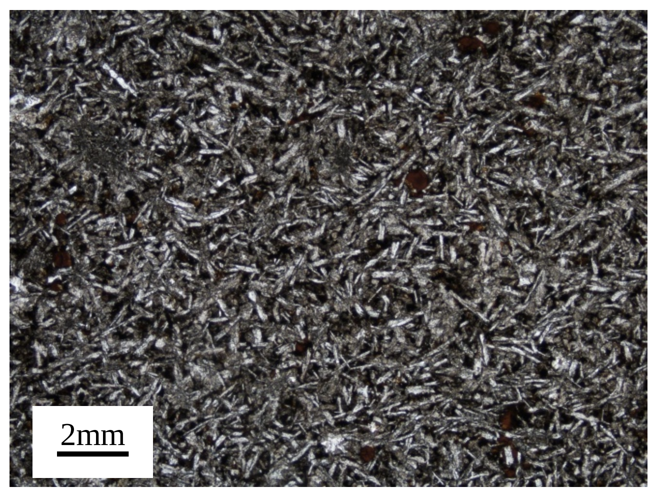

| | |
|---|---|
| Thin Section<br>Rock Type<br>MBSF<br>ODP ID | GIL 29<br>Basalt, sheet flow<br>514<br>1713644 |
| Overall Grain Size | Fine to medium grain (0.5-1.5mm) |
| Textures | Minerals do not show any relationship and no distinctive texture in this sample. |
| Alteration/ Replacements | Clay is replacing what could have been glass, based on the almost circular shape. |
| Notes | Opaque minerals with a blocky and fibrous habit are present, but both are ulvospinel based on the EMP analysis of other samples. |

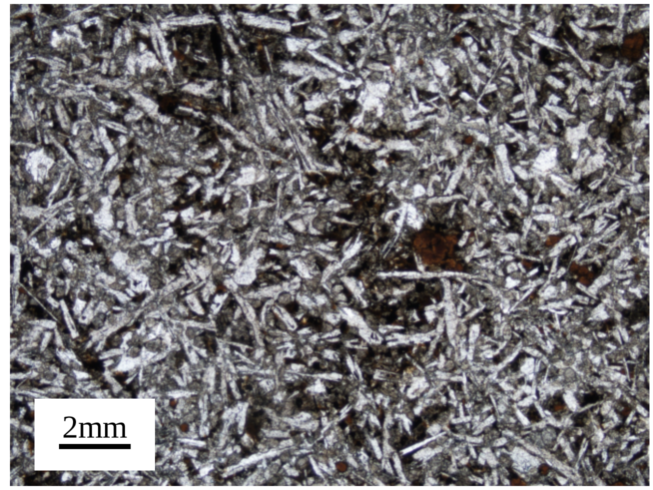


| | |
|---|---|
| Thin Section<br>Rock Type<br>MBSF<br>ODP ID | GIL 30<br>Basalt, sheet flow<br>578<br>1713700 |
| Overall Grain Size | Fine grain phenocrysts (0.1-0.3mm), groundmass (most abundant) is <0.1mm |
| Textures | Aphanitic, most of the sample is so fine grain that no microscope texture is even visible. |
| Alteration/ Replacements | Clay is replacing glass, often located in vesicles where the very center is unaltered glass. |
| Notes | Phenocrysts are plagioclase and clinopyroxene and are throughout the sample |

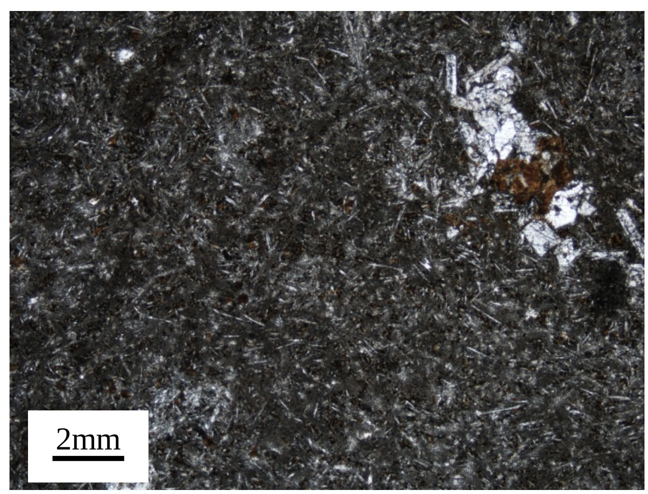

| | |
|---|---|
| Thin Section<br>Rock Type<br>MBSF<br>ODP ID | GIL 31<br>Basalt, sheet flow<br>619<br>1713701 |
| Overall Grain Size | Fine grain (on avg. 0.5mm), groundmass <0.1mm |
| Textures | Radiating intergrowths of plagioclase and clinopyroxene are present, often surrounded by the groundmass. |
| Alteration/ Replacements | Clay is present, often in small circles, therefore the original mineral is unknown (maybe clinopyroxene, or small vesicles) |
| Notes | Both blocky and fibrous opaque minerals are often contained to the groundmass, and are both ulvospinel. |

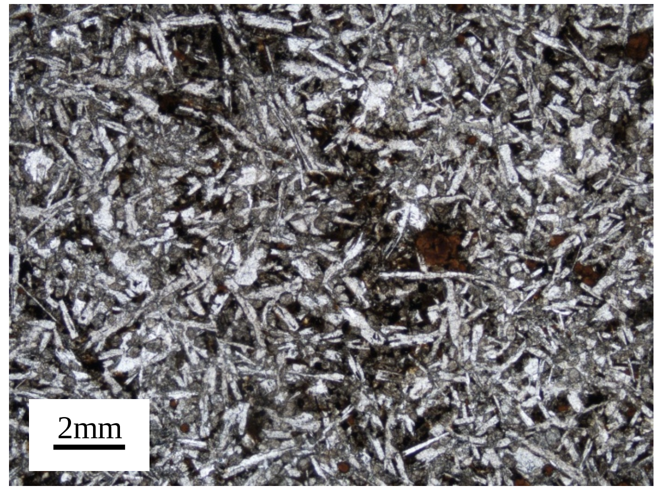


| | |
|---|---|
| Thin Section<br>Rock Type<br>MBSF<br>ODP ID | GIL 32<br>Basalt, sheet flow<br>660<br>1713703 |
| Overall Grain Size | Fine grain (0.2-0.5mm), groundmass <0.1mm |
| Textures | Relatively equigranular, with radiating intergrowths of plagioclase and clinopyroxene. |
| Alteration/ Replacements | Clay replaces what may be olivine based on shape, size, and distinctive fracturing. However this is only an assumption. |
| Notes | Blocky and fibrous opaque minerals are present, but both are ulvospinel. |

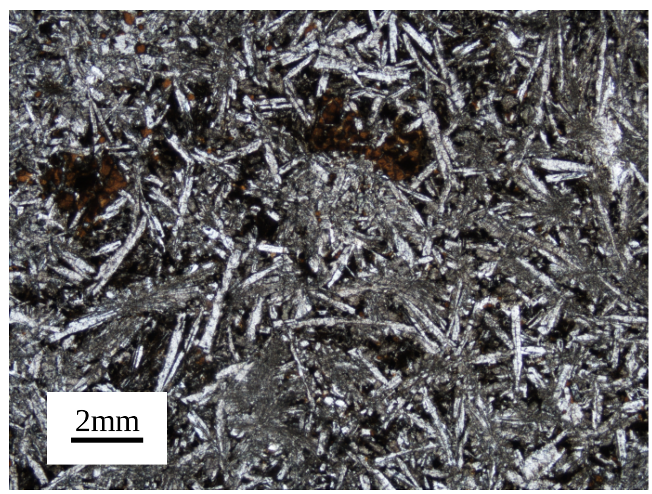

| | |
|---|---|
| Thin Section<br>Rock Type<br>MBSF<br>ODP ID | GIL 33<br>Basalt, sheet flow<br>715<br>1713716 |
| Overall Grain Size | Fine grain (0.4-1mm), groundmass <0.1mm |
| Textures | In some cases plagioclase and clinopyroxene are present in radiating intergrowths. |
| Alteration/ Replacements | Clay is abundant in this sample, and is located in concentrated areas. In some cases the center of the clay is glass; therefore the clay may be replacing glass. |
| Notes | Vesicles are present, but not abundant. |

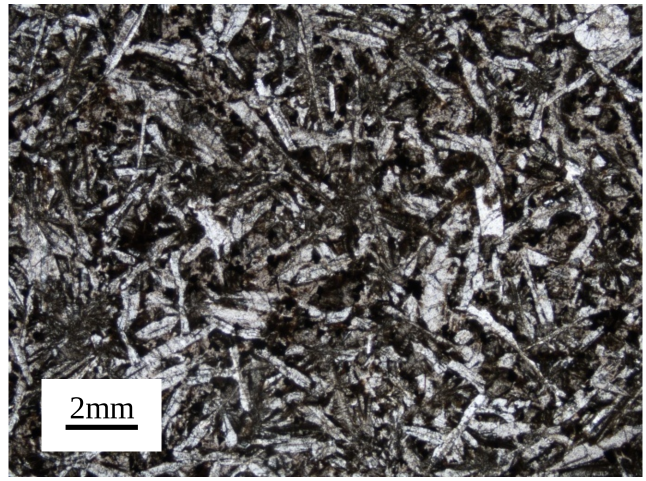


| | |
|---|---|
| Thin Section<br>Rock Type<br>MBSF<br>ODP ID | GIL 34<br>Basalt, sheet flow<br>716<br>1713740 |
| Overall Grain Size | Fine grain (0.1-0.3mm), groundmass <0.1mm |
| Textures | Radiating intergrowths of plagioclase and clinopyroxene are present. |
| Alteration/ Replacements | Clay is replacing an unknown; unfortunately there are no signs of the original mineral. Chlorite is also replacing an unknown in the groundmass, but only minor amounts |
| Notes | The groundmass in this sample has a green tinge in some areas; this may mean that some alteration to chlorite is occurring within the very fine grain groundmass. |

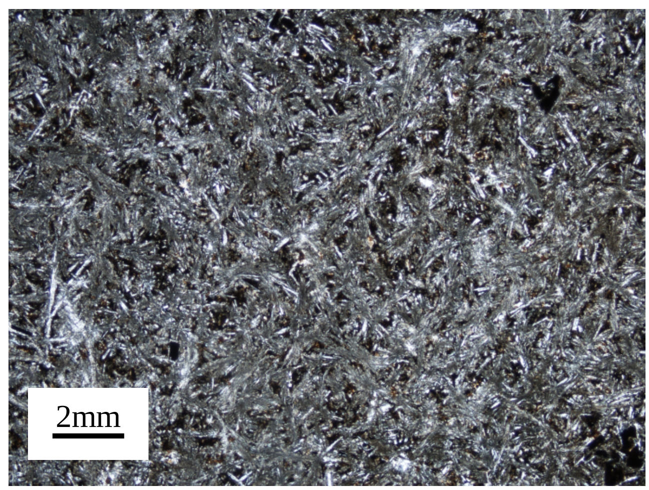

| | |
|---|---|
| Thin Section<br>Rock Type<br>MBSF<br>ODP ID | GIL 01<br>Basalt, sheet flow<br>772<br>1588048 |
| Overall Grain Size | Fine grain throughout (0.1-0.3mm), some phenocrysts up to 1mm. A groundmass of minerals <0.1mm is present. |
| Textures | Intergrowths of clinopyroxene and plagioclase are abundant throughout and often form a radiating texture. |
| Alteration/ Replacements | Replacement of what appears to be olivine (because of shape and fractures) by clay |
| Notes | Only blocky opaque minerals exist in this sample and are ulvospinel (if consistent with sample analyzed by EMP) |

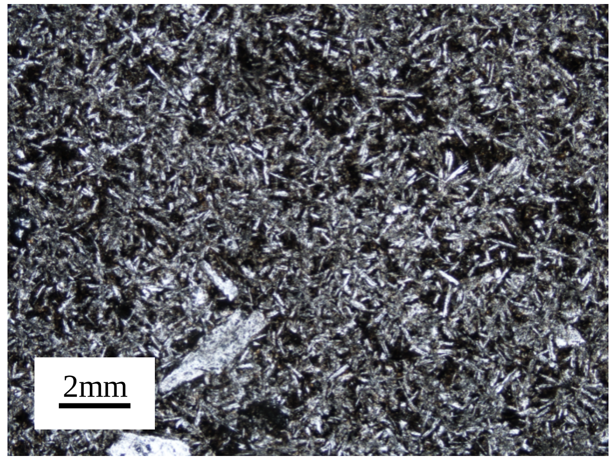


| | |
|---|---|
| Thin Section<br>Rock Type<br>MBSF<br>ODP ID | GIL 02<br>Basalt, massive<br>818<br>1588052 |
| Overall Grain Size | Medium grain throughout, but more variable (0.5-1mm) |
| Textures | Plagioclase and opaque minerals are equigranular throughout the sample however clinopyroxene is not equigranular. |
| Alteration/ Replacements | Vesicles are present (up to 1mm in diameter) and are altered around the rims to clay. |
| Notes | The vesicles are almost perfectly circular and often are rimmed by clay and contain glass in the center. Furthermore the clay is interstitially grown in this sample often with the opaque minerals. |

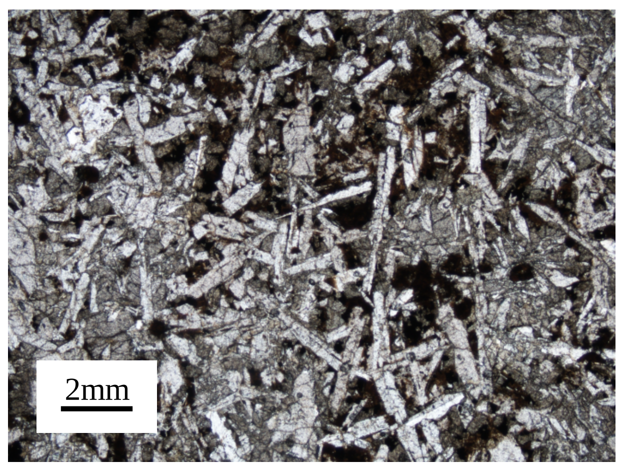

| | |
|---|---|
| Thin Section<br>Rock Type<br>MBSF<br>ODP ID | GIL 03<br>Basalt, massive<br>823<br>1588083 |
| Overall Grain Size | Varies throughout the sample, relatively fine grain (<0.1-1.2mm) |
| Textures | Inequigranular throughout. Plagioclase and clinopyroxene are intergrown with one another again and have a slight radiating texture. |
| Alteration/Replacements | Clay has replaced glass (based on the interstitially grown grains, and lack of habit) |
| Notes | Plagioclase can be very difficult to identify |

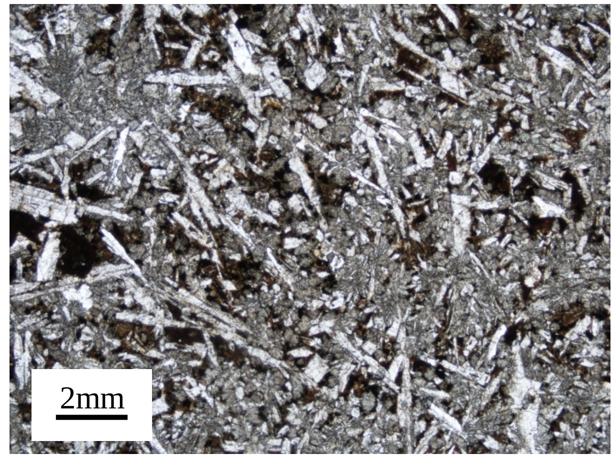


| | |
|---|---|
| Thin Section<br>Rock Type<br>MBSF<br>ODP ID | GIL 04<br>Basalt, sheet flow<br>842<br>1588149 |
| Overall Grain Size | Majority of sample is between 0.1-0.6mm, with phenocrysts up to 1.2mm and a groundmass <0.1mm. |
| Textures | The majority of the sample is intergrowths of radiating plagioclase and clinopyroxene. |
| Alteration/ Replacements | Smectite may replace glass in the groundmass (but this is not definite); it appears as a light brown colour in the groundmass. |
| Notes | Plagioclase can be very difficult to identify. |

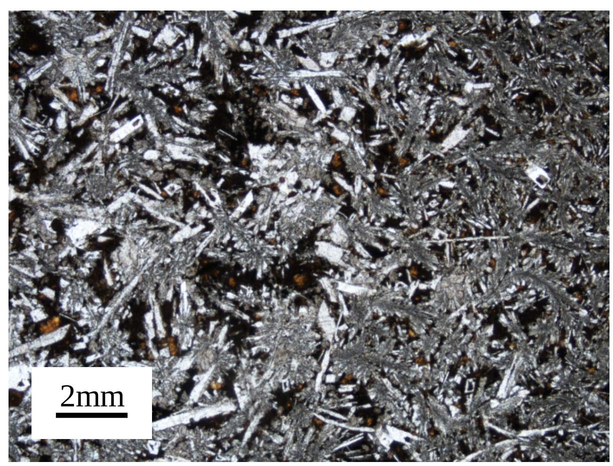

| | |
|---|---|
| Thin Section<br>Rock Type<br>MBSF<br>ODP ID | GIL 05<br>Basalt, sheet flow<br>908<br>1589676 |
| Overall Grain Size | Fine grain (0.1mm-0.5mm0, with a groundmass <0.1mm. |
| Textures | Relatively equigranular, intergrowths of radiating plagioclase and clinopyroxene are abundant. |
| Alteration/ Replacements | Clay has replaced an unknown mineral; it is found throughout the sample however no characteristic habits are visible to identify the original mineral. |
| Notes | The presence of orthopyroxene is questionable, although parallel extinction was observed the sample is relatively fine grain and was difficult to determine exactly. |

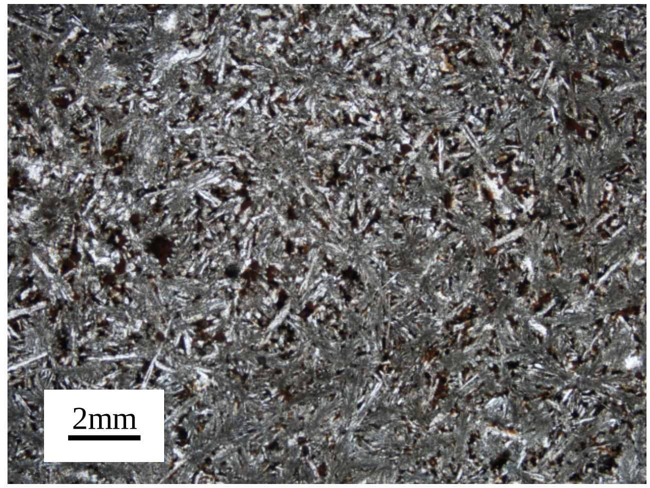


| | |
|---|---|
| Thin Section<br>Rock Type<br>MBSF<br>ODP ID | GIL 06<br>Basalt, massive<br>927<br>1588631 |
| Overall Grain Size | Fine grain (0.1-0.5mm), plagioclase is the only coarse-grained mineral (up to 1mm) |
| Textures | Intergrowths of radiating plagioclase and clinopyroxene. Interstitially grown clay. |
| Alteration/ Replacements | Clay replaces an unknown mineral |
| Notes | Thin section had been cracked and glued back together, making areas very hard/impossible to determine mineralogy. |

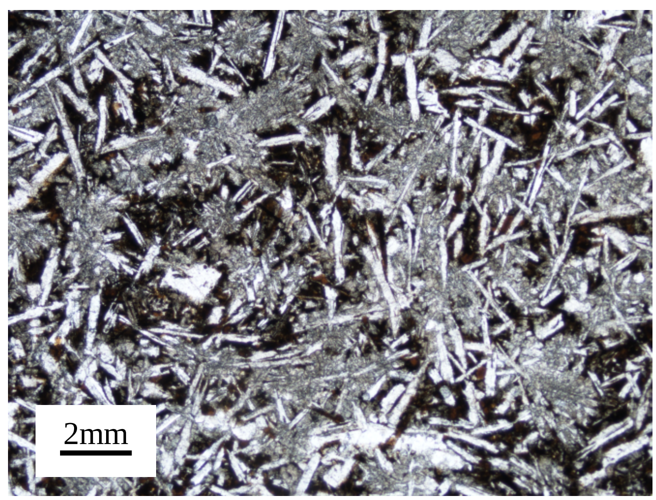

| | |
|---|---|
| Thin Section<br>Rock Type<br>MBSF<br>ODP ID | GIL 07<br>Basalt, massive<br>946<br>1588632 |
| Overall Grain Size | Fine grain (<0.1-0.3mm), with some phenocrysts of plagioclase. |
| Textures | Porphyritic, with intergrowths of radiating plagioclase and clinopyroxene. |
| Alteration/ Replacements | Clay is present, often in fracture zones or interstitially grown, may have replaced glass. |
| Notes | So fine grain that the pyroxene was difficult to identify, however based on previous samples it is classified as clinopyroxene. |

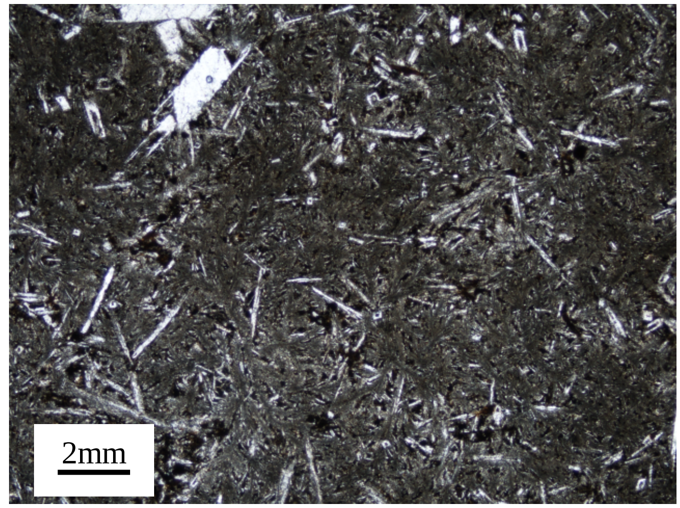


| | |
|---|---|
| Thin Section<br>Rock Type<br>MBSF<br>ODP ID | GIL 08<br>Basalt, massive<br>972<br>1588630 |
| Overall Grain Size | Medium grain (0.4-1.4mm), with finer opaque minerals (0.2-0.5mm) |
| Textures | Relatively similar textures throughout, with intergrowths of radiating plagioclase and clinopyroxene |
| Alteration/ Replacements | Clay replaces an unknown (possibly olivine) mineral, but is found in fractures and interstitially grown. |
| Notes | |

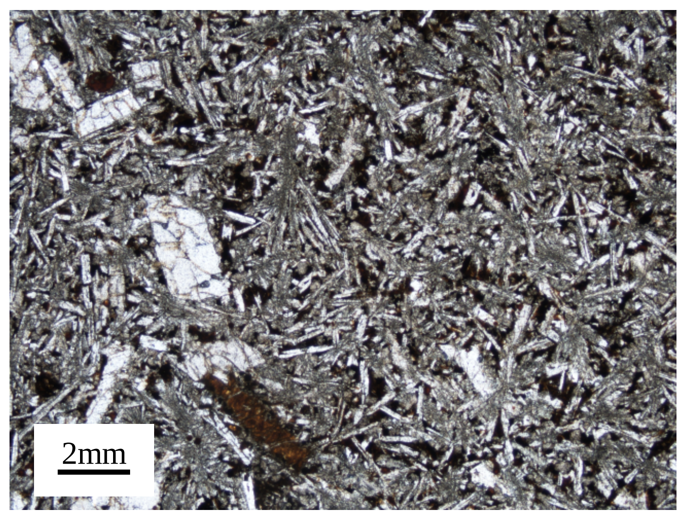

| | |
|---|---|
| Thin Section<br>Rock Type<br>MBSF<br>ODP ID | GIL 09<br>Basalt, massive<br>995<br>1588924 |
| Overall Grain Size | Fine grain (<0.1-0.3mm), phenocrysts up to 1.0mm |
| Textures | Porphyritic, with intergrowths of radiating plagioclase and clinopyroxene |
| Alteration/ Replacements | Clay replaces an unknown mineral, but is found in fractures and interstitially grown. |
| Notes | Opaque minerals and clay are often found together. |

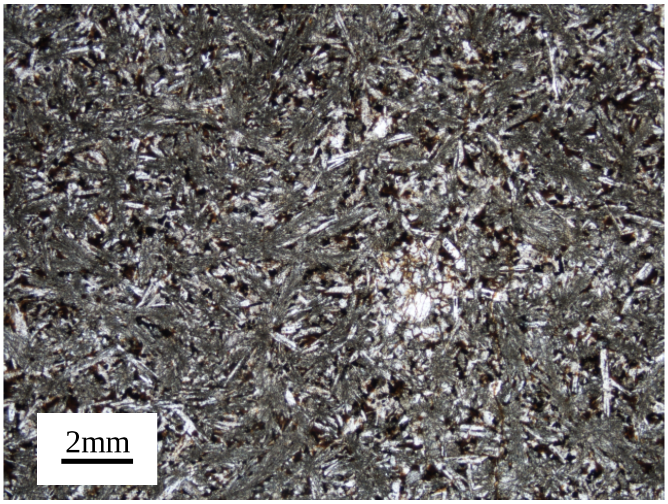


| | |
|---|---|
| Thin Section<br>Rock Type<br>MBSF<br>ODP ID | GIL 10<br>Basalt, dikes<br>1008<br>1588684 |
| Overall Grain Size | Varies drastically (0.5-2.5mm) |
| Textures | With the presence of quartz, plagioclase now has a myrmekitic texture. |
| Alteration/ Replacements | Clay present often in vesicles therefore could be a replacement of glass. |
| Notes | Clay may be surrounded by very fine grain clinopyroxene grains, however too fine grain to be certain. |

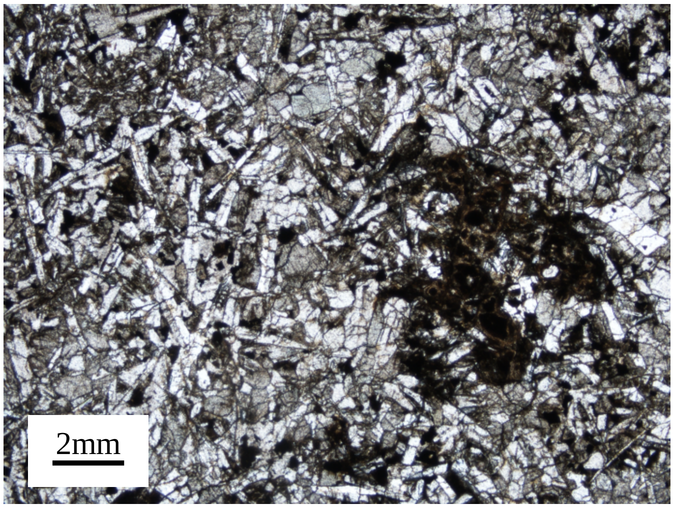

| | |
|---|---|
| Thin Section<br>Rock Type<br>MBSF<br>ODP ID | GIL 11<br>Basalt, dikes<br>1068<br>1588804 |
| Overall Grain Size | Fine grain (0.1-0.6mm) |
| Textures | Plagioclase and quartz interact forming a myrmekitic texture. |
| Alteration/ Replacements | Chlorite replacing an unknown mineral (possibly clinopyroxene) |
| Notes | First significant appearance of chlorite |

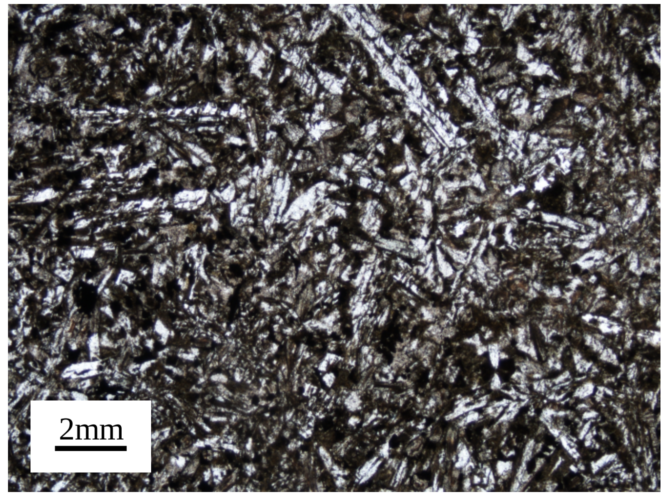


| | |
|---|---|
| Thin Section<br>Rock Type<br>MBSF<br>ODP ID | GIL 12<br>Basalt, dikes<br>1087<br>1588817 |
| Overall Grain Size | Plagioclase and clinopyroxene are fine grain (0.1-0.6mm), groundmass <0.1mm |
| Textures | Intergrowths of radiating plagioclase and clinopyroxene are present, along with areas of myrmekitic plagioclase. |
| Alteration/ Replacements | Chlorite replacing what appears to clinopyroxene |
| Notes | Groundmass is sporadic and located throughout the thin section |

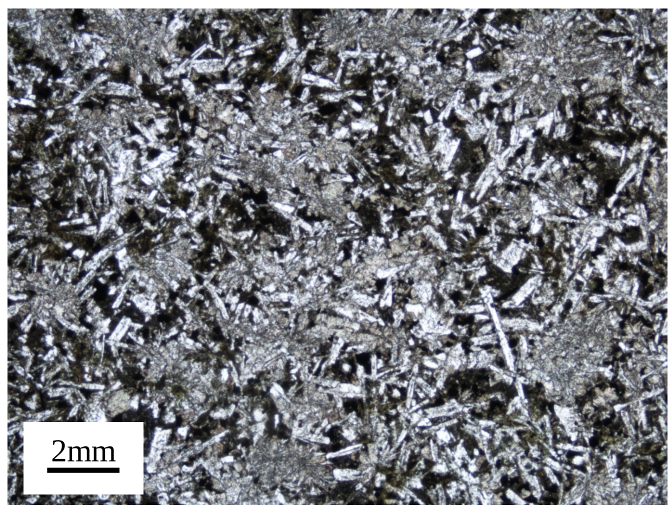

| | |
|---|---|
| Thin Section<br>Rock Type<br>MBSF<br>ODP ID | GIL 13<br>Basalt, dikes<br>1106<br>1588868 |
| Overall Grain Size | Fine grain (0.1-0.8mm) |
| Textures | Some myrmekitic texture, but not abundant. |
| Alteration/ Replacements | Chlorite replaces an unknown |
| Notes | Fibrous opaque minerals are more visible now, not just blocky opaque minerals. |

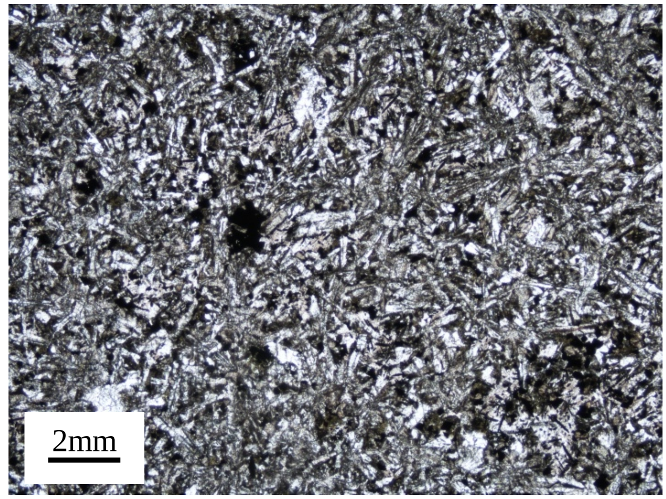


| | |
|---|---|
| in Section<br>Rock Type<br>MBSF<br>ODP ID | GIL 14<br>Basalt, dikes<br>1125<br>1589390 |
| Overall Grain Size | Fine to medium grain (0.5-1.3mm) |
| Textures | Intergrowths of plagioclase and clinopyroxene but no obvious radial patterns. Myrmekitic textures are visible but not abundant. |
| Alteration/ Replacements | Chlorite replaces an unknown, however is often interstitially grown. |
| Notes | At first epidote was thought to be present, but with no parallel extinction it was determined to be clinopyroxene. |

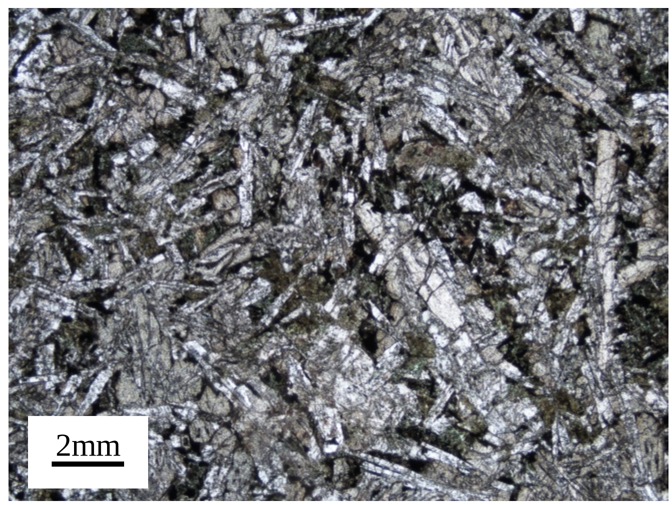

| | |
|---|---|
| Thin Section<br>Rock Type<br>MBSF<br>ODP ID | GIL 15<br>Basalt, dikes<br>1181<br>1589494 |
| Overall Grain Size | Fine grain (0.1-0.8mm) |
| Textures | Plagioclase and clinopyroxene are relatively equigranular. The myrmekitic texture is abundant due to an increase in quartz. |
| Alteration/ Replacements | Chlorite has replaced an unknown |
| Notes | Quartz has increased in this sample so much so that an area is completely quartz. The quartz is equigranular (approx. 0.5mm) and has no sign of alteration or deformation. |

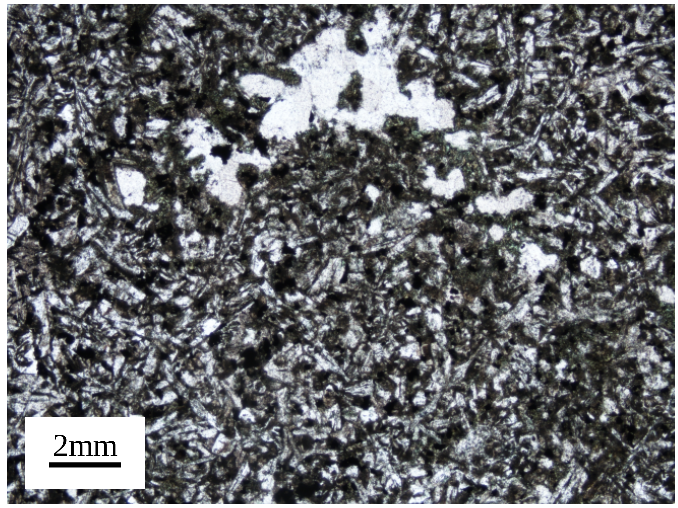


| | |
|---|---|
| Thin Section<br>Rock Type<br>MBSF<br>ODP ID | GIL 16<br>Basalt, dikes<br>1204<br>1589546 |
| Overall Grain Size | Fine grain (0.1-1mm). Groundmass <0.1mm |
| Textures | Plagioclase displays a radiating texture in some areas, and in other areas intergrowths of radiating plagioclase and clinopyroxene are present. |
| Alteration/ Replacements | Chlorite replaces an unknown. |
| Notes | With EMP work some of the opaque minerals were identified to be some kind of sulphide (located in an area of abundant chlorite). More analytical work will have to be done to determine what kind of sulphide is present. Ulvospinel is also present. |

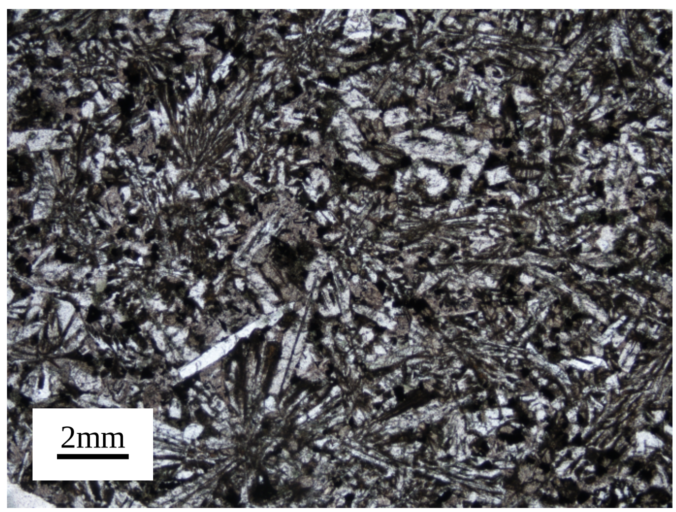

| | |
|---|---|
| Thin Section<br>Rock Type<br>MBSF<br>ODP ID | GIL 17<br>Basalt, dikes<br>1221<br>1589562 |
| Overall Grain Size | Fine grain (0.1-0.5mm), phenocrysts up to 1.5mm. Groundmass <0.1mm |
| Textures | Porphyritic. Intergrowths of radiating plagioclase and clinopyroxene are present. Sample is relatively equigranular. |
| Alteration/ Replacements | Chlorite replaces and unknown. |
| Notes | Section was badly damaged, cracked and glued back together. Epidote is thought to be present in tiny amounts, located in a fracture of a large plagioclase phenocryst. |

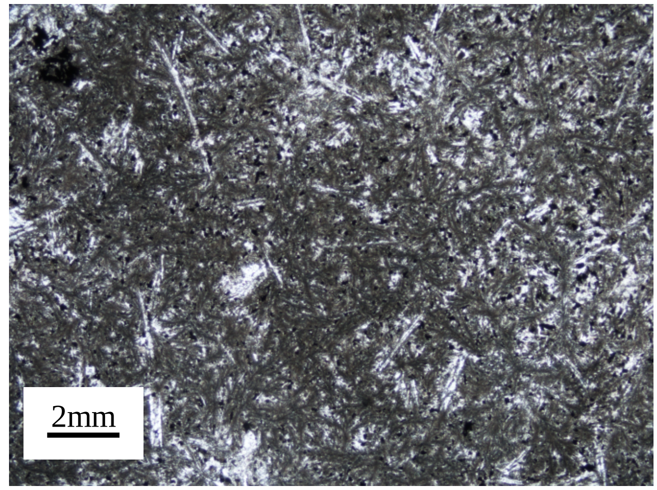


| | |
|---|---|
| Thin Section<br>Rock Type<br>MBSF<br>ODP ID | GIL 18<br>Basalt, dikes<br>1235<br>1589586 |
| Overall Grain Size | Fine grain (0.1-0.6mm), groundmass <0.1mm |
| Textures | Intergrowths of radiating plagioclase and clinopyroxene. |
| Alteration/ Replacements | Chlorite replaces an unknown |
| Notes | Although quartz is present, there is no obvious presence of a myrmekitic texture. |

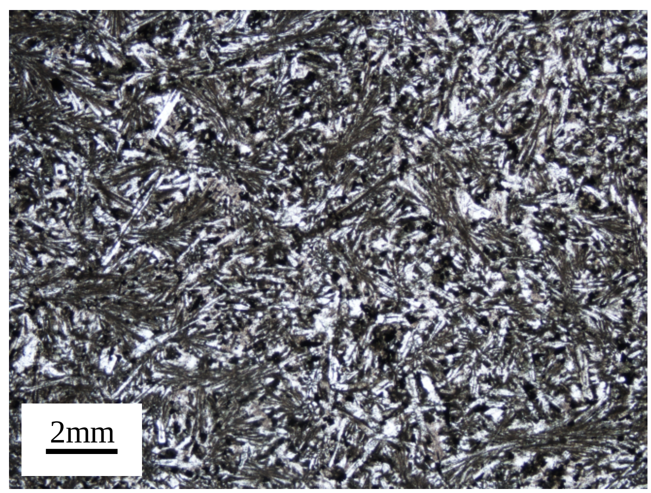

| | |
|---|---|
| Thin Section<br>Rock Type<br>MBSF<br>ODP ID | GIL 19<br>Basalt, dikes<br>1255<br>1589675 |
| Overall Grain Size | Fine grain (0.1-0.5mm), opaque minerals around 0.1mm |
| Textures | Relatively equigranular throughout, with radiating intergrowths of plagioclase and clinopyroxene. Myrmekitic visible on only one plagioclase crystal. |
| Alteration/ Replacements | Chlorite replaces an unknown (possibly clinopyroxene) |
| Notes | Opaque minerals are not spread evenly throughout the sample, but are more concentrated in certain areas. |

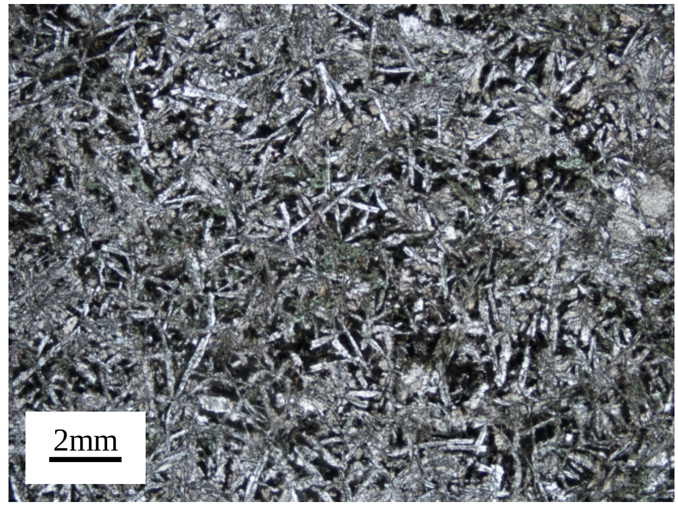


| | |
|---|---|
| Thin Section<br>Rock Type<br>MBSF<br>ODP ID | GIL 22<br>Basalt, dikes<br>1278 |
| Overall Grain Size | Fine grain (0.4-0.7mm), phenocrysts up to 1mm. |
| Textures | Relatively equigranular, porphyritic. Areas of radiating intergrowths of plagioclase and clinopyroxene are present, however not as abundant as other samples. |
| Alteration/ Replacements | Chlorite replaces an unknown (located in the groundmass, and in minor amounts) |
| Notes | |

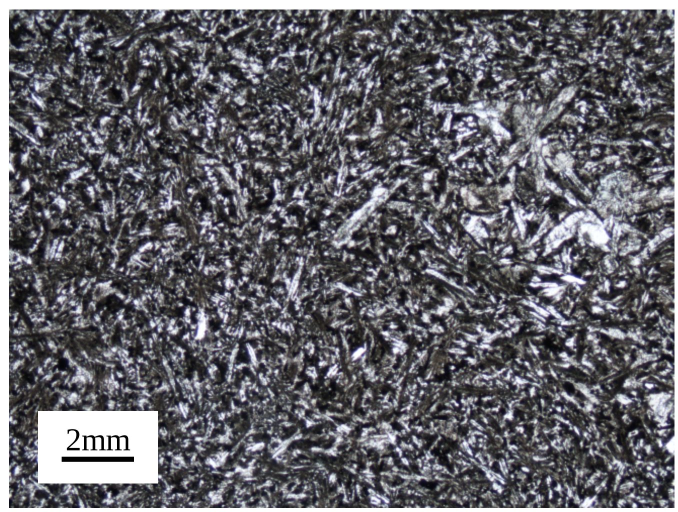

| | |
|---|---|
| Thin Section<br>Rock Type<br>MBSF<br>ODP ID | GIL 20<br>Basalt, dikes<br>1325<br>1713700 |
| Overall Grain Size | Fine grain (0.3-0.6mm) |
| Textures | Relatively equigranular with radiating intergrowths of plagioclase, opaque minerals and clinopyroxene. Myrmekitic texture is present in the plagioclase. |
| Alteration/Replacements | Chlorite replaces an unknown (possibly clinopyroxene) |
| Notes | Chlorite and clinopyroxene were sometimes difficult to tell apart. |

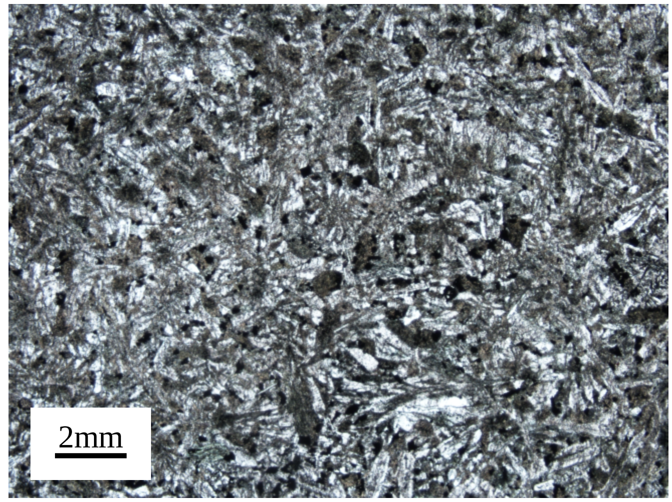


| | |
|---|---|
| Thin Section<br>Rock Type<br>MBSF<br>ODP ID | GIL 23<br>Basalt, dikes<br>1373<br>unknown |
| Overall Grain Size | Fine to medium grain, average size around 1mm |
| Textures | Some myrmekitic texture is visible, but only minor amounts. |
| Alteration/ Replacements | Alteration occurs throughout this sample, most often replaced by actinolite, hornblende, and chlorite. |
| Notes | In transition zone from Basalt to Gabbro. Orthopyroxene is present based on the parallel extinction. |

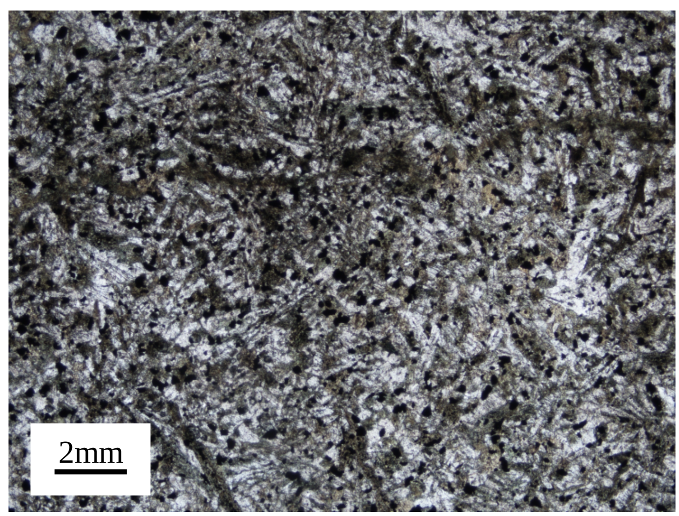

| | |
|---|---|
| Thin Section<br>Rock Type<br>MBSF<br>ODP ID | (48)<br>Basalt, Sheeted dikes<br>1374.9<br>unknown |
| Overall Grain Size | The general grain size is very fine, with the groundmass <0.1mm and the veins include grains between <0.1-0.5mm |
| Textures | Plagioclase grains are euhedral and fresh looking, the clinopyroxene is anhedral and distressed. Veins occur in this slide, however they are not smooth and even and they cross over each other. In areas it looks like clusters of actinolite and not so much a connected vein, but this could be due to the limited size of the slide. |
| Alteration/ Replacements | Actinolite is present in the veins, and possible alteration of the groundmass may have occurred. A clue to this is that the groundmass varies in colour throughout the slide. Due to the fine grain size it is hard to tell if this is due to change in a mineral or if it is just a change in the concentration of the minerals in that area. |
| Notes | A vein of quartz is present in this sample, however due to the small size and its location on the slide it was not counted in the point counts. Opaque minerals are present and abundant in the groundmass, but are equal in size and shape to the rest of the minerals. |

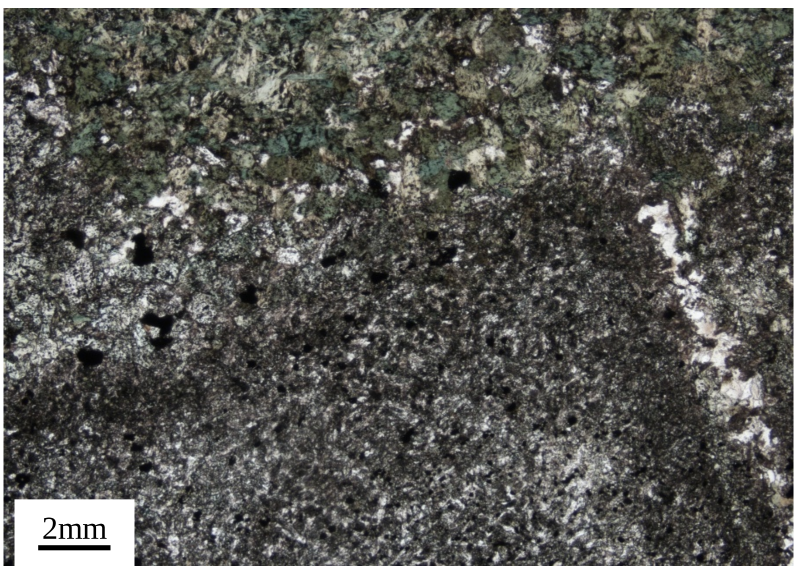

| | |
|---|---|
| Thin Section<br>Rock Type<br>MBSF<br>ODP ID | (49)<br>Basalt, sheeted dikes<br>1382.2<br>unknown |
| Overall Grain Size | General grain size is very fine. The groundmass is <0.1mm, but the size is relatively equal throughout. The veins vary between <0.1-0.3mm. |
| Textures | The groundmass is relatively equigranular throughout; the plagioclase is subhedral with clinopyroxene as anhedral. The veins are fibrous in texture (due to actinolite). One area with approx. 5 grains is up to0.5mm across is present in the groundmass, but that is the only area with significant grain size change. |
| Alteration/Replacements | Actinolite is present in the veins. One thing to note of importance is the area of coarse grains in the groundmass. It appears to be clinopyroxene altered to amphibole, which could be a sign the groundmass is altered as well, but this is not obvious in thin section. |
| Notes | Around the veins parallel areas of colour change in the groundmass occur, this could also be assign of alteration. Opaque minerals are present and abundant in the groundmass, but are equal in size and shape to the rest of the minerals. Quartz is present in the veins, but due to amount and location was not sufficient to be point counted. |

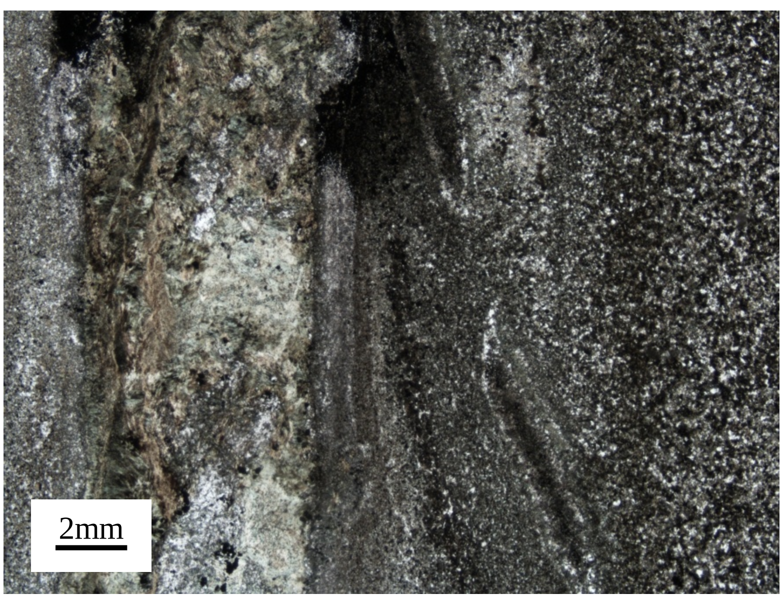

| | |
|---|---|
| Thin Section<br>Rock Type<br>MBSF<br>ODP ID | (51)<br>Basalt, sheeted dikes<br>1387.1<br>unknown |
| Overall Grain Size | General grain size is very fine. The groundmass is <0.1mm, but the size is relatively equal throughout. The veins vary between <0.1-0.5mm. Opaque minerals vary from <0.1-0.2mm. |
| Textures | The plagioclase seems to have become euhedral and fresh looking again, however the clinopyroxene remains anhedral and distressed, the fine grain plagioclase makes the groundmass look fibrous. Similar to previous sample there is one area with a few coarse grains (approx. 0.5mm), but this is the only area with a significant grain size change. |
| Alteration/Replacements | Actinolite is present in the veins. Similar to previous slide the coarse grain minerals appear to be altered clinopyroxene to amphibole, with one grain having captured the alteration. This, along with colour variations, could be a sign of alteration in the groundmass, but again due to the size of the grains an accurate analysis of what is believed to cpx cannot be optically done. |
| Notes | Quartz is present in the veins; due to its location it was included in the point counts. |

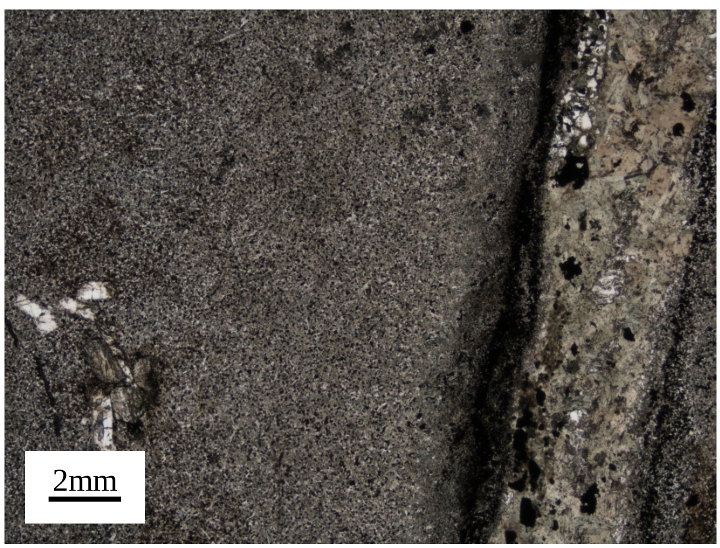

| | |
|---|---|
| Thin Section<br>Rock Type<br>MBSF<br>ODP ID | GIL 24<br>Gabbro<br>1413<br>unknown |
| Overall Grain Size | Fine grain (0.5-1mm) |
| Textures | Actinolite fibrous and when it replaces clinopyroxene, the cpx inherits the fibrous texture. Plagioclase is fresh. |
| Alteration/ Replacements | Chlorite and amphiboles (actinolite and hornblende) are replacing many of the clinopyroxene minerals in this sample. Epidote is present but in minor quantities. |
| Notes | |

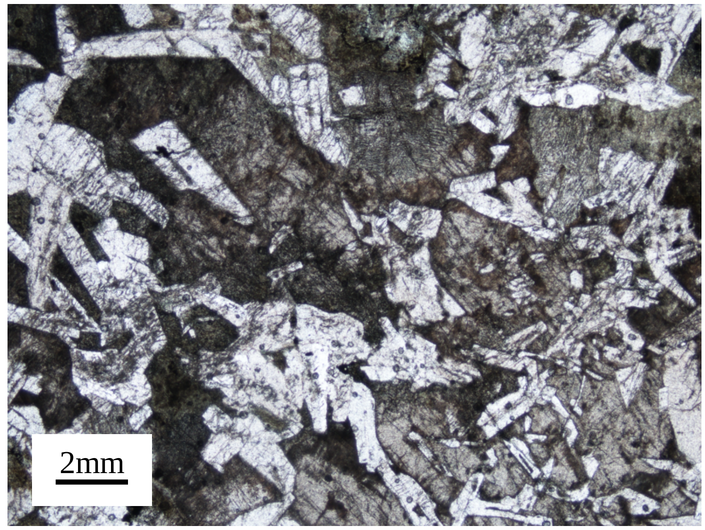


| | |
|---|---|
| Thin Section<br>Rock Type<br>MBSF<br>ODP ID | GIL 25<br>Gabbro<br>1448<br>unknown |
| Overall Grain Size | Medium to coarse grain (up to 5mm) |
| Textures | Actinolite is fibrous, and forms fibrous intergrowths with chlorite and hornblende. |
| Alteration/ Replacements | Epidote seems to be altered by a rim of opaque minerals. Amphiboles (actinolite and hornblende) and chlorite are replacing clinopyroxene throughout the sample. |
| Notes | This is the only rock where olivine was observed, and where the EMP analysis showed olivine. |

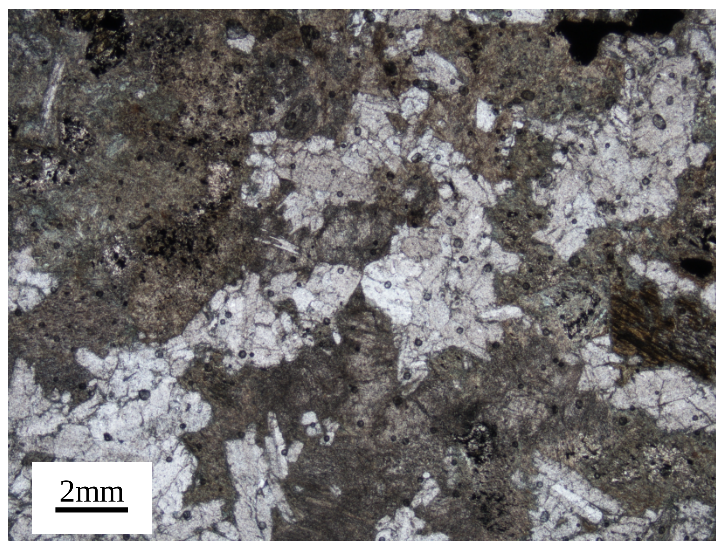

| | |
|---|---|
| Thin Section<br>Rock Type<br>MBSF<br>ODP ID | GIL 21<br>Basalt, dikes<br>1470<br>1609539 |
| Overall Grain Size | Fine grain, majority of grains between 0.4-1.0mm |
| Textures | Inequigranular, a slight ophitic texture. Actinolite is fibrous and forms intergrowths with hornblende. |
| Alteration/ Replacements | Amphibole (actinolite and hornblende) and chlorite are replacing most of the clinopyroxene in the sample |
| Notes | Quartz is not present |

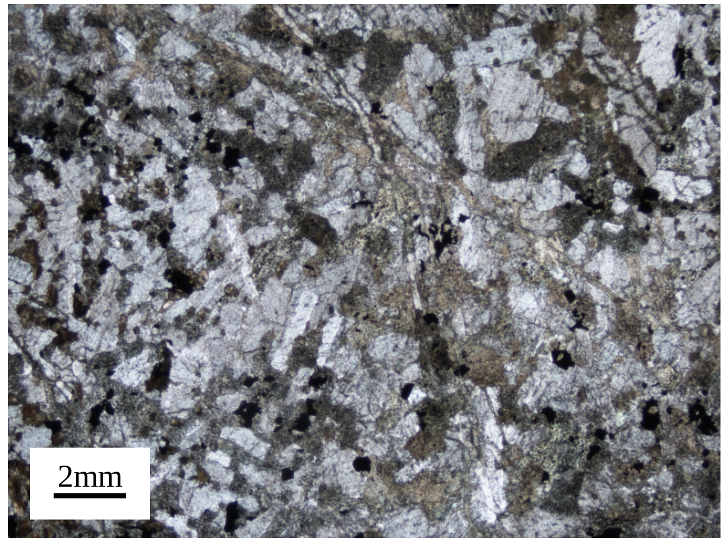


| | |
|---|---|
| Thin Section<br>Rock Type<br>MBSF<br>ODP ID | GIL 26<br>Gabbro<br>1488<br>unknown |
| Overall Grain Size | Fine to medium grain (0.3mm to 2.5mm) |
| Textures | Inequigranular. Actinolite is fibrous and forms intergrowths with hornblende. |
| Alteration/ Replacements | Chlorite and actinolite replace clinopyroxene, and possible primary hornblende |
| Notes | Low modal percentage of opaque minerals. |

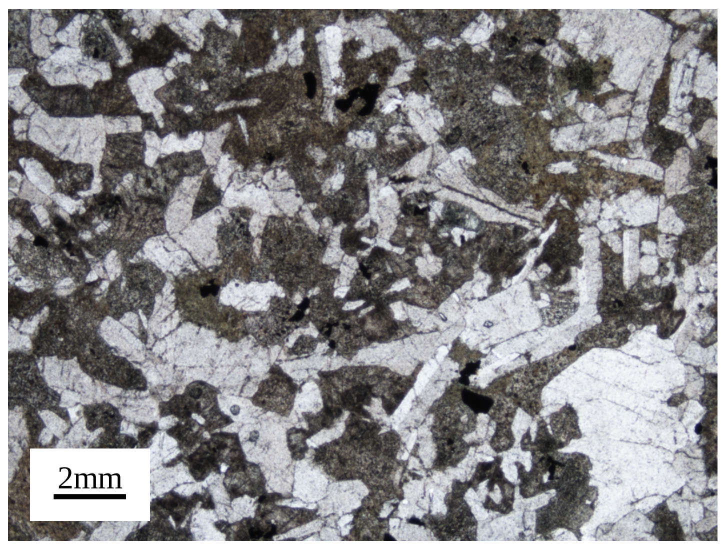

# APPENDIX B
# IODP Hole 1256D: Electron Microprobe Data

The following appendix includes the electron microprobe data collected from six representative thin sections from IODP Hole 1256D. The beginning of this appendix includes the backscatter electron images with the points of analysis marked in red. This marks correlate to the tables of data which are found after the images. The tables include the thin section name, the area of analysis, and the point of analysis. The tables have been organized into the minerals identified (ie: plagioclase, clinopyroxene, etc.). In some circumstances the EMP data collected were not suitable and were not used for this project. The points removed were ones that had total percentages less than 75% and did not represent the mineral being identified.

**Thin Section: GIL 48**
**Rock Type: Basalt, sheet flow**
**MBSF: 253**
**Area of analysis: 1**

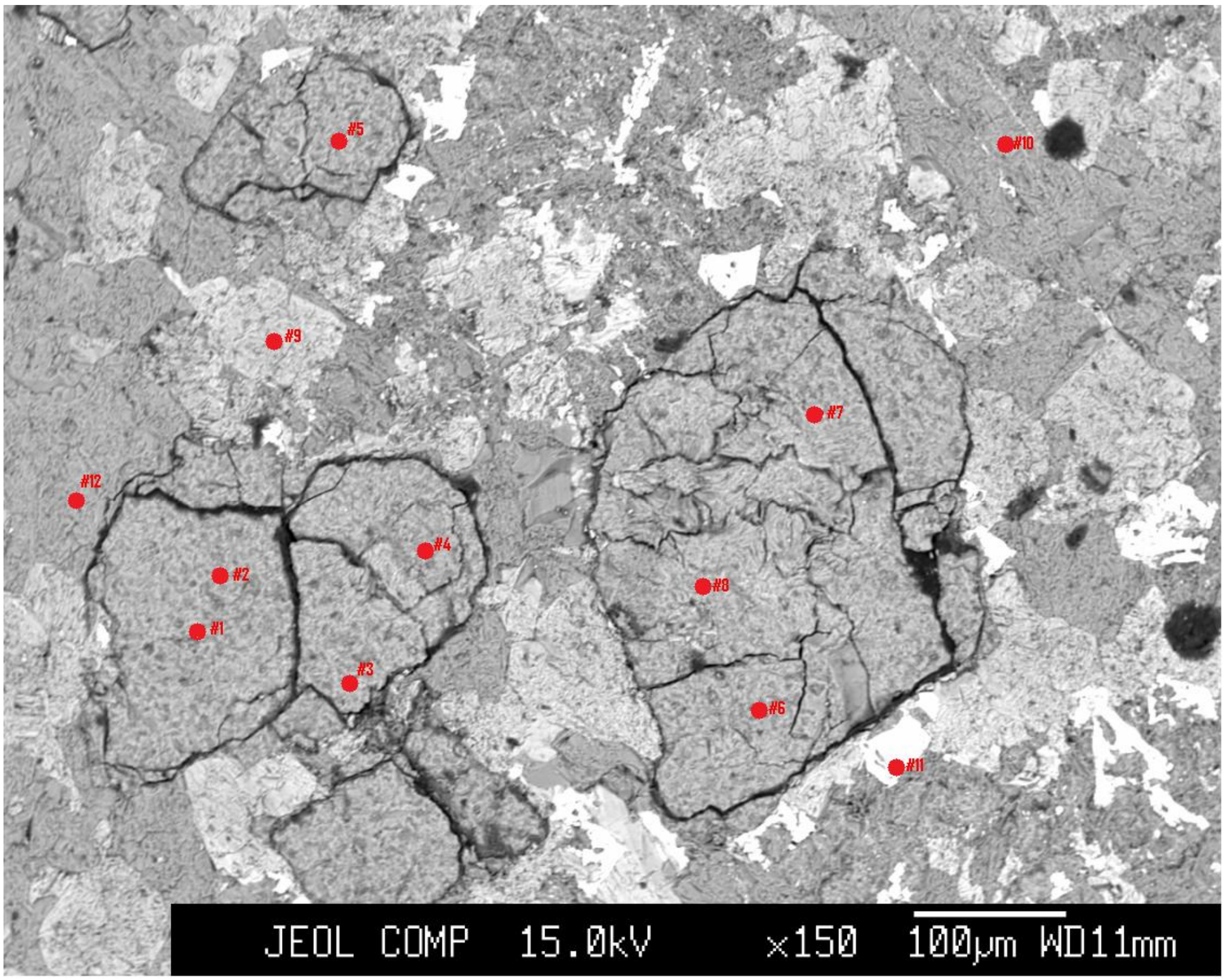

**Thin Section: GIL 48**
**Rock Type: Basalt, sheet flow**
**MBSF: 253**
**Area of analysis: 2**

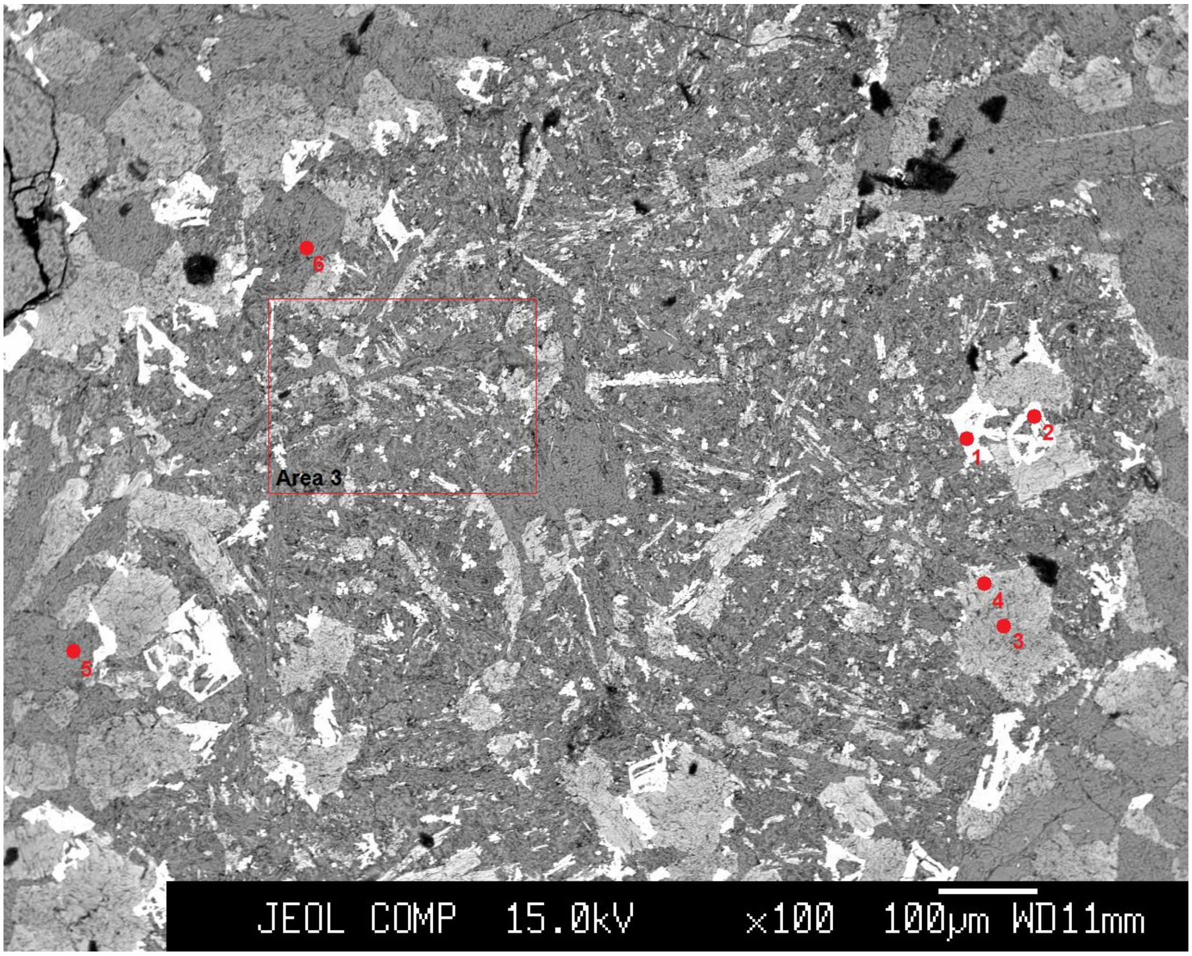

**Thin Section: GIL 48**
**Rock Type: Basalt, sheet flow**
**MBSF: 253**
**Area of analysis: 3**

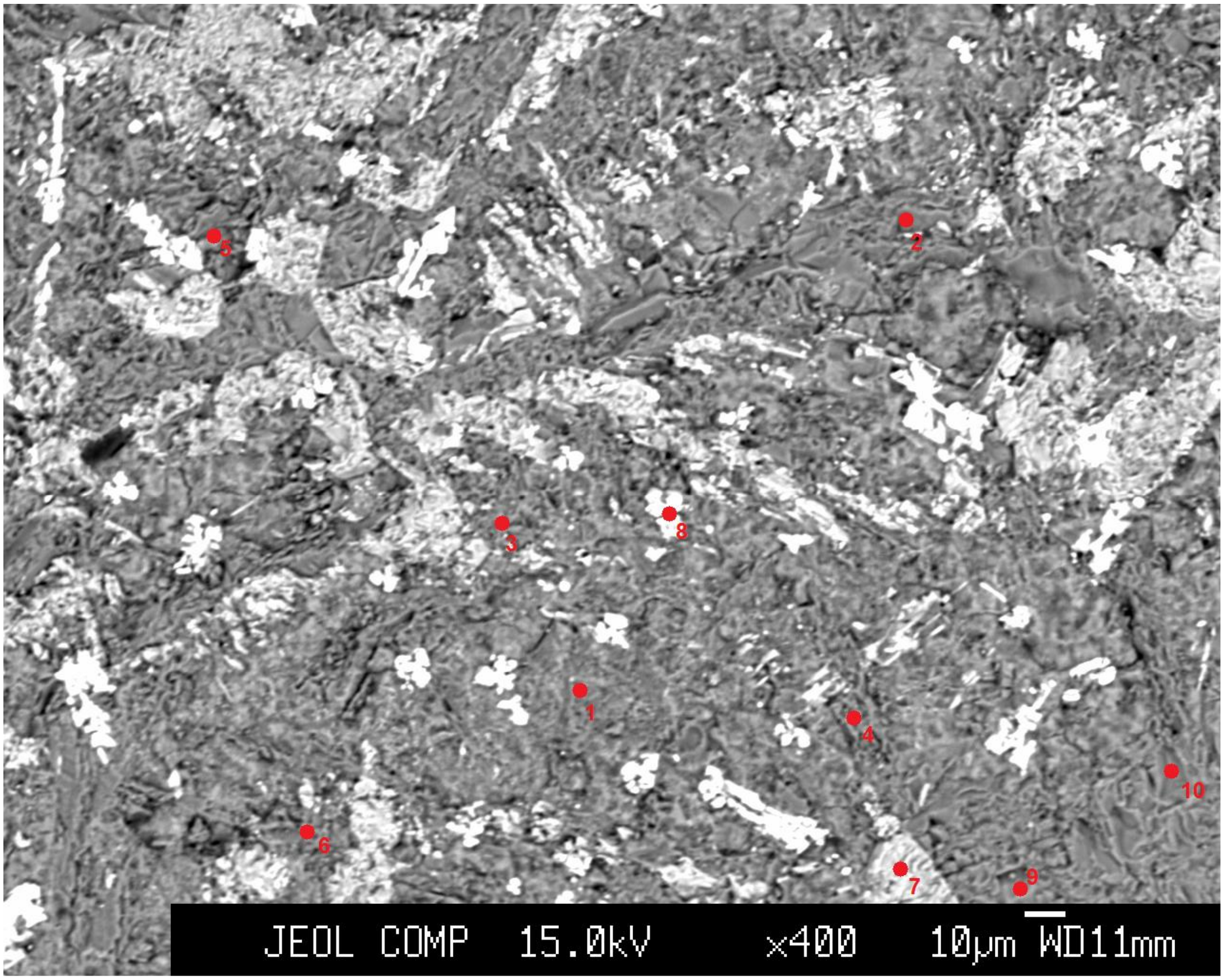

**Thin Section: GIL 49**
**Rock Type: Basalt, sheet flow**
**MBSF: 258**
**Area of analysis: 1**

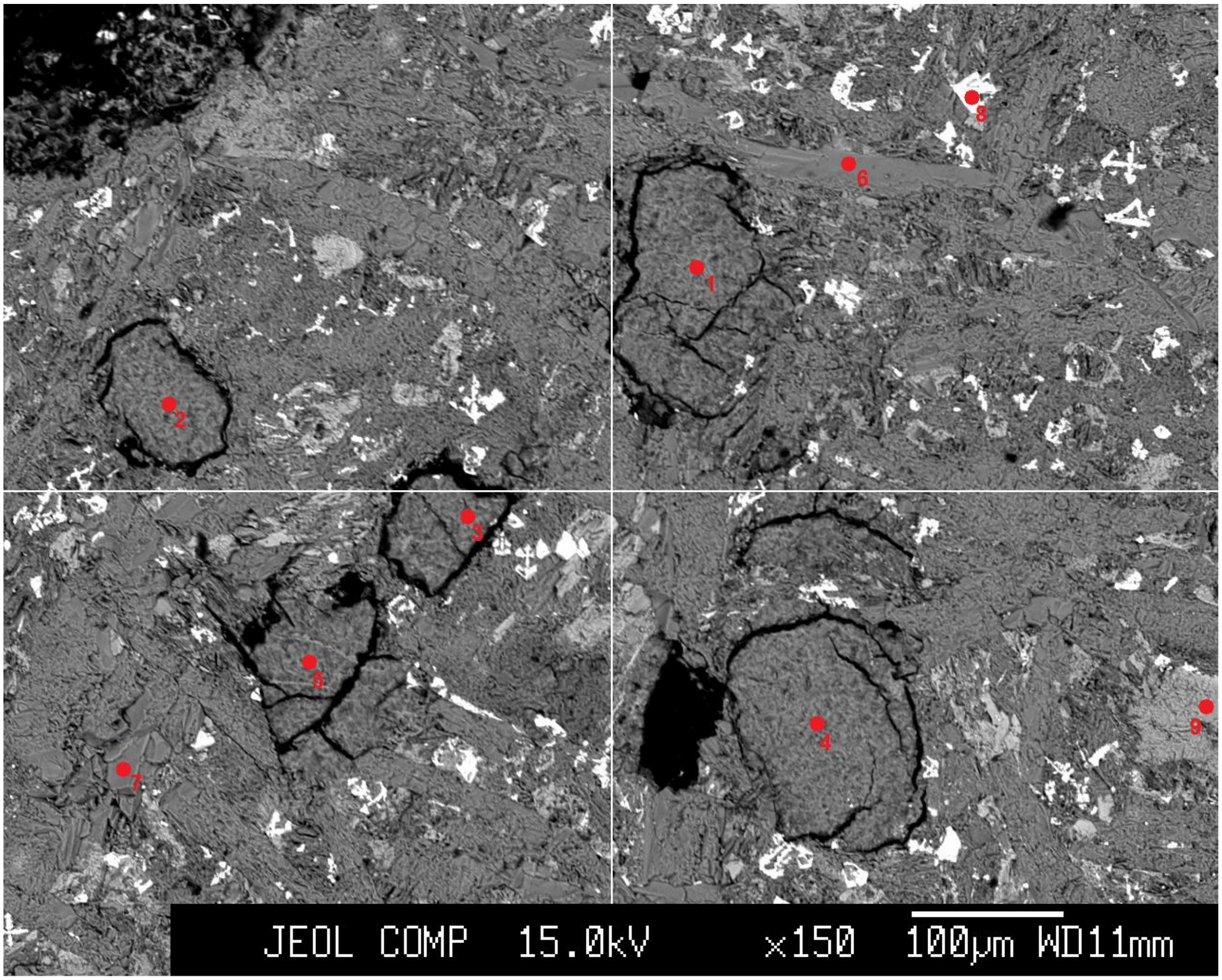

**Thin Section: GIL 49**
**Rock Type: Basalt, sheet flow**
**MBSF: 258**
**Area of analysis: 2**

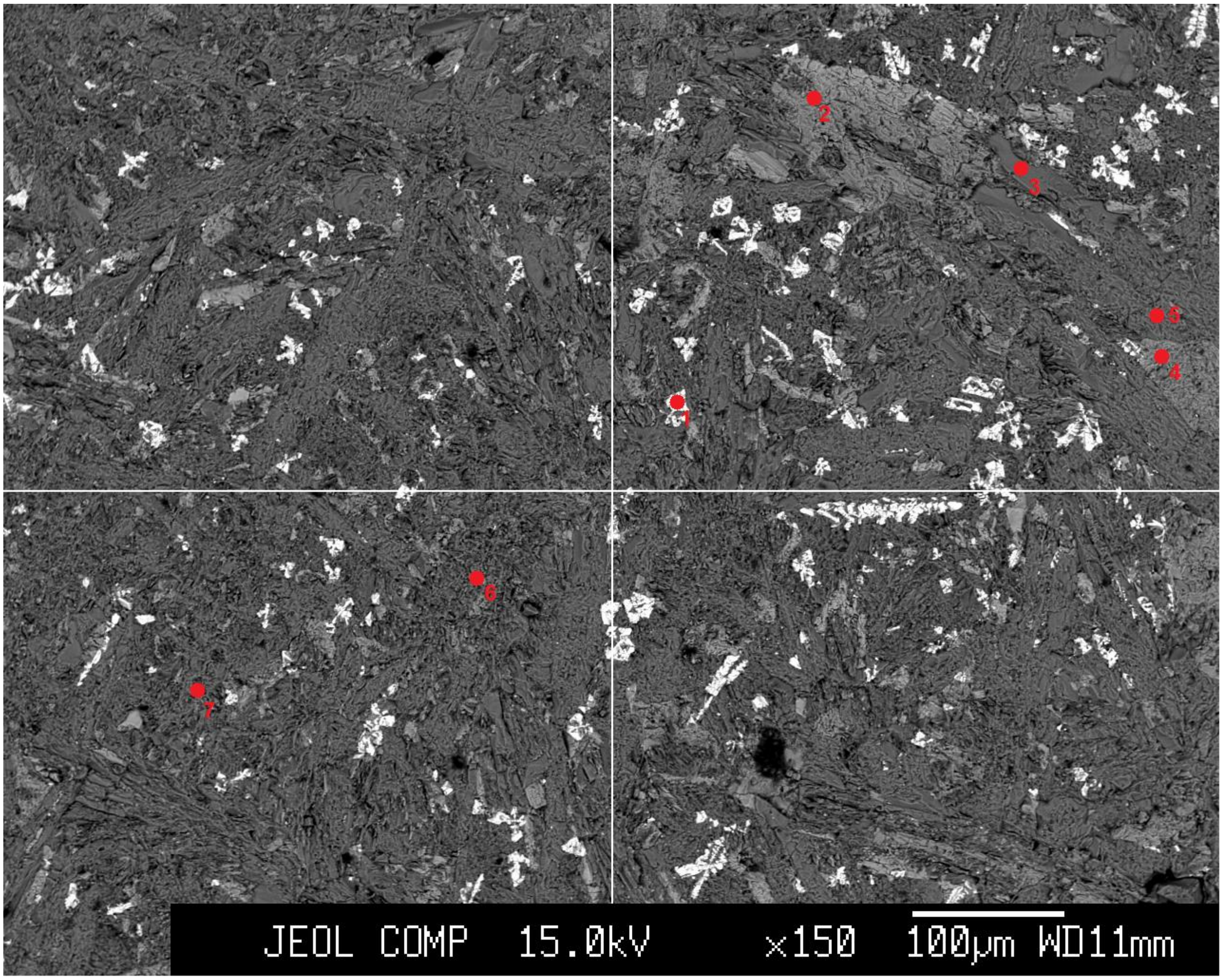

**Thin Section: GIL 49**
**Rock Type: Basalt, sheet flow**
**MBSF: 258**
**Area of analysis: 3**

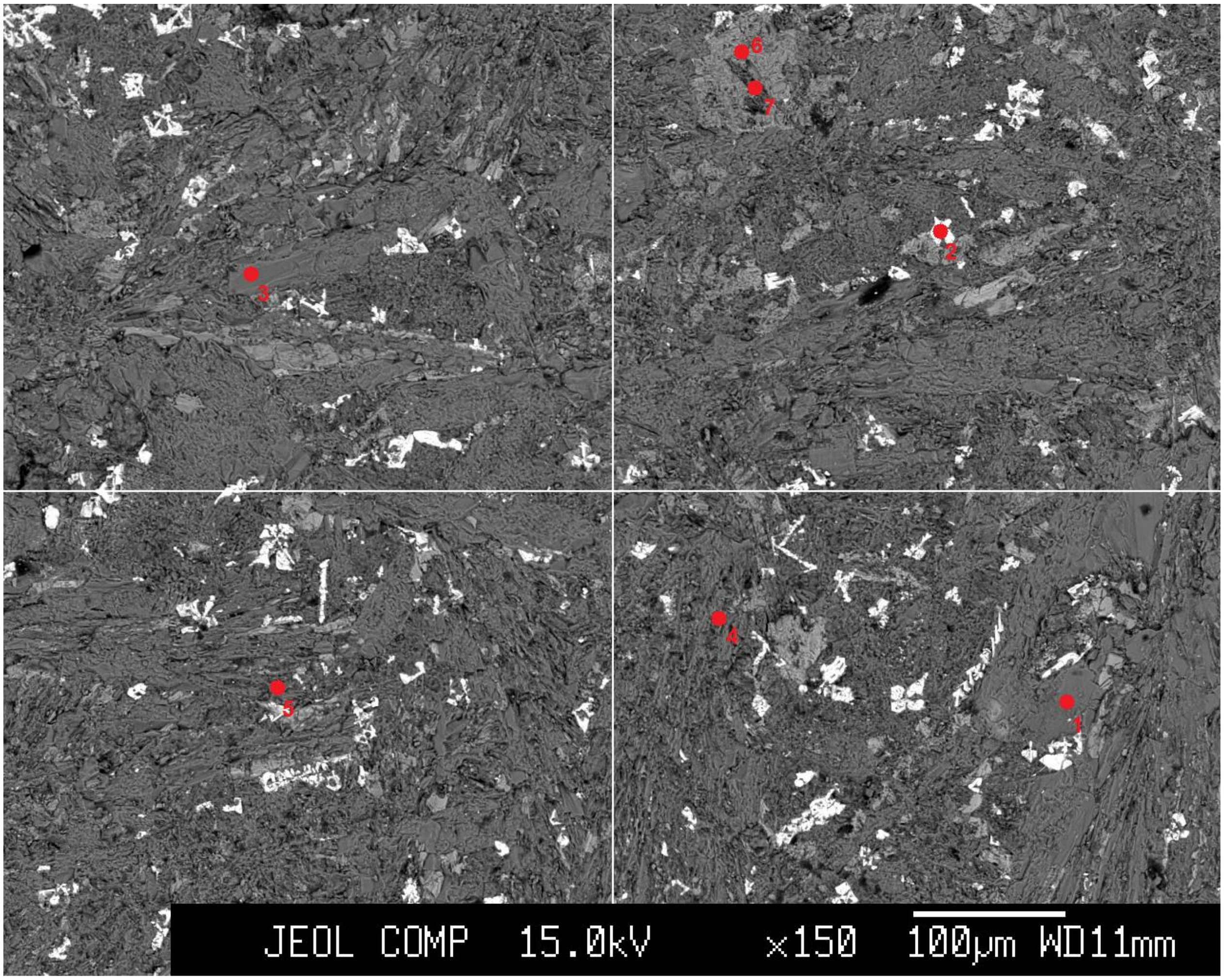

**Thin Section: GIL 35**
**Rock Type: Basalt, massive**
**MBSF: 285**
**Area of analysis: 1**

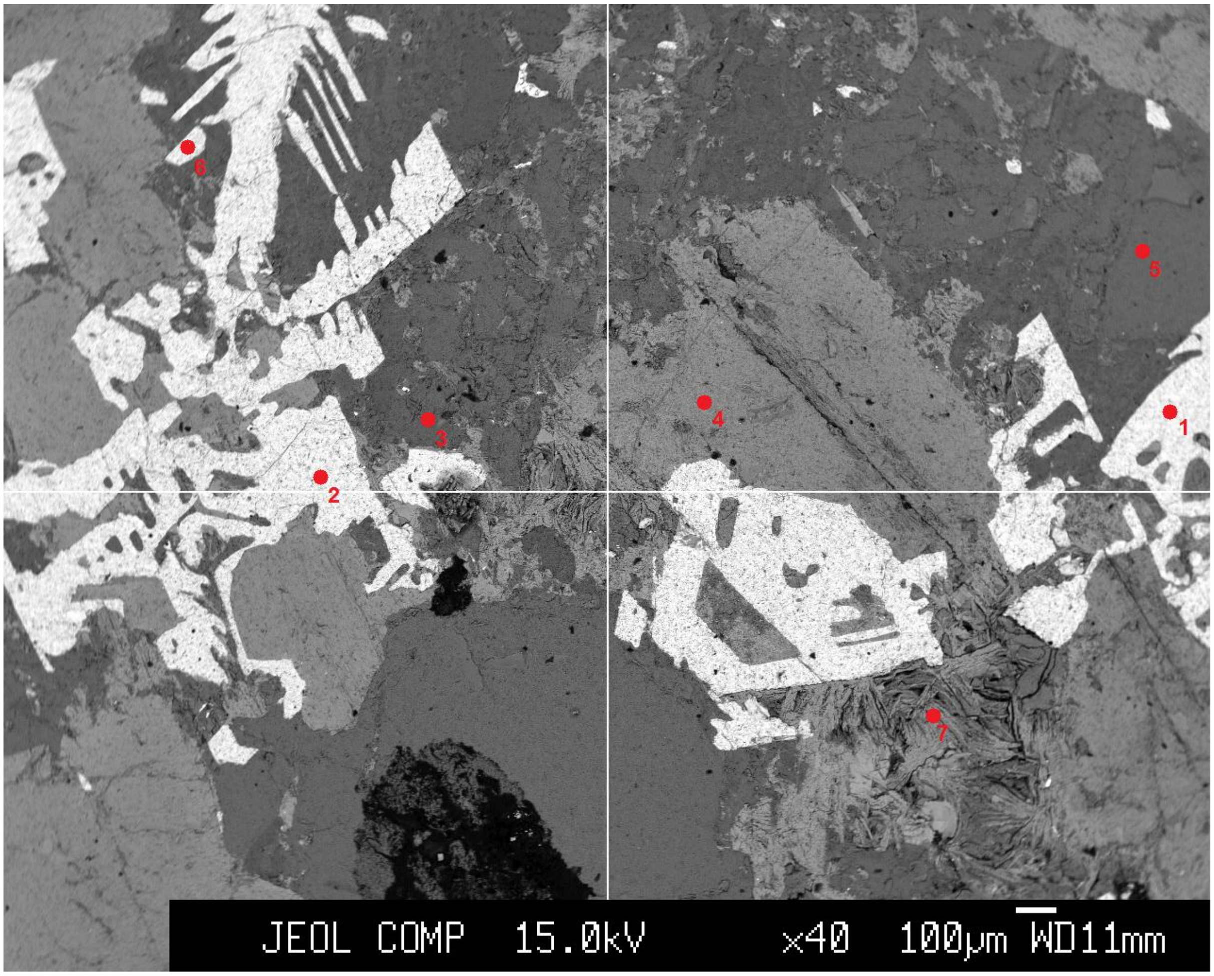

**Thin Section: GIL 35**
**Rock Type: Basalt, massive**
**MBSF: 285**
**Area of analysis: 2**

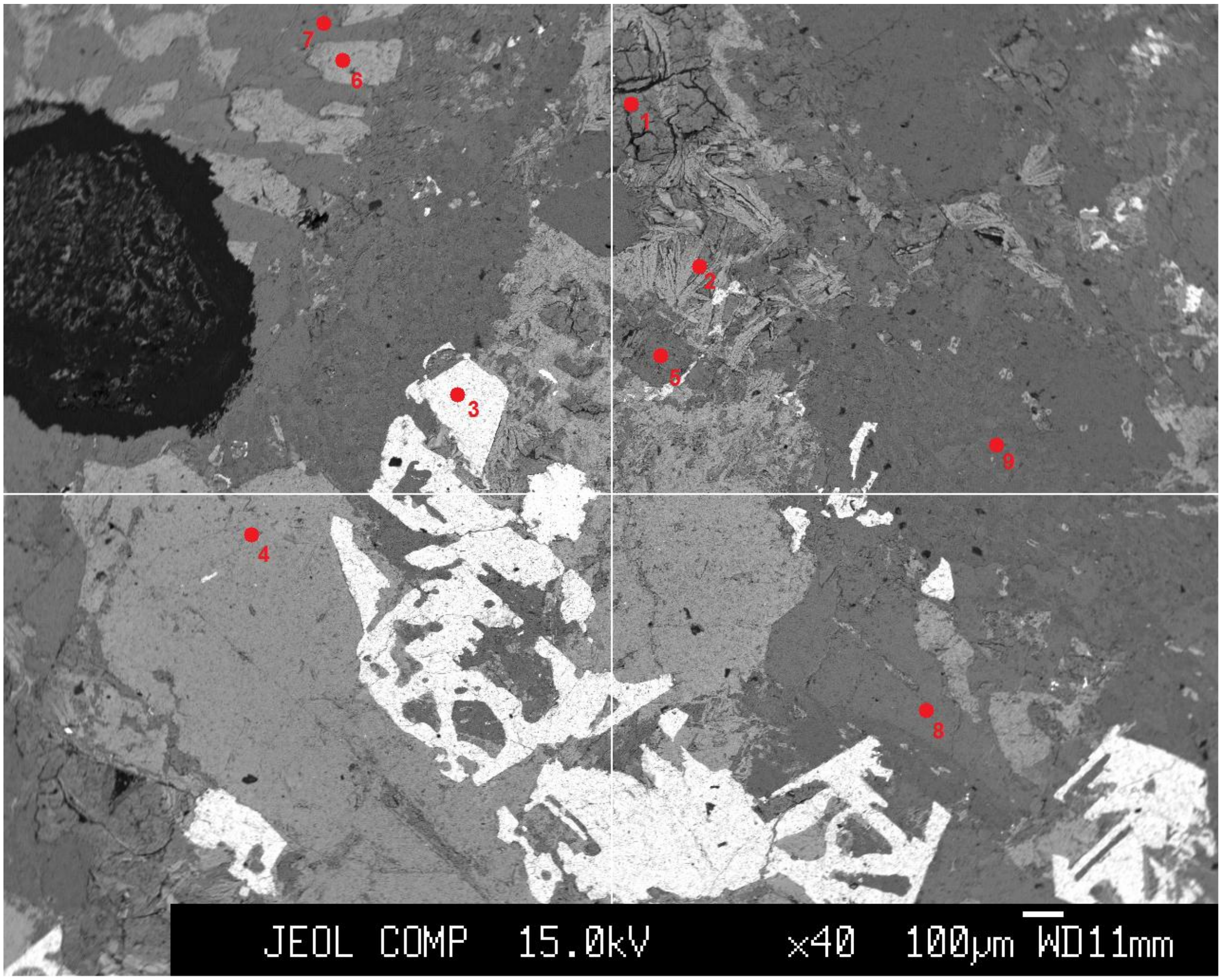

**Thin Section: GIL 16**
**Rock Type: Basalt, dikes**
**MBSF: 1204**
**Area of analysis: 1**

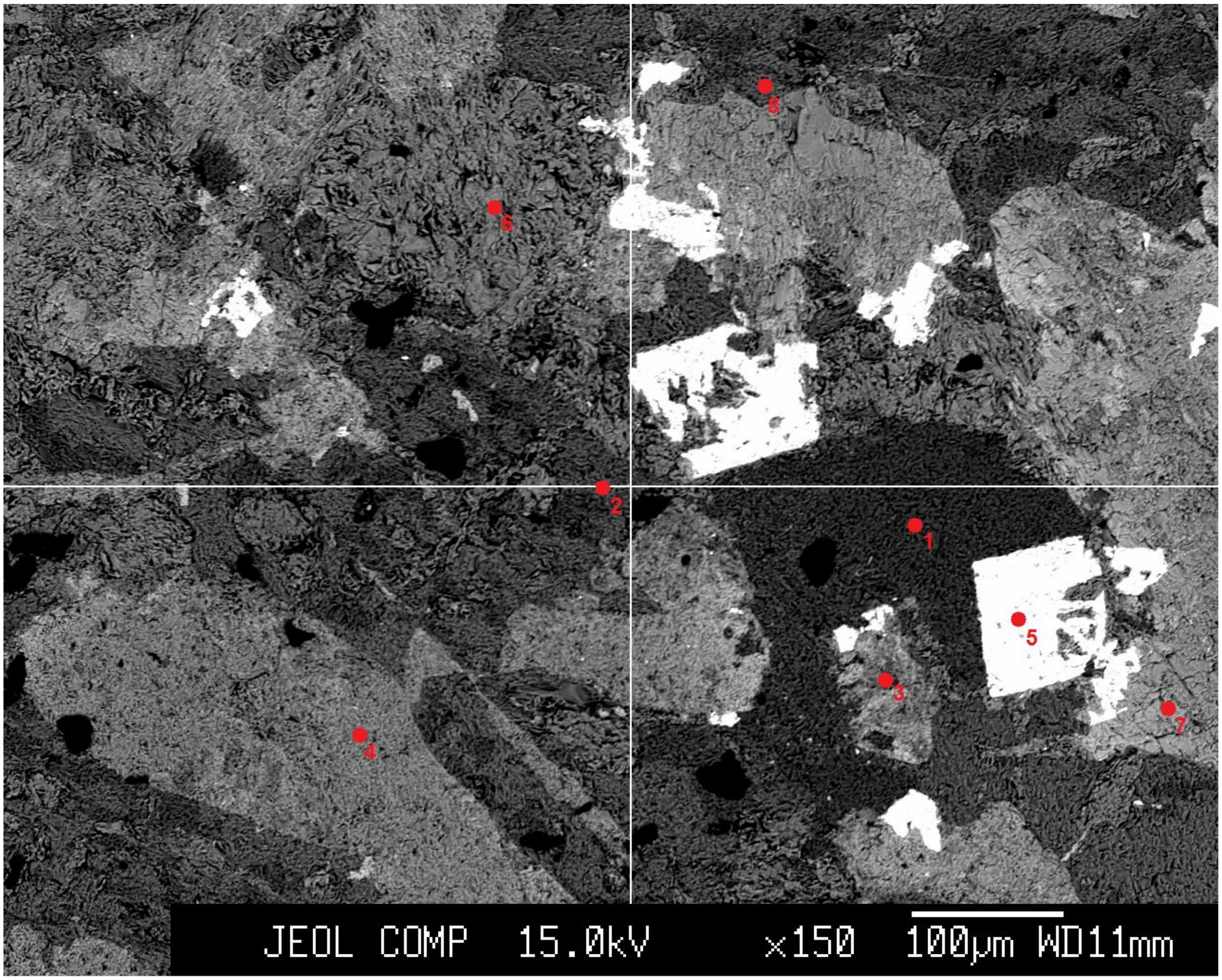

**Thin Section: GIL 16**
**Rock Type: Basalt, dikes**
**MBSF: 1204**
**Area of analysis: 2**

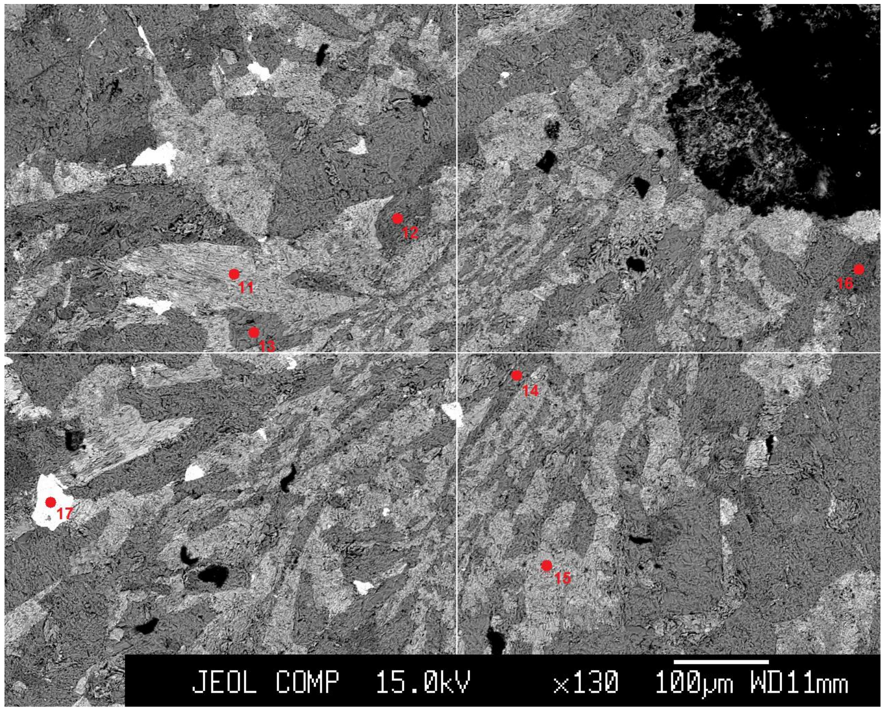


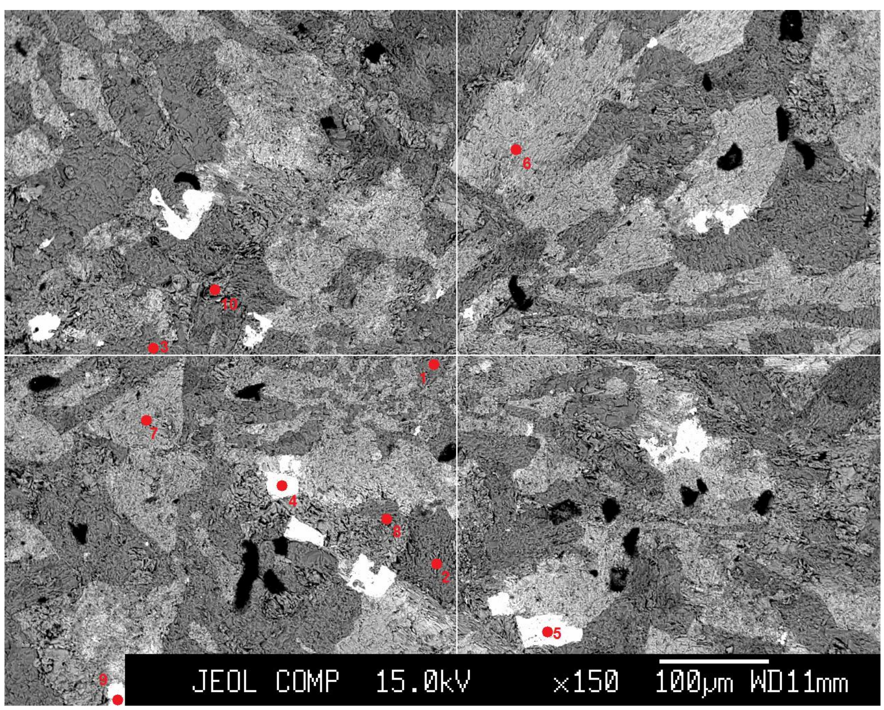

**Thin Section: GIL 16**
**Rock Type: Basalt, dikes**
**MBSF: 1204**
**Area of analysis: 3**

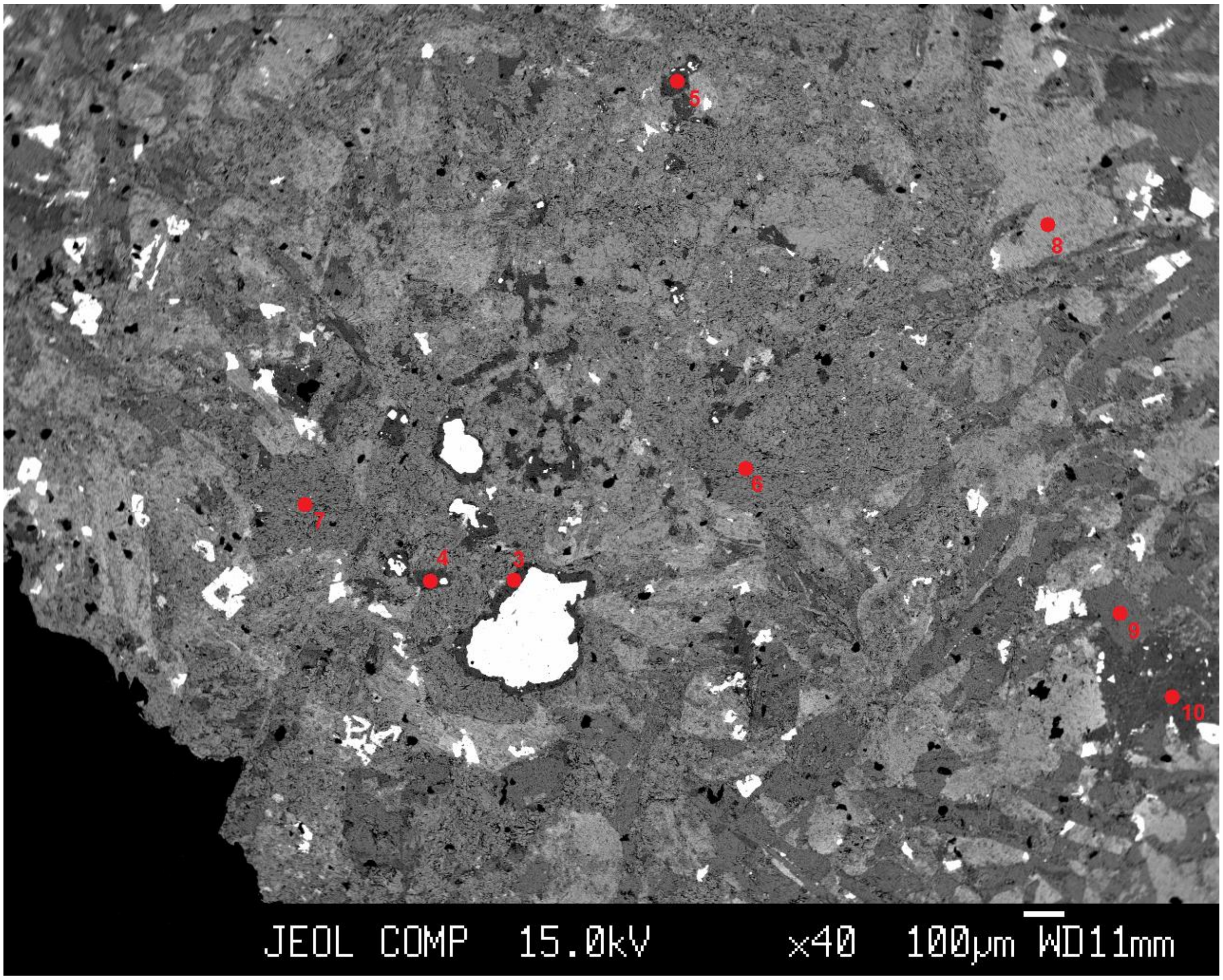

**Thin Section: GIL 23**
**Rock Type: Basalt, dikes**
**MBSF: 1373**
**Area of analysis: 1**

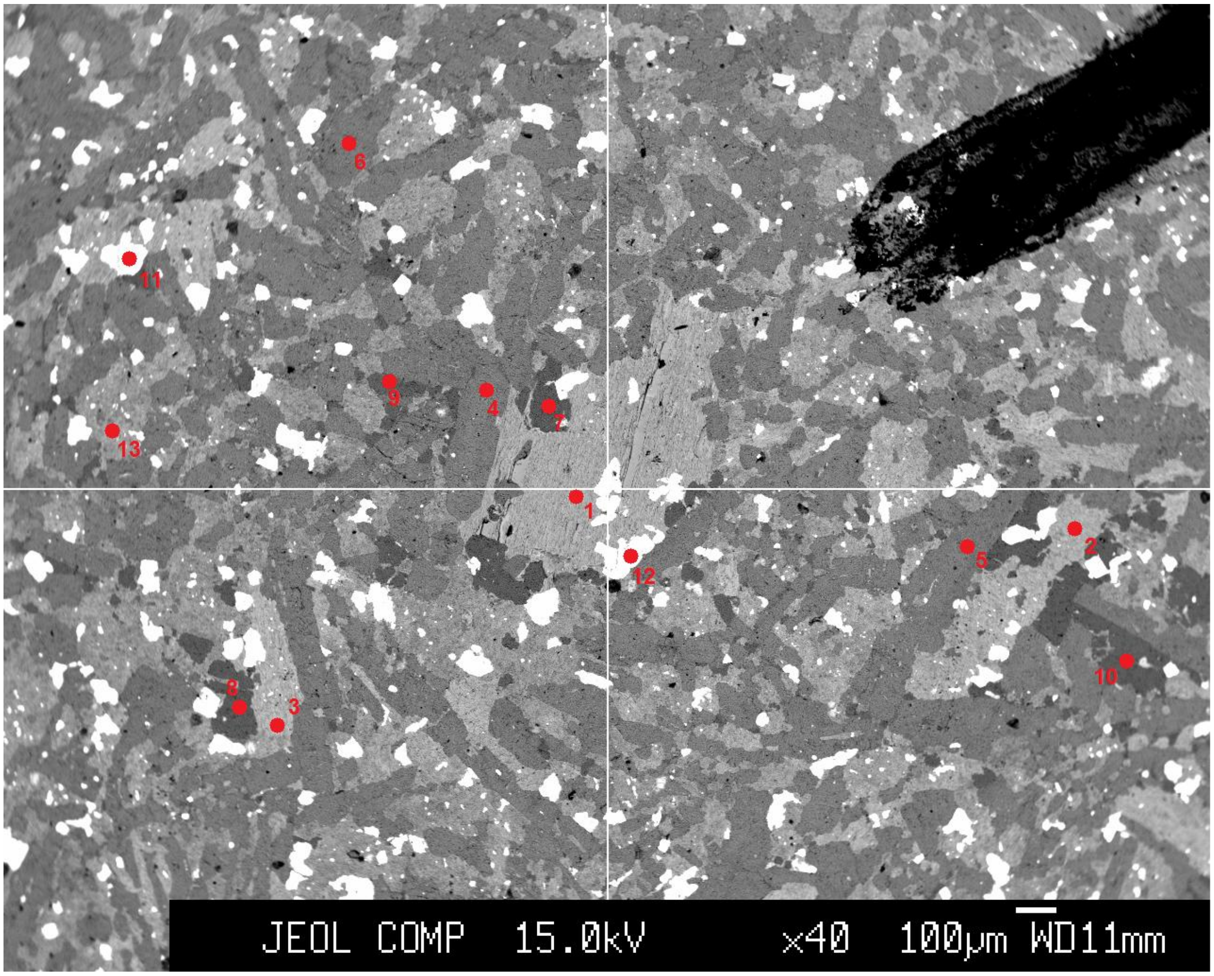

**Thin Section: GIL 23**
**Rock Type: Basalt, dikes**
**MBSF: 1373**
**Area of analysis: 2**

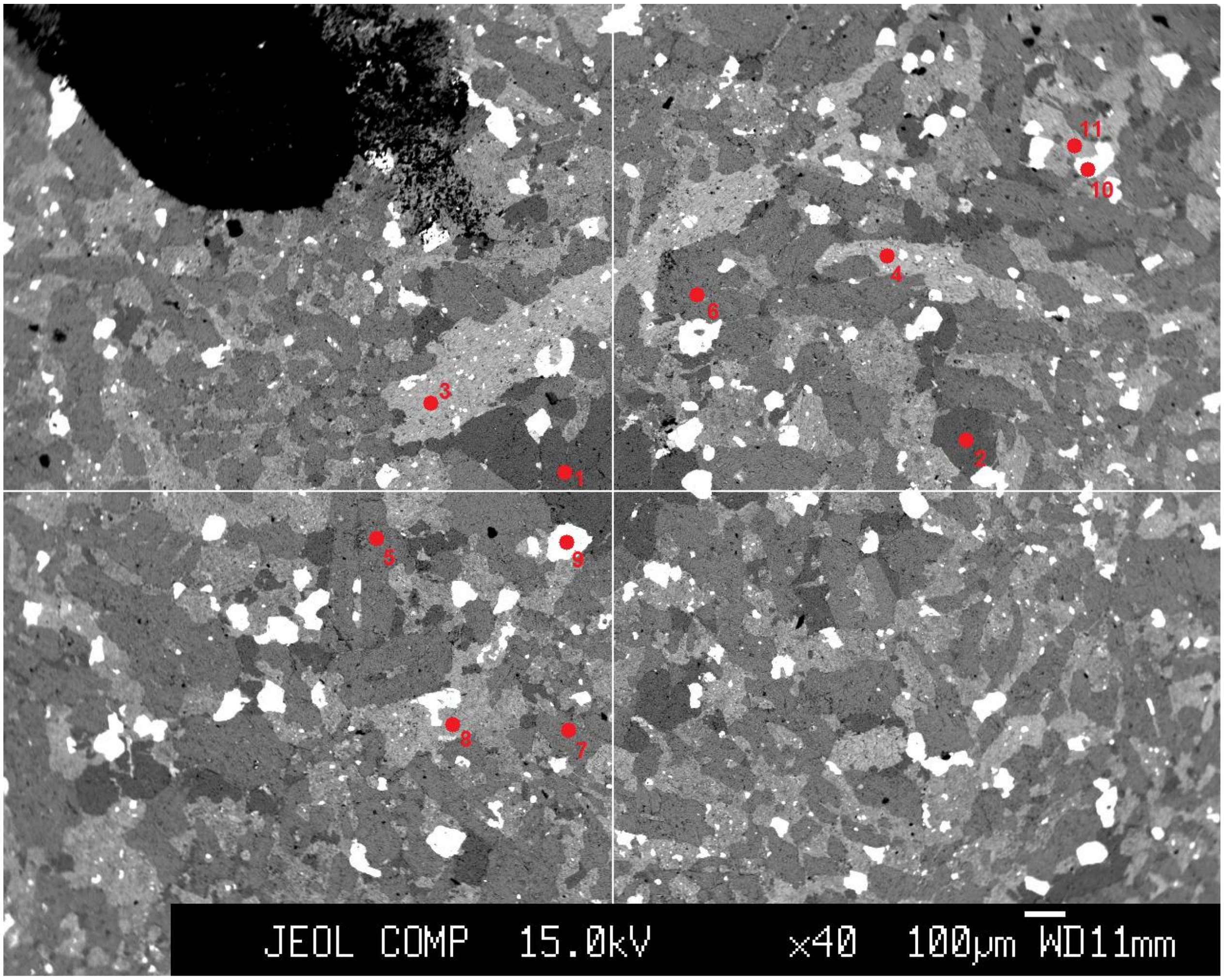

**Thin Section: GIL 25**
**Rock Type: Gabbro**
**MBSF: 1448**
**Area of analysis: 1**

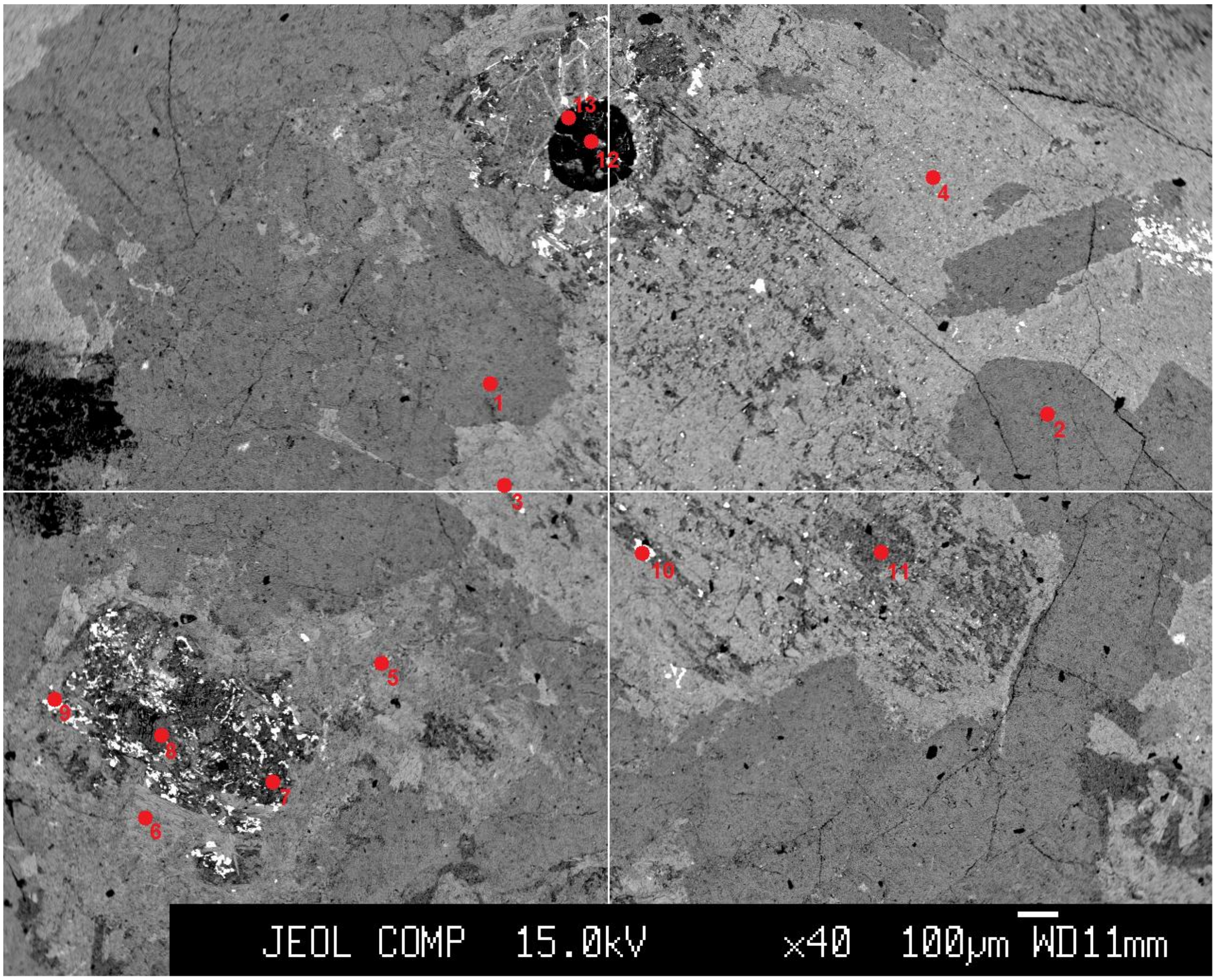

**Thin Section: GIL 25**
**Rock Type: Gabbro**
**MBSF: 1448**
**Area of analysis: 2**

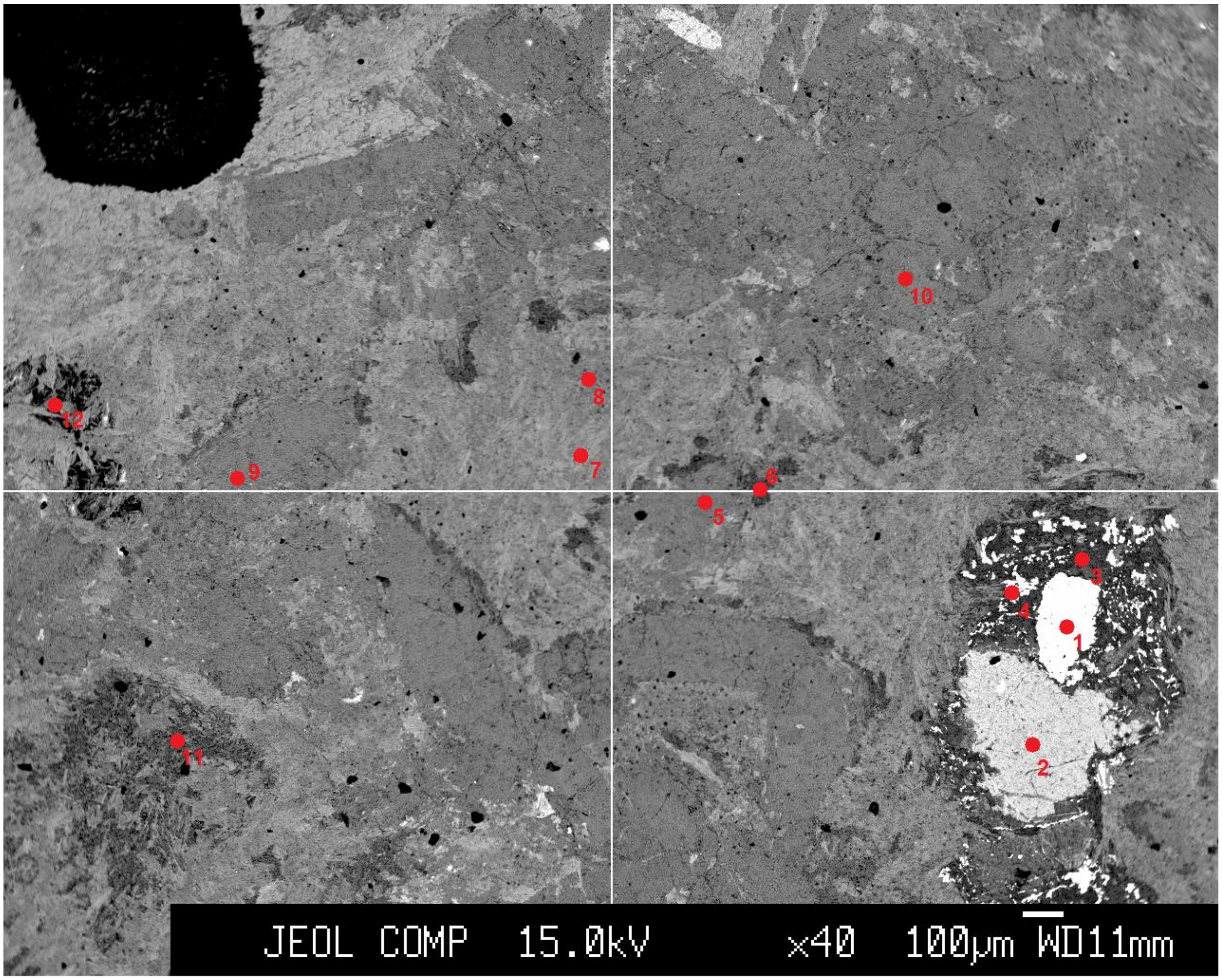

**Thin Section: GIL 25**
**Rock Type: Gabbro**
**MBSF: 1448**
**Area of analysis: 3**

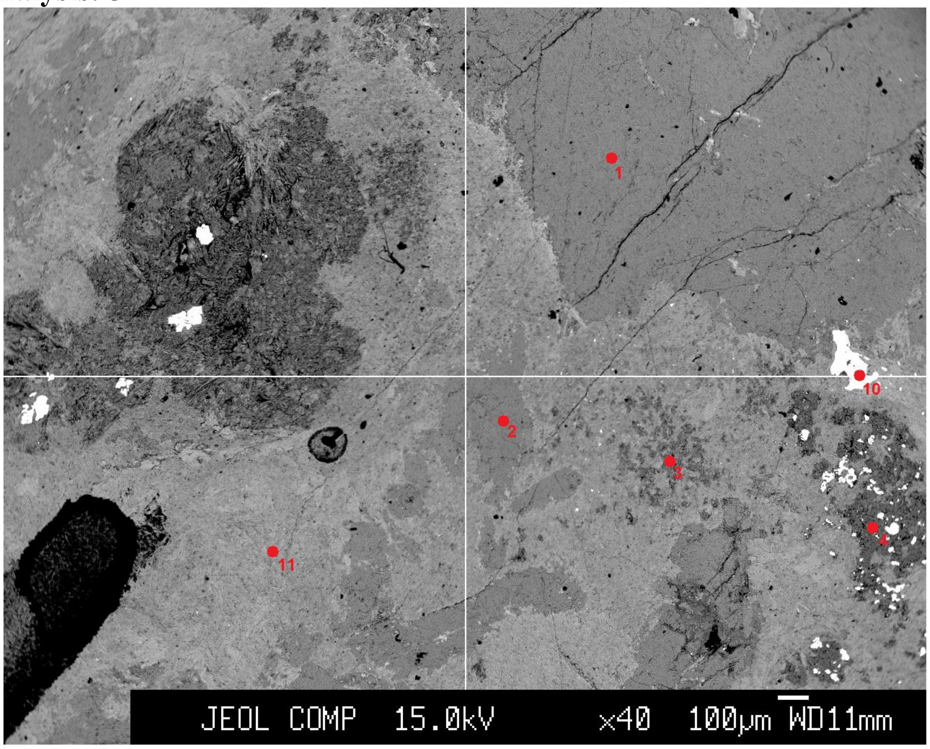


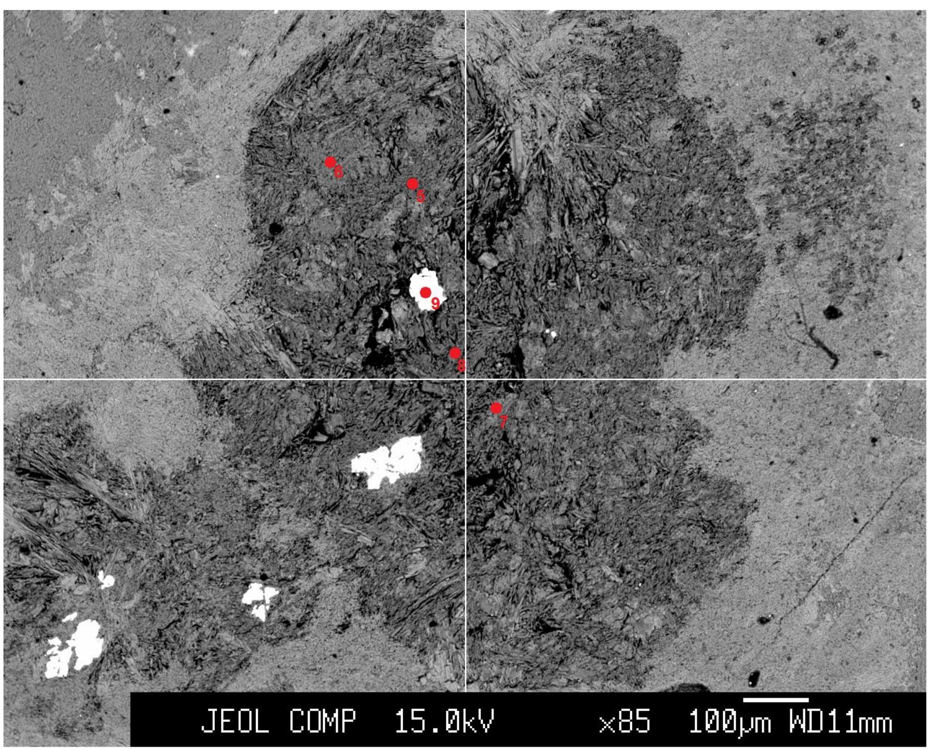

**Thin Section: GIL 25**
**Rock Type: Gabbro**
**MBSF: 1448**
**Area of analysis: 4**

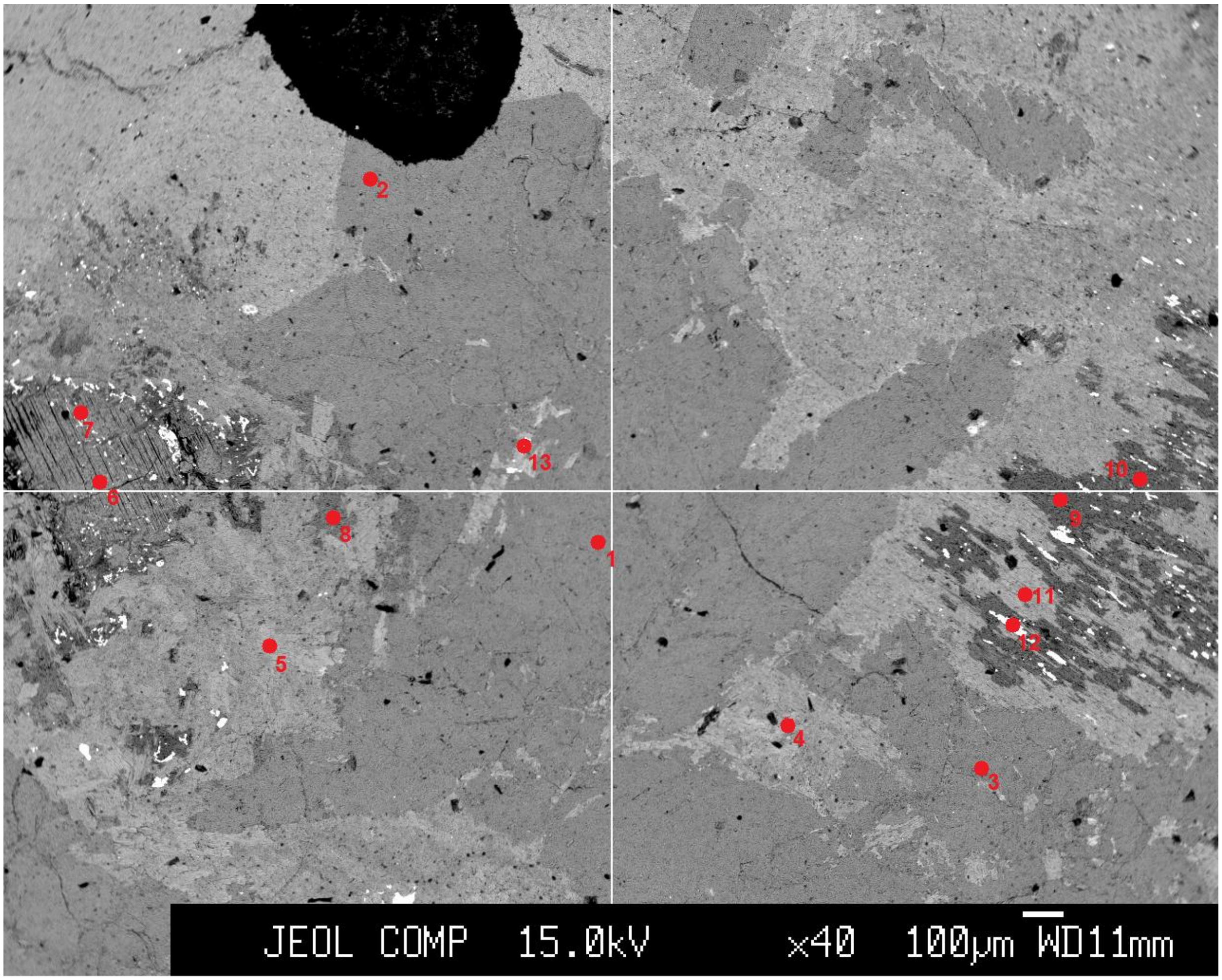

PLAGIOCLASE

| Slide | GIL 48 | GIL 48 | GIL 48 | GIL 48 | GIL 48 | GIL 48 | GIL 48 | GIL 49 | GIL 49 | GIL 49 | GIL 49 |
|---|---|---|---|---|---|---|---|---|---|---|---|
| **Depth (mbsf)** | **253** | **253** | **253** | **253** | **253** | **253** | **253** | **258** | **258** | **258** | **258** |
| **Area** | **1** | **2** | **2** | **3** | **3** | **3** | **3** | **1** | **2** | **2** | **3** |
| **Point** | **10** | **5** | **6** | **2** | **3** | **6** | **9** | **7** | **3** | **5** | **3** |
| SiO2 | 46.64 | 52.43 | 55.39 | 52.09 | 55.40 | 56.53 | 51.76 | 45.08 | 53.53 | 51.78 | 44.30 |
| TiO2 | 0.04 | 0.08 | 0.10 | 0.09 | 0.07 | 0.06 | 0.08 | 0.01 | 0.13 | 0.05 | 0.03 |
| Al2O3 | 25.11 | 26.01 | 25.76 | 20.57 | 22.26 | 22.25 | 23.83 | 25.32 | 24.61 | 25.39 | 21.19 |
| Cr2O3 | 0.00 | 0.01 | 0.01 | 0.00 | 0.00 | 0.00 | 0.00 | 0.00 | 0.00 | 0.00 | 0.00 |
| FeO | 0.75 | 0.96 | 1.17 | 1.15 | 1.22 | 1.31 | 1.02 | 0.76 | 1.17 | 0.93 | 1.20 |
| MnO | 0.02 | 0.00 | 0.00 | 0.01 | 0.02 | 0.01 | 0.00 | 0.00 | 0.00 | 0.04 | 0.00 |
| MgO | 0.17 | 0.15 | 0.10 | 0.07 | 0.15 | 0.18 | 0.15 | 0.24 | 0.26 | 0.22 | 0.11 |
| CaO | 13.64 | 11.73 | 10.57 | 7.91 | 7.91 | 7.63 | 9.64 | 13.41 | 9.91 | 11.56 | 11.24 |
| Na2O | 3.24 | 5.06 | 5.66 | 6.35 | 5.64 | 4.52 | 6.53 | 4.30 | 6.11 | 5.23 | 2.28 |
| K2O | 0.03 | 0.08 | 0.08 | 0.11 | 0.10 | 0.14 | 0.11 | 0.04 | 0.10 | 0.07 | 0.06 |
| **Total** | **89.64** | **96.50** | **98.84** | **88.34** | **92.77** | **92.63** | **93.10** | **89.16** | **95.84** | **95.27** | **80.41** |
| cations pfu per 8 oxygen | | | | | | | | | | | |
| Si | 2.386 | 2.474 | 2.539 | 2.664 | 2.678 | 2.716 | 2.532 | 2.334 | 2.538 | 2.478 | 2.503 |
| Ti | 0.002 | 0.002 | 0.003 | 0.003 | 0.002 | 0.002 | 0.003 | 0.000 | 0.005 | 0.002 | 0.002 |
| Al | 1.514 | 1.446 | 1.393 | 1.240 | 1.268 | 1.260 | 1.374 | 1.546 | 1.375 | 1.432 | 1.412 |
| Cr | 0.000 | 0.000 | 0.001 | 0.000 | 0.000 | 0.000 | 0.000 | 0.000 | 0.000 | 0.000 | 0.000 |
| Fe | 0.032 | 0.038 | 0.045 | 0.050 | 0.050 | 0.053 | 0.042 | 0.033 | 0.046 | 0.037 | 0.057 |
| Mn | 0.001 | 0.000 | 0.000 | 0.000 | 0.001 | 0.000 | 0.000 | 0.000 | 0.000 | 0.002 | 0.000 |
| Mg | 0.013 | 0.010 | 0.007 | 0.005 | 0.010 | 0.013 | 0.010 | 0.018 | 0.018 | 0.016 | 0.009 |
| Ca | 0.748 | 0.593 | 0.519 | 0.434 | 0.410 | 0.393 | 0.505 | 0.744 | 0.503 | 0.593 | 0.680 |
| Na | 0.322 | 0.463 | 0.503 | 0.630 | 0.529 | 0.421 | 0.619 | 0.432 | 0.562 | 0.486 | 0.250 |
| K | 0.002 | 0.005 | 0.005 | 0.007 | 0.006 | 0.009 | 0.006 | 0.002 | 0.006 | 0.004 | 0.005 |
| **Total** | **5.018** | **5.033** | **5.016** | **5.033** | **4.954** | **4.867** | **5.092** | **5.110** | **5.054** | **5.050** | **4.918** |
| | | | | | | | | | | | |
| Xan | 0.698 | 0.559 | 0.505 | 0.405 | 0.434 | 0.478 | 0.447 | 0.631 | 0.470 | 0.548 | 0.727 |
| Xab | 0.300 | 0.437 | 0.490 | 0.588 | 0.560 | 0.512 | 0.548 | 0.367 | 0.524 | 0.449 | 0.268 |
| Xor | 0.001 | 0.005 | 0.005 | 0.007 | 0.007 | 0.011 | 0.006 | 0.002 | 0.006 | 0.004 | 0.005 |

PLAGIOCLASE

| Slide | GIL 35 | GIL 35 | GIL 16 | GIL 16 | GIL 16 | GIL 16 | GIL 16 | GIL 16 | GIL 16 | GIL 16 |
|---|---|---|---|---|---|---|---|---|---|---|
| **Depth (mbsf)** | **285** | **285** | **1204** | **1204** | **1204** | **1204** | **1204** | **1204** | **1204** | **1204** |
| **Area** | **1** | **2** | **1** | **1** | **2** | **2** | **2** | **2** | **2** | **3** |
| **Point** | **5** | **7** | **2** | **8** | **1** | **3** | **8** | **12** | **14** | **10** |
| SiO2 | 59.11+B53 | 56.06 | 55.80 | 52.14 | 57.12 | 52.55 | 58.09 | 62.59 | 50.33 | 62.95 |
| TiO2 | 0.06 | 0.07 | 0.05 | 0.30 | 0.03 | 0.02 | 0.05 | 0.00 | 0.07 | 0.00 |
| Al2O3 | 26.00 | 25.61 | 25.68 | 27.91 | 26.53 | 28.14 | 24.83 | 20.90 | 19.70 | 13.34 |
| Cr2O3 | 0.00 | 0.00 | 0.00 | 0.00 | 0.00 | 0.00 | 0.00 | 0.00 | 0.00 | 0.00 |
| FeO | 0.62 | 0.66 | 1.15 | 1.17 | 1.19 | 0.88 | 1.63 | 0.36 | 0.68 | 4.44 |
| MnO | 0.00 | 0.01 | 0.00 | 0.01 | 0.00 | 0.00 | 0.00 | 0.00 | 0.00 | 0.00 |
| MgO | 0.04 | 0.06 | 0.12 | 0.15 | 0.19 | 0.19 | 0.08 | 0.00 | 0.17 | 2.36 |
| CaO | 9.33 | 9.79 | 9.80 | 12.59 | 10.47 | 13.03 | 8.85 | 3.41 | 6.35 | 1.33 |
| Na2O | 6.21 | 6.41 | 5.82 | 2.68 | 6.38 | 4.22 | 5.78 | 9.07 | 6.48 | 5.87 |
| K2O | 0.08 | 0.09 | 0.17 | 0.08 | 0.08 | 0.08 | 0.09 | 0.09 | 0.34 | 0.22 |
| **Total** | **101.45** | **98.76** | **98.59** | **97.02** | **101.97** | **99.12** | **99.41** | **96.43** | **84.12** | **90.50** |
| Cations pfu per 8 oxygen | | | 8 oxygen | | | | | | | |
| Si | 2.614 | 2.564 | 2.558 | 2.434 | 2.540 | 2.416 | 2.629 | 2.862 | 2.690 | 3.071 |
| Ti | 0.002 | 0.002 | 0.002 | 0.010 | 0.001 | 0.001 | 0.002 | 0.000 | 0.002 | 0.000 |
| Al | 1.355 | 1.381 | 1.388 | 1.535 | 1.390 | 1.525 | 1.324 | 1.126 | 1.241 | 0.767 |
| Cr | 0.000 | 0.000 | 0.000 | 0.000 | 0.000 | 0.000 | 0.000 | 0.000 | 0.000 | 0.000 |
| Fe | 0.023 | 0.025 | 0.044 | 0.046 | 0.044 | 0.034 | 0.062 | 0.014 | 0.030 | 0.181 |
| Mn | 0.000 | 0.001 | 0.000 | 0.001 | 0.000 | 0.000 | 0.000 | 0.000 | 0.000 | 0.000 |
| Mg | 0.002 | 0.004 | 0.008 | 0.010 | 0.013 | 0.013 | 0.006 | 0.000 | 0.014 | 0.171 |
| Ca | 0.442 | 0.479 | 0.482 | 0.630 | 0.498 | 0.642 | 0.429 | 0.167 | 0.363 | 0.070 |
| Na | 0.532 | 0.569 | 0.518 | 0.242 | 0.550 | 0.377 | 0.507 | 0.805 | 0.671 | 0.555 |
| K | 0.004 | 0.006 | 0.010 | 0.005 | 0.005 | 0.005 | 0.006 | 0.006 | 0.023 | 0.014 |
| **Total** | **4.975** | **5.030** | **5.010** | **4.913** | **5.042** | **5.013** | **4.964** | **4.981** | **5.034** | **4.829** |
| Xan | 0.452 | 0.455 | 0.477 | 0.718 | 0.473 | 0.627 | 0.455 | 0.171 | 0.343 | 0.109 |
| Xab | 0.544 | 0.540 | 0.513 | 0.276 | 0.522 | 0.368 | 0.539 | 0.823 | 0.635 | 0.870 |
| Xor | 0.004 | 0.005 | 0.010 | 0.005 | 0.005 | 0.005 | 0.006 | 0.006 | 0.022 | 0.021 |

PLAGIOCLASE

| Slide | GIL 23 | GIL 23 | GIL 23 | GIL 23 | GIL 23 | GIL 23 |
|---|---|---|---|---|---|---|
| **Depth (mbsf)** | **1373** | **1373** | **1373** | **1373** | **1373** | **1373** |
| **Area** | **1** | **1** | **1** | **2** | **2** | **2** |
| **Point** | **4** | **5** | **6** | **5** | **6** | **7** |
| SiO2 | 52.66 | 56.21 | 49.74 | 49.37 | 48.21 | 45.25 |
| TiO2 | 0.00 | 0.00 | 0.00 | 0.00 | 0.00 | 0.00 |
| Al2O3 | 28.16 | 24.41 | 25.09 | 24.77 | 25.10 | 24.39 |
| Cr2O3 | 0.00 | 0.00 | 0.00 | 0.00 | 0.00 | 0.00 |
| FeO | 0.63 | 1.15 | 0.62 | 0.66 | 0.71 | 0.54 |
| MnO | 0.00 | 0.00 | 0.00 | 0.00 | 0.00 | 0.00 |
| MgO | 0.09 | 0.54 | 0.04 | 0.09 | 0.08 | 0.04 |
| CaO | 11.07 | 10.12 | 10.34 | 10.14 | 10.32 | 10.49 |
| Na2O | 6.09 | 4.66 | 5.31 | 5.58 | 5.49 | 4.41 |
| K2O | 0.11 | 0.15 | 0.14 | 0.12 | 0.11 | 0.10 |
| **Total** | **98.81** | **97.24** | **91.29** | **90.74** | **90.02** | **85.23** |
| cations pfu per 8 oxygen | | | | | | |
| Si | 2.426 | 2.602 | 2.475 | 2.475 | 2.442 | 2.418 |
| Ti | 0.000 | 0.000 | 0.000 | 0.000 | 0.000 | 0.000 |
| Al | 1.530 | 1.332 | 1.472 | 1.463 | 1.498 | 1.536 |
| Cr | 0.000 | 0.000 | 0.000 | 0.000 | 0.000 | 0.000 |
| Fe | 0.024 | 0.045 | 0.026 | 0.028 | 0.030 | 0.024 |
| Mn | 0.000 | 0.000 | 0.000 | 0.000 | 0.000 | 0.000 |
| Mg | 0.006 | 0.038 | 0.003 | 0.007 | 0.006 | 0.003 |
| Ca | 0.546 | 0.502 | 0.551 | 0.545 | 0.560 | 0.601 |
| Na | 0.544 | 0.418 | 0.513 | 0.542 | 0.539 | 0.457 |
| K | 0.006 | 0.009 | 0.009 | 0.008 | 0.007 | 0.007 |
| **Total** | **5.084** | **4.946** | **5.050** | **5.070** | **5.083** | **5.047** |
| | | | | | | |
| Xan | 0.498 | 0.540 | 0.514 | 0.497 | 0.506 | 0.564 |
| Xab | 0.496 | 0.450 | 0.478 | 0.495 | 0.487 | 0.429 |
| Xor | 0.006 | 0.009 | 0.008 | 0.007 | 0.007 | 0.007 |

PLAGIOCLASE

| | | | | | | |
|---|---|---|---|---|---|---|
| **GIL 25** | **GIL 25** | **GIL 25** | **GIL 25** | **GIL 25** | **GIL 25** | **GIL 25** |
| **1448** | **1448** | **1448** | **1448** | **1448** | **1448** | **1448** |
| **1** | **1** | **2** | **2** | **3** | **4** | **4** |
| **1** | **2** | **5** | **9** | **2** | **1** | **3** |
| 45.14 | 46.99 | 45.78 | 50.92 | 47.14 | 46.94 | 48.02 |
| 0.00 | 0.00 | 0.00 | 0.00 | 0.00 | 0.00 | 0.06 |
| 29.23 | 26.46 | 27.29 | 31.01 | 29.32 | 29.69 | 26.01 |
| 0.00 | 0.00 | 0.00 | 0.00 | 0.00 | 0.00 | 0.00 |
| 0.52 | 0.47 | 0.41 | 0.65 | 0.97 | 0.74 | 0.74 |
| 0.00 | 0.00 | 0.00 | 0.00 | 0.00 | 0.00 | 0.00 |
| 0.03 | 0.10 | 0.04 | 0.00 | 0.14 | 0.02 | 0.25 |
| 15.35 | 13.23 | 13.17 | 15.03 | 14.96 | 15.91 | 12.01 |
| 2.10 | 4.01 | 4.22 | 2.94 | 2.57 | 2.52 | 4.19 |
| 0.01 | 0.13 | 0.03 | 0.07 | 0.15 | 0.10 | 0.45 |
| **92.37** | **91.39** | **90.94** | **100.61** | **95.24** | **95.94** | **91.73** |
| | | | | | | |
| 2.244 | 2.358 | 2.312 | 2.312 | 2.275 | 2.254 | 2.396 |
| 0.000 | 0.000 | 0.000 | 0.000 | 0.000 | 0.000 | 0.002 |
| 1.713 | 1.565 | 1.624 | 1.659 | 1.668 | 1.681 | 1.530 |
| 0.000 | 0.000 | 0.000 | 0.000 | 0.000 | 0.000 | 0.000 |
| 0.022 | 0.020 | 0.018 | 0.025 | 0.039 | 0.030 | 0.031 |
| 0.000 | 0.000 | 0.000 | 0.000 | 0.000 | 0.000 | 0.000 |
| 0.002 | 0.008 | 0.003 | 0.000 | 0.010 | 0.002 | 0.018 |
| 0.818 | 0.711 | 0.713 | 0.731 | 0.774 | 0.819 | 0.642 |
| 0.202 | 0.390 | 0.414 | 0.259 | 0.240 | 0.235 | 0.406 |
| 0.001 | 0.008 | 0.002 | 0.004 | 0.009 | 0.006 | 0.029 |
| **5.002** | **5.059** | **5.086** | **4.990** | **5.014** | **5.028** | **5.055** |
| | | | | | | |
| 0.801 | 0.641 | 0.631 | 0.735 | 0.757 | 0.772 | 0.597 |
| 0.198 | 0.351 | 0.366 | 0.261 | 0.235 | 0.222 | 0.377 |
| 0.001 | 0.007 | 0.002 | 0.004 | 0.009 | 0.006 | 0.027 |

CLINOPYROXENE

| Slide | GIL 48 | GIL 48 | GIL 48 | GIL 48 | GIL 48 | GIL 49 | GIL 49 | GIL 49 | GIL 49 |
|---|---|---|---|---|---|---|---|---|---|
| **Depth (mbsf)** | **253** | **253** | **253** | **253** | **253** | **258** | **258** | **258** | **258** |
| **Area** | **2** | **2** | **3** | **3** | **3** | **1** | **2** | **2** | **3** |
| **Point** | **3** | **4** | **1** | **4** | **7** | **9** | **2** | **4** | **7** |
| SiO2 | 51.65 | 43.57 | 52.38 | 45.53 | 42.53 | 42.49 | 35.68 | 42.99 | 38.72 |
| TiO2 | 0.28 | 1.34 | 0.38 | 0.91 | 2.00 | 1.13 | 1.21 | 1.19 | 0.13 |
| Al2O3 | 0.74 | 2.43 | 12.30 | 8.60 | 2.59 | 3.69 | 2.08 | 2.90 | 2.83 |
| Cr2O3 | 0.04 | 0.00 | 0.00 | 0.00 | 0.02 | 0.09 | 0.01 | 0.04 | 0.09 |
| FeO | 17.21 | 17.37 | 10.11 | 20.27 | 22.54 | 10.21 | 13.04 | 10.52 | 12.62 |
| MnO | 0.41 | 0.33 | 0.12 | 0.29 | 0.55 | 0.24 | 0.30 | 0.23 | 0.04 |
| MgO | 22.04 | 9.45 | 4.78 | 9.73 | 8.14 | 9.60 | 13.24 | 13.94 | 13.25 |
| CaO | 4.32 | 18.13 | 2.80 | 3.99 | 16.06 | 16.74 | 15.74 | 16.81 | 0.93 |
| Na2O | 0.31 | 0.39 | 4.26 | 1.95 | 0.29 | 0.36 | 0.31 | 0.33 | 0.91 |
| K2O | 0.05 | 0.04 | 1.03 | 0.51 | 0.01 | 0.02 | 0.02 | 0.02 | 0.21 |
| **Total** | **97.03** | **93.04** | **88.17** | **91.78** | **94.73** | **84.58** | **81.64** | **88.98** | **69.74** |
| cations pfu per 6 oxygen | | | | | | | | | |
| Si | 1.966 | 1.839 | 2.087 | 1.873 | 1.802 | 1.893 | 1.714 | 1.829 | 2.018 |
| Ti | 0.008 | 0.043 | 0.011 | 0.028 | 0.064 | 0.038 | 0.044 | 0.038 | 0.005 |
| Al | 0.033 | 0.121 | 0.578 | 0.417 | 0.130 | 0.194 | 0.118 | 0.145 | 0.174 |
| Cr | 0.001 | 0.000 | 0.000 | 0.000 | 0.001 | 0.003 | 0.000 | 0.001 | 0.004 |
| Fe | 0.548 | 0.613 | 0.337 | 0.697 | 0.799 | 0.380 | 0.524 | 0.374 | 0.550 |
| Mn | 0.013 | 0.011 | 0.004 | 0.010 | 0.020 | 0.009 | 0.013 | 0.008 | 0.002 |
| Mg | 1.250 | 0.595 | 0.284 | 0.597 | 0.514 | 0.638 | 0.948 | 0.884 | 1.030 |
| Ca | 0.176 | 0.820 | 0.119 | 0.176 | 0.729 | 0.799 | 0.810 | 0.766 | 0.052 |
| Na | 0.023 | 0.032 | 0.329 | 0.155 | 0.024 | 0.031 | 0.029 | 0.027 | 0.091 |
| K | 0.002 | 0.002 | 0.052 | 0.026 | 0.001 | 0.001 | 0.001 | 0.001 | 0.014 |
| **Total** | **4.021** | **4.076** | **3.803** | **3.981** | **4.082** | **3.986** | **4.199** | **4.075** | **3.940** |
| | | | | | | | | | |
| Xdi | 0.718 | 0.694 | 0.542 | 0.522 | 0.603 | 0.787 | 0.766 | 0.812 | 0.662 |
| Xhd | 0.364 | 0.703 | 0.613 | 0.590 | 0.741 | 0.646 | 0.581 | 0.561 | 0.369 |

CLINOPYROXENE

| Slide | GIL 35 | GIL 35 | GIL 35 | GIL 35 | GIL 16 | GIL 16 | GIL 16 | GIL 16 | GIL 16 |
|---|---|---|---|---|---|---|---|---|---|
| **Depth (mbsf)** | **285** | **285** | **285** | **285** | **1204** | **1204** | **1204** | **1204** | **1204** |
| **Area** | **2** | **2** | **2** | **2** | **1** | **2** | **2** | **2** | **3** |
| **Point** | **1** | **2** | **4** | **6** | **3** | **6** | **7** | **15** | **8** |
| SiO2 | 46.56 | 45.46 | 45.51 | 49.34 | 44.98 | 53.09 | 34.23 | 50.47 | 52.96 |
| TiO2 | 0.00 | 0.00 | 0.57 | 0.80 | 0.22 | 0.10 | 0.21 | 0.16 | 0.49 |
| Al2O3 | 3.84 | 4.69 | 1.07 | 1.23 | 1.67 | 1.31 | 3.84 | 1.41 | 3.04 |
| Cr2O3 | 0.00 | 0.00 | 0.00 | 0.00 | 0.03 | 0.11 | 0.12 | 0.05 | 0.00 |
| FeO | 18.01 | 19.44 | 16.99 | 20.93 | 17.30 | 14.65 | 14.20 | 15.23 | 8.56 |
| MnO | 0.05 | 0.03 | 0.43 | 0.58 | 0.35 | 0.46 | 0.28 | 0.41 | 0.07 |
| MgO | 14.75 | 14.71 | 10.07 | 10.52 | 11.30 | 11.18 | 12.02 | 10.46 | 18.04 |
| CaO | 1.41 | 1.08 | 15.50 | 16.07 | 8.08 | 19.47 | 13.53 | 14.75 | 19.12 |
| Na2O | 0.65 | 0.98 | 0.30 | 0.34 | 0.48 | 0.40 | 0.38 | 0.44 | 0.33 |
| K2O | 0.13 | 0.25 | 0.03 | 0.04 | 0.16 | 0.15 | 0.25 | 0.14 | 0.02 |
| **Total** | **85.40** | **86.64** | **90.47** | **99.85** | **84.57** | **100.90** | **79.06** | **93.51** | **102.63** |
| cations pfu per 6 oxyegn | | | | | | | | | |
| Si | 2.006 | 1.953 | 1.946 | 1.931 | 2.012 | 1.998 | 1.701 | 2.036 | 1.903 |
| Ti | 0.000 | 0.000 | 0.019 | 0.023 | 0.008 | 0.003 | 0.008 | 0.005 | 0.013 |
| Al | 0.195 | 0.238 | 0.054 | 0.056 | 0.088 | 0.058 | 0.224 | 0.067 | 0.129 |
| Cr | 0.000 | 0.000 | 0.000 | 0.000 | 0.001 | 0.003 | 0.005 | 0.002 | 0.000 |
| Fe | 0.649 | 0.698 | 0.608 | 0.685 | 0.647 | 0.461 | 0.590 | 0.514 | 0.257 |
| Mn | 0.002 | 0.001 | 0.016 | 0.019 | 0.013 | 0.014 | 0.012 | 0.014 | 0.002 |
| Mg | 0.947 | 0.942 | 0.642 | 0.614 | 0.753 | 0.627 | 0.890 | 0.629 | 0.967 |
| Ca | 0.065 | 0.050 | 0.710 | 0.674 | 0.388 | 0.785 | 0.720 | 0.638 | 0.736 |
| Na | 0.055 | 0.082 | 0.025 | 0.026 | 0.042 | 0.029 | 0.037 | 0.034 | 0.023 |
| K | 0.007 | 0.014 | 0.002 | 0.002 | 0.009 | 0.007 | 0.016 | 0.007 | 0.001 |
| **Total** | **3.927** | **3.978** | **4.022** | **4.032** | **3.962** | **3.986** | **4.204** | **3.946** | **4.033** |
| | | | | | | | | | |
| Xdi | 0.609 | 0.586 | 0.684 | 0.646 | 0.633 | 0.748 | 0.728 | 0.706 | 0.868 |
| Xhd | 0.429 | 0.442 | 0.667 | 0.682 | 0.575 | 0.660 | 0.592 | 0.642 | 0.506 |

CLINOPYROXENE

| Slide | GIL 23 | GIL 23 | GIL 25 | GIL 25 | GIL 25 | GIL 25 | GIL 25 | GIL 25 |
|---|---|---|---|---|---|---|---|---|
| **Depth (mbsf)** | **1373** | **1373** | **1448** | **1448** | **1448** | **1448** | **1448** | **1448** |
| **Area** | **1** | **2** | **1** | **1** | **1** | **2** | **2** | **3** |
| **Point** | **3** | **4** | **4** | **11** | **12** | **3** | **11** | **11** |
| SiO2 | 40.30 | 52.07 | 46.00 | 56.60 | 31.22 | 51.69 | 43.48 | 35.08 |
| TiO2 | 0.00 | 0.00 | 1.27 | 0.00 | 0.00 | 0.00 | 0.10 | 0.31 |
| Al2O3 | 0.30 | 0.64 | 5.32 | 0.90 | 0.25 | 0.00 | 7.20 | 6.08 |
| Cr2O3 | 0.00 | 0.00 | 0.00 | 0.00 | 0.00 | 0.00 | 0.00 | 0.04 |
| FeO | 12.25 | 12.19 | 9.75 | 5.79 | 32.77 | 1.94 | 13.03 | 10.91 |
| MnO | 0.21 | 0.29 | 0.02 | 0.00 | 0.00 | 0.00 | 0.23 | 0.14 |
| MgO | 11.89 | 13.54 | 15.11 | 23.04 | 13.84 | 24.24 | 19.93 | 15.75 |
| CaO | 17.71 | 20.86 | 12.92 | 5.90 | 0.80 | 0.00 | 5.77 | 10.59 |
| Na2O | 0.10 | 0.36 | 1.77 | 0.28 | 0.46 | 0.19 | 0.51 | 2.18 |
| K2O | 0.04 | 0.00 | 0.15 | 0.01 | 0.66 | 0.04 | 0.07 | 0.15 |
| **Total** | **82.80** | **99.95** | **92.30** | **92.51** | **79.99** | **78.09** | **90.31** | **81.23** |
| cations pfu per 6 oxygen | | | | | | | | |
| Si | 1.883 | 1.970 | 1.844 | 2.115 | 1.6632 | 2.194 | 1.771 | 1.648 |
| Ti | 0.000 | 0.000 | 0.038 | 0.000 | 0 | 0.000 | 0.003 | 0.011 |
| Al | 0.017 | 0.029 | 0.251 | 0.040 | 0.0156 | 0.000 | 0.346 | 0.337 |
| Cr | 0.000 | 0.000 | 0.000 | 0.000 | 0 | 0.000 | 0.000 | 0.001 |
| Fe | 0.479 | 0.386 | 0.327 | 0.181 | 1.4598 | 0.069 | 0.444 | 0.429 |
| Mn | 0.008 | 0.009 | 0.001 | 0.000 | 0 | 0.000 | 0.008 | 0.005 |
| Mg | 0.828 | 0.763 | 0.903 | 1.283 | 1.0992 | 1.534 | 1.210 | 1.103 |
| Ca | 0.887 | 0.845 | 0.555 | 0.236 | 0.0456 | 0.000 | 0.252 | 0.533 |
| Na | 0.009 | 0.026 | 0.137 | 0.020 | 0.0474 | 0.016 | 0.040 | 0.199 |
| K | 0.002 | 0.000 | 0.008 | 0.001 | 0.0444 | 0.002 | 0.004 | 0.009 |
| **Total** | **4.115** | **4.029** | **4.065** | **3.877** | **4.3758** | **3.816** | **4.077** | **4.276** |
| | | | | | | | | |
| Xdi | 0.779 | 0.803 | 0.817 | 0.893 | 0.440 | 0.957 | 0.764 | 0.790 |
| Xhd | 0.620 | 0.615 | 0.494 | 0.246 | 0.578 | 0.043 | 0.364 | 0.465 |

SMECTITE

| **Slide** | **GIL 48** | **GIL 48** | **GIL 48** | **GIL 48** | **GIL 48** | **GIL 48** | **GIL 48** | **GIL 48** |
|---|---|---|---|---|---|---|---|---|
| **Depth (mbsf)** | **253** | **253** | **253** | **253** | **253** | **253** | **253** | **253** |
| **Area** | **1** | **1** | **1** | **1** | **1** | **1** | **1** | **1** |
| **Point** | **1** | **3** | **4** | **5** | **6** | **7** | **8** | **2** |
| SiO2 | 37.07 | 45.01 | 46.03 | 40.27 | 39.89 | 48.25 | 49.84 | 52.14 |
| TiO2 | 0.18 | 0.20 | 0.19 | 0.16 | 0.19 | 0.21 | 0.22 | 0.21 |
| Al2O3 | 3.67 | 4.60 | 5.02 | 2.54 | 3.99 | 5.32 | 5.60 | 5.76 |
| Cr2O3 | 0.00 | 0.00 | 0.00 | 0.06 | 0.00 | 0.00 | 0.00 | 0.00 |
| FeO | 18.74 | 18.38 | 17.37 | 16.43 | 18.06 | 18.44 | 18.82 | 18.85 |
| MnO | 0.04 | 0.04 | 0.05 | 0.04 | 0.05 | 0.04 | 0.05 | 0.02 |
| MgO | 12.35 | 14.36 | 15.29 | 11.81 | 15.03 | 14.83 | 14.41 | 16.96 |
| CaO | 0.82 | 1.06 | 1.03 | 0.74 | 0.88 | 1.09 | 0.97 | 0.91 |
| Na2O | 0.46 | 0.82 | 0.72 | 0.43 | 0.76 | 0.89 | 0.66 | 0.82 |
| K2O | 0.64 | 0.65 | 0.59 | 0.40 | 0.56 | 0.54 | 0.47 | 0.65 |
| **Total** | **73.97** | **85.11** | **86.29** | **72.86** | **79.41** | **89.61** | **91.04** | **96.33** |
| cations pfu per 20 oyxgen | | | | | | | | |
| Si | 6.35 | 6.542 | 6.54 | 6.816 | 6.296 | 6.602 | 6.682 | 6.598 |
| Ti | 0.024 | 0.022 | 0.02 | 0.02 | 0.022 | 0.022 | 0.022 | 0.02 |
| Al | 0.742 | 0.788 | 0.84 | 0.506 | 0.742 | 0.858 | 0.884 | 0.86 |
| Cr | 0 | 0 | 0 | 0.008 | 0 | 0 | 0 | 0 |
| Fe | 2.684 | 2.234 | 2.064 | 2.326 | 2.384 | 2.11 | 2.11 | 1.996 |
| Mn | 0.006 | 0.004 | 0.006 | 0.006 | 0.008 | 0.004 | 0.006 | 0.002 |
| Mg | 3.154 | 3.11 | 3.238 | 2.978 | 3.538 | 3.026 | 2.88 | 3.2 |
| Ca | 0.15 | 0.166 | 0.156 | 0.134 | 0.148 | 0.16 | 0.14 | 0.124 |
| Na | 0.152 | 0.232 | 0.2 | 0.14 | 0.234 | 0.236 | 0.172 | 0.202 |
| K | 0.14 | 0.12 | 0.106 | 0.086 | 0.112 | 0.094 | 0.08 | 0.106 |
| **Total** | **13.402** | **13.22** | **13.172** | **13.022** | **13.486** | **13.114** | **12.976** | **13.108** |

SMECTITE

| **Slide** | **GIL 49** | **GIL 49** | **GIL 49** | **GIL 49** | **GIL 49** | **GIL 35** | **GIL 35** |
|---|---|---|---|---|---|---|---|
| **Depth (mbsf)** | **258** | **258** | **258** | **258** | **258** | **285** | **285** |
| **Area** | **1** | **1** | **1** | **1** | **1** | **2** | **2** |
| **Point** | **1** | **2** | **3** | **4** | **5** | **1** | **2** |
| SiO2 | 48.95 | 38.01 | 48.01 | 44.92 | 45.03 | 46.56 | 45.46 |
| TiO2 | 0.17 | 0.16 | 0.18 | 0.10 | 0.17 | 0.00 | 0.00 |
| Al2O3 | 3.08 | 2.26 | 2.90 | 2.73 | 2.68 | 3.84 | 4.69 |
| Cr2O3 | 0.00 | 0.02 | 0.07 | 0.01 | 0.00 | 0.00 | 0.00 |
| FeO | 17.78 | 17.67 | 17.68 | 17.46 | 17.51 | 18.01 | 19.44 |
| MnO | 0.07 | 0.09 | 0.09 | 0.07 | 0.05 | 0.05 | 0.03 |
| MgO | 13.96 | 11.33 | 13.62 | 10.70 | 11.88 | 14.75 | 14.71 |
| CaO | 0.87 | 1.26 | 1.11 | 1.27 | 0.94 | 1.41 | 1.08 |
| Na2O | 1.00 | 0.80 | 0.96 | 0.86 | 0.62 | 0.65 | 0.98 |
| K2O | 0.18 | 0.18 | 0.11 | 0.21 | 0.13 | 0.13 | 0.25 |
| **Total** | **86.07** | **71.78** | **84.73** | **78.34** | **79.02** | **85.40** | **86.64** |

cations pfu per 20 oxygen

| | | | | | | | |
|---|---|---|---|---|---|---|---|
| Si | 6.926 | 6.654 | 6.916 | 7.03 | 6.974 | 6.688 | 6.51 |
| Ti | 0.018 | 0.02 | 0.018 | 0.012 | 0.02 | 0 | 0 |
| Al | 0.514 | 0.466 | 0.492 | 0.504 | 0.49 | 0.65 | 0.792 |
| Cr | 0 | 0.002 | 0.008 | 0.002 | 0 | 0 | 0 |
| Fe | 2.104 | 2.586 | 2.13 | 2.286 | 2.268 | 2.164 | 2.328 |
| Mn | 0.008 | 0.014 | 0.01 | 0.01 | 0.006 | 0.006 | 0.004 |
| Mg | 2.944 | 2.956 | 2.924 | 2.498 | 2.742 | 3.158 | 3.14 |
| Ca | 0.132 | 0.236 | 0.172 | 0.214 | 0.156 | 0.216 | 0.166 |
| Na | 0.274 | 0.274 | 0.268 | 0.26 | 0.186 | 0.182 | 0.272 |
| K | 0.034 | 0.04 | 0.02 | 0.042 | 0.026 | 0.024 | 0.046 |
| **Total** | **12.954** | **13.248** | **12.96** | **12.858** | **12.868** | **13.09** | **13.26** |

CHLORITE

| Slide | GIL 16 | GIL 16 | GIL 16 | GIL 16 | GIL 25 | GIL 25 | GIL 25 | GIL 25 |
|---|---|---|---|---|---|---|---|---|
| **Depth (mbsf)** | **1204** | **1204** | **1204** | **1204** | **1448** | **1448** | **1448** | **1448** |
| **Area** | **1** | **2** | **3** | **3** | **2** | **3** | **3** | **4** |
| **Point** | **6** | **10** | **6** | **7** | **6** | **6** | **7** | **8** |
| SiO2 | 27.15 | 35.75 | 22.05 | 26.58 | 27.21 | 29.03 | 27.79 | 24.47 |
| TiO2 | 0.05 | 0.03 | 0.00 | 0.00 | 0.00 | 0.00 | 0.00 | 0.17 |
| Al2O3 | 15.98 | 17.31 | 13.79 | 16.35 | 16.99 | 14.31 | 12.98 | 13.12 |
| Cr2O3 | 0.02 | 0.03 | 0.00 | 0.00 | 0.00 | 0.03 | 0.03 | 0.00 |
| FeO | 24.98 | 19.46 | 22.90 | 23.54 | 11.63 | 12.73 | 13.10 | 14.86 |
| MnO | 0.22 | 0.26 | 0.08 | 0.07 | 0.00 | 0.04 | 0.05 | 0.14 |
| MgO | 16.06 | 6.87 | 13.54 | 16.72 | 19.64 | 24.28 | 22.24 | 19.21 |
| CaO | 0.29 | 1.57 | 0.34 | 0.20 | 0.73 | 0.51 | 0.64 | 0.17 |
| Na2O | 0.24 | 3.18 | 0.15 | 0.43 | 0.40 | 0.02 | 0.01 | 0.16 |
| K2O | 0.09 | 0.45 | 0.06 | 0.09 | 0.55 | 0.05 | 0.04 | 0.47 |
| **Total** | **85.08** | **84.90** | **72.91** | **83.97** | **77.15** | **80.99** | **76.88** | **72.78** |
| | | | | | | | | |
| cations pfu per 28 oxygen | | | | | | | | |
| Si | 5.928 | 7.473 | 5.692 | 5.841 | 6.096 | 6.210 | 6.303 | 5.998 |
| Ti | 0.008 | 0.006 | 0.000 | 0.000 | 0.000 | 0.000 | 0.000 | 0.031 |
| Al | 4.110 | 4.264 | 4.197 | 4.234 | 4.486 | 3.609 | 3.469 | 3.788 |
| Cr | 0.003 | 0.006 | 0.000 | 0.000 | 0.000 | 0.006 | 0.006 | 0.000 |
| Fe | 4.561 | 3.402 | 4.945 | 4.326 | 2.178 | 2.276 | 2.484 | 3.046 |
| Mn | 0.039 | 0.045 | 0.020 | 0.014 | 0.000 | 0.008 | 0.011 | 0.031 |
| Mg | 5.228 | 2.139 | 5.214 | 5.477 | 6.560 | 7.745 | 7.521 | 7.022 |
| Ca | 0.067 | 0.353 | 0.092 | 0.045 | 0.176 | 0.118 | 0.157 | 0.045 |
| Na | 0.104 | 1.288 | 0.073 | 0.182 | 0.174 | 0.006 | 0.003 | 0.076 |
| K | 0.025 | 0.120 | 0.022 | 0.025 | 0.157 | 0.014 | 0.011 | 0.148 |
| **Total** | **20.073** | **19.099** | **20.258** | **20.143** | **19.830** | **19.995** | **19.967** | **20.188** |

HORNBLENDE

| Slide | GIL 23 | GIL 23 | GIL 23 | GIL 23 | GIL 23 | GIL 23 | GIL 25 | GIL 25 | GIL 25 | GIL 25 |
|---|---|---|---|---|---|---|---|---|---|---|
| **Depth (mbsf)** | **1373** | **1373** | **1373** | **1373** | **1373** | **1373** | **1448** | **1448** | **1448** | **1448** |
| **Area** | **1** | **1** | **1** | **2** | **2** | **2** | **1** | **1** | **2** | **2** |
| **Point** | **1** | **2** | **13** | **3** | **8** | **11** | **5** | **6** | **7** | **8** |
| SiO2 | 44.99 | 49.30 | 51.39 | 49.26 | 48.89 | 48.96 | 47.26 | 41.67 | 42.08 | 45.05 |
| TiO2 | 1.01 | 0.00 | 0.00 | 0.13 | 0.14 | 0.00 | 0.38 | 0.02 | 0.01 | 0.16 |
| Al2O3 | 4.82 | 1.36 | 1.15 | 2.68 | 2.43 | 0.72 | 10.97 | 10.33 | 8.93 | 7.95 |
| Cr2O3 | 0.00 | 0.00 | 0.00 | 0.00 | 0.00 | 0.00 | 0.00 | 0.00 | 0.00 | 0.00 |
| FeO | 13.18 | 14.47 | 14.21 | 14.63 | 14.85 | 14.96 | 11.06 | 11.63 | 10.45 | 9.58 |
| MnO | 0.10 | 0.22 | 0.14 | 0.23 | 0.22 | 0.25 | 0.02 | 0.03 | 0.02 | 0.13 |
| MgO | 14.56 | 15.85 | 13.38 | 13.99 | 14.11 | 10.68 | 15.41 | 15.41 | 17.60 | 16.22 |
| CaO | 10.49 | 11.51 | 11.84 | 10.53 | 10.19 | 11.08 | 10.91 | 10.72 | 11.17 | 10.57 |
| Na2O | 2.01 | 0.51 | 0.93 | 0.46 | 0.62 | 0.13 | 2.73 | 2.90 | 2.57 | 2.25 |
| K2O | 0.31 | 0.11 | 0.44 | 0.06 | 0.15 | 0.04 | 0.16 | 0.16 | 0.10 | 0.33 |
| **Total** | **91.46** | **93.34** | **93.47** | **91.98** | **91.60** | **86.82** | **98.91** | **92.85** | **92.92** | **92.23** |
| | | | | | | | | | | |
| cations pfu per 23 oxygen | | | | | | | | | | |
| Si | 7.077 | 7.567 | 7.848 | 7.629 | 7.622 | 8.0523 | 6.744 | 6.445 | 6.475 | 6.889 |
| Ti | 0.120 | 0.000 | 0.000 | 0.016 | 0.016 | 0 | 0.041 | 0.002 | 0.002 | 0.018 |
| Al | 0.895 | 0.246 | 0.207 | 0.490 | 0.446 | 0.1403 | 1.845 | 1.881 | 1.619 | 1.433 |
| Cr | 0.000 | 0.000 | 0.000 | 0.000 | 0.000 | 0 | 0.000 | 0.000 | 0.000 | 0.000 |
| Fe | 1.734 | 1.858 | 1.815 | 1.895 | 1.937 | 2.0585 | 1.320 | 1.504 | 1.346 | 1.226 |
| Mn | 0.014 | 0.030 | 0.018 | 0.030 | 0.030 | 0.0345 | 0.002 | 0.005 | 0.002 | 0.016 |
| Mg | 3.413 | 3.627 | 3.045 | 3.229 | 3.280 | 2.6174 | 3.278 | 3.551 | 4.037 | 3.698 |
| Ca | 1.769 | 1.893 | 1.937 | 1.748 | 1.702 | 1.9527 | 1.668 | 1.776 | 1.840 | 1.732 |
| Na | 0.612 | 0.152 | 0.276 | 0.138 | 0.189 | 0.0414 | 0.757 | 0.869 | 0.766 | 0.667 |
| K | 0.062 | 0.021 | 0.085 | 0.012 | 0.030 | 0.0092 | 0.030 | 0.032 | 0.018 | 0.064 |
| **Total** | **15.698** | **15.396** | **15.233** | **15.189** | **15.254** | **14.9086** | **15.684** | **16.066** | **16.105** | **15.746** |

HORNBLENDE

| **Slide** | **GIL 25** | **GIL 25** | **GIL 25** | **GIL 25** | **GIL 25** | **GIL 25** | **GIL 25** | **GIL 25** | **GIL 25** | **GIL 25** | **GIL 25** |
|---|---|---|---|---|---|---|---|---|---|---|---|
| **Depth (mbsf)** | **1448** | **1448** | **1448** | **1448** | **1448** | **1448** | **1448** | **1448** | **1448** | **1448** | **1448** |
| **Area** | **3** | **3** | **3** | **3** | **4** | **4** | **4** | **4** | **4** | **4** | **4** |
| **Point** | **3** | **4** | **5** | **8** | **4** | **5** | **6** | **7** | **9** | **10** | **11** |
| SiO2 | 46.68 | 31.15 | 47.18 | 39.60 | 43.66 | 47.90 | 51.82 | 49.41 | 56.97 | 54.53 | 38.14 |
| TiO2 | 0.03 | 0.00 | 0.00 | 0.00 | 3.76 | 0.08 | 0.01 | 0.01 | 0.01 | 0.00 | 2.20 |
| Al2O3 | 9.03 | 11.92 | 5.14 | 5.18 | 10.77 | 7.30 | 3.28 | 2.56 | 1.09 | 0.94 | 7.11 |
| Cr2O3 | 0.00 | 0.00 | 0.00 | 0.00 | 0.04 | 0.00 | 0.01 | 0.03 | 0.00 | 0.00 | 0.04 |
| FeO | 12.51 | 11.48 | 8.53 | 9.30 | 12.89 | 9.48 | 19.02 | 19.54 | 6.10 | 6.83 | 11.88 |
| MnO | 0.10 | 0.04 | 0.00 | 0.01 | 0.14 | 0.14 | 0.08 | 0.08 | 0.00 | 0.02 | 0.13 |
| MgO | 22.32 | 18.26 | 21.72 | 20.64 | 12.68 | 15.45 | 17.96 | 17.07 | 26.60 | 23.93 | 10.96 |
| CaO | 1.91 | 2.44 | 0.98 | 1.15 | 11.18 | 10.91 | 1.19 | 0.97 | 0.30 | 1.24 | 11.25 |
| Na2O | 0.35 | 0.03 | 0.13 | 0.24 | 2.84 | 1.63 | 0.75 | 0.55 | 0.81 | 0.99 | 1.52 |
| K2O | 0.07 | 0.03 | 0.10 | 0.12 | 0.50 | 0.20 | 0.25 | 0.25 | 0.21 | 0.38 | 0.31 |
| **Total** | **93.00** | **75.34** | **83.79** | **76.25** | **98.47** | **93.10** | **94.38** | **90.47** | **92.11** | **88.87** | **83.55** |
| | | | | | | | | | | | |
| cations pfu per 23 oxygen | | | | | | | | | | | |
| Si | 6.898 | 5.831 | 7.526 | 7.091 | 6.399 | 7.185 | 7.721 | 7.733 | 8.094 | 8.110 | 6.631 |
| Ti | 0.002 | 0.000 | 0.000 | 0.000 | 0.414 | 0.009 | 0.000 | 0.000 | 0.002 | 0.000 | 0.288 |
| Al | 1.573 | 2.629 | 0.966 | 1.093 | 1.861 | 1.290 | 0.575 | 0.472 | 0.184 | 0.166 | 1.456 |
| Cr | 0.000 | 0.000 | 0.000 | 0.000 | 0.005 | 0.000 | 0.000 | 0.002 | 0.000 | 0.000 | 0.005 |
| Fe | 1.546 | 1.796 | 1.136 | 1.394 | 1.580 | 1.189 | 2.371 | 2.558 | 0.725 | 0.849 | 1.727 |
| Mn | 0.014 | 0.007 | 0.000 | 0.002 | 0.016 | 0.018 | 0.012 | 0.012 | 0.000 | 0.002 | 0.018 |
| Mg | 4.917 | 5.095 | 5.166 | 5.509 | 2.772 | 3.455 | 3.991 | 3.981 | 5.635 | 5.304 | 2.838 |
| Ca | 0.304 | 0.488 | 0.168 | 0.221 | 1.757 | 1.755 | 0.189 | 0.163 | 0.046 | 0.198 | 2.095 |
| Na | 0.101 | 0.012 | 0.041 | 0.083 | 0.807 | 0.474 | 0.219 | 0.168 | 0.223 | 0.285 | 0.513 |
| K | 0.012 | 0.007 | 0.021 | 0.028 | 0.094 | 0.039 | 0.048 | 0.051 | 0.039 | 0.071 | 0.069 |
| **Total** | **15.369** | **15.865** | **15.026** | **15.419** | **15.707** | **15.417** | **15.125** | **15.139** | **14.950** | **14.985** | **15.642** |

ACTINOLITE

| Slide | GIL 25 | GIL 25 | GIL 25 | GIL 25 | GIL 25 |
|---|---|---|---|---|---|
| **Depth (mbsf)** | **1448** | **1448** | **1448** | **1448** | **1448** |
| **Area** | **1** | **1** | **2** | **2** | **3** |
| **Point** | **3** | **4** | **7** | **8** | **11** |
| SiO2 | 54.72 | 46.00 | 42.08 | 45.05 | 35.08 |
| TiO2 | 0.20 | 1.27 | 0.01 | 0.16 | 0.31 |
| Al2O3 | 5.94 | 5.32 | 8.93 | 7.95 | 6.08 |
| Cr2O3 | 0.00 | 0.00 | 0.00 | 0.00 | 0.04 |
| FeO | 10.84 | 9.75 | 10.45 | 9.58 | 10.91 |
| MnO | 0.08 | 0.02 | 0.02 | 0.13 | 0.14 |
| MgO | 18.51 | 15.11 | 17.60 | 16.22 | 15.75 |
| CaO | 9.50 | 12.92 | 11.17 | 10.57 | 10.59 |
| Na2O | 1.81 | 1.77 | 2.57 | 2.25 | 2.18 |
| K2O | 0.14 | 0.15 | 0.10 | 0.33 | 0.15 |
| **Total** | **101.72** | **92.30** | **92.92** | **92.23** | **81.23** |
| cations pfu per 23 oxygen | | | | | |
| Si | 7.447 | 7.070 | 6.475 | 6.889 | 6.318 |
| Ti | 0.021 | 0.147 | 0.002 | 0.018 | 0.041 |
| Al | 0.952 | 0.964 | 1.619 | 1.433 | 1.290 |
| Cr | 0.000 | 0.000 | 0.000 | 0.000 | 0.005 |
| Fe | 1.233 | 1.254 | 1.346 | 1.226 | 1.645 |
| Mn | 0.009 | 0.002 | 0.002 | 0.016 | 0.021 |
| Mg | 3.756 | 3.462 | 4.037 | 3.698 | 4.230 |
| Ca | 1.385 | 2.128 | 1.840 | 1.732 | 2.045 |
| Na | 0.476 | 0.527 | 0.766 | 0.667 | 0.761 |
| K | 0.023 | 0.030 | 0.018 | 0.064 | 0.035 |
| **Total** | **15.304** | **15.583** | **16.105** | **15.746** | **16.392** |

ORTHOPYROXENE

| Slide | GIL 35 | GIL 16 | GIL 16 | GIL 16 |
|---|---|---|---|---|
| **Depth (mbsf)** | **285** | **1204** | **1204** | **1204** |
| **Area** | **1** | **1** | **1** | **2** |
| **Point** | **7** | **4** | **7** | **11** |
| SiO2 | 39.08 | 36.24 | 41.26 | 39.45 |
| TiO2 | 0.02 | 0.17 | 1.40 | 0.15 |
| Al2O3 | 7.20 | 6.46 | 6.17 | 10.11 |
| Cr2O3 | 0.00 | 0.10 | 0.06 | 0.04 |
| FeO | 30.48 | 20.84 | 20.12 | 23.83 |
| MnO | 0.18 | 0.37 | 0.38 | 0.43 |
| MgO | 11.75 | 10.70 | 11.78 | 10.83 |
| CaO | 1.36 | 9.42 | 9.25 | 6.11 |
| Na2O | 1.11 | 0.44 | 1.14 | 0.75 |
| K2O | 0.12 | 0.09 | 0.37 | 0.32 |
| **Total** | **91.30** | **84.83** | **91.92** | **92.02** |
| cations pfu per 6 oxygen | | | | |
| Si | 1.715 | 1.691 | 1.749 | 1.679 |
| Ti | 0.001 | 0.006 | 0.044 | 0.005 |
| Al | 0.373 | 0.355 | 0.308 | 0.507 |
| Cr | 0.000 | 0.004 | 0.002 | 0.001 |
| Fe | 1.119 | 0.813 | 0.713 | 0.848 |
| Mn | 0.007 | 0.014 | 0.014 | 0.016 |
| Mg | 0.769 | 0.745 | 0.744 | 0.688 |
| Ca | 0.064 | 0.471 | 0.420 | 0.279 |
| Na | 0.094 | 0.040 | 0.094 | 0.062 |
| K | 0.007 | 0.005 | 0.020 | 0.017 |
| **Total** | **4.147** | **4.145** | **4.108** | **4.102** |
| Xdi | 0.425 | 0.595 | 0.615 | 0.528 |
| Xhd | 0.604 | 0.628 | 0.599 | 0.616 |

QUARTZ

| Slide | GIL 35 | GIL 16 | GIL 16 | GIL 16 | GIL 23 | GIL 23 | GIL 23 | GIL 23 | GIL 23 | GIL 23 |
|---|---|---|---|---|---|---|---|---|---|---|
| **Depth (mbsf)** | **285** | **1204** | **1204** | **1204** | **1373** | **1373** | **1373** | **1373** | **1373** | **1373** |
| **Area** | **2** | **1** | **2** | **3** | **1** | **1** | **1** | **1** | **2** | **2** |
| **Point** | **9** | **1** | **16** | **3** | **7** | **8** | **9** | **10** | **1** | **2** |
| SiO2 | 89.72 | 94.70 | 94.78 | 91.39 | 90.82 | 95.19 | 93.06 | 92.69 | 94.67 | 89.97 |
| TiO2 | 0.03 | 0.04 | 0.00 | 0.00 | 0.00 | 0.00 | 0.00 | 0.00 | 0.00 | 0.00 |
| Al2O3 | 0.98 | 0.13 | 0.22 | 0.29 | 0.07 | 0.06 | 0.05 | 0.03 | 0.11 | 0.05 |
| Cr2O3 | 0.00 | 0.00 | 0.00 | 0.00 | 0.00 | 0.00 | 0.00 | 0.00 | 0.00 | 0.00 |
| FeO | 0.13 | 0.25 | 0.24 | 0.40 | 0.08 | 0.11 | 0.00 | 0.00 | 0.00 | 0.00 |
| MnO | 0.01 | 0.00 | 0.00 | 0.00 | 0.00 | 0.00 | 0.00 | 0.00 | 0.00 | 0.00 |
| MgO | 0.02 | 0.00 | 0.03 | 0.09 | 0.00 | 0.00 | 0.00 | 0.00 | 0.02 | 0.00 |
| CaO | 0.28 | 0.02 | 0.08 | 0.00 | 0.16 | 0.00 | 0.03 | 0.00 | 0.00 | 0.00 |
| Na2O | 0.57 | 0.05 | 0.08 | 0.07 | 0.31 | 0.02 | 0.15 | 0.03 | 0.19 | 0.04 |
| K2O | 0.05 | 0.03 | 0.06 | 0.02 | 0.12 | 0.00 | 0.04 | 0.01 | 0.05 | 0.00 |
| **Total** | **91.78** | **95.22** | **95.48** | **92.26** | **91.56** | **95.38** | **93.33** | **92.76** | **95.04** | **90.06** |
| cations pfu per 2 oxygen | | | | | | | | | | |
| Si | 0.985 | 0.997 | 0.996 | 0.994 | 0.996 | 0.999 | 0.998 | 1.000 | 0.998 | 0.999 |
| Ti | 0.000 | 0.000 | 0.000 | 0.000 | 0.000 | 0.000 | 0.000 | 0.000 | 0.000 | 0.000 |
| Al | 0.013 | 0.002 | 0.003 | 0.004 | 0.001 | 0.001 | 0.001 | 0.000 | 0.001 | 0.001 |
| Cr | 0.000 | 0.000 | 0.000 | 0.000 | 0.000 | 0.000 | 0.000 | 0.000 | 0.000 | 0.000 |
| Fe | 0.001 | 0.002 | 0.002 | 0.004 | 0.001 | 0.001 | 0.000 | 0.000 | 0.000 | 0.000 |
| Mn | 0.000 | 0.000 | 0.000 | 0.000 | 0.000 | 0.000 | 0.000 | 0.000 | 0.000 | 0.000 |
| Mg | 0.000 | 0.000 | 0.000 | 0.001 | 0.000 | 0.000 | 0.000 | 0.000 | 0.000 | 0.000 |
| Ca | 0.003 | 0.000 | 0.001 | 0.000 | 0.002 | 0.000 | 0.000 | 0.000 | 0.000 | 0.000 |
| Na | 0.012 | 0.001 | 0.002 | 0.002 | 0.007 | 0.000 | 0.003 | 0.001 | 0.004 | 0.001 |
| K | 0.001 | 0.000 | 0.001 | 0.000 | 0.002 | 0.000 | 0.001 | 0.000 | 0.001 | 0.000 |
| **Total** | **1.015** | **1.003** | **1.004** | **1.005** | **1.008** | **1.001** | **1.003** | **1.001** | **1.004** | **1.001** |

ULVOSPINEL

| Slide | GIL 48 | GIL 48 | GIL 48 | GIL 48 | GIL 49 | GIL 49 | GIL 49 | GIL 35 | GIL 35 | GIL 35 | GIL 35 |
|---|---|---|---|---|---|---|---|---|---|---|---|
| **Depth (mbsf)** | **253** | **253** | **253** | **253** | **258** | **258** | **258** | **285** | **285** | **285** | **285** |
| **Area** | **1** | **2** | **2** | **3** | **1** | **2** | **3** | **1** | **1** | **1** | **2** |
| **Point** | **11** | **1** | **2** | **8** | **8** | **1** | **2** | **1** | **2** | **6** | **3** |
| SiO2 | 0.38 | 0.27 | 0.41 | 4.92 | 1.75 | 0.97 | 2.85 | 0.43 | 1.40 | 0.52 | 0.21 |
| TiO2 | 21.79 | 21.29 | 22.18 | 20.88 | 20.25 | 21.63 | 21.47 | 22.75 | 22.75 | 19.04 | 22.81 |
| Al2O3 | 2.94 | 2.24 | 1.30 | 2.18 | 1.91 | 1.95 | 1.56 | 1.47 | 0.93 | 0.61 | 1.03 |
| Cr2O3 | 0.11 | 0.05 | 0.11 | 0.00 | 0.11 | 0.06 | 0.05 | 0.44 | 0.12 | 0.06 | 0.02 |
| FeO | 69.79 | 69.42 | 65.59 | 62.31 | 64.97 | 69.15 | 63.95 | 69.82 | 67.05 | 71.16 | 69.28 |
| MnO | 0.57 | 0.45 | 0.57 | 1.77 | 1.34 | 1.07 | 0.99 | 1.30 | 1.64 | 0.97 | 1.01 |
| MgO | 1.05 | 0.83 | 0.24 | 0.40 | 0.73 | 0.47 | 1.38 | 0.24 | 0.32 | 0.42 | 0.21 |
| CaO | 0.11 | 0.11 | 0.26 | 0.49 | 0.32 | 0.24 | 0.26 | 0.04 | 0.14 | 0.10 | 0.12 |
| Na2O | 0.05 | 0.03 | 0.04 | 0.19 | 0.19 | 0.18 | 0.25 | 0.00 | 0.06 | 0.03 | 0.18 |
| K2O | 0.02 | 0.02 | 0.03 | 0.05 | 0.07 | 0.04 | 0.04 | 0.03 | 0.04 | 0.02 | 0.05 |
| **Total** | **96.80** | **94.71** | **90.72** | **93.20** | **91.62** | **95.75** | **92.80** | **96.52** | **94.43** | **92.93** | **94.92** |
| | | | | | | | | | | | |
| cations pfu per 4 oxygen | | | | | | | | | | | |
| Si | 0.015 | 0.011 | 0.018 | 0.197 | 0.074 | 0.040 | 0.116 | 0.018 | 0.058 | 0.023 | 0.008 |
| Ti | 0.659 | 0.664 | 0.720 | 0.628 | 0.644 | 0.665 | 0.661 | 0.698 | 0.706 | 0.623 | 0.715 |
| Al | 0.139 | 0.110 | 0.066 | 0.103 | 0.095 | 0.094 | 0.076 | 0.070 | 0.045 | 0.031 | 0.051 |
| Cr | 0.004 | 0.002 | 0.004 | 0.000 | 0.004 | 0.002 | 0.002 | 0.014 | 0.004 | 0.002 | 0.001 |
| Fe | 2.348 | 2.408 | 2.369 | 2.083 | 2.298 | 2.363 | 2.189 | 2.381 | 2.313 | 2.589 | 2.414 |
| Mn | 0.019 | 0.016 | 0.021 | 0.060 | 0.048 | 0.037 | 0.034 | 0.045 | 0.057 | 0.036 | 0.036 |
| Mg | 0.063 | 0.051 | 0.016 | 0.024 | 0.046 | 0.029 | 0.084 | 0.014 | 0.019 | 0.027 | 0.013 |
| Ca | 0.004 | 0.005 | 0.012 | 0.021 | 0.014 | 0.010 | 0.012 | 0.002 | 0.006 | 0.005 | 0.005 |
| Na | 0.004 | 0.003 | 0.004 | 0.015 | 0.016 | 0.014 | 0.020 | 0.000 | 0.005 | 0.002 | 0.015 |
| K | 0.001 | 0.001 | 0.002 | 0.003 | 0.004 | 0.002 | 0.002 | 0.002 | 0.002 | 0.001 | 0.003 |
| **Total** | **3.257** | **3.271** | **3.231** | **3.133** | **3.242** | **3.256** | **3.196** | **3.243** | **3.216** | **3.340** | **3.261** |

ULVOSPINEL

| Slide | GIL 16 | GIL 16 | GIL 16 | GIL 16 | GIL 25 |
|---|---|---|---|---|---|
| **Depth (mbsf)** | **1204** | **1204** | **1204** | **1204** | **1448** |
| **Area** | **4** | **5** | **17** | **5** | **3** |
| **Point** | **2** | **2** | **2** | **1** | **10** |
| SiO2 | 6.17 | 0.74 | 1.99 | 3.99 | 0.40 |
| TiO2 | 22.98 | 20.23 | 28.37 | 18.01 | 28.55 |
| Al2O3 | 0.88 | 1.54 | 0.84 | 1.52 | 0.91 |
| Cr2O3 | 0.24 | 0.27 | 0.28 | 0.23 | 0.38 |
| FeO | 55.97 | 66.18 | 55.71 | 61.90 | 64.26 |
| MnO | 1.30 | 3.97 | 1.80 | 2.54 | 0.53 |
| MgO | 0.09 | 0.03 | 0.02 | 0.08 | 0.99 |
| CaO | 5.65 | 0.74 | 1.84 | 3.40 | 0.13 |
| Na2O | 0.22 | 0.30 | 0.29 | 0.54 | 0.26 |
| K2O | 0.09 | 0.11 | 0.09 | 0.18 | 0.09 |
| **Total** | **93.61** | **94.11** | **91.23** | **92.38** | **96.49** |
| cations pfu per 4 oxygen | | | | | |
| Si | 0.240 | 0.031 | 0.080 | 0.166 | 0.016 |
| Ti | 0.670 | 0.642 | 0.862 | 0.562 | 0.843 |
| Al | 0.040 | 0.076 | 0.040 | 0.074 | 0.042 |
| Cr | 0.007 | 0.009 | 0.009 | 0.008 | 0.012 |
| Fe | 1.816 | 2.334 | 1.884 | 2.149 | 2.109 |
| Mn | 0.042 | 0.142 | 0.062 | 0.089 | 0.018 |
| Mg | 0.006 | 0.002 | 0.001 | 0.005 | 0.058 |
| Ca | 0.235 | 0.033 | 0.080 | 0.151 | 0.005 |
| Na | 0.017 | 0.024 | 0.023 | 0.044 | 0.020 |
| K | 0.004 | 0.006 | 0.005 | 0.009 | 0.004 |
| **Total** | **3.077** | **3.300** | **3.046** | **3.258** | **3.127** |

Fe-OXIDES

| Slide | GIL 23 | GIL 23 | GIL 23 |
|---|---|---|---|
| **Depth (mbsf)** | **1373** | **1373** | **1373** |
| **Area** | **1** | **1** | **2** |
| **Point** | **11** | **12** | **9** |
| SiO2 | 0.36 | 0.38 | 0.36 |
| TiO2 | 4.42 | 6.47 | 3.76 |
| Al2O3 | 0.41 | 0.69 | 0.62 |
| Cr2O3 | 0.17 | 0.15 | 0.11 |
| FeO | 88.00 | 83.20 | 84.74 |
| MnO | 0.43 | 0.33 | 0.21 |
| MgO | 0.05 | 0.16 | 0.19 |
| CaO | 0.08 | 0.16 | 0.17 |
| Na2O | 0.16 | 0.26 | 1.04 |
| K2O | 0.08 | 0.10 | 0.15 |
| **Total** | **94.17** | **91.91** | **91.35** |
| | titano-magnetite | titano-magnetite | titano-magnetite |
| cations pfu per 4 oxygen | | | |
| Si | 0.018 | 0.019 | 0.018 |
| Ti | 0.161 | 0.236 | 0.141 |
| Al | 0.024 | 0.040 | 0.036 |
| Cr | 0.006 | 0.006 | 0.004 |
| Fe | 3.563 | 3.374 | 3.534 |
| Mn | 0.018 | 0.014 | 0.009 |
| Mg | 0.004 | 0.012 | 0.014 |
| Ca | 0.004 | 0.008 | 0.009 |
| Na | 0.015 | 0.024 | 0.101 |
| K | 0.005 | 0.006 | 0.010 |
| **Total** | **3.817** | **3.738** | **3.877** |

| Slide | GIL 23 | GIL 25 |
|---|---|---|
| **Depth (mbsf)** | **1373** | **1448** |
| **Area** | **2** | **4** |
| **Point** | **10** | **13** |
| SiO2 | 0.48 | 0.22 |
| TiO2 | 45.07 | 48.23 |
| Al2O3 | 0.30 | 0.12 |
| Cr2O3 | 0.00 | 0.00 |
| FeO | 49.94 | 47.08 |
| MnO | 1.45 | 3.09 |
| MgO | 0.27 | 0.11 |
| CaO | 0.15 | 0.25 |
| Na2O | 0.31 | 0.09 |
| K2O | 0.07 | 0.06 |
| **Total** | **98.05** | **99.25** |
| | ilmenite | ilmenite |
| cations pfu per 3 oxygen | | |
| Si | 0.0126 | 0.01 |
| Ti | 0.8982 | 0.94 |
| Al | 0.0096 | 0.00 |
| Cr | 0 | 0.00 |
| Fe | 1.1067 | 1.02 |
| Mn | 0.0327 | 0.07 |
| Mg | 0.0108 | 0.00 |
| Ca | 0.0045 | 0.01 |
| Na | 0.0162 | 0.00 |
| K | 0.0024 | 0.00 |
| **Total** | **2.094** | **2.06** |

Fe-OXIDES

| **Slide** | **GIL 25** | **GIL 25** | **GIL 25** | **GIL 25** | **GIL 25** | **GIL 25** |
|---|---|---|---|---|---|---|
| **Depth (mbsf)** | **1448** | **1448** | **1448** | **1448** | **1448** | **1448** |
| **Area** | **1** | **1** | **2** | **2** | **3** | **4** |
| **Point** | **9** | **10** | **1** | **4** | **9** | **12** |
| SiO2 | 2.17 | 2.39 | 16.77 | 2.22 | 0.30 | 12.22 |
| TiO2 | 0.28 | 0.68 | 0.46 | 0.06 | 0.24 | 0.37 |
| Al2O3 | 0.51 | 0.47 | 0.84 | 0.04 | 0.08 | 2.58 |
| Cr2O3 | 0.01 | 0.07 | 0.00 | 0.05 | 0.32 | 0.22 |
| FeO | 89.38 | 88.98 | 67.13 | 92.42 | 42.60 | 74.22 |
| MnO | 0.06 | 0.03 | 0.12 | 0.01 | 0.13 | 0.11 |
| MgO | 0.80 | 0.86 | 8.41 | 0.42 | 0.08 | 9.02 |
| CaO | 0.17 | 0.21 | 0.61 | 0.09 | 0.11 | 0.23 |
| Na2O | 0.09 | 0.51 | 0.95 | 0.20 | 0.16 | 0.49 |
| K2O | 0.05 | 0.10 | 0.10 | 0.06 | 0.10 | 0.17 |
| **Total** | **93.51** | **94.31** | **95.39** | **95.57** | **44.11** | **99.64** |
| | magnetite | magnetite | magnetite | magnetite | magnetite | magnetite |
| cations pfu per 4 oxygen | | | | | | |
| Si | 0.106 | 0.115 | 0.632 | 0.107 | 0.032 | 0.460 |
| Ti | 0.010 | 0.024 | 0.013 | 0.002 | 0.019 | 0.010 |
| Al | 0.030 | 0.026 | 0.037 | 0.002 | 0.010 | 0.114 |
| Cr | 0.000 | 0.003 | 0.000 | 0.002 | 0.026 | 0.007 |
| Fe | 3.648 | 3.576 | 2.116 | 3.729 | 3.783 | 2.336 |
| Mn | 0.002 | 0.002 | 0.004 | 0.000 | 0.012 | 0.004 |
| Mg | 0.058 | 0.062 | 0.473 | 0.030 | 0.012 | 0.506 |
| Ca | 0.009 | 0.011 | 0.025 | 0.005 | 0.013 | 0.009 |
| Na | 0.008 | 0.047 | 0.070 | 0.019 | 0.033 | 0.036 |
| K | 0.003 | 0.006 | 0.005 | 0.004 | 0.014 | 0.008 |
| **Total** | **3.875** | **3.873** | **3.374** | **3.900** | **3.954** | **3.490** |

OLIVINE

| **Slide** | **GIL 25** |
|---|---|
| **Depth (mbsf)** | **1448** |
| **Area** | **2** |
| **Point** | **2** |
| SiO2 | 35.66 |
| TiO2 | 0.00 |
| Al2O3 | 0.00 |
| Cr2O3 | 0.00 |
| FeO | 29.49 |
| MnO | 0.34 |
| MgO | 34.03 |
| CaO | 0.05 |
| Na2O | 0.08 |
| K2O | 0.00 |
| **Total** | **99.67** |
| cations pfu per 4 oxygen | |
| Si | 0.970 |
| Ti | 0.000 |
| Al | 0.000 |
| Cr | 0.000 |
| Fe | 0.670 |
| Mn | 0.008 |
| Mg | 1.379 |
| Ca | 0.002 |
| Na | 0.004 |
| K | 0.000 |
| **Total** | **3.034** |

# APPENDIX C
## Petrographic Descriptions of Kane Fracture Zone Thin Sections

The following appendix includes petrographic descriptions of 10 thin sections collected from the Kane Fracture Zone. Descriptions include thin section number, rock type, overall grain size, textures, replacement/alteration minerals, and anything noteworthy. The descriptions have been grouped into gabbros and basalts. With each petrographic description there is a photomicrograph of the thin section, all have been taken at the same optical zoom. All photos are in plane polarized light unless otherwise noted.

| | |
|---|---|
| Thin Section<br>Rock Type | KFZ85_010_08_2<br>Basalt |
| Overall Grain Size | Overall glassy, majority of thin section has no grains visible. Microphenocrysts of plagioclase laths (~1mm in length) and olivine are present (~0.5mm). Vesicles present vary between 0.1 mm-0.75 mm. |
| Textures | Glassy. Plagioclase forms as very thin laths, and olivine is euhedral or forms a swallow tail shape. |
| Alteration/ Replacements | Vesicles have possible clay material present in them, (brown colour), however EMP could not confirm this. No alteration is obvious. |
| Notes | Photomicrograph does not show much, plagioclase is more defined then seen here however this thin section is almost all glass, plane polarized light. |

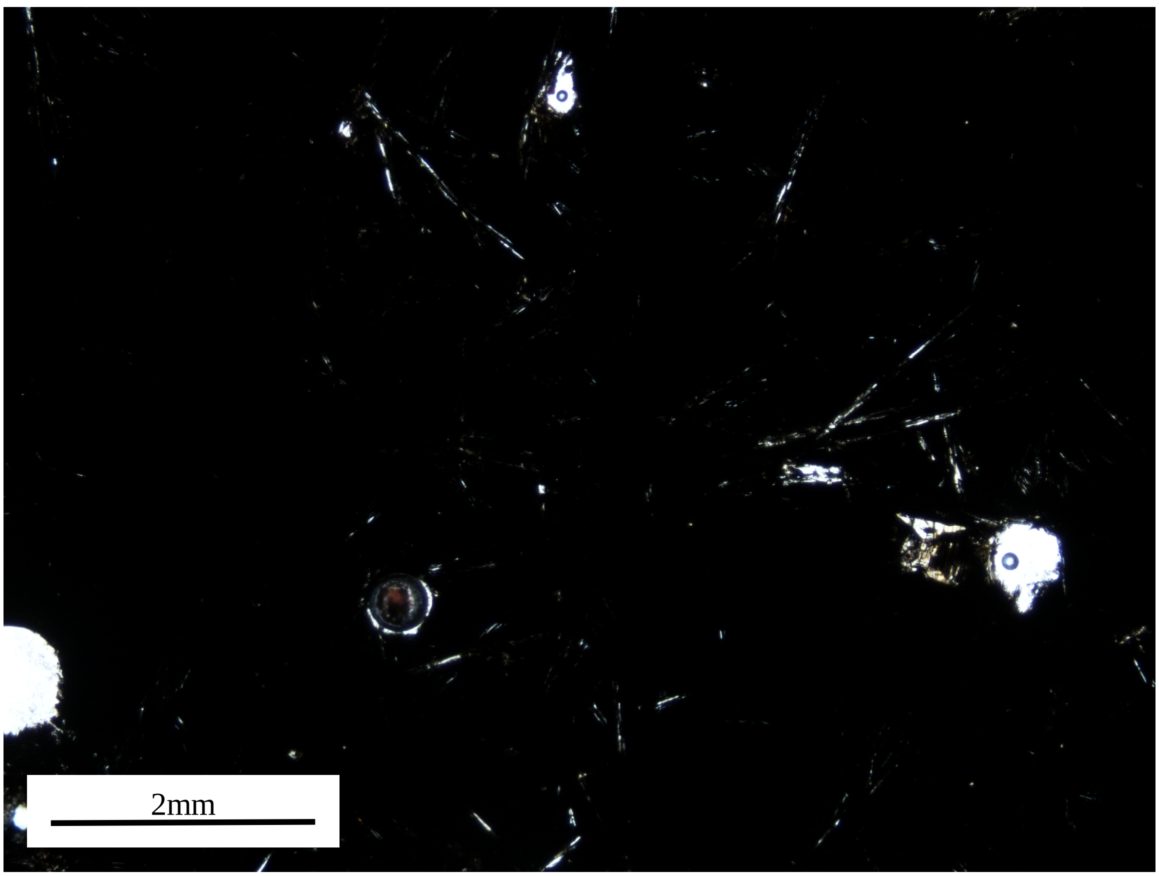

| | |
|---|---|
| Thin Section<br>Rock Type | KFZ85_010_09_6<br>Basalt |
| Overall Grain Size | Laths of plagioclase are ≤ 1mm in length. Olivine is fine-grain ~0.2mm. Vesicles are not common, but are ~ 1mm in diameter. |
| Textures | Plagioclase sporadically grows throughout the glass matrix; it does not follow a specific trend. Olivine is often found near the center of dense plagioclase growths. Olivine is euhedral to subhedral. |
| Alteration/ Replacements | No alteration occurs in this thin section. |
| Notes | Photo taken in plane polarized light. |

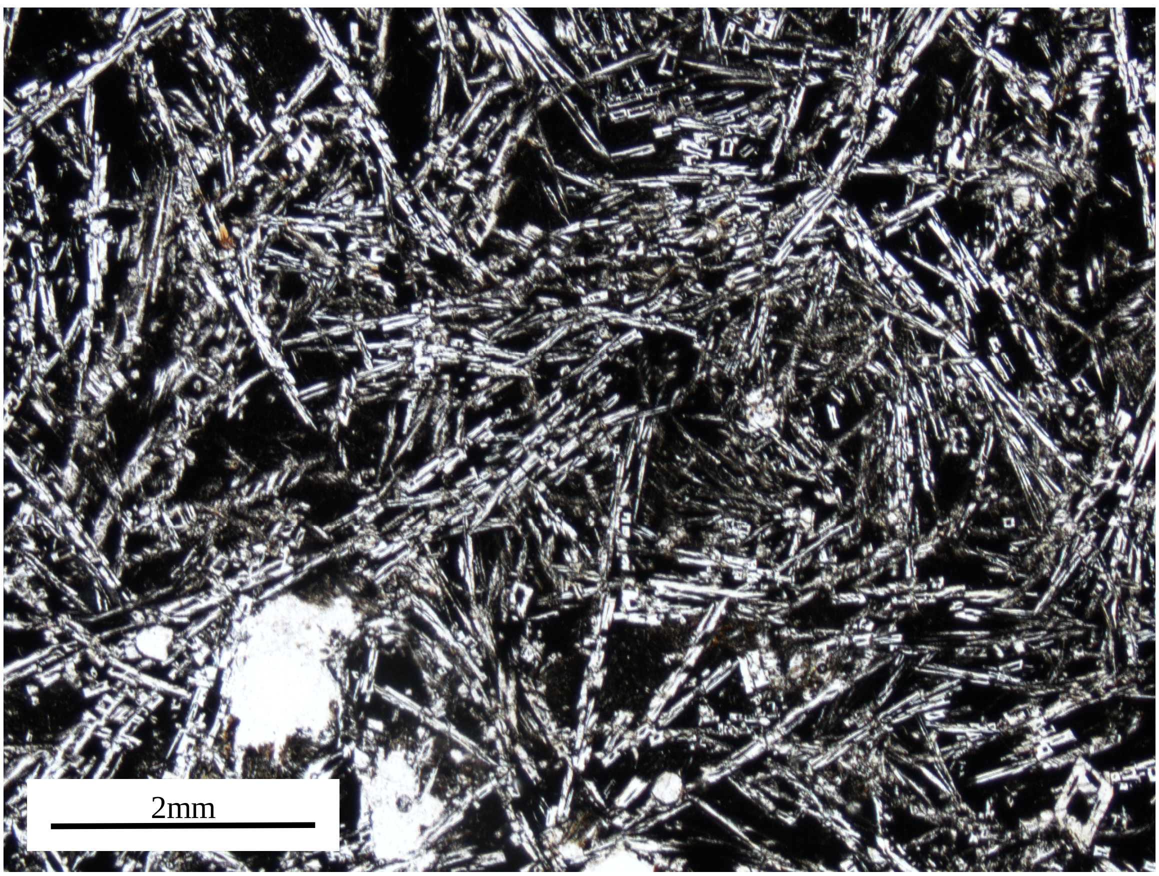

| | |
|---|---|
| Thin Section<br>Rock Type | KFZ85_010_08_1<br>Basalt |
| Overall Grain Size | Very fine grain (<0.1mm, possibly plagioclase), olivine microphenocrysts are ~0.3mm. Vesicles vary from 0.4-0.7mm in diameter. |
| Textures | Radiating minerals away from vesicles (too fine grain to determine the minerals). Vesicles are present throughout thin section. Olivine microphenocrysts are present. |
| Alteration/ Replacements | Alteration does not obviously occur in this sample. |
| Notes | The light for the camera has been set to very high to emphasis the radiating textures; this does not represent the true colour of the thin section. The brown areas are not areas of alteration. Plane polarized light. |

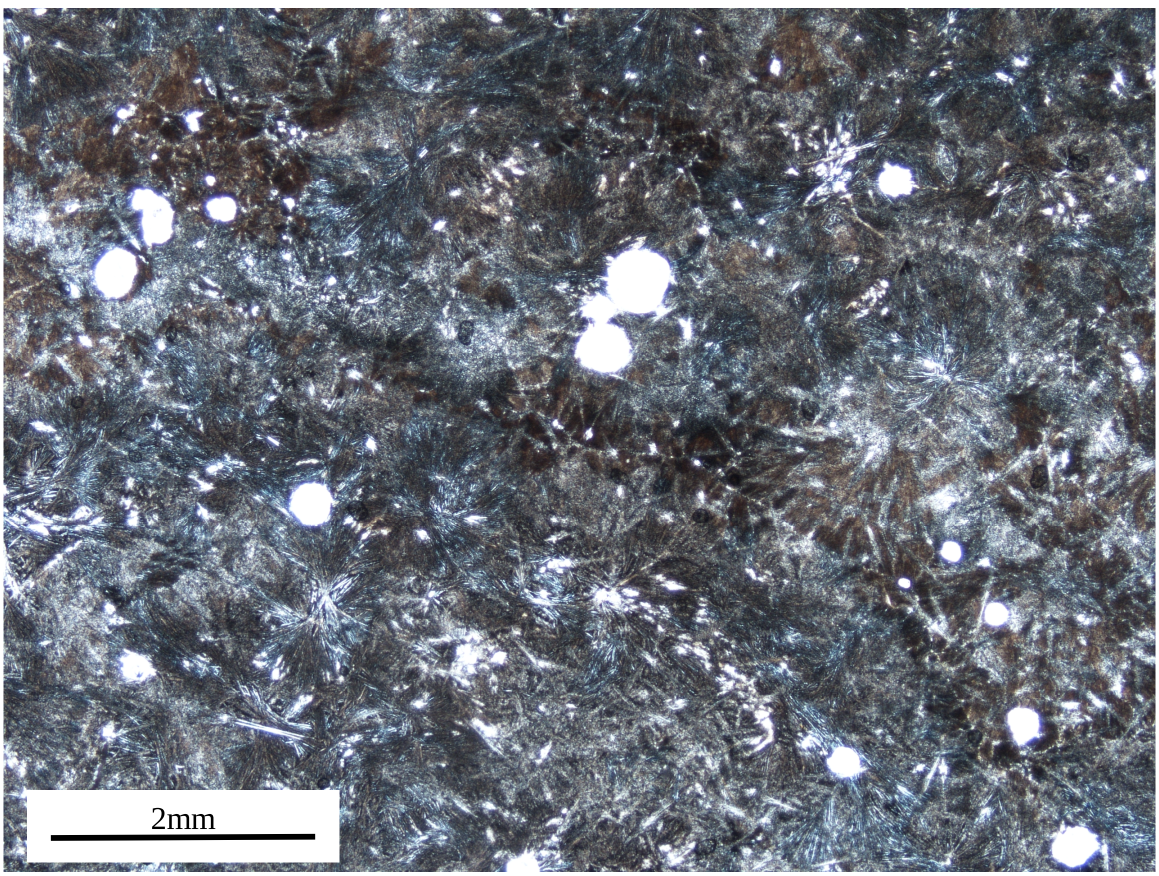

| | |
|---|---|
| Thin Section<br>Rock Type | KFZ85_010_11_4 (top)<br>Gabbro |
| Overall Grain Size | Coarse grain plagioclase and clinopyroxene (≤2-4mm). Secondary chlorite and actinolite are fine grain (<0.3mm). |
| Textures | Clinopyroxene is “dirty” like it has a brown “dust” covering; this could be a reaction to the alteration of clinopyroxene to chlorite and amphiboles. Inclusions of actinolite are present in the chlorite, chlorite thus appears fibrous. Rims of chlorite and actinolite enclose plagioclase and clinopyroxene. Intergrowths of fine-grain actinolite and hornblende are common. Plagioclase is fresh looking. |
| Alteration/ Replacements | Alteration of clinopyroxene to chlorite and amphiboles (actinolite and secondary hornblende) appears to occur. Alterations of hornblende to actinolite also possibly occur. Chlorite does not seem to be replacing plagioclase; simply acts as an enclosure around the plagioclase were it is replacing clinopyroxene. |
| Notes | Opaque minerals are present but only as trace minerals; amount was not recordable for modal percentages. |

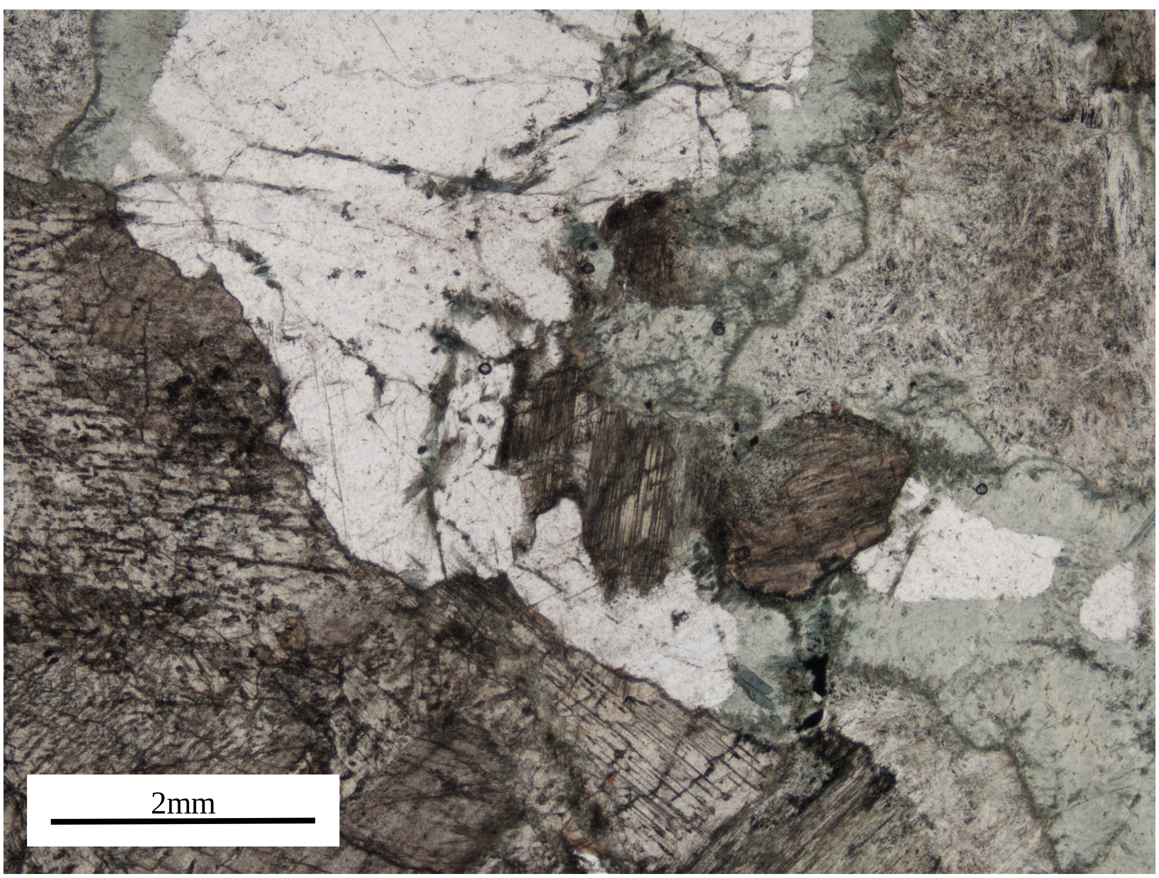

| | |
|---|---|
| Thin Section<br>Rock Type | KFZ85_010_11_4 (bottom)<br>Gabbro |
| Overall Grain Size | Coarse grain plagioclase and clinopyroxene (≤2-4mm). Secondary chlorite and actinolite are fine grain (<0.3mm). |
| Textures | Inclusions of actinolite are present in the chlorite that seems to replace clinopyroxene; these inclusions make the chlorite appear fibrous. Clinopyroxene appears dirty, as though there is a layer of brown dust on the surface. Plagioclase appears fresh. |
| Alteration/ Replacements | Chlorite and actinolite replace clinopyroxene. Plagioclase is fractured; actinolite may be present in those fractures however plagioclase is predominantly unaltered. |
| Notes | Opaque minerals are present but only as trace minerals; amount was not recordable for modal percentages. |

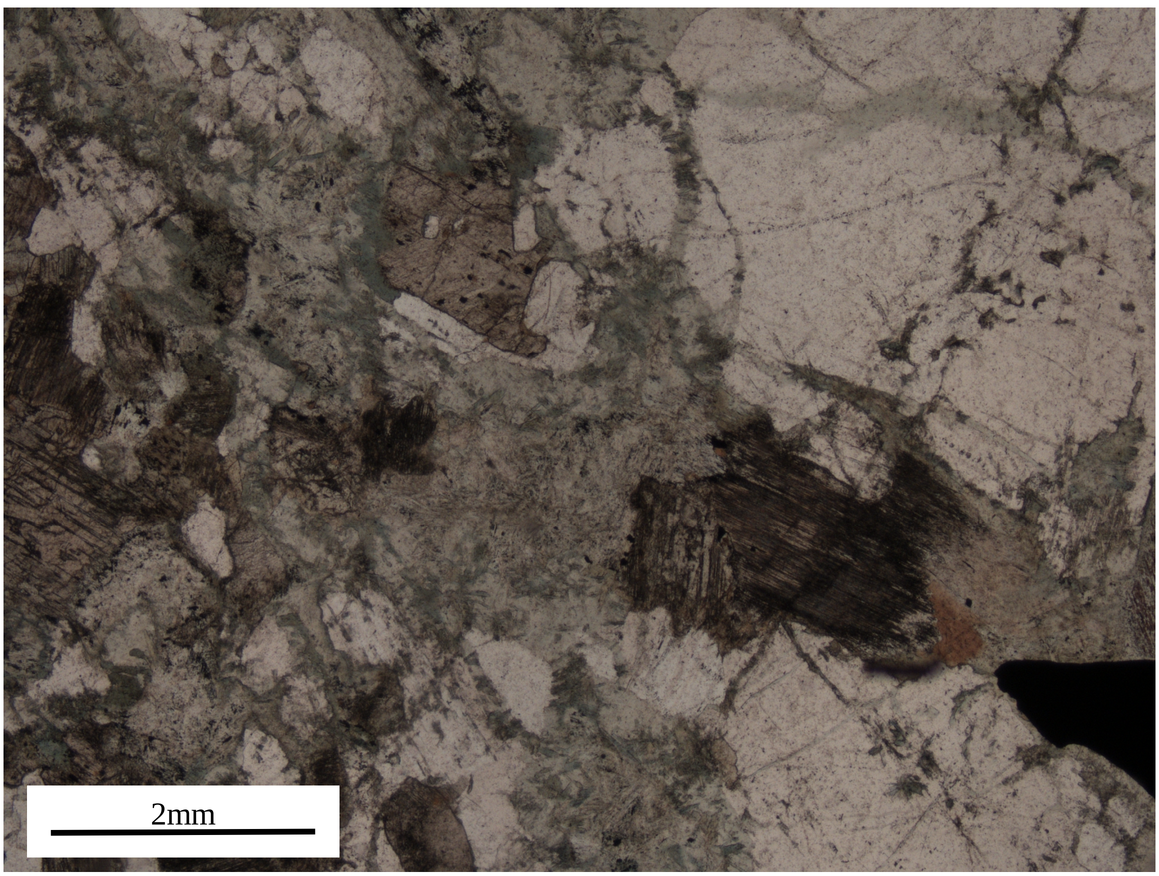

| | |
|---|---|
| Thin Section<br>Rock Type | KFZ85_010_14_2<br>Gabbro |
| Overall Grain Size | Coarse grain plagioclase and clinopyroxene (≤2-4mm). Secondary chlorite and actinolite are fine grain (<0.2mm). |
| Textures | Fine grain intergrowths of actinolite and hornblende give the thin section a fibrous texture (most visible in cross-polarized light). The fibrous masses are separated by the boundaries of the original mineral. |
| Alteration/ Replacements | The only areas that have not been altered to actinolite (and some secondary hornblende) are marked as clinopyroxene and plagioclase. The remainder of the image has been completely altered. |
| Notes | The vein running down the center is full of very fine-grain actinolite, which is most evident in cross-polarized light. Opaque minerals are present but only as trace minerals; amount was not recordable for modal percentages. |

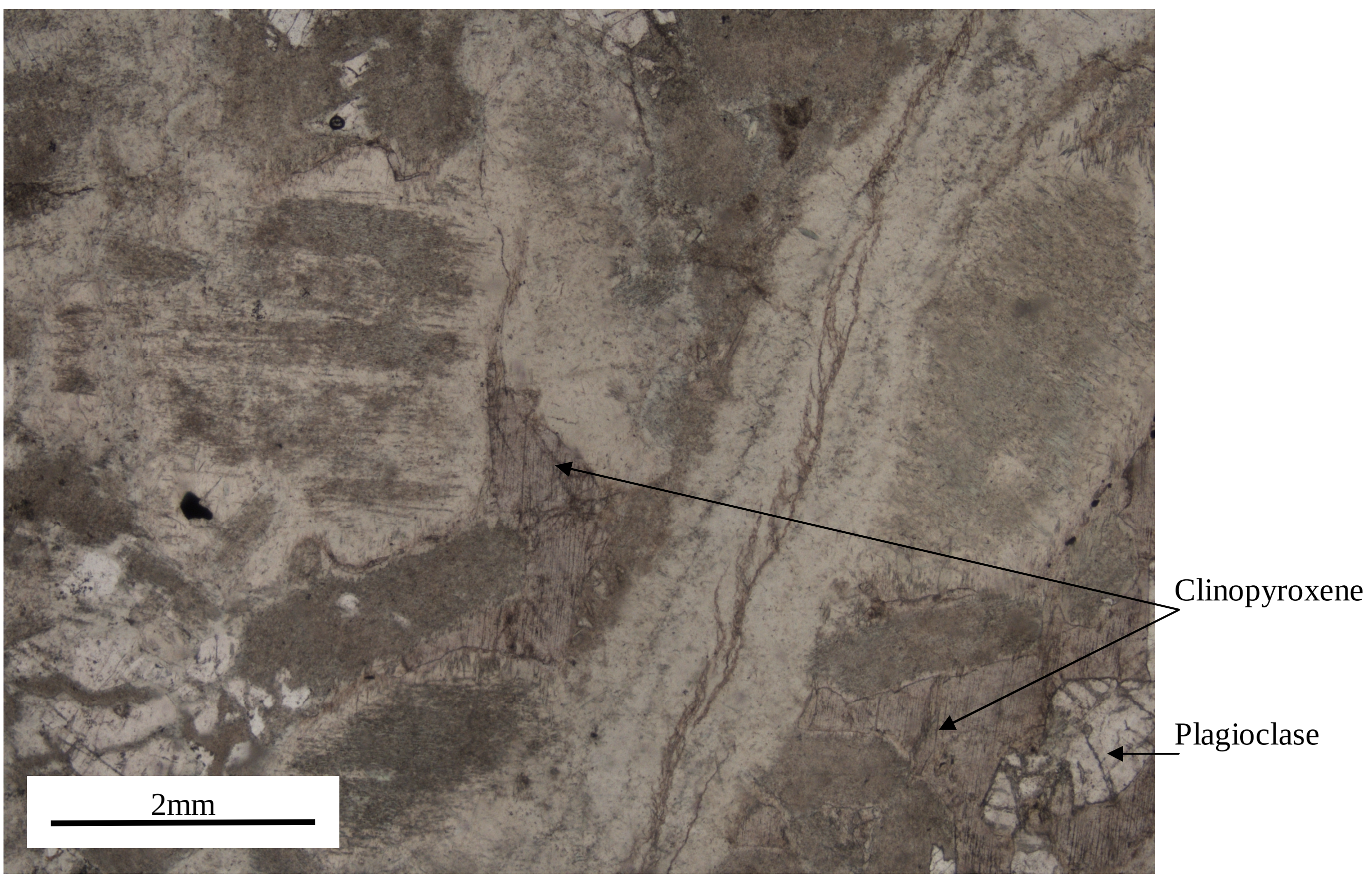

| | |
|---|---|
| Thin Section<br>Rock Type | KFZ85_010_12_14<br>Gabbro |
| Overall Grain Size | Coarse grain: plagioclase can reach up to 4mm, clinopyroxene ~2mm. Chlorite and actinolite are fine-grain, <0.1-0.3 mm. |
| Textures | All minerals are subhedral to anhedral, and due to alteration clinopyroxene and chlorite have a fibrous texture. Plagioclase has minimal fracturing that does not follow a pattern. |
| Alteration/ Replacements | Clinopyroxene is badly altered to actinolite and chlorite creating a fibrous texture. The clinopyroxene appears very dark in plane polarized light, most likely caused by significant alteration. Plagioclase contains actinolite along fractures, however plagioclase is predominantly unaltered. |
| Notes | Opaque minerals are present but only as trace minerals; amount was not recordable for modal percentages. |

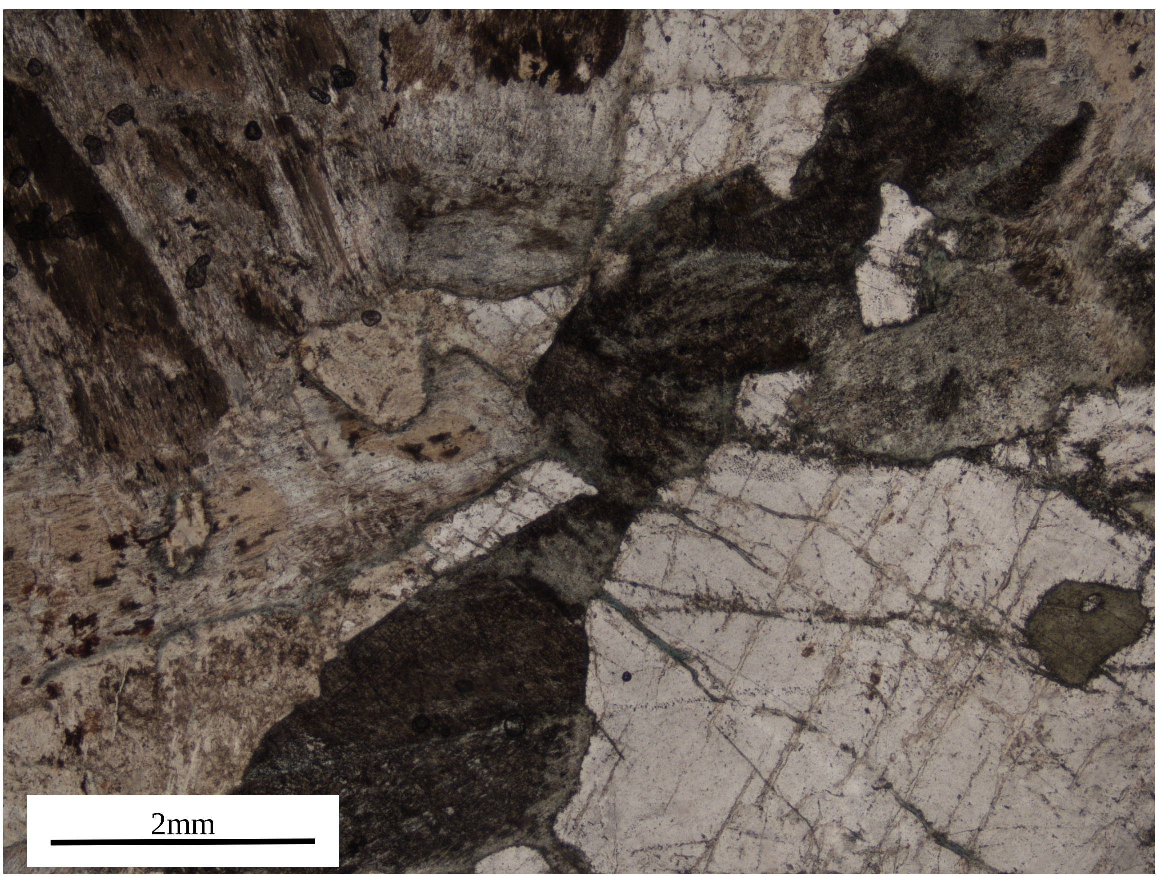

| | |
|---|---|
| Thin Section<br>Rock Type | KFZ85_010_12_11<br>Gabbro |
| Overall Grain Size | Plagioclase and clinopyroxene are coarse-grain, but variable. Plagioclase varies between 0.5 mm-2 mm, and clinopyroxene varies from 0.5 mm- 3 mm. Actinolite and chlorite are fine-grain, <0.2mm. |
| Textures | All minerals are subhedral to anhedral. Plagioclase does not appear fresh, but has not been altered. Clinopyroxene is “dirty” looking, and looks broken up. The fibrous texture as seen previously is no longer abundant and only occurs in small areas. Inclusions of actinolite in chlorite are not abundant. |
| Alteration/ Replacements | Clinopyroxene is being altered, but not to the same degree. Often actinolite is located at the center of the clinopyroxene grain it is replacing, and chlorite occurs along the rim of the clinopyroxene. |
| Notes | Opaque minerals are present but only as trace minerals; amount was not recordable for modal percentages. |

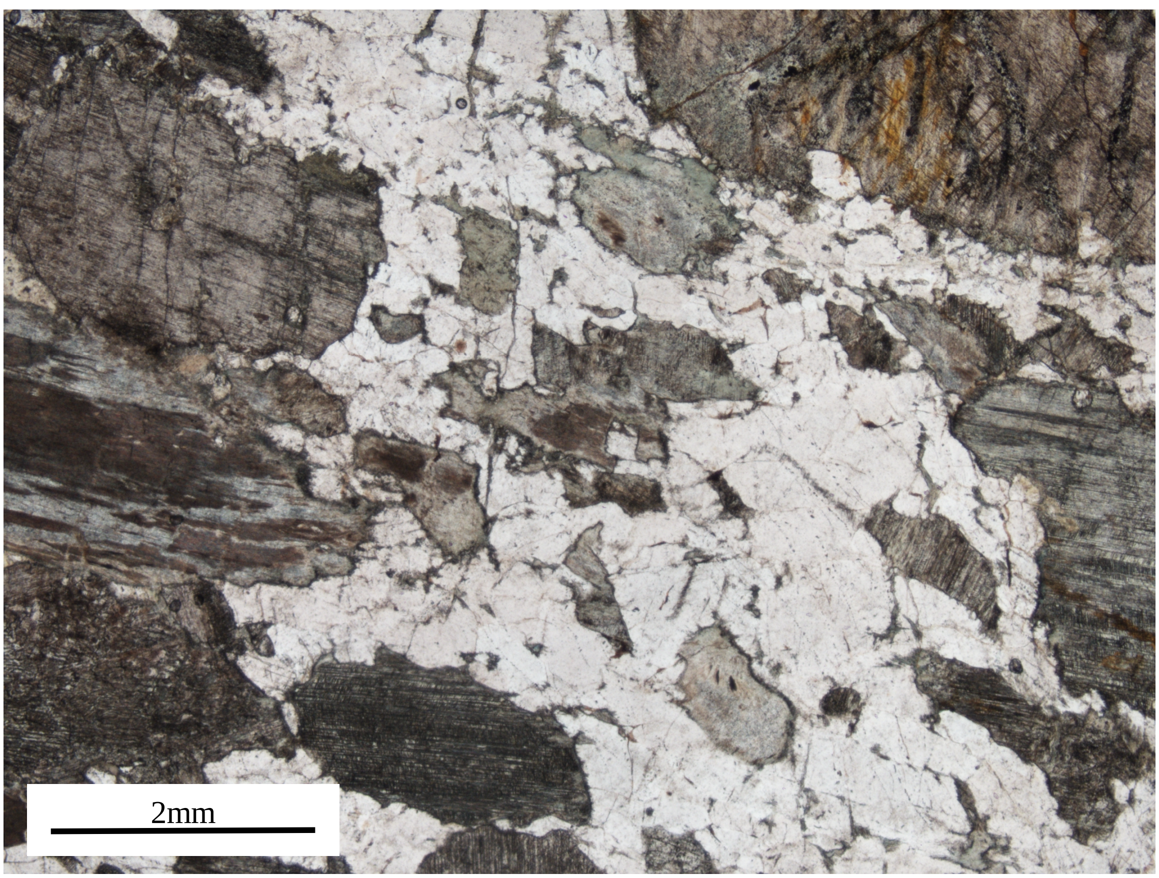

| | |
|---|---|
| Thin Section<br>Rock Type | KFZ85_010_11_2<br>Gabbro |
| Overall Grain Size | Plagioclase and clinopyroxene are coarse-grained, up to 3-4mm. Chlorite and actinolite are fine-grained between <0.1mm to 0.3mm |
| Textures | All minerals are anhedral. Plagioclase is relatively fresh, with minor fracturing. Clinopyroxene is “dirty” as though covered in dust. Fibrous actinolite is an inclusion in the chlorite rims around clinopyroxene. |
| Alteration/ Replacements | Chlorite forms a rim of clinopyroxene, where the chlorite has replaced the clinopyroxene. Actinolite can be found as inclusions in the chlorite. Chlorite is also present in the microfractures in the plagioclase. The degree of alteration seems to be less in this thin section; clinopyroxene is unaltered in many areas. |
| Notes | Opaque minerals are present but only as trace minerals; amount was not recordable for modal percentages. |

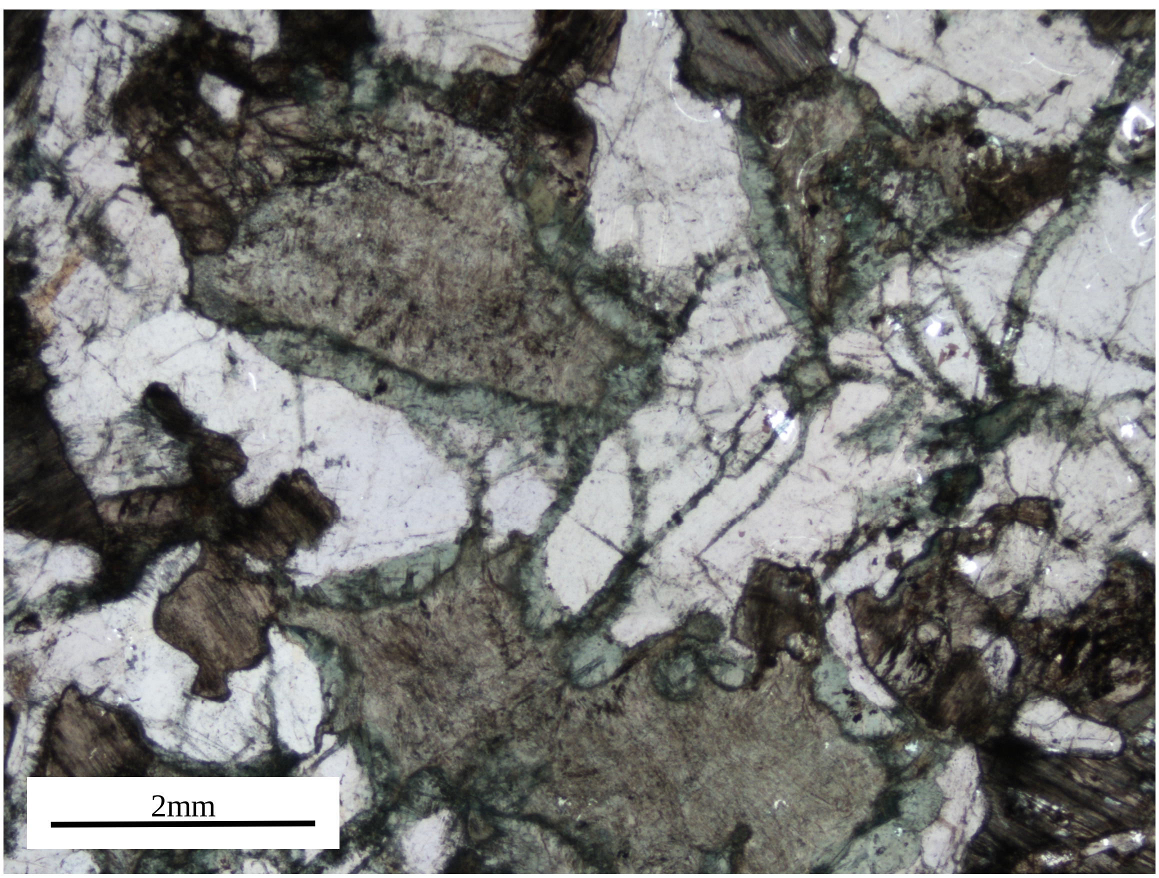

| | |
|---|---|
| Thin Section<br>Rock Type | KFZ85_010_12_7<br>Gabbro |
| Overall Grain Size | Plagioclase and clinopyroxene are coarse-grained (up to 5mm), whereas chlorite, actinolite and hornblende are fine grained (<0.3mm). |
| Textures | Plagioclase looks beaten up, but not altered. Lot’s of fractures occur in the plagioclase; clinopyroxene is very dirty looking and does not appear as a fresh mineral in this thin section. Small fibrous masses of intergrown actinolite, chlorite and hornblende are present. |
| Alteration/ Replacements | This may be one of the least altered thin sections. Clinopyroxene is altered to a certain extent; however actinolite and chlorite have not fully replaced clinopyroxene yet. |
| Notes | Opaque minerals are present but only as trace minerals; amount was not recordable for modal percentages. |

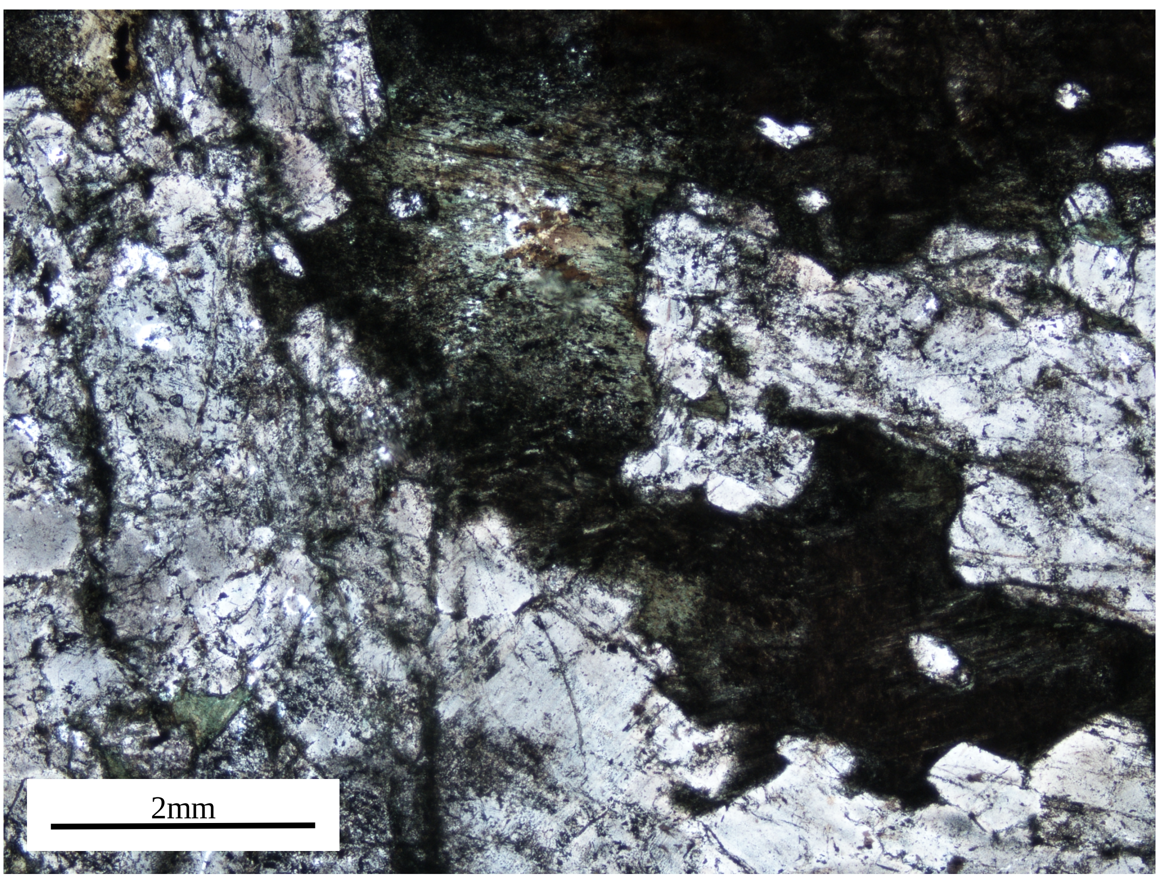

# APPENDIX D
## Kane Fracture Zone: Electron Microprobe Data

The following Appendix includes the electron microprobe data collected from three representative thin sections from the Kane Fracture Zone. The pages in the beginning are the back scatter electron images with the locations of the analyzed points marked in red. The remainder of the pages include tables of the points that have been separated into each mineral analyzed (ie: plagioclase, clinopyroxene, etc). Listed at the top of each table are the slide names, area of the slide that was analyzed, and the point number of each analysis for easy reference to the BSE images. In some circumstances data is not included as it was not used for this project. The points removed were ones that had totals less than 75% and did not accurately represent the mineral being analyzed.

**SLIDE: KFZ_010_08_02**
**Rock Type: Pillow Basalt**
**Area of analysis: 1**

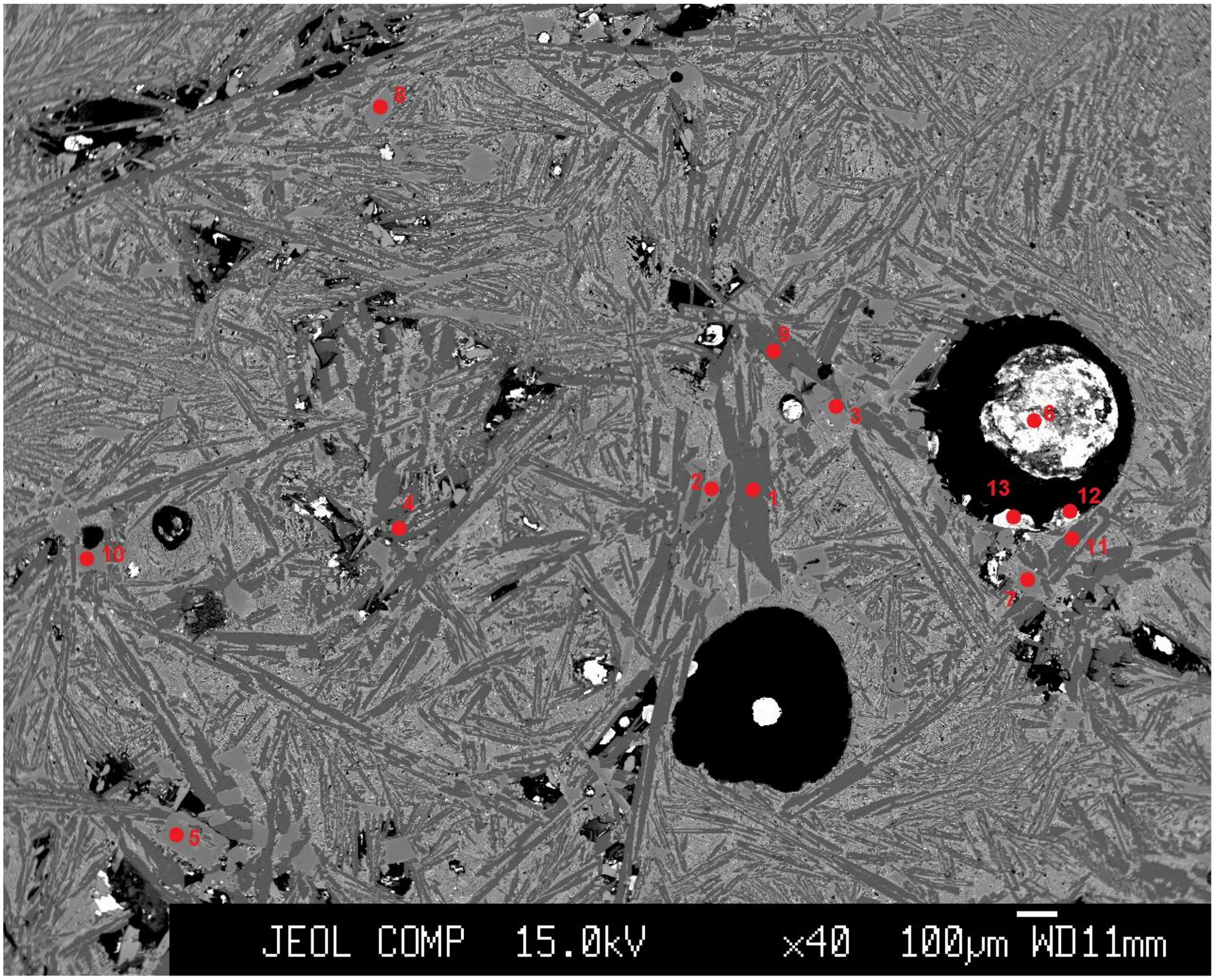

**SLIDE: KFZ_010_08_02**
**Rock Type: Pillow Basalt**
**Area of analysis: 2**

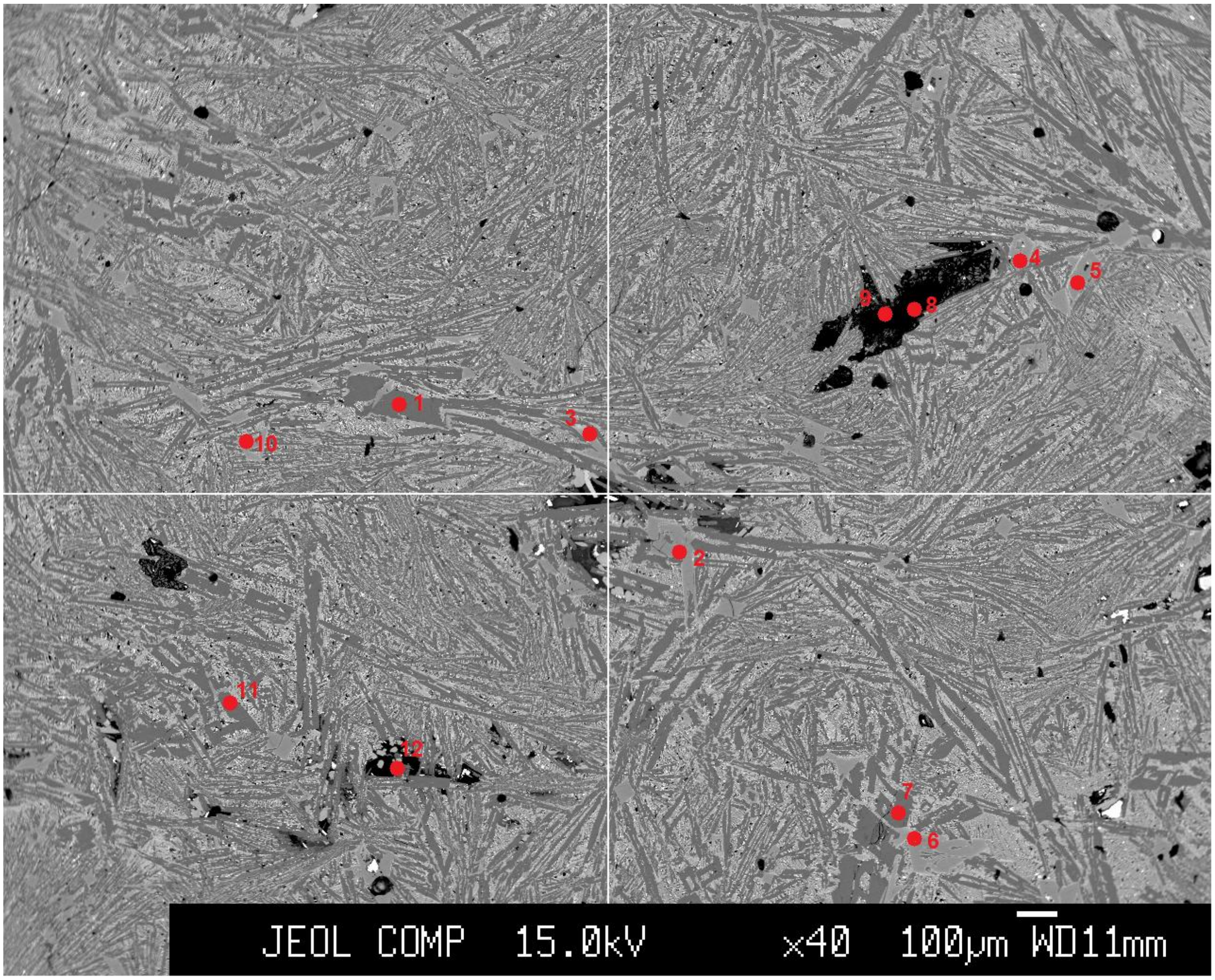

**SLIDE: KFZ_010_08_02**
**Rock Type: Pillow Basalt**
**Area of Analysis: 3**

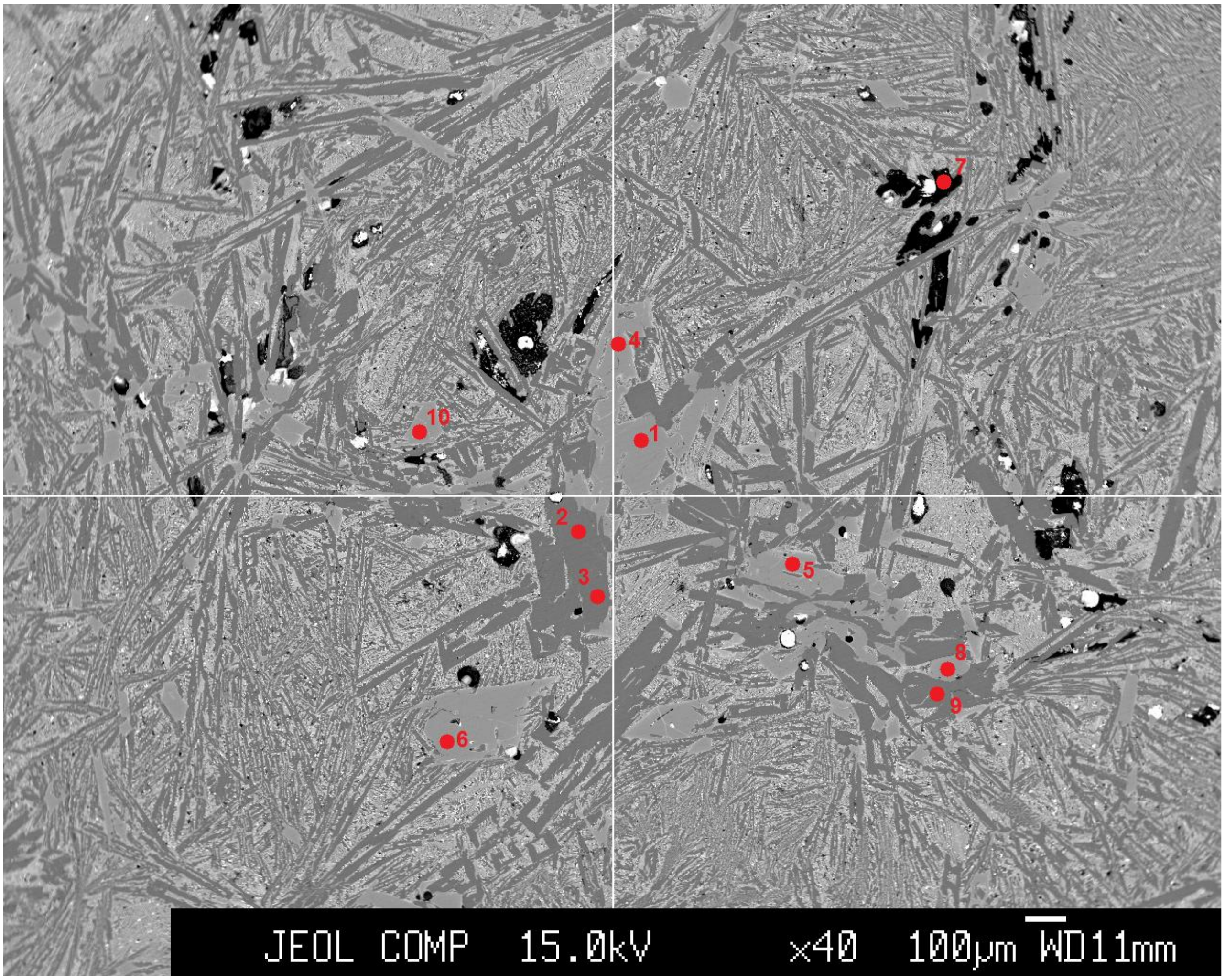

**SLIDE: KFZ_010_08_02**
**Rock Type: Pillow Basalt**
**Area of analysis: 4**

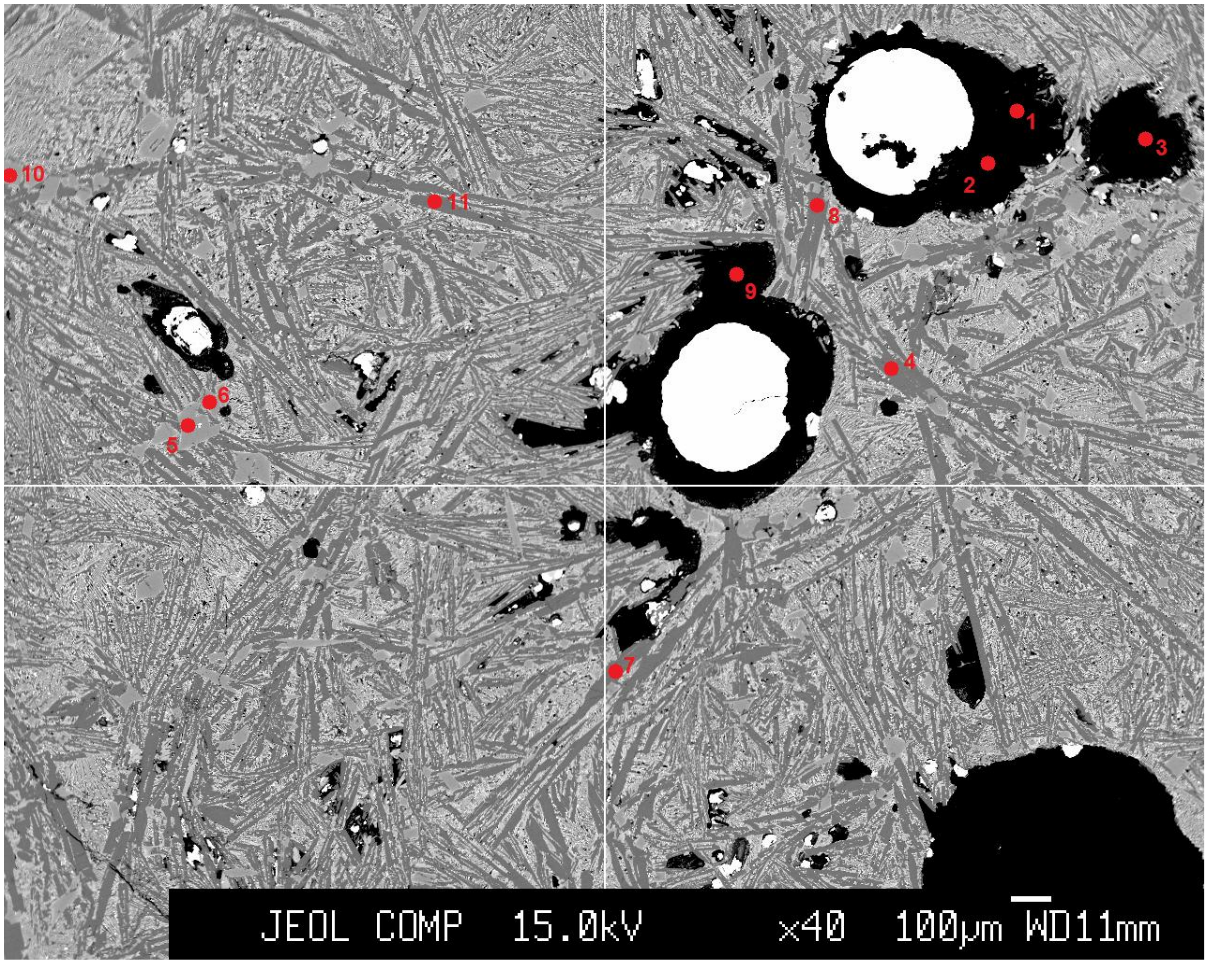

**SLIDE: KFZ_010_11_02**
**Rock Type: Gabbro**
**Area of analysis: 1**

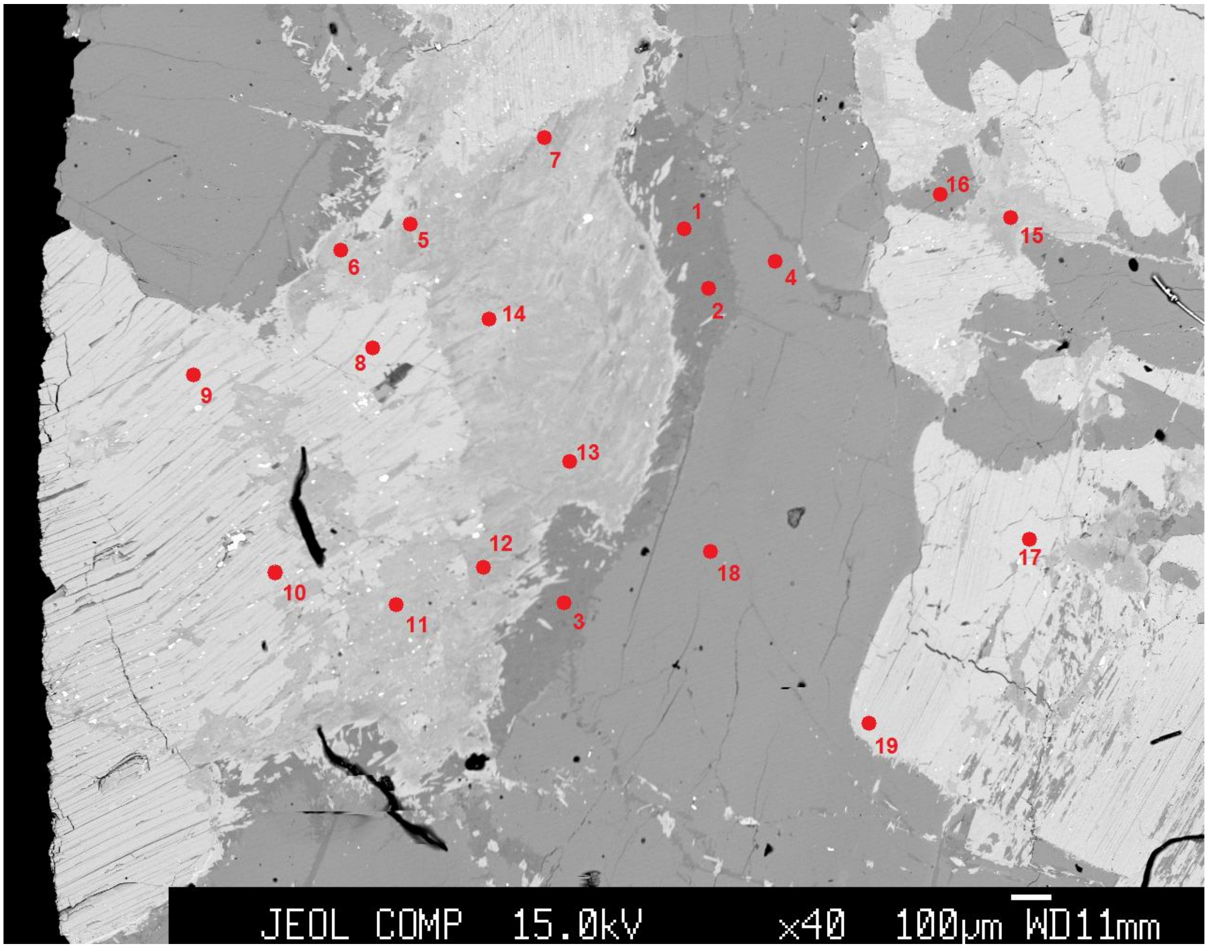

**SLIDE: KFZ_010_11_02**
**Rock Type: Gabbro**
**Area of analysis: 2**

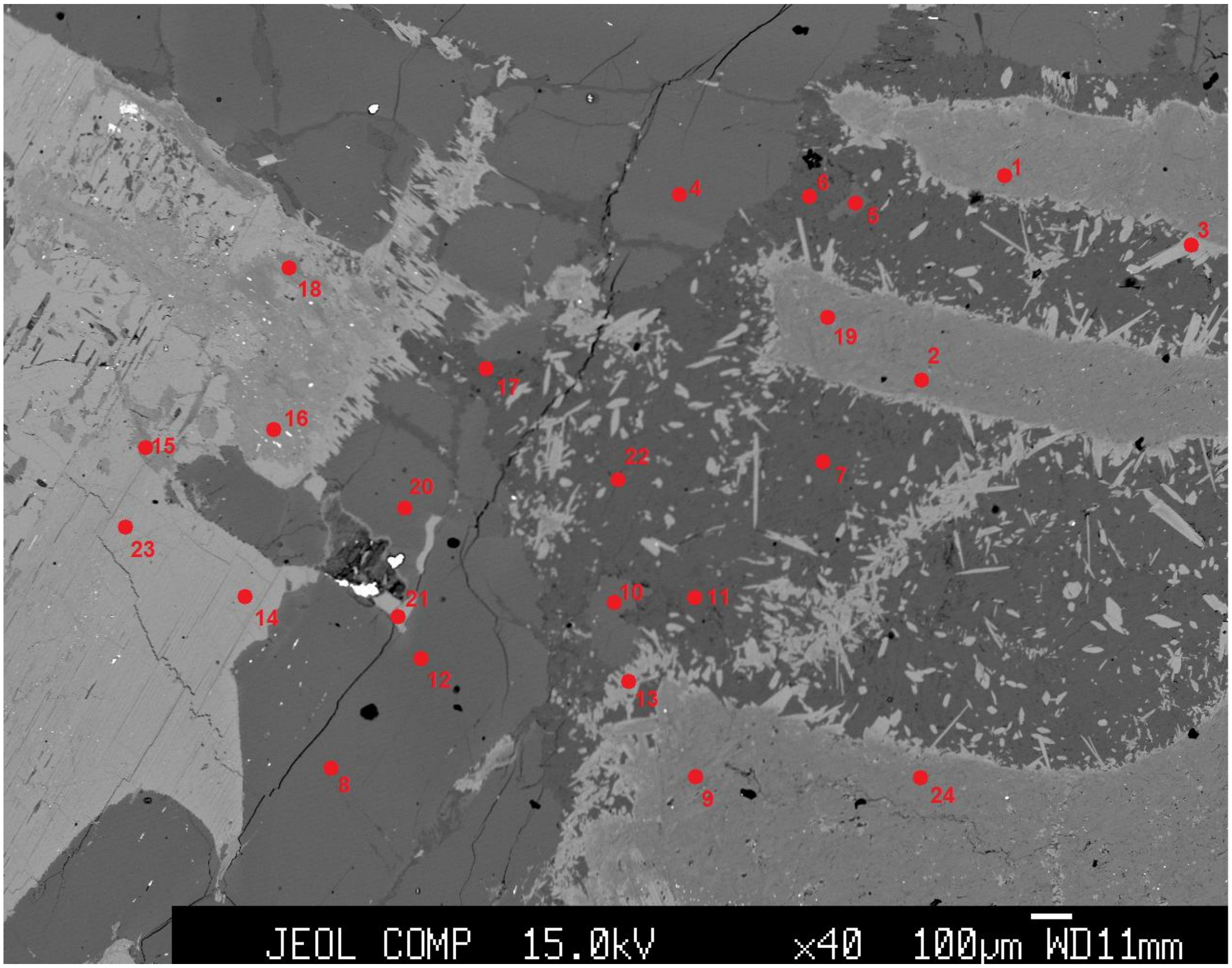

**SLIDE: KFZ_010_11_02**
**Rock Type: Gabbro**
**Area of analysis: 3**

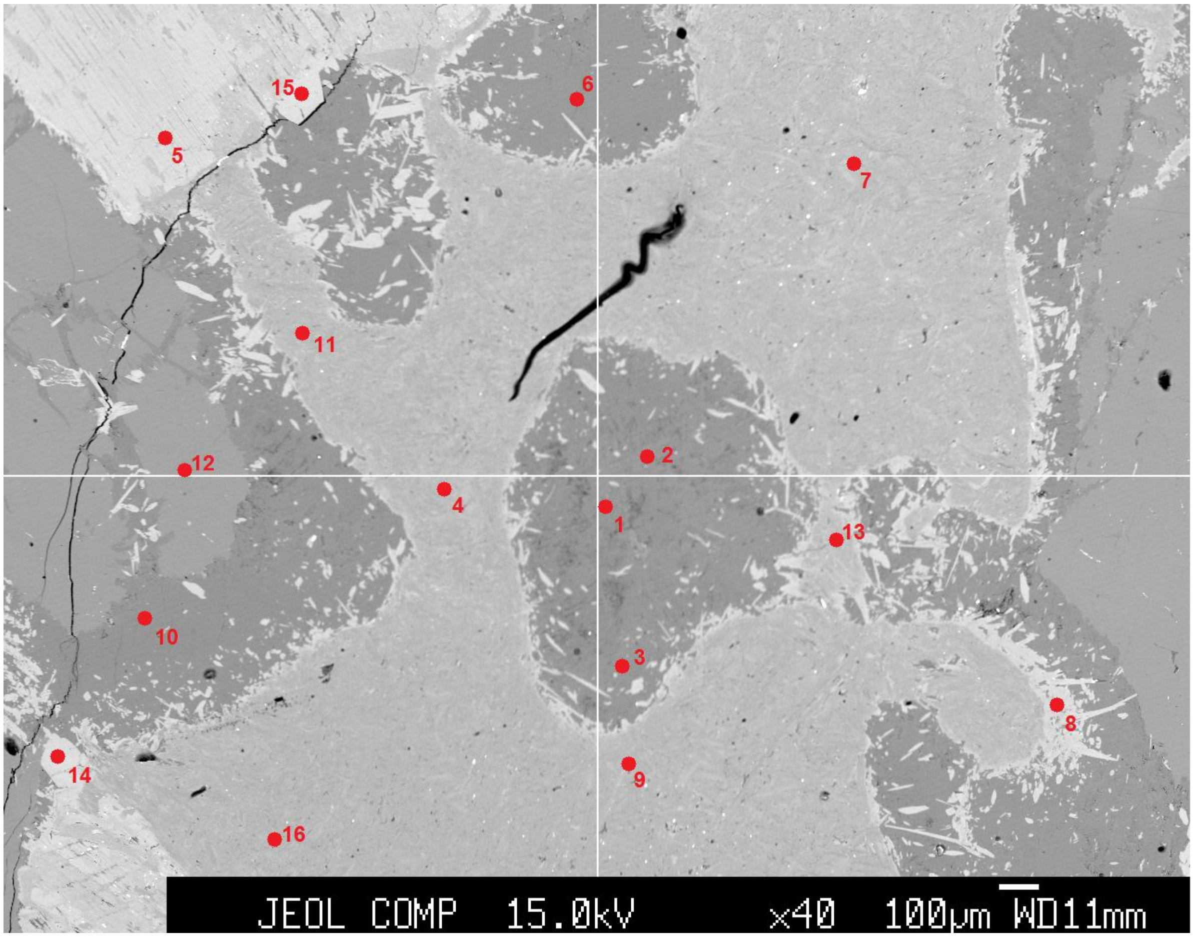

**SLIDE: KFZ_010_11_02**
**Rock Type: Gabbro**
**Area of analysis: 4**

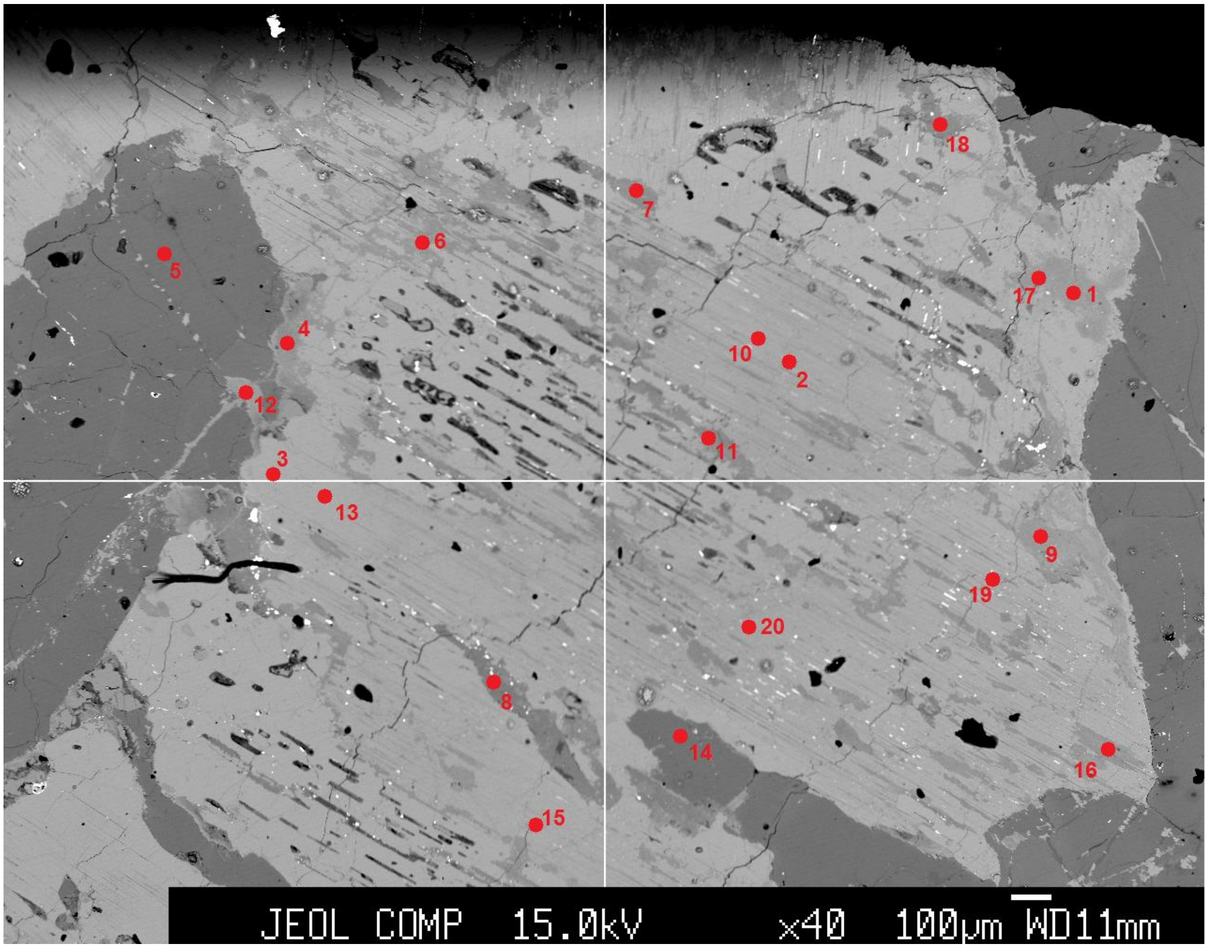

**SLIDE: KFZ_010_11_02**
**Rock Type: Gabbro**
**Area of analysis: 5**

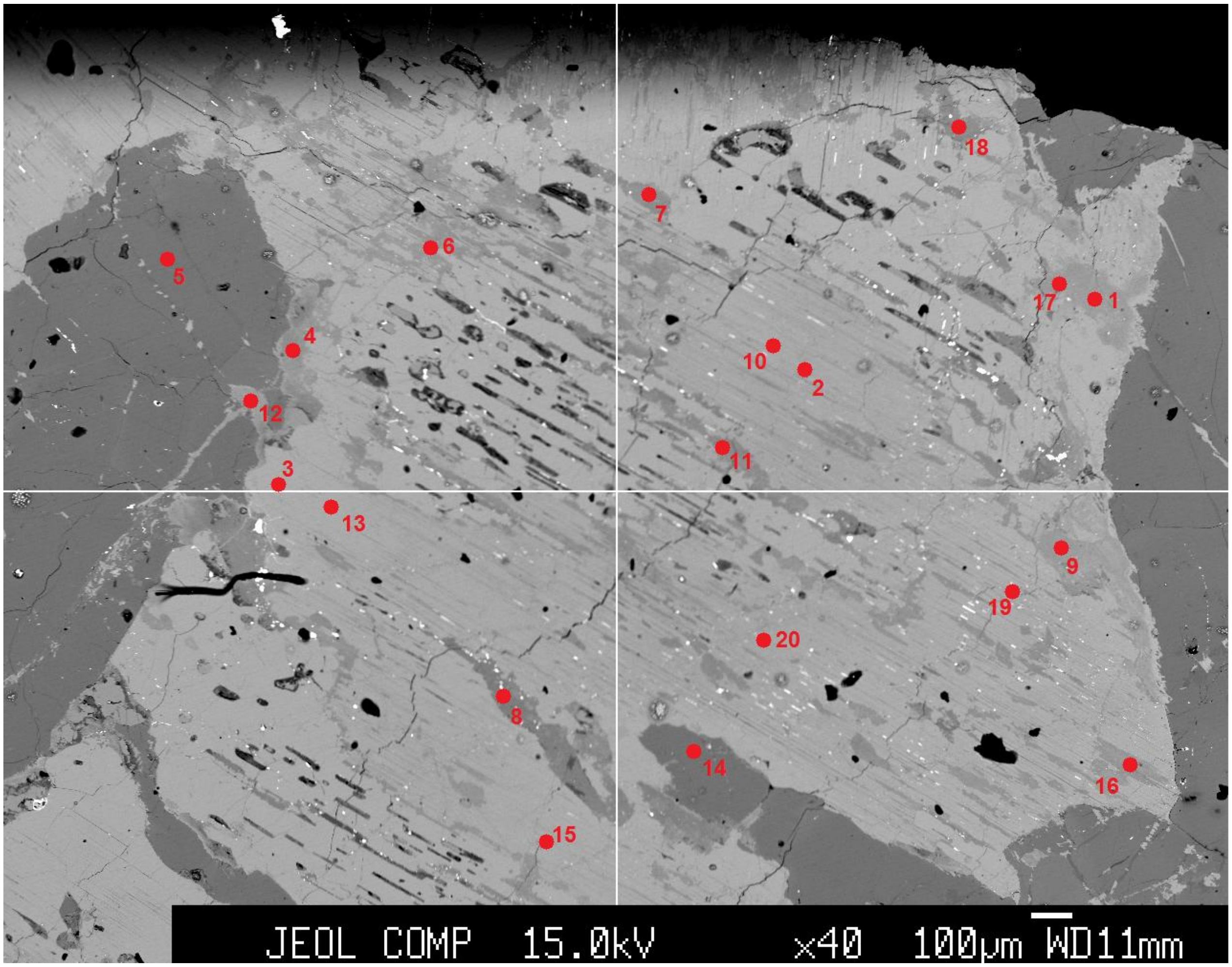

**SLIDE: KFZ_010_12_07**
**Rock Type: Gabbro**
**Area of analysis: 1**

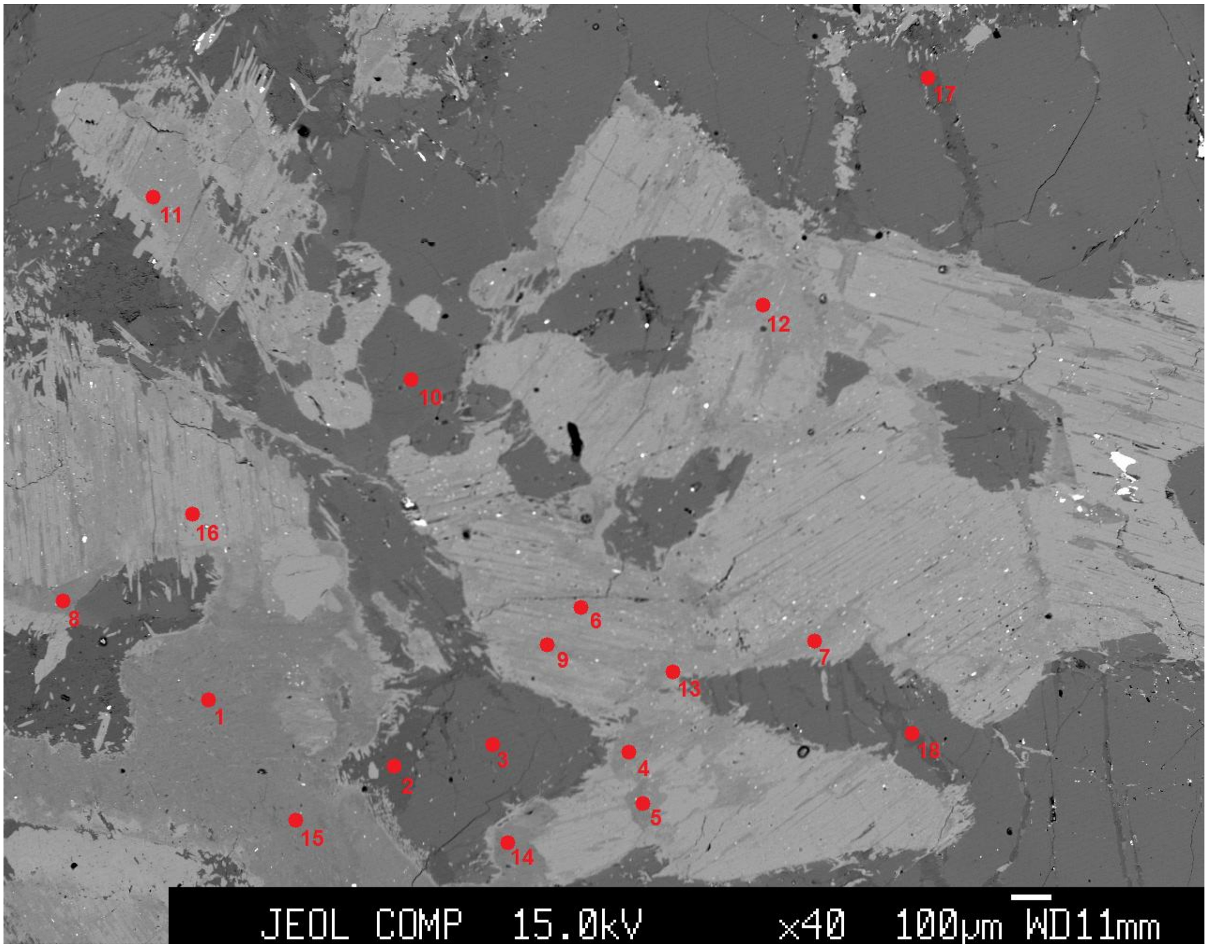

**SLIDE: KFZ_010_12_07**
**Rock Type: Gabbro**
**Area of analysis: 2**

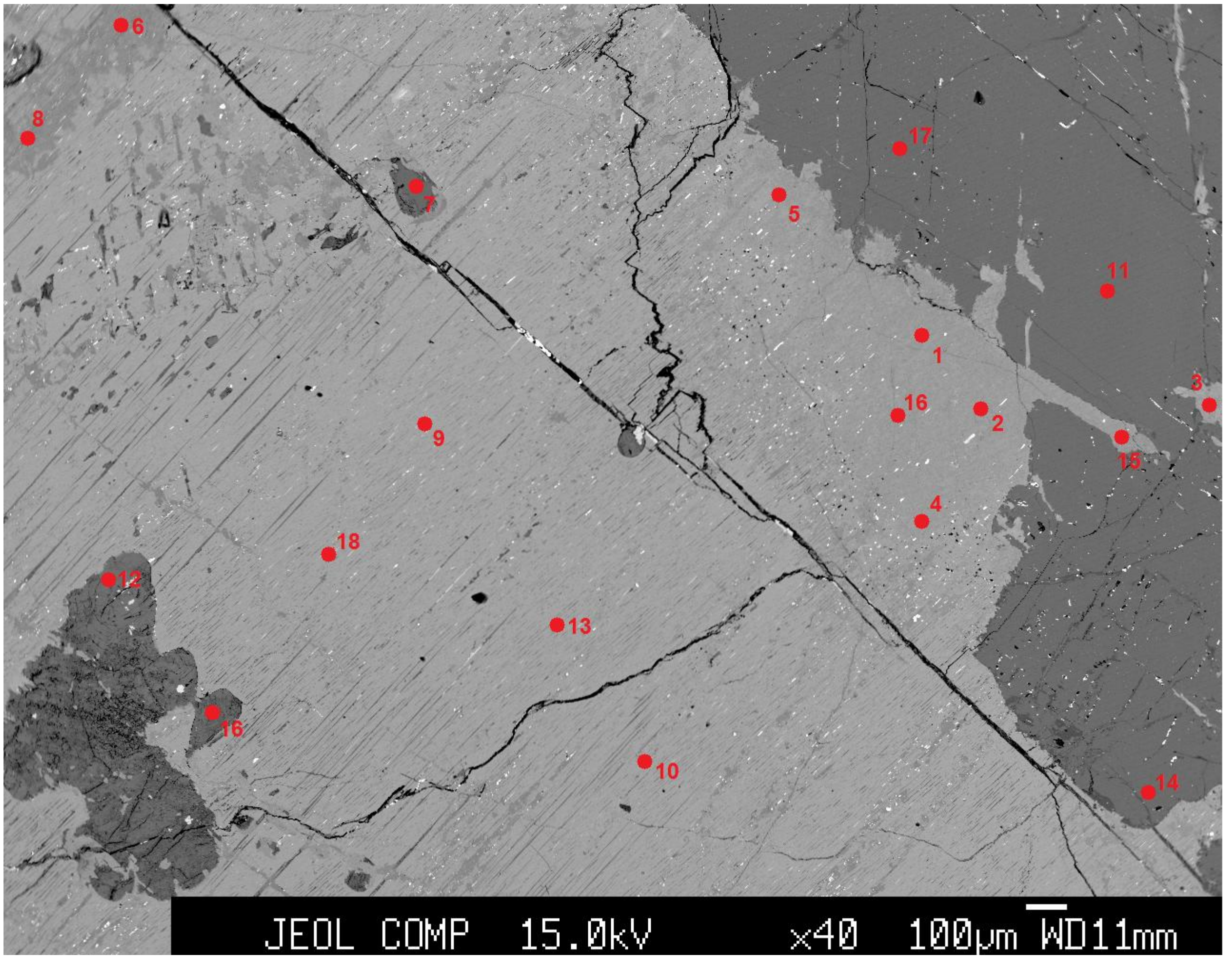

**SLIDE: KFZ_010_12_07**
**Rock Type: Gabbro**
**Area of analysis: 3**

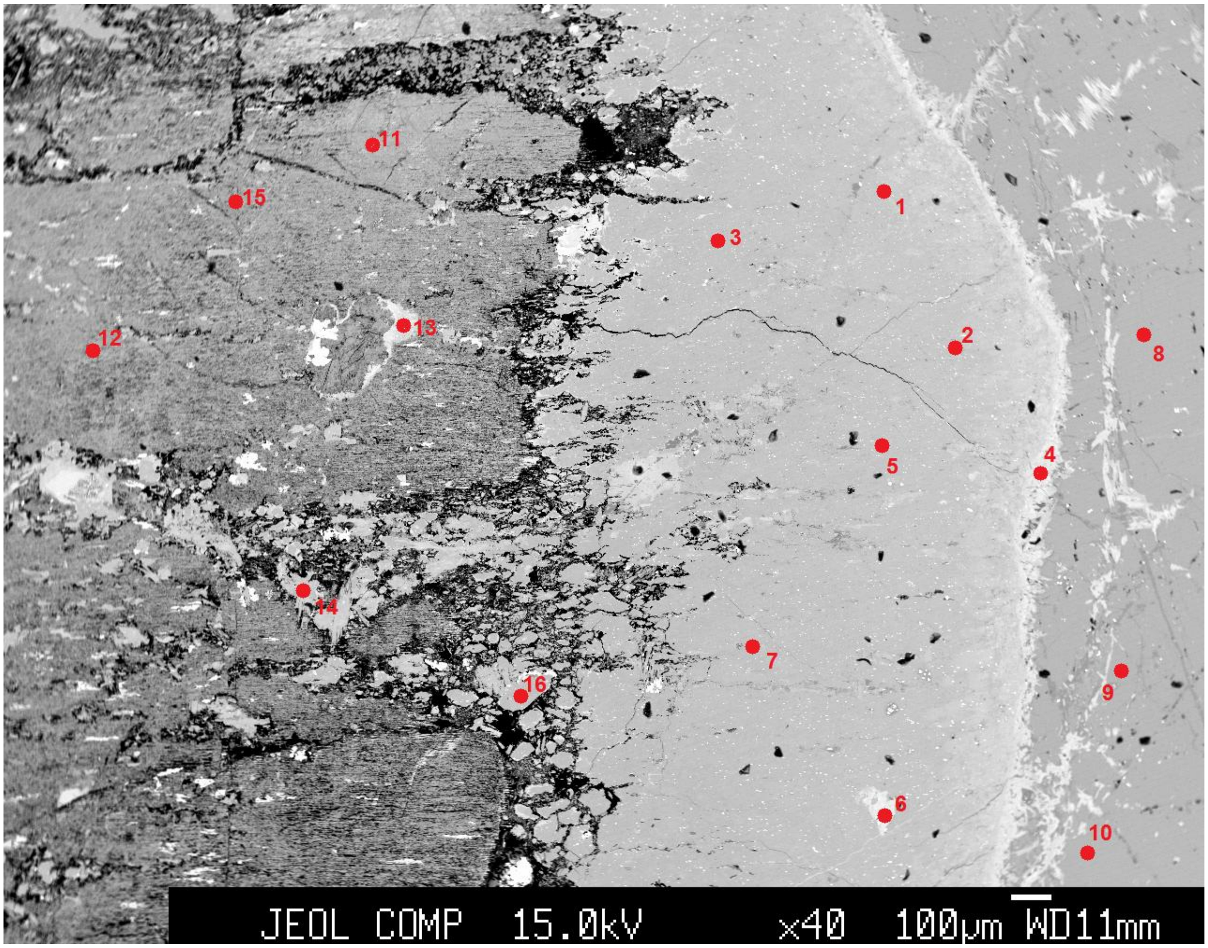

**SLIDE: KFZ_010_12_07**
**Rock Type: Gabbro**
**Area of analysis: 4**

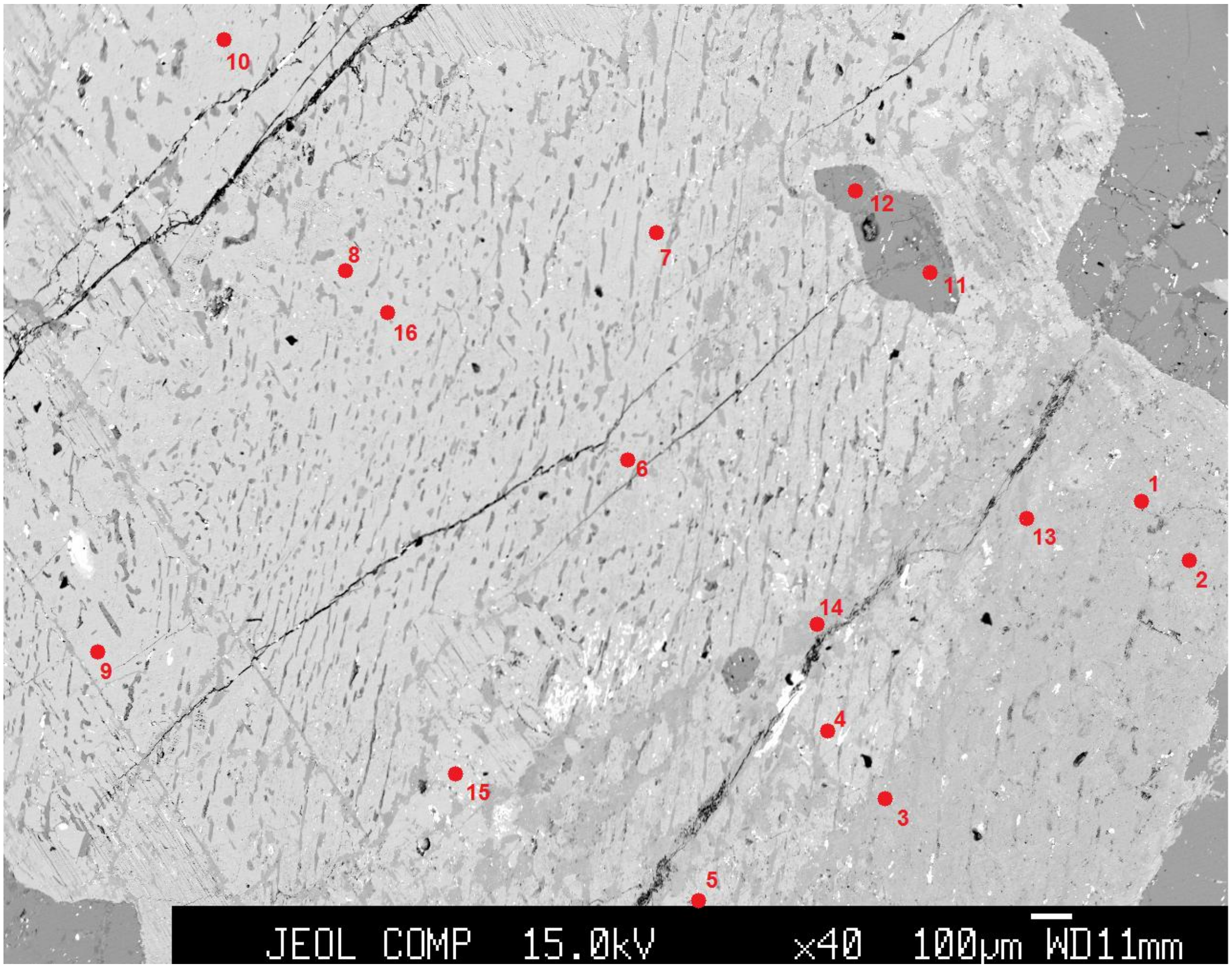

**SLIDE: KFZ_010_12_07**
**Rock Type: Gabbro**
**Area of analysis: 5**

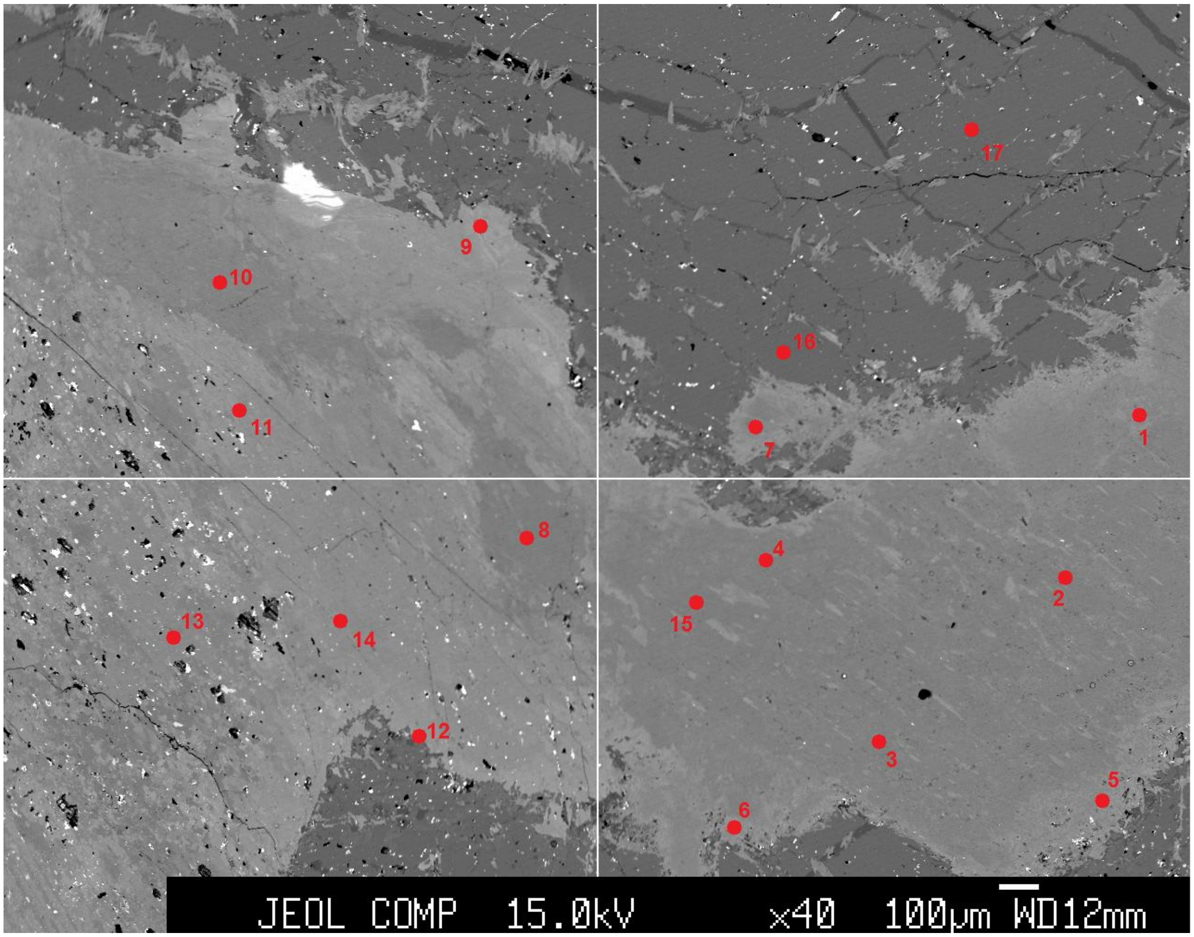

**SLIDE: KFZ_010_12_07**
**Rock Type: Gabbro**
**Area of analysis: 6**

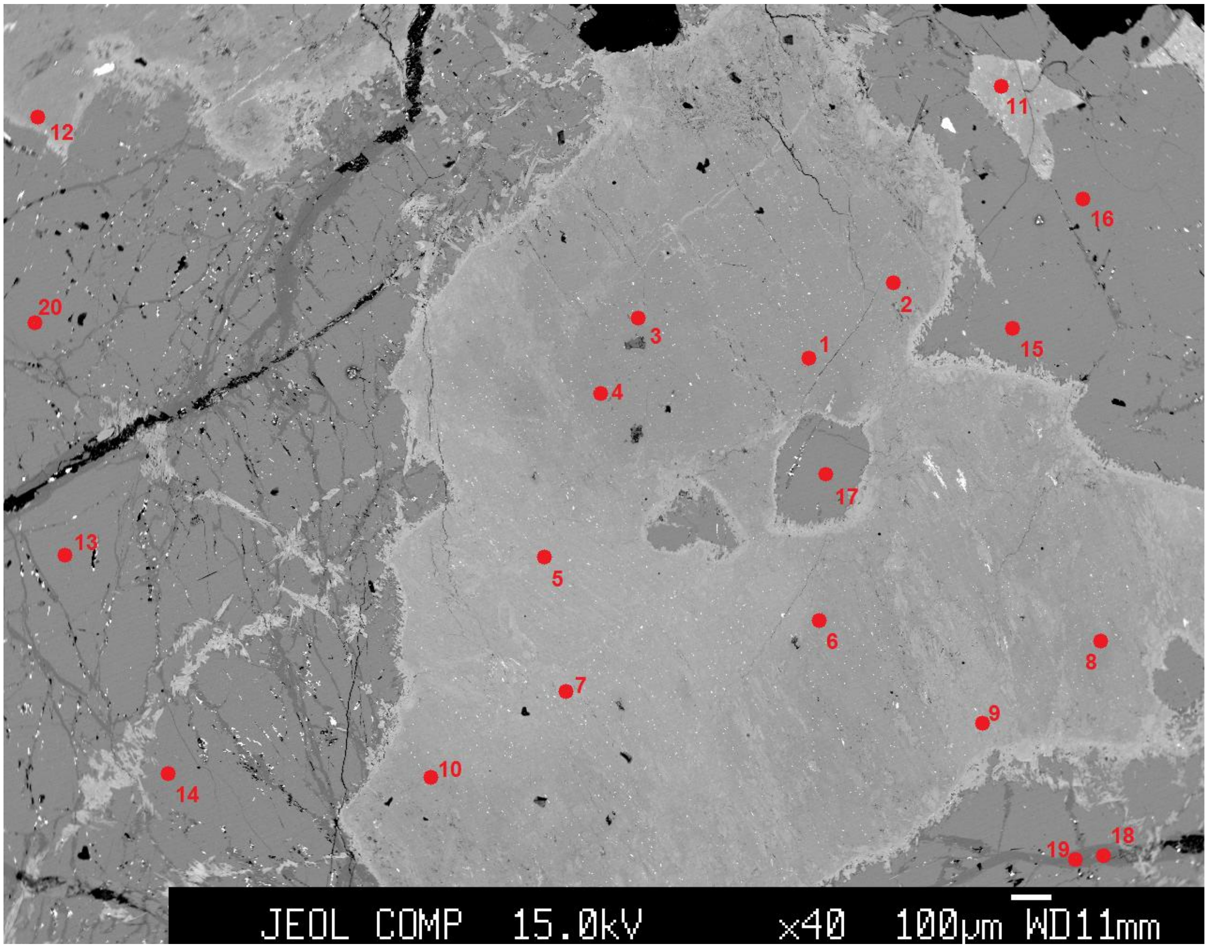

PLAGIOCLASE

| **Slide** | **KFZ_010_08_02** | **KFZ_010_08_02** | **KFZ_010_08_02** | **KFZ_010_08_02** | **KFZ_010_08_02** | **KFZ_010_08_02** | **KFZ_010_08_02** | **KFZ_010_08_02** | **KFZ_010_08_02** | **KFZ_010_08_02** |
|---|---|---|---|---|---|---|---|---|---|---|
| **Area** | **1** | **1** | **1** | **1** | **2** | **2** | **3** | **3** | **3** | **4** |
| **Point** | **1** | **4** | **9** | **11** | **7** | **11** | **2** | **3** | **9** | **4** |
| SiO2 | 51.37 | 53.54 | 52.41 | 52.12 | 52.09 | 52.49 | 51.50 | 51.55 | 50.83 | 51.73 |
| TiO2 | 0.06 | 0.12 | 0.04 | 0.07 | 0.12 | 0.14 | 0.06 | 0.07 | 0.09 | 0.09 |
| Al2O3 | 27.10 | 26.23 | 26.46 | 26.13 | 26.48 | 26.47 | 27.54 | 28.15 | 27.73 | 27.12 |
| Cr2O3 | 0.01 | 0.00 | 0.00 | 0.00 | 0.00 | 0.00 | 0.02 | 0.00 | 0.00 | 0.01 |
| FeO | 0.67 | 1.18 | 0.96 | 1.12 | 1.12 | 1.17 | 0.56 | 0.60 | 0.76 | 0.89 |
| Na2O | 4.60 | 5.17 | 5.02 | 4.97 | 4.85 | 4.98 | 4.59 | 4.40 | 4.36 | 4.70 |
| MnO | 0.00 | 0.02 | 0.00 | 0.00 | 0.01 | 0.03 | 0.02 | 0.01 | 0.02 | 0.01 |
| MgO | 0.23 | 0.34 | 0.23 | 0.27 | 0.33 | 0.38 | 0.20 | 0.20 | 0.20 | 0.27 |
| NiO | 0.01 | 0.00 | 0.00 | 0.00 | 0.00 | 0.02 | 0.00 | 0.02 | 0.00 | 0.00 |
| CaO | 12.30 | 11.24 | 11.83 | 11.76 | 12.16 | 12.07 | 12.37 | 12.69 | 12.77 | 12.36 |
| K2O | 0.06 | 0.08 | 0.06 | 0.07 | 0.14 | 0.07 | 0.05 | 0.06 | 0.05 | 0.06 |
| BaO | 0.03 | 0.02 | 0.00 | 0.00 | 0.00 | 0.00 | 0.03 | 0.00 | 0.00 | 0.03 |
| Total | **96.43** | **97.93** | **97.01** | **96.50** | **97.31** | **97.84** | **96.94** | **97.75** | **96.82** | **97.28** |
| cations per pfu 8 oxygen | | | | | | | | | | |
| Si | 2.426 | 2.486 | 2.461 | 2.462 | 2.445 | 2.450 | 2.418 | 2.402 | 2.396 | 2.426 |
| Ti | 0.002 | 0.004 | 0.002 | 0.002 | 0.004 | 0.005 | 0.002 | 0.002 | 0.003 | 0.003 |
| Al | 1.509 | 1.436 | 1.465 | 1.455 | 1.465 | 1.456 | 1.525 | 1.546 | 1.541 | 1.499 |
| Cr | 0.001 | 0.000 | 0.000 | 0.000 | 0.000 | 0.000 | 0.001 | 0.000 | 0.000 | 0.000 |
| Fe | 0.026 | 0.046 | 0.038 | 0.044 | 0.044 | 0.046 | 0.022 | 0.023 | 0.030 | 0.035 |
| Mn | 0.000 | 0.001 | 0.000 | 0.000 | 0.000 | 0.002 | 0.001 | 0.000 | 0.001 | 0.001 |
| Mg | 0.016 | 0.023 | 0.016 | 0.019 | 0.023 | 0.026 | 0.014 | 0.014 | 0.014 | 0.019 |
| Ni | 0.000 | 0.000 | 0.000 | 0.000 | 0.000 | 0.001 | 0.000 | 0.001 | 0.000 | 0.000 |
| Ca | 0.622 | 0.559 | 0.595 | 0.595 | 0.611 | 0.604 | 0.622 | 0.634 | 0.645 | 0.622 |
| Na | 0.421 | 0.466 | 0.457 | 0.455 | 0.442 | 0.450 | 0.418 | 0.398 | 0.398 | 0.427 |
| K | 0.003 | 0.005 | 0.004 | 0.004 | 0.008 | 0.004 | 0.003 | 0.004 | 0.003 | 0.004 |
| Ba | 0.001 | 0.000 | 0.000 | 0.000 | 0.000 | 0.000 | 0.001 | 0.000 | 0.000 | 0.001 |
| Total | **5.029** | **5.027** | **5.037** | **5.038** | **5.042** | **5.045** | **5.028** | **5.022** | **5.031** | **5.038** |
| | | | | | | | | | | |
| Xan | 0.595 | 0.543 | 0.564 | 0.564 | 0.576 | 0.571 | 0.597 | 0.612 | 0.616 | 0.590 |
| Xab | 0.402 | 0.452 | 0.433 | 0.432 | 0.416 | 0.426 | 0.400 | 0.384 | 0.381 | 0.406 |
| Xor | 0.003 | 0.005 | 0.004 | 0.004 | 0.008 | 0.004 | 0.003 | 0.004 | 0.003 | 0.004 |

PLAGIOCLASE

| Slide | KFZ_010_08_02 | KFZ_010_08_02 | KFZ_010_08_02 | KFZ_010_11_2 | KFZ_010_11_2 | KFZ_010_11_2 | KFZ_010_11_2 | KFZ_010_11_2 | KFZ_010_11_2 | KFZ_010_11_2 |
|---|---|---|---|---|---|---|---|---|---|---|
| **Area** | **4** | **4** | **4** | **1** | **1** | **1** | **2** | **2** | **2** | **2** |
| **Point** | **7** | **8** | **11** | **4** | **16** | **18** | **4** | **5** | **8** | **10** |
| SiO2 | 53.20 | 51.84 | 54.42 | 51.37 | 51.93 | 51.21 | 52.58 | 51.66 | 52.03 | 51.94 |
| TiO2 | 0.12 | 0.09 | 0.15 | 0.04 | 0.05 | 0.05 | 0.04 | 0.04 | 0.05 | 0.03 |
| Al2O3 | 26.07 | 27.82 | 25.68 | 29.72 | 28.94 | 29.20 | 29.44 | 29.74 | 29.91 | 29.60 |
| Cr2O3 | 0.01 | 0.00 | 0.00 | 0.00 | 0.00 | 0.00 | 0.00 | 0.00 | 0.00 | 0.00 |
| FeO | 1.14 | 0.82 | 1.16 | 0.31 | 0.31 | 0.26 | 0.27 | 0.52 | 0.31 | 0.37 |
| Na2O | 5.26 | 4.43 | 5.67 | 4.26 | 4.59 | 4.24 | 4.60 | 4.20 | 4.19 | 4.39 |
| MnO | 0.01 | 0.01 | 0.02 | 0.00 | 0.00 | 0.00 | 0.00 | 0.00 | 0.00 | 0.02 |
| MgO | 0.27 | 0.22 | 0.29 | 0.04 | 0.01 | 0.02 | 0.04 | 0.03 | 0.02 | 0.03 |
| NiO | 0.01 | 0.00 | 0.00 | 0.00 | 0.00 | 0.00 | 0.00 | 0.00 | 0.00 | 0.00 |
| CaO | 11.28 | 12.75 | 10.76 | 13.30 | 12.67 | 13.18 | 12.82 | 13.27 | 13.43 | 13.25 |
| K2O | 0.06 | 0.07 | 0.07 | 0.05 | 0.03 | 0.04 | 0.04 | 0.05 | 0.04 | 0.04 |
| BaO | 0.03 | 0.00 | 0.00 | 0.00 | 0.00 | 0.00 | 0.00 | 0.00 | 0.00 | 0.00 |
| Total | **97.46** | **98.06** | **98.21** | **99.10** | **98.52** | **98.19** | **99.83** | **99.52** | **99.99** | **99.68** |
| cations per pfu 8 oxygen | | | | | | | | | | |
| Si | 2.485 | 2.410 | 2.518 | 2.361 | 2.396 | 2.374 | 2.393 | 2.365 | 2.368 | 2.373 |
| Ti | 0.004 | 0.003 | 0.005 | 0.002 | 0.002 | 0.002 | 0.002 | 0.002 | 0.002 | 0.001 |
| Al | 1.435 | 1.525 | 1.400 | 1.610 | 1.574 | 1.595 | 1.579 | 1.605 | 1.605 | 1.594 |
| Cr | 0.000 | 0.000 | 0.000 | 0.000 | 0.000 | 0.000 | 0.000 | 0.000 | 0.000 | 0.000 |
| Fe | 0.044 | 0.032 | 0.045 | 0.012 | 0.012 | 0.010 | 0.010 | 0.020 | 0.012 | 0.014 |
| Mn | 0.000 | 0.000 | 0.001 | 0.000 | 0.000 | 0.000 | 0.000 | 0.000 | 0.000 | 0.001 |
| Mg | 0.018 | 0.015 | 0.020 | 0.002 | 0.001 | 0.002 | 0.002 | 0.002 | 0.002 | 0.002 |
| Ni | 0.001 | 0.000 | 0.000 | 0.000 | 0.000 | 0.000 | 0.000 | 0.000 | 0.000 | 0.000 |
| Ca | 0.565 | 0.635 | 0.534 | 0.655 | 0.626 | 0.654 | 0.626 | 0.650 | 0.655 | 0.649 |
| Na | 0.477 | 0.400 | 0.509 | 0.380 | 0.410 | 0.382 | 0.406 | 0.373 | 0.370 | 0.389 |
| K | 0.004 | 0.004 | 0.004 | 0.003 | 0.002 | 0.002 | 0.002 | 0.003 | 0.002 | 0.002 |
| Ba | 0.001 | 0.000 | 0.000 | 0.000 | 0.000 | 0.000 | 0.000 | 0.000 | 0.000 | 0.000 |
| Total | **5.034** | **5.025** | **5.034** | **5.025** | **5.022** | **5.021** | **5.021** | **5.021** | **5.016** | **5.024** |
| | | | | | | | | | | |
| Xan | 0.540 | 0.611 | 0.510 | 0.631 | 0.603 | 0.630 | 0.605 | 0.634 | 0.638 | 0.624 |
| Xab | 0.456 | 0.385 | 0.486 | 0.366 | 0.395 | 0.367 | 0.392 | 0.363 | 0.360 | 0.374 |
| Xor | 0.004 | 0.004 | 0.004 | 0.003 | 0.002 | 0.002 | 0.002 | 0.003 | 0.002 | 0.002 |

# PLAGIOCLASE

| Slide | KFZ_010_11_2 | KFZ_010_11_2 | KFZ_010_11_2 | KFZ_010_11_2 | KFZ_010_11_2 | KFZ_010_11_2 | KFZ_010_11_2 | KFZ_010_11_2 | KFZ_010_12_7 | KFZ_010_12_7 | KFZ_010_12_7 |
|---|---|---|---|---|---|---|---|---|---|---|---|
| **Area** | **2** | **2** | **3** | **4** | **4** | **5** | **5** | **5** | **1** | **1** | **1** |
| **Point** | **12** | **20** | **12** | **5** | **14** | **3** | **10** | **17** | **7** | **11** | **14** |
| SiO2 | 53.56 | 51.37 | 51.84 | 51.62 | 52.31 | 52.44 | 52.10 | 51.32 | 54.58 | 54.58 | 54.39 |
| TiO2 | 0.03 | 0.02 | 0.05 | 0.00 | 0.00 | 0.00 | 0.05 | 0.08 | 0.05 | 0.05 | 0.07 |
| Al2O3 | 28.85 | 29.76 | 29.35 | 29.19 | 29.65 | 29.00 | 29.42 | 29.26 | 27.18 | 27.37 | 26.77 |
| Cr2O3 | 0.00 | 0.00 | 0.00 | 0.00 | 0.00 | 0.00 | 0.02 | 0.00 | 0.00 | 0.00 | 0.00 |
| FeO | 0.24 | 0.30 | 0.36 | 0.34 | 0.38 | 0.32 | 0.33 | 0.61 | 0.30 | 0.30 | 0.43 |
| Na2O | 5.08 | 4.19 | 4.37 | 2.72 | 4.64 | 4.75 | 4.44 | 4.33 | 5.99 | 5.74 | 5.87 |
| MnO | 0.00 | 0.00 | 0.00 | 0.00 | 0.00 | 0.00 | 0.00 | 0.00 | 0.00 | 0.00 | 0.00 |
| MgO | 0.02 | 0.02 | 0.05 | 0.00 | 0.03 | 0.04 | 0.03 | 0.30 | 0.01 | 0.01 | 0.04 |
| NiO | 0.00 | 0.00 | 0.00 | 0.04 | 0.00 | 0.00 | 0.00 | 0.00 | 0.00 | 0.00 | 0.00 |
| CaO | 12.00 | 13.36 | 13.00 | 12.84 | 12.89 | 12.41 | 12.87 | 13.01 | 10.26 | 10.67 | 10.46 |
| K2O | 0.07 | 0.06 | 0.06 | 0.04 | 0.05 | 0.05 | 0.05 | 0.04 | 0.03 | 0.06 | 0.06 |
| BaO | 0.00 | 0.00 | 0.00 | 0.00 | 0.00 | 0.00 | 0.00 | 0.00 | 0.00 | 0.00 | 0.00 |
| Total | **99.86** | **99.07** | **99.09** | **96.80** | **99.95** | **99.00** | **99.30** | **98.94** | **98.40** | **98.77** | **98.11** |
| cations pfu per 8 oxygen | | | | | | | | | | | |
| Si | 2.431 | 2.361 | 2.380 | 2.406 | 2.381 | 2.406 | 2.385 | 2.365 | 2.504 | 2.496 | 2.506 |
| Ti | 0.001 | 0.001 | 0.002 | 0.000 | 0.000 | 0.000 | 0.002 | 0.002 | 0.002 | 0.002 | 0.002 |
| Al | 1.544 | 1.612 | 1.589 | 1.604 | 1.591 | 1.568 | 1.587 | 1.590 | 1.470 | 1.475 | 1.454 |
| Cr | 0.000 | 0.000 | 0.000 | 0.000 | 0.000 | 0.000 | 0.001 | 0.000 | 0.000 | 0.000 | 0.000 |
| Fe | 0.009 | 0.011 | 0.014 | 0.013 | 0.014 | 0.012 | 0.013 | 0.023 | 0.011 | 0.011 | 0.017 |
| Mn | 0.000 | 0.000 | 0.000 | 0.000 | 0.000 | 0.000 | 0.000 | 0.000 | 0.000 | 0.000 | 0.000 |
| Mg | 0.002 | 0.002 | 0.003 | 0.000 | 0.002 | 0.002 | 0.002 | 0.021 | 0.001 | 0.001 | 0.003 |
| Ni | 0.000 | 0.000 | 0.000 | 0.002 | 0.000 | 0.000 | 0.000 | 0.000 | 0.000 | 0.000 | 0.000 |
| Ca | 0.584 | 0.658 | 0.639 | 0.642 | 0.629 | 0.610 | 0.631 | 0.642 | 0.505 | 0.523 | 0.517 |
| Na | 0.447 | 0.373 | 0.389 | 0.246 | 0.410 | 0.422 | 0.394 | 0.386 | 0.534 | 0.510 | 0.525 |
| K | 0.004 | 0.003 | 0.004 | 0.002 | 0.003 | 0.003 | 0.002 | 0.002 | 0.002 | 0.003 | 0.003 |
| Ba | 0.000 | 0.000 | 0.000 | 0.000 | 0.000 | 0.000 | 0.000 | 0.000 | 0.000 | 0.000 | 0.000 |
| Total | **5.022** | **5.021** | **5.019** | **4.916** | **5.030** | **5.025** | **5.018** | **5.033** | **5.027** | **5.022** | **5.028** |
| | | | | | | | | | | | |
| Xan | 0.564 | 0.637 | 0.619 | 0.721 | 0.604 | 0.589 | 0.614 | 0.623 | 0.485 | 0.505 | 0.495 |
| Xab | 0.432 | 0.360 | 0.377 | 0.277 | 0.393 | 0.408 | 0.384 | 0.375 | 0.513 | 0.492 | 0.502 |
| Xor | 0.004 | 0.003 | 0.004 | 0.003 | 0.003 | 0.003 | 0.002 | 0.002 | 0.002 | 0.003 | 0.003 |

# PLAGIOCLASE

| **Slide** | **KFZ_010_12_7** | **KFZ_010_12_7** | **KFZ_010_12_7** | **KFZ_010_12_7** | **KFZ_010_12_7** | **KFZ_010_12_7** | **KFZ_010_12_7** | **KFZ_010_12_7** | **KFZ_010_12_7** | **KFZ_010_12_7** | **KFZ_010_12_7** |
|---|---|---|---|---|---|---|---|---|---|---|---|
| **Area** | **1** | **2** | **2** | **2** | **3** | **3** | **3** | **3** | **4** | **5** | **6** |
| **Point** | **17** | **8** | **9** | **10** | **9** | **10** | **17** | **19** | **12** | **16** | **18** |
| SiO2 | 54.32 | 54.34 | 54.27 | 54.29 | 54.76 | 53.89 | 53.81 | 54.64 | 54.66 | 53.90 | 67.85 |
| TiO2 | 0.09 | 0.06 | 0.08 | 0.09 | 0.08 | 0.01 | 0.02 | 0.04 | 0.02 | 0.02 | 0.00 |
| Al2O3 | 27.04 | 26.98 | 27.29 | 27.30 | 26.72 | 27.06 | 26.91 | 26.96 | 27.13 | 26.70 | 19.49 |
| Cr2O3 | 0.00 | 0.00 | 0.00 | 0.00 | 0.00 | 0.00 | 0.00 | 0.00 | 0.00 | 0.00 | 0.00 |
| FeO | 0.39 | 0.31 | 0.30 | 0.40 | 0.25 | 0.29 | 0.31 | 0.28 | 0.30 | 0.24 | 0.05 |
| Na2O | 6.01 | 6.13 | 6.08 | 5.83 | 6.13 | 6.03 | 5.92 | 6.03 | 6.02 | 5.90 | 11.83 |
| MnO | 0.00 | 0.00 | 0.00 | 0.00 | 0.00 | 0.00 | 0.00 | 0.00 | 0.00 | 0.00 | 0.00 |
| MgO | 0.00 | 0.01 | 0.01 | 0.00 | 0.03 | 0.01 | 0.00 | 0.03 | 0.01 | 0.01 | 0.00 |
| NiO | 0.00 | 0.00 | 0.00 | 0.00 | 0.00 | 0.00 | 0.00 | 0.00 | 0.00 | 0.00 | 0.00 |
| CaO | 10.34 | 10.76 | 10.53 | 10.79 | 10.24 | 10.51 | 10.45 | 10.53 | 10.46 | 10.43 | 0.31 |
| K2O | 0.04 | 0.07 | 0.03 | 0.07 | 0.05 | 0.09 | 0.05 | 0.09 | 0.07 | 0.03 | 0.05 |
| BaO | 0.04 | 0.00 | 0.00 | 0.00 | 0.00 | 0.00 | 0.00 | 0.00 | 0.00 | 0.00 | 0.00 |
| **Total** | **98.26** | **98.66** | **98.60** | **98.76** | **98.26** | **97.91** | **97.47** | **98.60** | **98.67** | **97.23** | **99.58** |
| cations pfu per 8 oxygen | | | | | | | | | | | |
| Si | 2.499 | 2.494 | 2.490 | 2.488 | 2.517 | 2.491 | 2.496 | 2.506 | 2.503 | 2.505 | 2.9816 |
| Ti | 0.003 | 0.002 | 0.002 | 0.003 | 0.003 | 0.000 | 0.001 | 0.002 | 0.001 | 0.001 | 0 |
| Al | 1.467 | 1.460 | 1.476 | 1.474 | 1.447 | 1.474 | 1.472 | 1.457 | 1.465 | 1.462 | 1.0096 |
| Cr | 0.000 | 0.000 | 0.000 | 0.000 | 0.000 | 0.000 | 0.000 | 0.000 | 0.000 | 0.000 | 0 |
| Fe | 0.015 | 0.012 | 0.012 | 0.015 | 0.010 | 0.011 | 0.012 | 0.011 | 0.011 | 0.010 | 0.0016 |
| Mn | 0.000 | 0.000 | 0.000 | 0.000 | 0.000 | 0.000 | 0.000 | 0.000 | 0.000 | 0.000 | 0 |
| Mg | 0.000 | 0.001 | 0.001 | 0.000 | 0.002 | 0.001 | 0.000 | 0.002 | 0.001 | 0.001 | 0 |
| Ni | 0.000 | 0.000 | 0.000 | 0.000 | 0.000 | 0.000 | 0.000 | 0.000 | 0.000 | 0.000 | 0 |
| Ca | 0.510 | 0.529 | 0.518 | 0.530 | 0.504 | 0.521 | 0.519 | 0.518 | 0.514 | 0.519 | 0.0144 |
| Na | 0.537 | 0.546 | 0.541 | 0.518 | 0.546 | 0.541 | 0.532 | 0.537 | 0.534 | 0.531 | 1.008 |
| K | 0.002 | 0.004 | 0.002 | 0.004 | 0.002 | 0.006 | 0.002 | 0.006 | 0.004 | 0.002 | 0.0024 |
| Ba | 0.001 | 0.000 | 0.000 | 0.000 | 0.000 | 0.000 | 0.000 | 0.000 | 0.000 | 0.000 | 0 |
| **Total** | **5.035** | **5.049** | **5.042** | **5.034** | **5.031** | **5.045** | **5.035** | **5.037** | **5.033** | **5.030** | **5.0184** |
| | | | | | | | | | | | |
| Xan | 0.486 | 0.490 | 0.488 | 0.503 | 0.479 | 0.488 | 0.493 | 0.488 | 0.488 | 0.494 | 0.014 |
| Xab | 0.512 | 0.506 | 0.510 | 0.493 | 0.519 | 0.507 | 0.505 | 0.506 | 0.508 | 0.505 | 0.984 |
| Xor | 0.002 | 0.004 | 0.002 | 0.004 | 0.002 | 0.005 | 0.002 | 0.005 | 0.004 | 0.002 | 0.002 |

# PLAGIOCLASE

| Slide | KFZ_010_12_ 7 | KFZ_010_12_ 7 | KFZ_010_12_ 7 | KFZ_010_12_ 7 | KFZ_010_12_ 7 | KFZ_010_12_ 7 | KFZ_010_12_ 7 |
|---|---|---|---|---|---|---|---|
| **Area** | **6** | **6** | **6** | **6** | **6** | **6** | **6** |
| **Point** | **19** | **13** | **14** | **15** | **16** | **17** | **20** |
| SiO2 | 65.50 | 54.44 | 54.62 | 54.38 | 54.66 | 54.16 | 54.26 |
| TiO2 | 0.00 | 0.07 | 0.14 | 0.04 | 0.09 | 0.07 | 0.12 |
| Al2O3 | 19.37 | 27.76 | 27.15 | 27.37 | 27.13 | 27.67 | 27.12 |
| Cr2O3 | 0.00 | 0.00 | 0.00 | 0.00 | 0.00 | 0.00 | 0.00 |
| FeO | 0.00 | 0.37 | 0.43 | 0.27 | 0.28 | 0.30 | 0.40 |
| Na2O | 11.48 | 5.58 | 5.83 | 5.88 | 6.01 | 5.80 | 5.88 |
| MnO | 0.00 | 0.00 | 0.00 | 0.00 | 0.00 | 0.00 | 0.00 |
| MgO | 0.00 | 0.04 | 0.01 | 0.02 | 0.00 | 0.01 | 0.03 |
| NiO | 0.00 | 0.00 | 0.00 | 0.01 | 0.00 | 0.00 | 0.00 |
| CaO | 0.70 | 11.37 | 10.72 | 10.85 | 10.46 | 10.94 | 10.76 |
| K2O | 0.05 | 0.05 | 0.07 | 0.06 | 0.06 | 0.04 | 0.07 |
| BaO | 0.00 | 0.00 | 0.00 | 0.00 | 0.00 | 0.00 | 0.00 |
| **Total** | **97.09** | **99.68** | **98.97** | **98.88** | **98.69** | **99.00** | **98.64** |
| cations pfu per 8 oxygen | | | | | | | |
| Si | 2.9576 | 2.474 | 2.497 | 2.488 | 2.502 | 2.476 | 2.490 |
| Ti | 0 | 0.002 | 0.005 | 0.002 | 0.003 | 0.002 | 0.004 |
| Al | 1.0312 | 1.486 | 1.463 | 1.476 | 1.464 | 1.491 | 1.467 |
| Cr | 0 | 0.000 | 0.000 | 0.000 | 0.000 | 0.000 | 0.000 |
| Fe | 0 | 0.014 | 0.016 | 0.010 | 0.010 | 0.012 | 0.015 |
| Mn | 0 | 0.000 | 0.000 | 0.000 | 0.000 | 0.000 | 0.000 |
| Mg | 0 | 0.002 | 0.001 | 0.002 | 0.000 | 0.001 | 0.002 |
| Ni | 0 | 0.000 | 0.000 | 0.000 | 0.000 | 0.000 | 0.000 |
| Ca | 0.0336 | 0.554 | 0.526 | 0.532 | 0.513 | 0.536 | 0.529 |
| Na | 1.0048 | 0.491 | 0.517 | 0.522 | 0.534 | 0.514 | 0.523 |
| K | 0.0032 | 0.003 | 0.004 | 0.003 | 0.003 | 0.002 | 0.004 |
| Ba | 0 | 0.000 | 0.000 | 0.000 | 0.000 | 0.000 | 0.000 |
| **Total** | **5.0312** | **5.026** | **5.028** | **5.035** | **5.030** | **5.036** | **5.036** |
| Xan | 0.032 | 0.528 | 0.502 | 0.503 | 0.489 | 0.509 | 0.501 |
| Xab | 0.965 | 0.469 | 0.494 | 0.494 | 0.508 | 0.489 | 0.495 |
| Xor | 0.003 | 0.003 | 0.004 | 0.003 | 0.003 | 0.002 | 0.004 |

CLINOPYROXE

| Slide | KFZ_010_11_2 | KFZ_010_11_2 | KFZ_010_11_2 | KFZ_010_11_2 | KFZ_010_11_2 | KFZ_010_11_2 | KFZ_010_11_2 | KFZ_010_11_2 | KFZ_010_11_2 | KFZ_010_11_2 | KFZ_010_11_2 |
|---|---|---|---|---|---|---|---|---|---|---|---|
| **Area** | **1** | **1** | **2** | **2** | **2** | **2** | **2** | **2** | **2** | **2** | **2** |
| **Point** | **17** | **19** | **1** | **2** | **9** | **14** | **15** | **16** | **18** | **19** | **21** |
| SiO2 | 50.69 | 50.75 | 56.03 | 54.77 | 55.08 | 50.60 | 54.00 | 51.42 | 54.44 | 55.72 | 51.00 |
| TiO2 | 0.90 | 0.57 | 0.00 | 0.00 | 0.01 | 0.63 | 0.17 | 0.29 | 0.43 | 0.02 | 0.88 |
| Al2O3 | 2.79 | 3.18 | 0.73 | 1.62 | 1.98 | 3.22 | 2.56 | 4.87 | 2.19 | 1.24 | 2.72 |
| Cr2O3 | 0.24 | 0.20 | 0.00 | 0.00 | 0.00 | 0.14 | 0.12 | 0.07 | 0.13 | 0.00 | 0.14 |
| FeO | 6.43 | 6.47 | 10.18 | 6.14 | 6.59 | 6.68 | 8.28 | 9.47 | 7.53 | 6.39 | 6.51 |
| Na2O | 0.41 | 0.42 | 0.27 | 0.31 | 0.44 | 0.39 | 0.61 | 1.17 | 0.57 | 0.34 | 0.43 |
| MnO | 0.22 | 0.23 | 0.45 | 0.17 | 0.16 | 0.20 | 0.21 | 0.17 | 0.19 | 0.23 | 0.18 |
| MgO | 15.41 | 16.49 | 20.92 | 20.55 | 20.51 | 16.10 | 18.82 | 17.86 | 19.45 | 20.94 | 15.58 |
| NiO | 0.02 | 0.04 | 0.08 | 0.07 | 0.08 | 0.05 | 0.04 | 0.01 | 0.02 | 0.06 | 0.02 |
| CaO | 21.58 | 19.38 | 8.72 | 11.85 | 12.12 | 21.11 | 12.50 | 11.24 | 12.22 | 11.96 | 21.96 |
| K2O | 0.01 | 0.05 | 0.02 | 0.05 | 0.03 | 0.01 | 0.02 | 0.05 | 0.02 | 0.02 | 0.01 |
| BaO | 0.00 | 0.00 | 0.00 | 0.00 | 0.00 | 0.00 | 0.00 | 0.00 | 0.00 | 0.01 | 0.00 |
| Total | **98.70** | **97.80** | **97.39** | **95.51** | **97.01** | **99.12** | **97.32** | **96.63** | **97.19** | **96.94** | **99.44** |
| | | | | | | | | | | | |
| cations pfu per 6 oxygen | | | | | | | | | | | |
| Si | 1.900 | 1.907 | 2.061 | 2.036 | 2.023 | 1.888 | 1.999 | 1.930 | 2.008 | 2.043 | 1.900 |
| Ti | 0.025 | 0.016 | 0.000 | 0.000 | 0.001 | 0.017 | 0.005 | 0.008 | 0.012 | 0.001 | 0.025 |
| Al | 0.123 | 0.141 | 0.032 | 0.071 | 0.086 | 0.142 | 0.112 | 0.215 | 0.095 | 0.053 | 0.119 |
| Cr | 0.007 | 0.006 | 0.000 | 0.000 | 0.000 | 0.004 | 0.004 | 0.002 | 0.004 | 0.000 | 0.004 |
| Fe | 0.202 | 0.203 | 0.313 | 0.191 | 0.202 | 0.208 | 0.256 | 0.297 | 0.232 | 0.196 | 0.203 |
| Mn | 0.007 | 0.007 | 0.014 | 0.005 | 0.005 | 0.006 | 0.007 | 0.005 | 0.006 | 0.007 | 0.005 |
| Mg | 0.862 | 0.923 | 1.147 | 1.139 | 1.123 | 0.896 | 1.038 | 1.000 | 1.069 | 1.145 | 0.865 |
| Ni | 0.001 | 0.001 | 0.002 | 0.002 | 0.002 | 0.002 | 0.001 | 0.000 | 0.001 | 0.002 | 0.001 |
| Ca | 0.867 | 0.781 | 0.344 | 0.472 | 0.477 | 0.844 | 0.496 | 0.452 | 0.483 | 0.470 | 0.877 |
| Na | 0.030 | 0.031 | 0.019 | 0.022 | 0.031 | 0.028 | 0.044 | 0.085 | 0.040 | 0.025 | 0.031 |
| K | 0.001 | 0.002 | 0.001 | 0.002 | 0.001 | 0.001 | 0.001 | 0.002 | 0.001 | 0.001 | 0.001 |
| Ba | 0.000 | 0.000 | 0.000 | 0.000 | 0.000 | 0.000 | 0.000 | 0.000 | 0.000 | 0.000 | 0.000 |
| Total | **4.025** | **4.020** | **3.934** | **3.941** | **3.951** | **4.036** | **3.961** | **3.997** | **3.952** | **3.943** | **4.030** |
| | | | | | | | | | | | |
| Xdi | 0.892 | 0.890 | 0.820 | 0.891 | 0.885 | 0.890 | 0.854 | 0.828 | 0.867 | 0.888 | 0.893 |
| Xhd | 0.552 | 0.514 | 0.361 | 0.367 | 0.376 | 0.539 | 0.419 | 0.427 | 0.399 | 0.366 | 0.554 |

CLINOPYROXE

| **Slide** | **KFZ_010_11_2** | **KFZ_010_11_2** | **KFZ_010_11_2** | **KFZ_010_11_2** | **KFZ_010_11_2** | **KFZ_010_11_2** | **KFZ_010_11_2** | **KFZ_010_11_2** | **KFZ_010_11_2** | **KFZ_010_11_2** | **KFZ_010_11_2** |
|---|---|---|---|---|---|---|---|---|---|---|---|
| **Area** | **2** | **2** | **3** | **3** | **3** | **3** | **3** | **3** | **3** | **4** | **4** |
| **Point** | **23** | **25** | **4** | **5** | **7** | **9** | **11** | **13** | **16** | **1** | **2** |
| SiO2 | 51.20 | 55.23 | 56.71 | 51.70 | 55.06 | 55.39 | 56.43 | 54.10 | 54.91 | 53.21 | 51.76 |
| TiO2 | 0.65 | 0.00 | 0.00 | 0.52 | 0.06 | 0.02 | 0.06 | 0.09 | 0.06 | 0.19 | 0.61 |
| Al2O3 | 2.66 | 2.10 | 0.67 | 2.91 | 1.85 | 1.66 | 1.14 | 3.07 | 1.66 | 3.09 | 3.05 |
| Cr2O3 | 0.15 | 0.02 | 0.01 | 0.25 | 0.00 | 0.01 | 0.00 | 0.03 | 0.00 | 0.10 | 0.21 |
| FeO | 6.44 | 6.12 | 4.87 | 6.15 | 7.21 | 7.64 | 6.27 | 8.60 | 7.72 | 8.69 | 5.69 |
| Na2O | 0.43 | 0.51 | 0.18 | 0.46 | 0.46 | 0.41 | 0.31 | 0.77 | 0.37 | 0.70 | 0.43 |
| MnO | 0.20 | 0.18 | 0.18 | 0.17 | 0.14 | 0.23 | 0.20 | 0.30 | 0.23 | 0.19 | 0.16 |
| MgO | 15.48 | 20.62 | 21.08 | 16.15 | 20.13 | 19.94 | 20.97 | 19.30 | 20.16 | 18.55 | 15.85 |
| NiO | 0.02 | 0.06 | 0.05 | 0.06 | 0.12 | 0.11 | 0.04 | 0.03 | 0.10 | 0.02 | 0.03 |
| CaO | 21.76 | 12.73 | 12.59 | 20.34 | 11.70 | 11.89 | 12.13 | 10.93 | 10.92 | 11.49 | 21.75 |
| K2O | 0.01 | 0.01 | 0.04 | 0.02 | 0.04 | 0.05 | 0.04 | 0.05 | 0.08 | 0.04 | 0.01 |
| BaO | 0.07 | 0.00 | 0.00 | 0.00 | 0.00 | 0.00 | 0.00 | 0.00 | 0.00 | 0.00 | 0.00 |
| Total | **99.06** | **97.59** | **96.39** | **98.73** | **96.77** | **97.35** | **97.60** | **97.26** | **96.22** | **96.27** | **99.57** |
| | | | | | | | | | | | |
| cations pfu per 6 oxygen | | | | | | | | | | | |
| Si | 1.912 | 2.015 | 2.075 | 1.923 | 2.030 | 2.035 | 2.052 | 1.997 | 2.037 | 1.991 | 1.913 |
| Ti | 0.018 | 0.000 | 0.000 | 0.014 | 0.002 | 0.001 | 0.002 | 0.002 | 0.002 | 0.005 | 0.017 |
| Al | 0.117 | 0.091 | 0.029 | 0.128 | 0.080 | 0.072 | 0.049 | 0.134 | 0.073 | 0.136 | 0.133 |
| Cr | 0.004 | 0.001 | 0.001 | 0.007 | 0.000 | 0.001 | 0.000 | 0.001 | 0.000 | 0.003 | 0.006 |
| Fe | 0.201 | 0.187 | 0.149 | 0.191 | 0.223 | 0.235 | 0.191 | 0.265 | 0.239 | 0.272 | 0.176 |
| Mn | 0.007 | 0.005 | 0.005 | 0.005 | 0.004 | 0.007 | 0.006 | 0.010 | 0.007 | 0.006 | 0.005 |
| Mg | 0.862 | 1.122 | 1.150 | 0.896 | 1.106 | 1.092 | 1.136 | 1.062 | 1.115 | 1.034 | 0.873 |
| Ni | 0.001 | 0.002 | 0.001 | 0.002 | 0.004 | 0.004 | 0.001 | 0.001 | 0.003 | 0.001 | 0.001 |
| Ca | 0.871 | 0.498 | 0.494 | 0.811 | 0.462 | 0.468 | 0.473 | 0.433 | 0.434 | 0.461 | 0.862 |
| Na | 0.031 | 0.037 | 0.013 | 0.033 | 0.033 | 0.029 | 0.022 | 0.055 | 0.027 | 0.050 | 0.031 |
| K | 0.001 | 0.001 | 0.002 | 0.001 | 0.002 | 0.002 | 0.002 | 0.002 | 0.004 | 0.002 | 0.001 |
| Ba | 0.001 | 0.000 | 0.000 | 0.000 | 0.000 | 0.000 | 0.000 | 0.000 | 0.000 | 0.000 | 0.000 |
| Total | **4.025** | **3.959** | **3.919** | **4.012** | **3.946** | **3.945** | **3.933** | **3.962** | **3.941** | **3.962** | **4.016** |
| | | | | | | | | | | | |
| Xdi | 0.893 | 0.894 | 0.914 | 0.897 | 0.874 | 0.866 | 0.891 | 0.845 | 0.863 | 0.843 | 0.906 |
| Xhd | 0.552 | 0.378 | 0.358 | 0.526 | 0.381 | 0.390 | 0.367 | 0.394 | 0.375 | 0.413 | 0.542 |

## CLINOPYROXE

| Slide | KFZ_010_11_2 | KFZ_010_11_2 | KFZ_010_11_2 | KFZ_010_11_2 | KFZ_010_11_2 | KFZ_010_11_2 | KFZ_010_11_2 | KFZ_010_11_2 | KFZ_010_11_2 | KFZ_010_11_2 | KFZ_010_11_2 |
|---|---|---|---|---|---|---|---|---|---|---|---|
| **Area** | **4** | **4** | **4** | **4** | **4** | **4** | **4** | **4** | **4** | **4** | **4** |
| **Point** | **3** | **4** | **6** | **7** | **8** | **9** | **10** | **11** | **13** | **15** | **16** |
| SiO2 | 51.88 | 54.28 | 51.51 | 46.33 | 56.61 | 53.07 | 50.87 | 53.34 | 52.71 | 52.03 | 53.25 |
| TiO2 | 0.54 | 0.09 | 0.10 | 0.01 | 0.00 | 0.19 | 0.61 | 0.29 | 0.48 | 0.48 | 0.26 |
| Al2O3 | 2.30 | 2.50 | 1.75 | 0.82 | 1.15 | 3.55 | 3.48 | 2.44 | 2.09 | 2.60 | 3.22 |
| Cr2O3 | 0.16 | 0.06 | 0.19 | 0.16 | 0.01 | 0.03 | 0.22 | 0.19 | 0.14 | 0.19 | 0.12 |
| FeO | 6.42 | 7.44 | 6.96 | 6.25 | 4.24 | 8.76 | 5.68 | 5.64 | 9.01 | 6.16 | 7.95 |
| Na2O | 0.42 | 0.55 | 0.00 | 0.00 | 0.35 | 0.72 | 0.48 | 0.43 | 0.29 | 0.45 | 0.70 |
| MnO | 0.17 | 0.22 | 0.15 | 0.26 | 0.20 | 0.17 | 0.16 | 0.16 | 0.21 | 0.17 | 0.15 |
| MgO | 16.13 | 19.29 | 0.60 | 0.00 | 22.07 | 18.14 | 15.47 | 18.05 | 19.68 | 16.12 | 18.55 |
| NiO | 0.06 | 0.05 | 0.12 | 0.02 | 0.00 | 0.00 | 0.01 | 0.04 | 0.08 | 0.01 | 0.00 |
| CaO | 21.16 | 11.66 | 13.01 | 12.21 | 12.48 | 12.39 | 21.50 | 18.11 | 15.32 | 21.37 | 12.61 |
| K2O | 0.02 | 0.03 | 0.01 | 0.02 | 0.02 | 0.04 | 0.02 | 0.02 | 0.01 | 0.03 | 0.04 |
| BaO | 0.00 | 0.00 | 0.00 | 0.00 | 0.00 | 0.00 | 0.01 | 0.00 | 0.00 | 0.00 | 0.00 |
| Total | **99.25** | **96.18** | **74.41** | **66.07** | **97.13** | **97.07** | **98.51** | **98.71** | **100.01** | **99.61** | **96.84** |
| | | | | | | | | | | | |
| cations pfu per 6 oxygen | | | | | | | | | | | |
| Si | 1.927 | 2.017 | 2.426 | 2.463 | 2.051 | 1.975 | 1.901 | 1.960 | 1.931 | 1.924 | 1.980 |
| Ti | 0.015 | 0.002 | 0.004 | 0.001 | 0.000 | 0.005 | 0.017 | 0.008 | 0.013 | 0.013 | 0.007 |
| Al | 0.101 | 0.110 | 0.097 | 0.052 | 0.049 | 0.156 | 0.153 | 0.106 | 0.091 | 0.113 | 0.141 |
| Cr | 0.005 | 0.002 | 0.007 | 0.007 | 0.001 | 0.001 | 0.007 | 0.005 | 0.004 | 0.005 | 0.004 |
| Fe | 0.200 | 0.232 | 0.274 | 0.278 | 0.128 | 0.272 | 0.178 | 0.173 | 0.276 | 0.190 | 0.247 |
| Mn | 0.005 | 0.007 | 0.006 | 0.011 | 0.006 | 0.005 | 0.005 | 0.005 | 0.007 | 0.005 | 0.005 |
| Mg | 0.893 | 1.069 | 0.042 | 0.000 | 1.192 | 1.006 | 0.862 | 0.989 | 1.075 | 0.888 | 1.028 |
| Ni | 0.002 | 0.001 | 0.004 | 0.001 | 0.000 | 0.000 | 0.001 | 0.001 | 0.002 | 0.001 | 0.000 |
| Ca | 0.842 | 0.464 | 0.656 | 0.695 | 0.484 | 0.494 | 0.861 | 0.713 | 0.601 | 0.847 | 0.502 |
| Na | 0.031 | 0.040 | 0.000 | 0.000 | 0.025 | 0.052 | 0.035 | 0.031 | 0.021 | 0.032 | 0.050 |
| K | 0.001 | 0.001 | 0.001 | 0.001 | 0.001 | 0.002 | 0.001 | 0.001 | 0.001 | 0.002 | 0.002 |
| Ba | 0.000 | 0.000 | 0.000 | 0.000 | 0.000 | 0.000 | 0.000 | 0.000 | 0.000 | 0.000 | 0.000 |
| Total | **4.022** | **3.945** | **3.518** | **3.508** | **3.937** | **3.970** | **4.021** | **3.992** | **4.022** | **4.021** | **3.967** |
| | | | | | | | | | | | |
| Xdi | 0.894 | 0.866 | 0.714 | 0.706 | 0.926 | 0.844 | 0.904 | 0.905 | 0.856 | 0.899 | 0.859 |
| Xhd | 0.537 | 0.393 | 0.951 | 0.988 | 0.338 | 0.431 | 0.545 | 0.472 | 0.448 | 0.537 | 0.420 |

CLINOPYROXE

| Slide | KFZ_010_11_2 | KFZ_010_11_2 | KFZ_010_11_2 | KFZ_010_11_2 | KFZ_010_11_2 | KFZ_010_11_2 | KFZ_010_11_2 | KFZ_010_11_2 | KFZ_010_11_2 | KFZ_010_11_2 | KFZ_010_11_2 |
|---|---|---|---|---|---|---|---|---|---|---|---|
| **Area** | **4** | **4** | **5** | **5** | **5** | **5** | **5** | **5** | **5** | **5** | **5** |
| **Point** | **17** | **20** | **1** | **4** | **5** | **6** | **7** | **8** | **9** | **11** | **12** |
| SiO2 | 53.81 | 52.43 | 54.15 | 51.62 | 52.65 | 52.00 | 51.85 | 54.49 | 50.93 | 53.53 | 51.60 |
| TiO2 | 0.16 | 0.36 | 0.07 | 0.29 | 0.38 | 0.48 | 0.53 | 0.18 | 0.44 | 0.29 | 0.35 |
| Al2O3 | 2.49 | 2.44 | 2.25 | 4.91 | 3.28 | 3.17 | 4.23 | 2.34 | 5.07 | 2.36 | 4.33 |
| Cr2O3 | 0.04 | 0.17 | 0.00 | 0.05 | 0.18 | 0.20 | 0.18 | 0.06 | 0.21 | 0.14 | 0.19 |
| FeO | 8.52 | 5.64 | 9.56 | 7.95 | 8.82 | 9.45 | 8.96 | 7.74 | 10.05 | 8.82 | 8.80 |
| Na2O | 0.52 | 0.41 | 0.43 | 1.14 | 0.65 | 0.63 | 0.91 | 0.53 | 1.18 | 0.47 | 0.84 |
| MnO | 0.17 | 0.17 | 0.36 | 0.15 | 0.13 | 0.12 | 0.13 | 0.18 | 0.21 | 0.15 | 0.20 |
| MgO | 18.60 | 16.44 | 19.32 | 18.25 | 17.60 | 17.30 | 17.35 | 19.23 | 16.69 | 17.95 | 17.64 |
| NiO | 0.04 | 0.00 | 0.02 | 0.00 | 0.00 | 0.00 | 0.02 | 0.00 | 0.03 | 0.00 | 0.02 |
| CaO | 12.25 | 21.41 | 9.75 | 12.09 | 12.56 | 12.71 | 12.07 | 11.56 | 11.65 | 12.77 | 12.25 |
| K2O | 0.03 | 0.02 | 0.05 | 0.05 | 0.02 | 0.03 | 0.04 | 0.03 | 0.05 | 0.04 | 0.06 |
| BaO | 0.00 | 0.00 | 0.00 | 0.00 | 0.00 | 0.00 | 0.00 | 0.00 | 0.00 | 0.00 | 0.00 |
| Total | **96.64** | **99.49** | **95.96** | **96.50** | **96.29** | **96.09** | **96.28** | **96.33** | **96.50** | **96.53** | **96.28** |
| | | | | | | | | | | | |
| cations pfu per 6 oxygen | | | | | | | | | | | |
| Si | 2.006 | 1.934 | 2.026 | 1.930 | 1.978 | 1.967 | 1.951 | 2.022 | 1.924 | 2.004 | 1.942 |
| Ti | 0.004 | 0.010 | 0.002 | 0.008 | 0.011 | 0.014 | 0.015 | 0.005 | 0.013 | 0.008 | 0.010 |
| Al | 0.109 | 0.106 | 0.099 | 0.216 | 0.145 | 0.141 | 0.188 | 0.103 | 0.226 | 0.104 | 0.192 |
| Cr | 0.001 | 0.005 | 0.000 | 0.001 | 0.005 | 0.006 | 0.005 | 0.002 | 0.006 | 0.004 | 0.005 |
| Fe | 0.266 | 0.174 | 0.299 | 0.248 | 0.277 | 0.299 | 0.282 | 0.240 | 0.317 | 0.276 | 0.277 |
| Mn | 0.005 | 0.005 | 0.011 | 0.005 | 0.004 | 0.004 | 0.004 | 0.005 | 0.007 | 0.005 | 0.007 |
| Mg | 1.033 | 0.904 | 1.077 | 1.017 | 0.985 | 0.976 | 0.973 | 1.064 | 0.940 | 1.001 | 0.989 |
| Ni | 0.001 | 0.000 | 0.001 | 0.000 | 0.000 | 0.000 | 0.001 | 0.000 | 0.001 | 0.000 | 0.001 |
| Ca | 0.489 | 0.847 | 0.391 | 0.485 | 0.506 | 0.515 | 0.487 | 0.460 | 0.472 | 0.512 | 0.494 |
| Na | 0.038 | 0.029 | 0.032 | 0.083 | 0.047 | 0.046 | 0.067 | 0.038 | 0.086 | 0.034 | 0.062 |
| K | 0.001 | 0.001 | 0.002 | 0.002 | 0.001 | 0.002 | 0.002 | 0.001 | 0.002 | 0.002 | 0.003 |
| Ba | 0.000 | 0.000 | 0.000 | 0.000 | 0.000 | 0.000 | 0.000 | 0.000 | 0.000 | 0.000 | 0.000 |
| Total | **3.954** | **4.017** | **3.940** | **3.997** | **3.961** | **3.970** | **3.974** | **3.940** | **3.993** | **3.952** | **3.982** |
| | | | | | | | | | | | |
| Xdi | 0.849 | 0.907 | 0.826 | 0.856 | 0.841 | 0.831 | 0.836 | 0.861 | 0.813 | 0.844 | 0.840 |
| Xhd | 0.421 | 0.529 | 0.388 | 0.418 | 0.442 | 0.454 | 0.440 | 0.395 | 0.455 | 0.439 | 0.436 |

CLINOPYROXE

| Slide | KFZ_010_11_2 | KFZ_010_11_2 | KFZ_010_11_2 | KFZ_010_11_2 | KFZ_010_12_7 | KFZ_010_12_7 | KFZ_010_12_7 | KFZ_010_12_7 | KFZ_010_12_7 | KFZ_010_12_7 | KFZ_010_12_7 |
|---|---|---|---|---|---|---|---|---|---|---|---|
| **Area** | **5** | **5** | **5** | **5** | **1** | **1** | **1** | **1** | **1** | **1** | **1** |
| **Point** | **13** | **14** | **15** | **16** | **1** | **2** | **3** | **4** | **5** | **6** | **8** |
| SiO2 | 53.20 | 54.57 | 56.07 | 51.46 | 50.01 | 50.13 | 49.46 | 51.37 | 50.74 | 53.65 | 53.53 |
| TiO2 | 0.38 | 0.28 | 0.11 | 0.84 | 0.55 | 0.48 | 0.31 | 0.38 | 0.51 | 0.32 | 0.19 |
| Al2O3 | 2.58 | 1.86 | 0.81 | 2.57 | 5.31 | 5.11 | 3.94 | 3.08 | 3.65 | 0.65 | 2.41 |
| Cr2O3 | 0.21 | 0.10 | 0.00 | 0.23 | 0.03 | 0.06 | 0.00 | 0.03 | 0.00 | 0.00 | 0.00 |
| FeO | 9.61 | 7.02 | 6.49 | 6.32 | 11.44 | 10.23 | 10.51 | 10.93 | 10.54 | 17.86 | 7.59 |
| Na2O | 0.49 | 0.47 | 0.20 | 0.42 | 1.06 | 0.99 | 0.78 | 0.55 | 0.74 | 0.10 | 0.51 |
| MnO | 0.18 | 0.24 | 0.22 | 0.18 | 0.18 | 0.11 | 0.17 | 0.15 | 0.15 | 0.78 | 0.19 |
| MgO | 17.20 | 19.51 | 20.28 | 15.63 | 15.62 | 16.07 | 15.77 | 15.92 | 16.32 | 20.08 | 18.84 |
| NiO | 0.02 | 0.03 | 0.08 | 0.03 | 0.03 | 0.03 | 0.03 | 0.04 | 0.02 | 0.04 | 0.01 |
| CaO | 12.74 | 11.96 | 12.76 | 21.98 | 12.41 | 12.51 | 12.15 | 12.53 | 12.56 | 2.50 | 13.08 |
| K2O | 0.04 | 0.04 | 0.03 | 0.03 | 0.06 | 0.05 | 0.04 | 0.05 | 0.06 | 0.03 | 0.05 |
| BaO | 0.00 | 0.00 | 0.00 | 0.00 | 0.04 | 0.00 | 0.01 | 0.01 | 0.02 | 0.00 | 0.00 |
| Total | **96.66** | **96.08** | **97.05** | **99.69** | **96.73** | **95.77** | **93.18** | **95.03** | **95.30** | **96.00** | **96.41** |
| cations pfu per 6 oxygen | | | | | | | | | | | |
| Si | 1.997 | 2.028 | 2.057 | 1.909 | 11.419 | 11.488 | 11.668 | 11.869 | 11.693 | 12.280 | 11.988 |
| Ti | 0.011 | 0.008 | 0.003 | 0.023 | 0.094 | 0.083 | 0.054 | 0.065 | 0.086 | 0.054 | 0.032 |
| Al | 0.115 | 0.082 | 0.035 | 0.112 | 1.429 | 1.379 | 1.094 | 0.839 | 0.990 | 0.176 | 0.637 |
| Cr | 0.006 | 0.003 | 0.000 | 0.007 | 0.004 | 0.011 | 0.000 | 0.004 | 0.000 | 0.000 | 0.000 |
| Fe | 0.302 | 0.218 | 0.199 | 0.196 | 2.185 | 1.962 | 2.074 | 2.110 | 2.030 | 3.420 | 1.422 |
| Mn | 0.005 | 0.008 | 0.007 | 0.005 | 0.036 | 0.022 | 0.036 | 0.029 | 0.029 | 0.151 | 0.036 |
| Mg | 0.962 | 1.081 | 1.109 | 0.864 | 5.317 | 5.490 | 5.544 | 5.483 | 5.609 | 6.851 | 6.289 |
| Ni | 0.001 | 0.001 | 0.002 | 0.001 | 0.007 | 0.007 | 0.007 | 0.007 | 0.004 | 0.007 | 0.000 |
| Ca | 0.512 | 0.476 | 0.502 | 0.874 | 3.035 | 3.071 | 3.071 | 3.103 | 3.103 | 0.612 | 3.139 |
| Na | 0.036 | 0.034 | 0.014 | 0.030 | 0.472 | 0.439 | 0.356 | 0.245 | 0.331 | 0.047 | 0.223 |
| K | 0.002 | 0.002 | 0.001 | 0.001 | 0.018 | 0.014 | 0.014 | 0.014 | 0.018 | 0.007 | 0.014 |
| Ba | 0.000 | 0.000 | 0.000 | 0.000 | 0.004 | 0.000 | 0.000 | 0.000 | 0.000 | 0.000 | 0.000 |
| Total | **3.949** | **3.940** | **3.930** | **4.023** | **24.019** | **23.965** | **23.918** | **23.767** | **23.897** | **23.609** | **23.785** |
| | | | | | | | | | | | |
| Xdi | 0.828 | 0.873 | 0.887 | 0.896 | 0.790 | 0.812 | 0.803 | 0.801 | 0.809 | 0.676 | 0.866 |
| Xhd | 0.457 | 0.389 | 0.386 | 0.552 | 0.494 | 0.477 | 0.480 | 0.486 | 0.477 | 0.365 | 0.419 |

CLINOPYROXE

| Slide | KFZ_010_12_7 | KFZ_010_12_7 | KFZ_010_12_7 | KFZ_010_12_7 | KFZ_010_12_7 | KFZ_010_12_7 | KFZ_010_12_7 | KFZ_010_12_7 | KFZ_010_12_7 | KFZ_010_12_7 | KFZ_010_12_7 |
|---|---|---|---|---|---|---|---|---|---|---|---|
| **Area** | **1** | **1** | **1** | **1** | **1** | **6** | **6** | **6** | **6** | **6** | **6** |
| **Point** | **10** | **13** | **15** | **16** | **18** | **1** | **2** | **3** | **4** | **5** | **6** |
| SiO2 | 50.1344 | 51.4842 | 48.9414 | 48.5705 | 51.1409 | 55.5123 | 55.973 | 56.0674 | 56.047 | 49.4784 | 56.177 |
| TiO2 | 0.8762 | 0.4797 | 0.5646 | 1.144 | 0.8001 | 0.1828 | 0.1372 | 0.1923 | 0.1576 | 0.327 | 0.1001 |
| Al2O3 | 2.4263 | 1.6627 | 5.7904 | 5.8308 | 2.3516 | 1.4936 | 1.4332 | 1.1484 | 1.1284 | 4.502 | 1.045 |
| Cr2O3 | 0.0117 | 0.0121 | 0 | 0.0813 | 0.0318 | 0 | 0 | 0 | 0 | 0 | 0 |
| FeO | 7.3166 | 8.4514 | 11.3534 | 12.5717 | 6.9094 | 3.8285 | 4.1148 | 3.0883 | 3.0152 | 7.7359 | 4.4956 |
| Na2O | 0.4884 | 0.324 | 1.1415 | 1.0758 | 0.5063 | 0.4454 | 0.3553 | 0.3252 | 0.2509 | 0.9576 | 0.2793 |
| MnO | 0.2067 | 0.2756 | 0.143 | 0.2051 | 0.2396 | 0.0227 | 0.0192 | 0.0507 | 0 | 0.146 | 0.039 |
| MgO | 14.5675 | 14.0635 | 15.209 | 14.6212 | 14.6308 | 21.9695 | 21.942 | 22.4093 | 22.1856 | 17.5959 | 21.8844 |
| NiO | 0.0218 | 0.0313 | 0.0413 | 0.0374 | 0.0325 | 0.0242 | 0 | 0.0141 | 0.0416 | 0.0543 | 0 |
| CaO | 22.0647 | 21.1465 | 12.3681 | 12.2183 | 22.3194 | 12.8005 | 12.9506 | 12.8221 | 13.1865 | 11.3866 | 12.187 |
| K2O | 0.0192 | 0.048 | 0.069 | 0.0344 | 0.0127 | 0.0239 | 0.0168 | 0.0286 | 0.0122 | 0.0652 | 0.0294 |
| BaO | 0.0602 | 0.0042 | 0.0382 | 0.0133 | 0 | 0 | 0 | 0 | 0 | 0 | 0 |
| Total | **98.1937** | **97.9833** | **95.66** | **96.4039** | **98.9752** | **96.3035** | **96.9421** | **96.1465** | **96.0251** | **92.249** | **96.2368** |
| cations pfu per 6 oxygen | | | | | | | | | | | |
| Si | 11.419 | 11.736 | 11.315 | 11.214 | 11.513 | 12.179 | 12.208 | 12.265 | 12.280 | 11.606 | 12.323 |
| Ti | 0.151 | 0.083 | 0.097 | 0.198 | 0.137 | 0.029 | 0.022 | 0.032 | 0.025 | 0.058 | 0.018 |
| Al | 0.652 | 0.446 | 1.577 | 1.588 | 0.623 | 0.385 | 0.367 | 0.295 | 0.292 | 1.246 | 0.270 |
| Cr | 0.004 | 0.004 | 0.000 | 0.014 | 0.007 | 0.000 | 0.000 | 0.000 | 0.000 | 0.000 | 0.000 |
| Fe | 1.393 | 1.613 | 2.196 | 2.426 | 1.300 | 0.702 | 0.749 | 0.565 | 0.551 | 1.519 | 0.824 |
| Mn | 0.040 | 0.054 | 0.029 | 0.040 | 0.047 | 0.004 | 0.004 | 0.011 | 0.000 | 0.029 | 0.007 |
| Mg | 4.946 | 4.777 | 5.242 | 5.033 | 4.910 | 7.186 | 7.132 | 7.308 | 7.243 | 6.152 | 7.157 |
| Ni | 0.004 | 0.007 | 0.007 | 0.007 | 0.007 | 0.004 | 0.000 | 0.004 | 0.007 | 0.011 | 0.000 |
| Ca | 5.386 | 5.166 | 3.064 | 3.024 | 5.386 | 3.010 | 3.028 | 3.006 | 3.096 | 2.862 | 2.866 |
| Na | 0.216 | 0.144 | 0.511 | 0.482 | 0.220 | 0.191 | 0.151 | 0.137 | 0.108 | 0.436 | 0.119 |
| K | 0.007 | 0.014 | 0.022 | 0.011 | 0.004 | 0.007 | 0.004 | 0.007 | 0.004 | 0.018 | 0.007 |
| Ba | 0.004 | 0.000 | 0.004 | 0.000 | 0.000 | 0.000 | 0.000 | 0.000 | 0.000 | 0.000 | 0.000 |
| **Total** | **24.224** | **24.044** | **24.062** | **24.037** | **24.152** | **23.695** | **23.666** | **23.630** | **23.605** | **23.940** | **23.591** |
| | | | | | | | | | | | |
| Xdi | 0.878 | 0.856 | 0.789 | 0.766 | 0.884 | 0.935 | 0.931 | 0.947 | 0.949 | 0.853 | 0.923 |
| Xhd | 0.576 | 0.584 | 0.499 | 0.518 | 0.574 | 0.340 | 0.346 | 0.328 | 0.335 | 0.415 | 0.340 |

CLINOPYROXE

| Slide | KFZ_010_12_7 | KFZ_010_12_7 | KFZ_010_12_7 | KFZ_010_12_7 | KFZ_010_12_7 | KFZ_010_12_7 | KFZ_010_12_7 | KFZ_010_12_7 | KFZ_010_12_7 | KFZ_010_12_7 | KFZ_010_12_7 |
|---|---|---|---|---|---|---|---|---|---|---|---|
| **Area** | **6** | **6** | **6** | **6** | **6** | **6** | **2** | **2** | **2** | **2** | **2** |
| **Point** | **7** | **8** | **9** | **10** | **11** | **12** | **1** | **2** | **3** | **5** | **6** |
| SiO2 | 52.8979 | 56.3245 | 54.967 | 54.7725 | 52.77 | 51.09 | 54.99 | 54.94 | 55.07 | 55.69 | 51.08 |
| TiO2 | 0.1269 | 0.1217 | 0.0816 | 0.241 | 0.43 | 0.32 | 0.34 | 0.13 | 0.91 | 0.10 | 0.83 |
| Al2O3 | 2.9873 | 1.115 | 1.6547 | 1.3252 | 3.62 | 3.92 | 1.16 | 1.24 | 1.19 | 1.29 | 3.18 |
| Cr2O3 | 0 | 0 | 0 | 0 | 0.01 | 0.05 | 0.03 | 0.00 | 0.01 | 0.02 | 0.08 |
| FeO | 8.0946 | 3.6375 | 5.0853 | 6.9757 | 6.93 | 6.19 | 4.30 | 3.72 | 3.52 | 3.72 | 7.18 |
| Na2O | 0.6571 | 0.2895 | 0.3928 | 0.329 | 0.86 | 0.73 | 0.39 | 0.36 | 0.42 | 0.45 | 1.01 |
| MnO | 0.1705 | 0.0105 | 0.1099 | 0.1985 | 0.14 | 0.17 | 0.19 | 0.10 | 0.03 | 0.06 | 0.21 |
| MgO | 18.7476 | 22.0164 | 21.1704 | 20.065 | 19.37 | 19.92 | 21.71 | 22.17 | 22.45 | 22.06 | 14.58 |
| NiO | 0.0336 | 0 | 0.0017 | 0.0403 | 0.02 | 0.02 | 0.00 | 0.00 | 0.00 | 0.00 | 0.05 |
| CaO | 11.5101 | 12.7337 | 12.2951 | 12.2101 | 11.87 | 10.33 | 12.00 | 12.19 | 12.73 | 12.57 | 21.42 |
| K2O | 0.036 | 0.0164 | 0.0344 | 0.0218 | 0.05 | 0.07 | 0.07 | 0.03 | 0.04 | 0.03 | 0.03 |
| BaO | 0.0016 | 0 | 0 | 0 | 0.00 | 0.00 | 0.00 | 0.00 | 0.01 | 0.00 | 0.01 |
| Total | **95.2633** | **96.2652** | **95.793** | **96.1792** | **96.08** | **92.81** | **95.18** | **94.88** | **96.38** | **95.98** | **99.66** |
| cations pfu per 6 oxygen | | | | | | | | | | | |
| Si | 11.966 | 12.319 | 12.179 | 12.200 | 11.801 | 11.750 | 12.222 | 12.215 | 12.078 | 12.240 | 11.419 |
| Ti | 0.022 | 0.022 | 0.014 | 0.040 | 0.072 | 0.054 | 0.058 | 0.022 | 0.151 | 0.018 | 0.140 |
| Al | 0.796 | 0.288 | 0.432 | 0.349 | 0.954 | 1.062 | 0.306 | 0.324 | 0.306 | 0.335 | 0.835 |
| Cr | 0.000 | 0.000 | 0.000 | 0.000 | 0.000 | 0.007 | 0.004 | 0.000 | 0.004 | 0.004 | 0.014 |
| Fe | 1.530 | 0.666 | 0.943 | 1.300 | 1.296 | 1.192 | 0.799 | 0.691 | 0.644 | 0.684 | 1.343 |
| Mn | 0.032 | 0.004 | 0.022 | 0.036 | 0.025 | 0.032 | 0.036 | 0.018 | 0.004 | 0.011 | 0.040 |
| Mg | 6.322 | 7.178 | 6.991 | 6.664 | 6.455 | 6.829 | 7.193 | 7.348 | 7.340 | 7.229 | 4.860 |
| Ni | 0.007 | 0.000 | 0.000 | 0.007 | 0.004 | 0.004 | 0.000 | 0.000 | 0.000 | 0.000 | 0.011 |
| Ca | 2.790 | 2.984 | 2.920 | 2.916 | 2.844 | 2.545 | 2.858 | 2.902 | 2.992 | 2.959 | 5.130 |
| Na | 0.288 | 0.122 | 0.169 | 0.140 | 0.374 | 0.324 | 0.166 | 0.155 | 0.180 | 0.191 | 0.439 |
| K | 0.011 | 0.004 | 0.011 | 0.007 | 0.014 | 0.022 | 0.022 | 0.007 | 0.011 | 0.007 | 0.007 |
| Ba | 0.000 | 0.000 | 0.000 | 0.000 | 0.000 | 0.000 | 0.000 | 0.000 | 0.000 | 0.000 | 0.000 |
| **Total** | **23.764** | **23.591** | **23.684** | **23.659** | **23.843** | **23.825** | **23.663** | **23.684** | **23.710** | **23.681** | **24.239** |
| | | | | | | | | | | | |
| Xdi | 0.854 | 0.938 | 0.911 | 0.878 | 0.876 | 0.885 | 0.923 | 0.935 | 0.941 | 0.936 | 0.878 |
| Xhd | 0.405 | 0.337 | 0.355 | 0.386 | 0.390 | 0.353 | 0.336 | 0.328 | 0.331 | 0.335 | 0.569 |

CLINOPYROXE

| Slide | KFZ_010_12_7 | KFZ_010_12_7 | KFZ_010_12_7 | KFZ_010_12_7 | KFZ_010_12_7 | KFZ_010_12_7 | KFZ_010_12_7 | KFZ_010_12_7 | KFZ_010_12_7 | KFZ_010_12_7 | KFZ_010_12_7 |
|---|---|---|---|---|---|---|---|---|---|---|---|
| **Area** | **2** | **2** | **2** | **2** | **3** | **3** | **3** | **3** | **3** | **3** | **3** |
| **Point** | **7** | **13** | **14** | **16** | **1** | **2** | **5** | **6** | **7** | **8** | **11** |
| SiO2 | 52.58 | 53.25 | 52.80 | 55.97 | 52.36 | 51.32 | 52.87 | 49.95 | 48.73 | 50.66 | 50.25 |
| TiO2 | 0.08 | 0.39 | 0.23 | 0.12 | 0.68 | 0.57 | 0.27 | 0.81 | 0.65 | 0.70 | 0.30 |
| Al2O3 | 1.33 | 2.13 | 3.92 | 0.97 | 2.98 | 4.09 | 2.10 | 2.15 | 2.60 | 2.12 | 4.07 |
| Cr2O3 | 0.04 | 0.05 | 0.02 | 0.01 | 0.08 | 0.07 | 0.05 | 0.02 | 0.04 | 0.04 | 0.03 |
| FeO | 4.93 | 7.46 | 7.10 | 3.08 | 9.12 | 10.51 | 10.24 | 8.32 | 8.73 | 7.27 | 9.59 |
| Na2O | 0.24 | 0.42 | 0.98 | 0.24 | 0.70 | 0.97 | 0.58 | 0.51 | 0.52 | 0.52 | 0.93 |
| MnO | 0.14 | 0.11 | 0.24 | 0.00 | 0.14 | 0.16 | 0.22 | 0.27 | 0.36 | 0.35 | 0.08 |
| MgO | 20.68 | 19.04 | 20.51 | 22.33 | 18.11 | 17.00 | 17.54 | 14.54 | 14.48 | 13.99 | 16.75 |
| NiO | 0.00 | 0.03 | 0.01 | 0.01 | 0.01 | 0.02 | 0.02 | 0.03 | 0.03 | 0.05 | 0.01 |
| CaO | 11.95 | 13.10 | 10.89 | 13.27 | 11.67 | 12.10 | 12.02 | 21.67 | 20.45 | 23.03 | 12.53 |
| K2O | 0.05 | 0.03 | 0.04 | 0.02 | 0.03 | 0.05 | 0.05 | 0.03 | 0.17 | 0.04 | 0.08 |
| BaO | 0.00 | 0.05 | 0.00 | 0.00 | 0.00 | 0.02 | 0.00 | 0.02 | 0.04 | 0.00 | 0.02 |
| Total | **92.02** | **96.04** | **96.74** | **96.02** | **95.89** | **96.88** | **95.96** | **98.32** | **96.80** | **98.77** | **94.64** |
| cations pfu per 6 oxygen | | | | | | | | | | | |
| Si | 12.146 | 11.970 | 11.714 | 12.272 | 11.851 | 11.617 | 12.024 | 11.412 | 11.329 | 11.495 | 11.624 |
| Ti | 0.014 | 0.065 | 0.036 | 0.022 | 0.115 | 0.097 | 0.047 | 0.140 | 0.115 | 0.119 | 0.054 |
| Al | 0.364 | 0.565 | 1.026 | 0.252 | 0.796 | 1.091 | 0.565 | 0.580 | 0.713 | 0.565 | 1.109 |
| Cr | 0.007 | 0.011 | 0.004 | 0.000 | 0.014 | 0.014 | 0.011 | 0.004 | 0.007 | 0.007 | 0.004 |
| Fe | 0.950 | 1.404 | 1.318 | 0.565 | 1.728 | 1.991 | 1.948 | 1.591 | 1.696 | 1.379 | 1.854 |
| Mn | 0.025 | 0.022 | 0.047 | 0.000 | 0.029 | 0.032 | 0.043 | 0.054 | 0.072 | 0.068 | 0.018 |
| Mg | 7.124 | 6.383 | 6.782 | 7.301 | 6.109 | 5.735 | 5.947 | 4.954 | 5.018 | 4.730 | 5.774 |
| Ni | 0.000 | 0.007 | 0.000 | 0.000 | 0.004 | 0.004 | 0.004 | 0.004 | 0.007 | 0.011 | 0.004 |
| Ca | 2.959 | 3.154 | 2.588 | 3.118 | 2.830 | 2.934 | 2.927 | 5.306 | 5.094 | 5.598 | 3.107 |
| Na | 0.108 | 0.184 | 0.421 | 0.101 | 0.310 | 0.425 | 0.259 | 0.223 | 0.234 | 0.230 | 0.414 |
| K | 0.014 | 0.007 | 0.011 | 0.007 | 0.007 | 0.014 | 0.014 | 0.011 | 0.050 | 0.011 | 0.025 |
| Ba | 0.000 | 0.004 | 0.000 | 0.000 | 0.000 | 0.000 | 0.000 | 0.004 | 0.004 | 0.000 | 0.000 |
| **Total** | **23.713** | **23.774** | **23.951** | **23.641** | **23.796** | **23.958** | **23.789** | **24.286** | **24.343** | **24.214** | **23.990** |
| | | | | | | | | | | | |
| Xdi | 0.912 | 0.870 | 0.873 | 0.949 | 0.836 | 0.811 | 0.817 | 0.862 | 0.851 | 0.877 | 0.826 |
| Xhd | 0.354 | 0.416 | 0.364 | 0.335 | 0.426 | 0.461 | 0.449 | 0.579 | 0.572 | 0.592 | 0.461 |

CLINOPYROXE

| Slide | KFZ_010_12_7 | KFZ_010_12_7 | KFZ_010_12_7 | KFZ_010_12_7 | KFZ_010_12_7 | KFZ_010_12_7 | KFZ_010_12_7 | KFZ_010_12_7 | KFZ_010_12_7 | KFZ_010_12_7 | KFZ_010_12_7 |
|---|---|---|---|---|---|---|---|---|---|---|---|
| **Area** | **3** | **3** | **3** | **3** | **3** | **3** | **4** | **4** | **4** | **4** | **4** |
| **Point** | **12** | **13** | **14** | **15** | **16** | **18** | **1** | **2** | **3** | **4** | **5** |
| SiO2 | 50.48 | 49.84 | 50.22 | 51.04 | 49.06 | 53.42 | 52.54 | 52.74 | 52.68 | 50.52 | 50.86 |
| TiO2 | 0.50 | 0.54 | 0.40 | 0.31 | 0.74 | 0.21 | 0.26 | 0.33 | 0.33 | 0.79 | 0.62 |
| Al2O3 | 4.88 | 5.53 | 1.62 | 3.93 | 5.89 | 2.96 | 2.80 | 2.66 | 2.61 | 2.24 | 1.67 |
| Cr2O3 | 0.00 | 0.03 | 0.00 | 0.00 | 0.02 | 0.02 | 0.00 | 0.03 | 0.00 | 0.01 | 0.04 |
| FeO | 7.90 | 10.90 | 5.66 | 9.39 | 10.66 | 7.45 | 7.31 | 8.16 | 7.79 | 6.73 | 5.93 |
| Na2O | 1.19 | 1.16 | 0.35 | 0.81 | 1.31 | 0.53 | 0.67 | 0.57 | 0.55 | 0.55 | 0.38 |
| MnO | 0.04 | 0.19 | 0.09 | 0.15 | 0.19 | 0.07 | 0.22 | 0.04 | 0.18 | 0.16 | 0.15 |
| MgO | 17.80 | 15.68 | 14.79 | 17.04 | 16.04 | 18.67 | 18.91 | 18.06 | 18.64 | 14.44 | 14.88 |
| NiO | 0.01 | 0.01 | 0.00 | 0.03 | 0.03 | 0.01 | 0.01 | 0.00 | 0.00 | 0.02 | 0.00 |
| CaO | 12.51 | 12.44 | 22.85 | 12.60 | 12.08 | 12.93 | 12.47 | 12.99 | 12.76 | 22.64 | 23.83 |
| K2O | 0.10 | 0.09 | 0.03 | 0.06 | 0.05 | 0.07 | 0.05 | 0.06 | 0.03 | 0.04 | 0.02 |
| BaO | 0.00 | 0.02 | 0.00 | 0.00 | 0.00 | 0.00 | 0.00 | 0.00 | 0.00 | 0.00 | 0.04 |
| Total | **95.40** | **96.43** | **96.04** | **95.36** | **96.05** | **96.32** | **95.24** | **95.65** | **95.58** | **98.14** | **98.41** |
| cations pfu per 6 oxygen | | | | | | | | | | | |
| Si | 11.491 | 11.394 | 11.617 | 11.686 | 11.257 | 11.952 | 11.898 | 11.941 | 11.916 | 11.488 | 11.527 |
| Ti | 0.086 | 0.094 | 0.072 | 0.054 | 0.126 | 0.036 | 0.043 | 0.058 | 0.058 | 0.133 | 0.104 |
| Al | 1.310 | 1.490 | 0.443 | 1.062 | 1.591 | 0.778 | 0.745 | 0.713 | 0.698 | 0.601 | 0.446 |
| Cr | 0.000 | 0.004 | 0.000 | 0.000 | 0.004 | 0.004 | 0.000 | 0.004 | 0.000 | 0.000 | 0.007 |
| Fe | 1.505 | 2.084 | 1.094 | 1.796 | 2.045 | 1.393 | 1.386 | 1.544 | 1.472 | 1.278 | 1.123 |
| Mn | 0.007 | 0.036 | 0.018 | 0.029 | 0.036 | 0.014 | 0.043 | 0.007 | 0.036 | 0.032 | 0.029 |
| Mg | 6.041 | 5.342 | 5.101 | 5.818 | 5.486 | 6.224 | 6.383 | 6.095 | 6.286 | 4.896 | 5.029 |
| Ni | 0.000 | 0.000 | 0.000 | 0.007 | 0.004 | 0.000 | 0.004 | 0.000 | 0.000 | 0.004 | 0.000 |
| Ca | 3.053 | 3.046 | 5.663 | 3.092 | 2.970 | 3.100 | 3.024 | 3.150 | 3.092 | 5.515 | 5.785 |
| Na | 0.526 | 0.511 | 0.158 | 0.360 | 0.583 | 0.230 | 0.295 | 0.248 | 0.241 | 0.241 | 0.166 |
| K | 0.029 | 0.025 | 0.011 | 0.014 | 0.014 | 0.018 | 0.014 | 0.018 | 0.011 | 0.011 | 0.007 |
| Ba | 0.000 | 0.000 | 0.000 | 0.000 | 0.000 | 0.000 | 0.000 | 0.000 | 0.000 | 0.000 | 0.004 |
| **Total** | **24.052** | **24.030** | **24.178** | **23.918** | **24.120** | **23.749** | **23.839** | **23.782** | **23.810** | **24.203** | **24.228** |
| | | | | | | | | | | | |
| Xdi | 0.857 | 0.798 | 0.906 | 0.830 | 0.803 | 0.869 | 0.868 | 0.856 | 0.861 | 0.888 | 0.904 |
| Xhd | 0.430 | 0.488 | 0.569 | 0.455 | 0.476 | 0.419 | 0.407 | 0.435 | 0.419 | 0.580 | 0.577 |

## CLINOPYROXE

| Slide | KFZ_010_12_7 | KFZ_010_12_7 | KFZ_010_12_7 | KFZ_010_12_7 | KFZ_010_12_7 | KFZ_010_12_7 | KFZ_010_12_7 | KFZ_010_12_7 | KFZ_010_12_7 | KFZ_010_12_7 | KFZ_010_12_7 |
|---|---|---|---|---|---|---|---|---|---|---|---|
| **Area** | **4** | **4** | **4** | **4** | **4** | **4** | **4** | **4** | **4** | **5** | **5** |
| **Point** | **6** | **7** | **8** | **9** | **10** | **13** | **14** | **15** | **16** | **2** | **3** |
| SiO2 | 50.73 | 50.30 | 50.88 | 50.87 | 51.06 | 53.98 | 53.29 | 51.01 | 51.08 | 50.97 | 50.49 |
| TiO2 | 0.74 | 0.78 | 0.76 | 0.75 | 0.39 | 0.21 | 0.53 | 0.76 | 0.53 | 0.19 | 0.25 |
| Al2O3 | 2.18 | 2.38 | 2.17 | 2.21 | 2.69 | 1.84 | 2.45 | 2.13 | 1.62 | 4.45 | 4.93 |
| Cr2O3 | 0.00 | 0.03 | 0.05 | 0.05 | 0.00 | 0.00 | 0.02 | 0.00 | 0.00 | 0.00 | 0.00 |
| FeO | 6.45 | 6.96 | 7.23 | 7.32 | 5.33 | 7.68 | 7.22 | 6.97 | 6.60 | 7.39 | 7.39 |
| Na2O | 0.51 | 0.49 | 0.51 | 0.49 | 0.60 | 0.40 | 0.48 | 0.46 | 0.39 | 1.08 | 1.15 |
| MnO | 0.17 | 0.24 | 0.22 | 0.23 | 0.11 | 0.17 | 0.20 | 0.22 | 0.22 | 0.17 | 0.14 |
| MgO | 14.75 | 14.62 | 15.09 | 14.78 | 18.35 | 18.91 | 18.98 | 14.97 | 15.60 | 18.71 | 18.44 |
| NiO | 0.01 | 0.02 | 0.03 | 0.00 | 0.00 | 0.01 | 0.00 | 0.01 | 0.00 | 0.00 | 0.00 |
| CaO | 22.77 | 22.38 | 21.61 | 22.15 | 13.61 | 13.06 | 12.70 | 21.20 | 21.01 | 11.78 | 12.31 |
| K2O | 0.04 | 0.05 | 0.05 | 0.04 | 0.04 | 0.04 | 0.05 | 0.04 | 0.03 | 0.03 | 0.06 |
| BaO | 0.06 | 0.00 | 0.05 | 0.05 | 0.00 | 0.02 | 0.00 | 0.00 | 0.00 | 0.00 | 0.00 |
| Total | **98.42** | **98.25** | **98.65** | **98.95** | **92.18** | **96.31** | **95.92** | **97.77** | **97.07** | **94.76** | **95.16** |
| cations pfu per 6 oxygen | | | | | | | | | | | |
| Si | 11.495 | 11.437 | 11.502 | 11.484 | 11.894 | 12.092 | 11.966 | 11.588 | 11.664 | 11.614 | 11.488 |
| Ti | 0.126 | 0.133 | 0.130 | 0.130 | 0.068 | 0.036 | 0.090 | 0.130 | 0.090 | 0.032 | 0.043 |
| Al | 0.583 | 0.637 | 0.580 | 0.587 | 0.738 | 0.486 | 0.648 | 0.572 | 0.436 | 1.195 | 1.321 |
| Cr | 0.000 | 0.004 | 0.011 | 0.007 | 0.000 | 0.000 | 0.004 | 0.000 | 0.000 | 0.000 | 0.000 |
| Fe | 1.220 | 1.325 | 1.368 | 1.382 | 1.040 | 1.436 | 1.357 | 1.325 | 1.260 | 1.408 | 1.408 |
| Mn | 0.032 | 0.047 | 0.043 | 0.043 | 0.022 | 0.032 | 0.040 | 0.043 | 0.043 | 0.032 | 0.029 |
| Mg | 4.982 | 4.957 | 5.083 | 4.975 | 6.372 | 6.314 | 6.354 | 5.069 | 5.306 | 6.354 | 6.257 |
| Ni | 0.004 | 0.004 | 0.007 | 0.000 | 0.000 | 0.004 | 0.000 | 0.004 | 0.000 | 0.000 | 0.000 |
| Ca | 5.526 | 5.454 | 5.234 | 5.357 | 3.395 | 3.136 | 3.056 | 5.159 | 5.141 | 2.876 | 2.999 |
| Na | 0.223 | 0.216 | 0.223 | 0.212 | 0.270 | 0.173 | 0.205 | 0.202 | 0.173 | 0.475 | 0.508 |
| K | 0.011 | 0.014 | 0.014 | 0.011 | 0.014 | 0.011 | 0.014 | 0.011 | 0.011 | 0.007 | 0.014 |
| Ba | 0.007 | 0.000 | 0.004 | 0.004 | 0.000 | 0.004 | 0.000 | 0.000 | 0.000 | 0.000 | 0.000 |
| **Total** | **24.214** | **24.232** | **24.199** | **24.192** | **23.818** | **23.728** | **23.735** | **24.106** | **24.127** | **23.998** | **24.070** |
| | | | | | | | | | | | |
| Xdi | 0.893 | 0.884 | 0.880 | 0.879 | 0.902 | 0.865 | 0.871 | 0.882 | 0.889 | 0.865 | 0.866 |
| Xhd | 0.574 | 0.575 | 0.563 | 0.573 | 0.410 | 0.419 | 0.408 | 0.559 | 0.545 | 0.401 | 0.412 |

CLINOPYROXE

| Slide | KFZ_010_12_7 | KFZ_010_12_7 | KFZ_010_12_7 | KFZ_010_12_7 | KFZ_010_12_7 | KFZ_010_12_7 | KFZ_010_12_7 | KFZ_010_12_7 | KFZ_010_12_7 | KFZ_010_12_7 |
|---|---|---|---|---|---|---|---|---|---|---|
| **Area** | **5** | **5** | **5** | **5** | **5** | **5** | **5** | **5** | **5** | **5** |
| **Point** | **4** | **7** | **8** | **9** | **10** | **11** | **12** | **13** | **14** | **15** |
| SiO2 | 50.72 | 52.44 | 54.24 | 48.61 | 52.01 | 53.29 | 50.04 | 53.30 | 52.87 | 54.66 |
| TiO2 | 0.24 | 0.13 | 0.07 | 0.23 | 0.04 | 0.15 | 0.43 | 0.15 | 0.22 | 0.05 |
| Al2O3 | 4.67 | 3.12 | 1.46 | 5.70 | 3.02 | 1.01 | 3.60 | 1.31 | 1.64 | 1.14 |
| Cr2O3 | 0.00 | 0.00 | 0.00 | 0.00 | 0.00 | 0.18 | 0.02 | 0.00 | 0.02 | 0.00 |
| FeO | 8.16 | 7.16 | 6.82 | 13.03 | 7.77 | 11.59 | 11.20 | 7.77 | 9.52 | 5.73 |
| Na2O | 1.13 | 0.79 | 0.34 | 1.18 | 0.70 | 0.29 | 0.94 | 0.33 | 0.39 | 0.27 |
| MnO | 0.21 | 0.21 | 0.22 | 0.39 | 0.17 | 0.25 | 0.27 | 0.18 | 0.20 | 0.16 |
| MgO | 18.13 | 19.25 | 19.91 | 14.80 | 18.58 | 16.95 | 16.38 | 19.16 | 17.96 | 20.36 |
| NiO | 0.00 | 0.00 | 0.00 | 0.02 | 0.00 | 0.00 | 0.03 | 0.00 | 0.00 | 0.00 |
| CaO | 11.50 | 11.81 | 12.25 | 11.20 | 11.90 | 11.76 | 12.06 | 12.63 | 12.46 | 12.40 |
| K2O | 0.04 | 0.04 | 0.03 | 0.05 | 0.04 | 0.02 | 0.04 | 0.03 | 0.03 | 0.03 |
| BaO | 0.00 | 0.00 | 0.00 | 0.00 | 0.00 | 0.00 | 0.00 | 0.00 | 0.00 | 0.00 |
| Total | **94.81** | **94.94** | **95.34** | **95.19** | **94.23** | **95.49** | **95.01** | **94.86** | **95.30** | **94.80** |
| cations pfu per 6 oxygen | | | | | | | | | | |
| Si | 11.588 | 11.880 | 12.186 | 11.354 | 11.909 | 12.229 | 11.621 | 12.125 | 12.074 | 12.280 |
| Ti | 0.043 | 0.022 | 0.011 | 0.040 | 0.007 | 0.025 | 0.076 | 0.025 | 0.036 | 0.007 |
| Al | 1.256 | 0.832 | 0.389 | 1.570 | 0.814 | 0.274 | 0.983 | 0.353 | 0.439 | 0.302 |
| Cr | 0.000 | 0.000 | 0.000 | 0.000 | 0.000 | 0.032 | 0.004 | 0.000 | 0.004 | 0.000 |
| Fe | 1.559 | 1.357 | 1.282 | 2.545 | 1.490 | 2.225 | 2.174 | 1.480 | 1.818 | 1.076 |
| Mn | 0.043 | 0.040 | 0.043 | 0.076 | 0.032 | 0.047 | 0.054 | 0.036 | 0.040 | 0.029 |
| Mg | 6.178 | 6.502 | 6.671 | 5.152 | 6.343 | 5.796 | 5.670 | 6.498 | 6.113 | 6.818 |
| Ni | 0.000 | 0.000 | 0.000 | 0.004 | 0.000 | 0.000 | 0.004 | 0.000 | 0.000 | 0.000 |
| Ca | 2.815 | 2.866 | 2.948 | 2.804 | 2.920 | 2.891 | 3.002 | 3.082 | 3.049 | 2.984 |
| Na | 0.500 | 0.346 | 0.148 | 0.533 | 0.310 | 0.130 | 0.425 | 0.148 | 0.173 | 0.119 |
| K | 0.014 | 0.011 | 0.007 | 0.014 | 0.011 | 0.007 | 0.011 | 0.007 | 0.007 | 0.011 |
| Ba | 0.000 | 0.000 | 0.000 | 0.000 | 0.000 | 0.000 | 0.000 | 0.000 | 0.000 | 0.000 |
| **Total** | **23.998** | **23.857** | **23.684** | **24.095** | **23.839** | **23.659** | **24.026** | **23.756** | **23.753** | **23.630** |
| | | | | | | | | | | |
| Xdi | 0.849 | 0.870 | 0.879 | 0.752 | 0.859 | 0.793 | 0.796 | 0.863 | 0.831 | 0.899 |
| Xhd | 0.413 | 0.392 | 0.387 | 0.506 | 0.409 | 0.467 | 0.475 | 0.411 | 0.442 | 0.372 |

OLIVINE

| Slide | KFZ_010_08_02 | KFZ_010_08_02 | KFZ_010_08_02 | KFZ_010_08_02 | KFZ_010_08_02 | KFZ_010_08_02 | KFZ_010_08_02 | KFZ_010_08_02 | KFZ_010_08_02 | KFZ_010_08_02 | KFZ_010_08_02 |
|---|---|---|---|---|---|---|---|---|---|---|---|
| **Area** | **1** | **1** | **1** | **1** | **1** | **1** | **2** | **2** | **2** | **2** | **2** |
| **Point** | **2** | **3** | **5** | **7** | **8** | **10** | **2** | **3** | **4** | **5** | **6** |
| SiO2 | 37.33 | 37.31 | 37.66 | 38.42 | 38.01 | 37.69 | 38.37 | 36.94 | 37.53 | 37.72 | 37.57 |
| TiO2 | 0.05 | 0.06 | 0.04 | 0.00 | 0.02 | 0.03 | 0.02 | 0.10 | 0.06 | 0.05 | 0.03 |
| Al2O3 | 0.00 | 0.05 | 0.00 | 0.05 | 0.04 | 0.02 | 0.00 | 0.29 | 0.02 | 0.00 | 0.00 |
| Cr2O3 | 0.06 | 0.07 | 0.07 | 0.04 | 0.04 | 0.05 | 0.02 | 0.03 | 0.04 | 0.04 | 0.01 |
| FeO | 18.14 | 19.39 | 17.74 | 17.41 | 17.66 | 17.65 | 18.15 | 20.39 | 18.35 | 17.66 | 17.93 |
| Na2O | 0.01 | 0.02 | 0.01 | 0.01 | 0.01 | 0.01 | 0.01 | 0.07 | 0.01 | 0.00 | 0.02 |
| MnO | 0.30 | 0.35 | 0.32 | 0.28 | 0.30 | 0.29 | 0.32 | 0.31 | 0.29 | 0.30 | 0.27 |
| MgO | 41.50 | 40.93 | 42.19 | 42.43 | 42.07 | 42.04 | 42.09 | 38.15 | 41.99 | 42.42 | 42.24 |
| NiO | 0.18 | 0.16 | 0.17 | 0.16 | 0.15 | 0.16 | 0.16 | 0.10 | 0.12 | 0.16 | 0.12 |
| CaO | 0.32 | 0.36 | 0.32 | 0.25 | 0.28 | 0.30 | 0.27 | 0.38 | 0.30 | 0.32 | 0.31 |
| K2O | 0.02 | 0.03 | 0.03 | 0.02 | 0.03 | 0.03 | 0.03 | 0.10 | 0.02 | 0.03 | 0.03 |
| BaO | 0.11 | 0.07 | 0.07 | 0.00 | 0.00 | 0.02 | 0.02 | 0.01 | 0.03 | 0.00 | 0.00 |
| Total | **98.01** | **98.79** | **98.61** | **99.07** | **98.61** | **98.30** | **99.46** | **96.87** | **98.75** | **98.71** | **98.53** |
| cations pfu per 4 oxygen | | | | | | | | | | | |
| Si | 0.978 | 0.976 | 0.978 | 0.9888 | 0.9852 | 0.9812 | 0.988 | 0.989 | 0.976 | 0.978 | 0.977 |
| Ti | 0.001 | 0.001 | 0.001 | 0 | 0.0004 | 0.0004 | 0.000 | 0.002 | 0.001 | 0.001 | 0.001 |
| Al | 0.000 | 0.002 | 0.000 | 0.0016 | 0.0012 | 0.0008 | 0.000 | 0.009 | 0.001 | 0.000 | 0.000 |
| Cr | 0.001 | 0.001 | 0.002 | 0.0008 | 0.0008 | 0.0012 | 0.000 | 0.000 | 0.001 | 0.001 | 0.000 |
| Fe | 0.398 | 0.424 | 0.385 | 0.3748 | 0.3828 | 0.384 | 0.390 | 0.456 | 0.399 | 0.383 | 0.390 |
| Mn | 0.007 | 0.008 | 0.007 | 0.006 | 0.0064 | 0.0064 | 0.007 | 0.007 | 0.006 | 0.006 | 0.006 |
| Mg | 1.621 | 1.595 | 1.634 | 1.6276 | 1.6252 | 1.6308 | 1.614 | 1.523 | 1.627 | 1.639 | 1.637 |
| Ni | 0.004 | 0.003 | 0.004 | 0.0032 | 0.0032 | 0.0036 | 0.003 | 0.002 | 0.002 | 0.004 | 0.002 |
| Ca | 0.009 | 0.010 | 0.009 | 0.0072 | 0.0076 | 0.0084 | 0.008 | 0.011 | 0.008 | 0.009 | 0.008 |
| Na | 0.001 | 0.001 | 0.000 | 0.0004 | 0.0008 | 0.0008 | 0.001 | 0.004 | 0.000 | 0.000 | 0.001 |
| K | 0.000 | 0.001 | 0.001 | 0.0008 | 0.0008 | 0.0008 | 0.001 | 0.004 | 0.001 | 0.001 | 0.001 |
| Ba | 0.001 | 0.001 | 0.001 | 0 | 0 | 0.0004 | 0.000 | 0.000 | 0.000 | 0.000 | 0.000 |
| Total | **3.020** | **3.022** | **3.021** | **3.0112** | **3.0148** | **3.0192** | **3.014** | **3.008** | **3.023** | **3.021** | **3.024** |

# OLIVINE

| Slide | KFZ_010_08_02 | KFZ_010_08_02 | KFZ_010_08_02 | KFZ_010_08_02 | KFZ_010_08_02 | KFZ_010_08_02 | KFZ_010_08_02 | KFZ_010_08_02 | KFZ_010_08_02 | KFZ_010_08_02 |
|---|---|---|---|---|---|---|---|---|---|---|
| **Area** | **2** | **3** | **3** | **3** | **3** | **3** | **3** | **4** | **4** | **4** |
| **Point** | **10** | **1** | **4** | **5** | **6** | **8** | **10** | **5** | **6** | **10** |
| SiO2 | 38.09 | 37.45 | 37.64 | 37.88 | 37.16 | 37.10 | 37.57 | 37.75 | 38.54 | 38.14 |
| TiO2 | 0.04 | 0.03 | 0.07 | 0.08 | 0.03 | 0.04 | 0.05 | 0.05 | 0.05 | 0.06 |
| Al2O3 | 0.01 | 0.00 | 0.00 | 0.00 | 0.00 | 0.00 | 0.00 | 0.00 | 0.00 | 0.02 |
| Cr2O3 | 0.02 | 0.06 | 0.07 | 0.08 | 0.07 | 0.06 | 0.07 | 0.06 | 0.05 | 0.04 |
| FeO | 18.44 | 17.61 | 17.60 | 18.18 | 17.56 | 18.20 | 18.11 | 17.39 | 17.70 | 17.69 |
| Na2O | 0.01 | 0.03 | 0.01 | 0.01 | 0.03 | 0.01 | 0.01 | 0.02 | 0.03 | 0.04 |
| MnO | 0.33 | 0.32 | 0.32 | 0.31 | 0.30 | 0.33 | 0.34 | 0.31 | 0.32 | 0.31 |
| MgO | 41.36 | 42.51 | 42.18 | 42.06 | 42.39 | 41.82 | 42.13 | 42.64 | 42.70 | 42.29 |
| NiO | 0.11 | 0.16 | 0.17 | 0.19 | 0.17 | 0.13 | 0.17 | 0.17 | 0.18 | 0.15 |
| CaO | 0.36 | 0.30 | 0.31 | 0.35 | 0.30 | 0.32 | 0.31 | 0.29 | 0.33 | 0.34 |
| K2O | 0.03 | 0.03 | 0.03 | 0.02 | 0.02 | 0.03 | 0.03 | 0.03 | 0.03 | 0.05 |
| BaO | 0.00 | 0.09 | 0.04 | 0.06 | 0.04 | 0.11 | 0.07 | 0.06 | 0.05 | 0.06 |
| Total | **98.80** | **98.60** | **98.44** | **99.23** | **98.09** | **98.17** | **98.87** | **98.78** | **99.98** | **99.18** |
| cations pfu per 4 oxygen | | | | | | | | | | |
| Si | 0.988 | 0.973 | 0.978 | 0.979 | 0.971 | 0.972 | 0.976 | 0.977 | 0.985 | 0.984 |
| Ti | 0.001 | 0.001 | 0.002 | 0.002 | 0.001 | 0.001 | 0.001 | 0.001 | 0.001 | 0.001 |
| Al | 0.000 | 0.000 | 0.000 | 0.000 | 0.000 | 0.000 | 0.000 | 0.000 | 0.000 | 0.001 |
| Cr | 0.000 | 0.001 | 0.002 | 0.002 | 0.002 | 0.001 | 0.002 | 0.001 | 0.001 | 0.001 |
| Fe | 0.400 | 0.383 | 0.383 | 0.393 | 0.384 | 0.399 | 0.393 | 0.376 | 0.378 | 0.382 |
| Mn | 0.007 | 0.007 | 0.007 | 0.007 | 0.007 | 0.007 | 0.008 | 0.007 | 0.007 | 0.007 |
| Mg | 1.600 | 1.647 | 1.635 | 1.621 | 1.651 | 1.633 | 1.630 | 1.646 | 1.627 | 1.626 |
| Ni | 0.002 | 0.003 | 0.004 | 0.004 | 0.004 | 0.003 | 0.004 | 0.004 | 0.004 | 0.003 |
| Ca | 0.010 | 0.008 | 0.009 | 0.010 | 0.008 | 0.009 | 0.009 | 0.008 | 0.009 | 0.009 |
| Na | 0.000 | 0.002 | 0.001 | 0.001 | 0.002 | 0.001 | 0.000 | 0.001 | 0.002 | 0.002 |
| K | 0.001 | 0.001 | 0.001 | 0.001 | 0.001 | 0.001 | 0.001 | 0.001 | 0.001 | 0.002 |
| Ba | 0.000 | 0.001 | 0.000 | 0.001 | 0.000 | 0.001 | 0.001 | 0.001 | 0.000 | 0.001 |
| Total | **3.012** | **3.028** | **3.021** | **3.019** | **3.030** | **3.028** | **3.024** | **3.022** | **3.015** | **3.017** |

CHLORITE

| Slide | KFZ_010_11_2 | KFZ_010_11_2 | KFZ_010_11_2 | KFZ_010_11_2 | KFZ_010_11_2 | KFZ_010_11_2 | KFZ_010_11_2 | KFZ_010_11_2 | KFZ_010_11_2 | KFZ_010_11_2 |
|---|---|---|---|---|---|---|---|---|---|---|
| **Area** | **1** | **1** | **1** | **2** | **2** | **2** | **2** | **2** | **3** | **3** |
| **Point** | **1** | **2** | **3** | **6** | **7** | **11** | **17** | **22** | **1** | **2** |
| SiO2 | 27.97 | 28.25 | 28.70 | 28.61 | 28.55 | 28.23 | 27.86 | 28.15 | 28.85 | 28.18 |
| TiO2 | 0.03 | 0.02 | 0.00 | 0.00 | 0.00 | 0.00 | 0.00 | 0.00 | 0.00 | 0.02 |
| Al2O3 | 20.67 | 20.32 | 19.51 | 20.08 | 20.16 | 20.48 | 19.73 | 20.88 | 20.36 | 20.22 |
| Cr2O3 | 0.00 | 0.00 | 0.00 | 0.00 | 0.00 | 0.00 | 0.00 | 0.00 | 0.00 | 0.00 |
| FeO | 12.17 | 12.23 | 12.02 | 12.27 | 12.70 | 12.97 | 12.37 | 13.00 | 12.24 | 12.14 |
| Na2O | 0.03 | 0.03 | 0.04 | 0.00 | 0.00 | 0.00 | 0.04 | 0.00 | 0.04 | 0.02 |
| MnO | 0.06 | 0.08 | 0.10 | 0.08 | 0.06 | 0.07 | 0.07 | 0.09 | 0.09 | 0.12 |
| MgO | 24.39 | 24.93 | 25.01 | 25.27 | 24.84 | 24.36 | 23.93 | 24.19 | 24.86 | 24.52 |
| NiO | 0.04 | 0.04 | 0.04 | 0.00 | 0.04 | 0.03 | 0.03 | 0.05 | 0.04 | 0.02 |
| CaO | 0.03 | 0.02 | 0.03 | 0.01 | 0.00 | 0.06 | 0.12 | 0.03 | 0.08 | 0.06 |
| K2O | 0.03 | 0.01 | 0.08 | 0.00 | 0.05 | 0.06 | 0.03 | 0.05 | 0.03 | 0.04 |
| BaO | 0.00 | 0.00 | 0.00 | 0.00 | 0.00 | 0.00 | 0.00 | 0.00 | 0.00 | 0.00 |
| Total | **85.41** | **85.93** | **85.55** | **86.33** | **86.41** | **86.26** | **84.20** | **86.45** | **86.59** | **85.33** |
| | | | | | | | | | | |
| cations pfu per 28 oxygen | | | | | | | | | | |
| Si | 5.625 | 5.650 | 5.762 | 5.692 | 5.690 | 5.645 | 5.698 | 5.617 | 5.720 | 5.673 |
| Ti | 0.006 | 0.003 | 0.000 | 0.000 | 0.000 | 0.000 | 0.000 | 0.000 | 0.000 | 0.003 |
| Al | 4.900 | 4.788 | 4.617 | 4.710 | 4.735 | 4.827 | 4.757 | 4.911 | 4.757 | 4.799 |
| Cr | 0.000 | 0.000 | 0.000 | 0.000 | 0.000 | 0.000 | 0.000 | 0.000 | 0.000 | 0.000 |
| Fe | 2.047 | 2.047 | 2.019 | 2.041 | 2.117 | 2.170 | 2.117 | 2.170 | 2.030 | 2.044 |
| Mn | 0.008 | 0.014 | 0.017 | 0.014 | 0.011 | 0.011 | 0.014 | 0.014 | 0.014 | 0.020 |
| Mg | 7.311 | 7.431 | 7.484 | 7.496 | 7.378 | 7.260 | 7.297 | 7.193 | 7.347 | 7.358 |
| Ni | 0.006 | 0.006 | 0.006 | 0.000 | 0.006 | 0.006 | 0.006 | 0.008 | 0.006 | 0.003 |
| Ca | 0.006 | 0.006 | 0.008 | 0.003 | 0.000 | 0.014 | 0.028 | 0.006 | 0.017 | 0.014 |
| Na | 0.014 | 0.011 | 0.014 | 0.000 | 0.000 | 0.000 | 0.014 | 0.003 | 0.017 | 0.006 |
| K | 0.008 | 0.003 | 0.020 | 0.000 | 0.014 | 0.017 | 0.008 | 0.014 | 0.008 | 0.008 |
| Ba | 0.000 | 0.000 | 0.000 | 0.000 | 0.000 | 0.000 | 0.000 | 0.000 | 0.000 | 0.000 |
| Total | **19.933** | **19.958** | **19.947** | **19.958** | **19.950** | **19.950** | **19.939** | **19.939** | **19.916** | **19.930** |

# CHLORITE

| Slide | KFZ_010_11_2 | KFZ_010_11_2 | KFZ_010_11_2 | KFZ_010_11_2 | KFZ_010_12_7 | KFZ_010_12_7 |
|---|---|---|---|---|---|---|
| **Area** | **3** | **3** | **3** | **5** | **1** | **4** |
| **Point** | **3** | **6** | **10** | **2** | **12** | **11** |
| SiO2 | 28.00 | 28.27 | 28.57 | 28.81 | 31.47 | 32.51 |
| TiO2 | 0.00 | 0.01 | 0.02 | 0.00 | 0.02 | 0.00 |
| Al2O3 | 19.44 | 20.89 | 19.61 | 20.59 | 16.80 | 18.85 |
| Cr2O3 | 0.00 | 0.00 | 0.00 | 0.00 | 0.00 | 0.00 |
| FeO | 11.95 | 12.35 | 11.92 | 12.28 | 13.99 | 13.50 |
| Na2O | 0.02 | 0.01 | 0.00 | 0.52 | 0.19 | 1.25 |
| MnO | 0.09 | 0.10 | 0.10 | 0.08 | 0.65 | 0.36 |
| MgO | 23.94 | 24.41 | 24.92 | 25.26 | 22.77 | 20.80 |
| NiO | 0.05 | 0.05 | 0.02 | 0.03 | 0.00 | 0.02 |
| CaO | 0.10 | 0.04 | 0.02 | 0.03 | 0.17 | 0.25 |
| K2O | 0.06 | 0.05 | 0.07 | 0.04 | 0.16 | 0.09 |
| BaO | 0.00 | 0.00 | 0.00 | 0.00 | 0.00 | 0.00 |
| Total | **83.65** | **86.19** | **85.26** | **87.63** | **86.2233** | **87.6327** |
| | | | | | | |
| cations pfu per 28 oxygen | | | | | | |
| Si | 5.751 | 5.636 | 5.748 | 5.656 | 6.325 | 6.387 |
| Ti | 0.000 | 0.000 | 0.003 | 0.000 | 0.003 | 0.000 |
| Al | 4.707 | 4.908 | 4.651 | 4.766 | 3.979 | 4.365 |
| Cr | 0.000 | 0.000 | 0.000 | 0.000 | 0.000 | 0.000 |
| Fe | 2.052 | 2.058 | 2.008 | 2.016 | 2.352 | 2.218 |
| Mn | 0.017 | 0.017 | 0.017 | 0.014 | 0.112 | 0.059 |
| Mg | 7.328 | 7.258 | 7.476 | 7.392 | 6.821 | 6.093 |
| Ni | 0.008 | 0.008 | 0.003 | 0.006 | 0.000 | 0.003 |
| Ca | 0.022 | 0.008 | 0.006 | 0.006 | 0.036 | 0.053 |
| Na | 0.008 | 0.006 | 0.000 | 0.199 | 0.076 | 0.476 |
| K | 0.017 | 0.014 | 0.020 | 0.008 | 0.039 | 0.022 |
| Ba | 0.000 | 0.000 | 0.000 | 0.000 | 0.000 | 0.000 |
| Total | **19.911** | **19.916** | **19.930** | **20.062** | **19.743** | **19.678** |

HORNBLLENDE

| Slide | KFZ_010_11_2 | KFZ_010_11_2 | KFZ_010_11_2 | KFZ_010_11_2 | KFZ_010_12_7 | KFZ_010_12_7 | KFZ_010_12_7 |
|---|---|---|---|---|---|---|---|
| **Area** | **4** | **4** | **3** | **3** | **5** | **5** | **5** |
| **Point** | **12** | **19** | **14** | **15** | **1** | **5** | **6** |
| SiO2 | 48.28 | 44.71 | 42.19 | 42.51 | 45.87 | 48.26 | 44.67 |
| TiO2 | 0.16 | 0.20 | 0.17 | 0.25 | 0.26 | 0.34 | 0.36 |
| Al2O3 | 8.29 | 6.58 | 14.21 | 13.49 | 8.84 | 7.71 | 10.54 |
| Cr2O3 | 0.00 | 0.58 | 0.04 | 0.03 | 0.00 | 0.00 | 0.00 |
| FeO | 10.52 | 11.84 | 13.24 | 13.06 | 8.84 | 8.27 | 10.03 |
| Na2O | 1.72 | 0.36 | 2.85 | 2.89 | 2.03 | 1.77 | 2.36 |
| MnO | 0.18 | 0.11 | 0.17 | 0.13 | 0.11 | 0.15 | 0.12 |
| MgO | 15.68 | 18.77 | 12.32 | 12.59 | 16.34 | 17.14 | 15.29 |
| NiO | 0.04 | 0.07 | 0.06 | 0.02 | 0.00 | 0.00 | 0.00 |
| CaO | 11.56 | 8.54 | 12.28 | 12.16 | 11.95 | 11.78 | 12.02 |
| K2O | 0.06 | 0.19 | 0.16 | 0.14 | 0.09 | 0.06 | 0.12 |
| BaO | 0.00 | 0.00 | 0.00 | 0.00 | 0.00 | 0.00 | 0.00 |
| Total | **96.49** | **91.94** | **97.69** | **97.27** | **94.32** | **95.48** | **95.51** |
| Cations pfu per 23 oxygen | | | | | | | |
| Si | 7.033 | 6.870 | 6.242 | 6.307 | 6.833 | 7.043 | 6.626 |
| Ti | 0.016 | 0.023 | 0.018 | 0.028 | 0.028 | 0.037 | 0.039 |
| Al | 1.424 | 1.191 | 2.479 | 2.360 | 1.553 | 1.325 | 1.842 |
| Cr | 0.000 | 0.071 | 0.005 | 0.005 | 0.000 | 0.000 | 0.000 |
| Fe | 1.281 | 1.520 | 1.638 | 1.622 | 1.102 | 1.010 | 1.244 |
| Mn | 0.023 | 0.014 | 0.021 | 0.016 | 0.014 | 0.018 | 0.014 |
| Mg | 3.404 | 4.299 | 2.716 | 2.785 | 3.627 | 3.728 | 3.381 |
| Ni | 0.005 | 0.009 | 0.007 | 0.002 | 0.000 | 0.000 | 0.000 |
| Ca | 1.803 | 1.405 | 1.946 | 1.932 | 1.907 | 1.842 | 1.911 |
| Na | 0.485 | 0.106 | 0.819 | 0.830 | 0.587 | 0.499 | 0.679 |
| K | 0.012 | 0.037 | 0.030 | 0.028 | 0.016 | 0.012 | 0.023 |
| Ba | 0.000 | 0.000 | 0.000 | 0.000 | 0.000 | 0.000 | 0.000 |
| Total | **15.486** | **15.548** | **15.923** | **15.914** | **15.668** | **15.516** | **15.760** |

ACTINOLITE

| Slide | KFZ_010_11_2 | KFZ_010_11_2 | KFZ_010_11_2 | KFZ_010_12_7 |
|---|---|---|---|---|
| **Area** | **3** | **2** | **2** | **2** |
| **Point** | **8** | **3** | **13** | **4** |
| SiO2 | 44.58 | 44.47 | 43.30 | 44.63 |
| TiO2 | 0.11 | 0.15 | 0.05 | 0.26 |
| Al2O3 | 11.94 | 11.44 | 14.80 | 11.38 |
| Cr2O3 | 0.03 | 0.01 | 0.00 | 0.03 |
| FeO | 11.35 | 11.81 | 10.59 | 10.64 |
| Na2O | 2.41 | 2.45 | 2.80 | 2.54 |
| MnO | 0.12 | 0.11 | 0.16 | 0.11 |
| MgO | 14.03 | 14.21 | 13.37 | 14.63 |
| NiO | 0.04 | 0.02 | 0.00 | 0.02 |
| CaO | 12.25 | 12.45 | 12.15 | 12.24 |
| K2O | 0.11 | 0.14 | 0.11 | 0.14 |
| BaO | 0.03 | 0.00 | 0.00 | 0.03 |
| Total | **97.00** | **97.26** | **97.33** | **96.67** |
| | | | | |
| cations pfu per 23 oxygen | | | | |
| Si | 6.548 | 6.541 | 6.320 | 6.567 |
| Ti | 0.012 | 0.016 | 0.007 | 0.030 |
| Al | 2.068 | 1.983 | 2.546 | 1.973 |
| Cr | 0.002 | 0.002 | 0.000 | 0.005 |
| Fe | 1.394 | 1.454 | 1.293 | 1.309 |
| Mn | 0.016 | 0.014 | 0.021 | 0.014 |
| Mg | 3.073 | 3.114 | 2.910 | 3.209 |
| Ni | 0.005 | 0.002 | 0.000 | 0.002 |
| Ca | 1.927 | 1.962 | 1.902 | 1.930 |
| Na | 0.688 | 0.699 | 0.791 | 0.725 |
| K | 0.021 | 0.025 | 0.021 | 0.025 |
| Ba | 0.002 | 0.000 | 0.000 | 0.002 |
| Total | **15.755** | **15.815** | **15.813** | **15.792** |